DECODING BRAIN FUNCTION THROUGH GENETICS

EDITED BY: Noriyoshi Usui, Guang-Zhong Wang, Kazuya Toriumi and Stefano Berto

PUBLISHED IN: Frontiers in Genetics and Frontiers in Neuroscience

frontiers Research Topics

ISSN 1664-8714
ISBN 978-2-88976-057-2
DOI 10.3389/978-2-88976-057-2

About Frontiers

Frontiers is more than just an open-access publisher of scholarly articles: it is a pioneering approach to the world of academia, radically improving the way scholarly research is managed. The grand vision of Frontiers is a world where all people have an equal opportunity to seek, share and generate knowledge. Frontiers provides immediate and permanent online open access to all its publications, but this alone is not enough to realize our grand goals.

Frontiers Journal Series

The Frontiers Journal Series is a multi-tier and interdisciplinary set of open-access, online journals, promising a paradigm shift from the current review, selection and dissemination processes in academic publishing. All Frontiers journals are driven by researchers for researchers; therefore, they constitute a service to the scholarly community. At the same time, the Frontiers Journal Series operates on a revolutionary invention, the tiered publishing system, initially addressing specific communities of scholars, and gradually climbing up to broader public understanding, thus serving the interests of the lay society, too.

Dedication to Quality

Each Frontiers article is a landmark of the highest quality, thanks to genuinely collaborative interactions between authors and review editors, who include some of the world's best academicians. Research must be certified by peers before entering a stream of knowledge that may eventually reach the public - and shape society; therefore, Frontiers only applies the most rigorous and unbiased reviews.
Frontiers revolutionizes research publishing by freely delivering the most outstanding research, evaluated with no bias from both the academic and social point of view. By applying the most advanced information technologies, Frontiers is catapulting scholarly publishing into a new generation.

What are Frontiers Research Topics?

Frontiers Research Topics are very popular trademarks of the Frontiers Journals Series: they are collections of at least ten articles, all centered on a particular subject. With their unique mix of varied contributions from Original Research to Review Articles, Frontiers Research Topics unify the most influential researchers, the latest key findings and historical advances in a hot research area! Find out more on how to host your own Frontiers Research Topic or contribute to one as an author by contacting the Frontiers Editorial Office: frontiersin.org/about/contact

DECODING BRAIN FUNCTION THROUGH GENETICS

Topic Editors:
Noriyoshi Usui, Osaka University, Japan
Guang-Zhong Wang, Shanghai Institute of Nutrition and Health, Chinese Academy of Sciences (CAS), China
Kazuya Toriumi, Tokyo Metropolitan Institute of Medical Science, Japan
Stefano Berto, University of Texas Southwestern Medical Center, United States

Citation: Usui, N., Wang, G.-Z., Toriumi, K., Berto, S., eds. (2022). Decoding Brain Function Through Genetics. Lausanne: Frontiers Media SA.
doi: 10.3389/978-2-88976-057-2

Table of Contents

frontiers | Frontiers in Genetics

EDITORIAL
published: 11 April 2022
doi: 10.3389/fgene.2022.874350

Editorial: Decoding Brain Function Through Genetics

Kazuya Toriumi[1], *Guang-Zhong Wang*[2], *Stefano Berto*[3] *and Noriyoshi Usui*[4,5,6,7]*

[1]Schizophrenia Research Project, Department of Psychiatry and Behavioral Sciences, Tokyo Metropolitan Institute of Medical Science, Tokyo, Japan, [2]Shanghai Institute of Nutrition and Health, University of Chinese Academy of Sciences, Chinese Academy of Sciences, Shanghai, China, [3]Department of Neuroscience, Medical University of South Carolina, Charleston, SC, United States, [4]Department of Neuroscience and Cell Biology, Graduate School of Medicine, Osaka University, Osaka, Japan, [5]United Graduate School of Child Development, Osaka University, Suita, Japan, [6]Global Center for Medical Engineering and Informatics, Osaka University, Osaka, Japan, [7]Addiction Research Unit, Osaka Psychiatric Research Center, Osaka Psychiatric Medical Center, Osaka, Japan

Keywords: neurogenomics, epigenetics, transcriptome, brain function, neurodevelopmental disorders (NDDs), psychiatric disorders, single nucleotide polymorphism (SNP), polygenic risk score (PRS)

Editorial on the Research Topic

Decoding Brain Function Through Genetics

Recently, several attempts have been made to explore the mechanisms underlying brain function using neurogenomics (Kang et al., 2011; Snyder et al., 2020; Yuste et al., 2020; Jourdon et al., 2021). Neurogenomics offers comprehensive perspectives on the profound impact of genomic alterations on brain function and facilitates an understanding of the complex interactions between genetics and the surrounding environment. It also aids in understanding the pathogenesis of brain disorders such as neurodevelopmental disorders (NDDs) and psychiatric disorders (Bogdan et al., 2013; Smoller et al., 2019; Pattabiraman et al., 2020; Lee et al., 2021). Our research presents a broad range of insights into the neurogenomic techniques used to decode brain physiology and pathophysiology (NDDs and psychiatric disorders). Specifically, this research topic included functional assessments of genetic polymorphisms and epigenetic studies using patient genome data or polygenic risk scores (PRSs) and comprehensive transcriptome studies using brain disease-related mouse models.

Firstly, studies discussing the discovery of single nucleotide polymorphisms (SNPs) or PRSs associated with brain diseases and their pharmacological effects were introduced. Wei et al. demonstrated that the rs187406 C>T polymorphism in the endothelin receptor type A gene (*EDNRA*) increased the susceptibility to large artery atherosclerotic stroke (Wei et al.). Iino et al. identified schizophrenia-associated SNPs in the aldo-keto reductase family 1 member A1 gene (*AKR1A1*). Although one of the SNPs located on the first nucleotide of the exon is a silent mutation, it results in exon skipping, thereby decreasing *AKR1A1* expression and functional activity (Iino et al.). Kasai et al. showed that short tandem repeats (STRs) in the cannabinoid receptor 1 gene (*CNR1*) were associated with analgesic requirements post-orthognathic cosmetic surgery (Kasai et al.). Blasi et al. showed that the rs363043 C>T SNPs of the synaptosomal-associated protein 25 (*SNAP25*) gene in children with borderline intellectual disability had reduced perceptual reasoning index and intelligence quotient (IQ) scores (Blasi et al.). In a cohort study of the general Japanese population, Takahashi et al. reported that the adult body mass index (BMI)-PRSs are associated with working memory in children (Takahashi et al.). This association was found to be related to reduced cortical thickness in the left inferior parietal lobe and left superior serratus gyrus. The abovementioned studies provide novel insights into the genetic factors associated with brain dysfunction, such as SNPs, STRs, and PRSs.

OPEN ACCESS

Edited and reviewed by:
Sarah H Elsea,
Baylor College of Medicine,
United States

***Correspondence:**
Noriyoshi Usui
usui@anat1.med.osaka-u.ac.jp

Specialty section:
This article was submitted to Neurogenomics, a section of the journal Frontiers in Genetics

Received: *12 February 2022*
Accepted: *23 March 2022*
Published: *11 April 2022*

Citation:
Toriumi K, Wang G-Z, Berto S and Usui N (2022) Editorial: Decoding Brain Function Through Genetics. Front. Genet. 13:874350. doi: 10.3389/fgene.2022.874350

Secondly, two reports that evaluated DNA methylation as an epigenetic alteration were introduced. Fujisawa et al. reported a relationship between genome-wide methylation differences and brain structure in the development of attention-deficit hyperactivity disorder (ADHD) (Fujisawa et al.). Their study identified 61 methylation sites in monozygotic twins discordant for ADHD and showed increased methylation rates in the sortilin-related VPS10 domain-containing receptor 2 gene (*SORCS2*). Furthermore, the methylation rate in *SORCS2* was associated with a decrease in the gray matter volume in the precentral and posterior orbital gyri, which are both involved in language processing and emotional control. Nishitani et al. defined the aging rate based on DNA methylation frequency and analyzed the relationship between reproductive efforts (parity status, number of deliveries, motherhood period, and cumulative motherhood period) and the aging rate (Nishitani et al.). They showed that increased reproductive effort was associated with slower aging in mothers with four or fewer children. Nishitani et al. reported that increased left precuneus gray matter volume mediated the relationship between parity status and aging deceleration, suggesting that mothers may benefit from aging deceleration due to structural changes in the precuneus. Thus, therapeutic and preventive strategies targeting alterations can be pursued by identifying epigenetic alterations related to disease onset. Epigenomics is important in understanding the onset of psychiatric disorders that are strongly influenced by environmental factors.

Finally, three reports on animal models of brain disorders using genetic analysis were introduced. Usui et al. reported that postnatal mice exposed to stress in their early life demonstrated social deficits, anxiety-like behavior, and abnormalities in cell architecture, such as a decrease in the number of neurons in the prefrontal cortex (Usui et al.). RNA sequencing identified 15 genes related to transcriptional regulation, stress, and synaptic signaling in the stressed group, indicating that these changes caused behavioral deficits. Lim et al. found increased neuropilin-1 (*NRP1*) expression in the brain and blood of model mice with Alzheimer's disease (AD) and the postmortem brain tissue of patients with AD (Lim et al.). Lim et al. suggested that the increased *NRP1* expression in the elderly may be responsible for the increased severity of severe acute respiratory syndrome coronavirus 2 (SARS-CoV-2) infection, suggesting that this gene is involved in the infectivity of the SARS-CoV-2 virus. Xie et al. reported that heterozygous mice with a serotonin transporter binding protein, N-ethylmaleimide-sensitive factor (Nsf), showed autism spectrum disorder-like behaviors and impairments of synaptic plasticity and glutamate-serotonin neurotransmission in the hippocampus (Xie et al.). Next-generation sequencing is a powerful tool that can provide comprehensive transcriptome analysis that will assist researchers in exploring the molecular mechanisms underlying brain diseases. Future studies combined with those from the latest single-cell transcriptome and epigenomics (Armand et al., 2021; Diez and Sepulcre, 2021) will provide more in-depth knowledge on the molecular and cellular mechanisms of brain diseases and dysfunction.

In conclusion, decoding the brain function through genetic analysis is in its nascent stages. Further technological developments will deepen our understanding of the role of genomics in brain function while simultaneously adding to its complexity. Currently, there is a gap between genomic observations and actual brain function. Therefore, future studies should take up the challenge of exploring the undiscovered brain functions. However, the diversity of the papers on this research topic leads us to believe that genetics has great potential to enhance our understanding of brain function.

AUTHOR CONTRIBUTIONS

KT: Writing - Original Draft, Writing - Review and Editing, Funding acquisition. G-ZW: Writing - Review and Editing. SB: Writing - Review and Editing. NU: Conceptualization, Writing - Original Draft, Writing - Review and Editing, Project administration, Supervision, Funding acquisition. All authors contributed to the article and approved the submitted version.

FUNDING

This work was supported by Japan Society for the Promotion of Science (JSPS) Program for Advancing Strategic International Networks to Accelerate the Circulation of Talented Researchers (S2603) to KT, SB, and NU; JSPS Grant-in-Aid for Scientific Research (C) (16H05380) to KT, (18K06977) to KT, (20K06872) to NU; JSPS Grant-in-Aid for Early-Career Scientists (18K14814) to NU; Kanae Foundation for the Promotion of Medical Science to KT; Uehara Memorial Foundation to NU; Takeda Science Foundation to NU; SENSHIN Medical Research Foundation to KT, and NU; Osaka Medical Research Foundation for Intractable Diseases to NU; Public Health Science Foundation to NU; Eli Lilly Japan Research Grant to NU.

REFERENCES

Armand, E. J., Li, J., Xie, F., Luo, C., and Mukamel, E. A. (2021). Single-Cell Sequencing of Brain Cell Transcriptomes and Epigenomes. *Neuron* 109, 11–26. doi:10.1016/j.neuron.2020.12.010

Bogdan, R., Hyde, L. W., and Hariri, A. R. (2013). A Neurogenetics Approach to Understanding Individual Differences in Brain, Behavior, and Risk for Psychopathology. *Mol. Psychiatry* 18, 288–299. doi:10.1038/mp.2012.35

Diez, I., and Sepulcre, J. (2021). Unveiling the Neuroimaging-Genetic Intersections in the Human Brain. *Curr. Opin. Neurol.* 34, 480–487. doi:10.1097/wco.0000000000000952

Jourdon, A., Scuderi, S., Capauto, D., Abyzov, A., and Vaccarino, F. M. (2021). PsychENCODE and beyond: Transcriptomics and Epigenomics of Brain Development and Organoids. *Neuropsychopharmacology* 46, 70–85. doi:10.1038/s41386-020-0763-3

Kang, H. J., Kawasawa, Y. I., Cheng, F., Zhu, Y., Xu, X., Li, M., et al. (2011). Spatio-temporal Transcriptome of the Human Brain. *Nature* 478, 483–489. doi:10.1038/nature10523

Lee, P. H., Feng, Y. A., and Smoller, J. W. (2021). Pleiotropy and Cross-Disorder Genetics Among Psychiatric Disorders. *Biol. Psychiatry* 89, 20–31. doi:10.1016/j.biopsych.2020.09.026

Pattabiraman, K., Muchnik, S. K., and Sestan, N. (2020). The Evolution of the Human Brain and Disease Susceptibility. *Curr. Opin. Genet. Dev.* 65, 91–97. doi:10.1016/j.gde.2020.05.004

Smoller, J. W., Andreassen, O. A., Edenberg, H. J., Faraone, S. V., Glatt, S. J., and Kendler, K. S. (2019). Psychiatric Genetics and the Structure of Psychopathology. *Mol. Psychiatry* 24, 409–420. doi:10.1038/s41380-017-0010-4

Snyder, M. P., Gingeras, T. R., Moore, J. E., Weng, Z., Gerstein, M. B., Ren, B., et al. (2020). Perspectives on ENCODE. *Nature* 583, 693–698. doi:10.1038/s41586-020-2449-8

Yuste, R., Hawrylycz, M., Aalling, N., Aguilar-Valles, A., Arendt, D., Armañanzas, R., et al. (2020). A Community-Based Transcriptomics Classification and Nomenclature of Neocortical Cell Types. *Nat. Neurosci.* 23, 1456–1468. doi:10.1038/s41593-020-0685-8

Conflict of Interest: The authors declare that the research was conducted in the absence of any commercial or financial relationships that could be construed as a potential conflict of interest.

frontiers in Neuroscience

BRIEF RESEARCH REPORT
published: 26 August 2021
doi: 10.3389/fnins.2021.715048

SNAP-25 Single Nucleotide Polymorphisms, Brain Morphology and Intelligence in Children With Borderline Intellectual Functioning: A Mediation Analysis

Valeria Blasi[1], Elisabetta Bolognesi[1], Cristian Ricci[2], Gisella Baglio[1], Milena Zanzottera[1], Maria Paola Canevini[3,4], Mauro Walder[5], Monia Cabinio[1], Michela Zanette[1], Francesca Baglio[1], Mario Clerici[1,6]† and Franca Rosa Guerini[1]†*

[1] IRCCS Fondazione Don Carlo Gnocchi ONLUS, Milan, Italy, [2] Pediatric Epidemiology, Department of Pediatrics, Medical Faculty, Leipzig University, Leipzig, Germany, [3] Epilepsy Center, ASST S. Paolo and S. Carlo Hospital, Milan, Italy, [4] Department of Health Sciences, University of Milan, Milan, Italy, [5] Child Neuropsychiatry Unit – ASST S. Paolo and S. Carlo Hospital, Milan, Italy, [6] Department of Pathophysiology and Transplantation, University of Milan, Milan, Italy

Borderline intellectual functioning (BIF) is a multifactorial condition in which both genetic and environmental factors are likely to contribute to the clinical outcome. Abnormal cortical development and lower IQ scores were shown to be correlated in BIF children, but the genetic components of this condition and their possible connection with intelligence and brain morphology have never been investigated in BIF. The synaptosomal-associated protein of 25 kD (SNAP-25) is involved in synaptic plasticity, neural maturation, and neurotransmission, affecting intellectual functioning. We investigated *SNAP-25* polymorphisms in BIF and correlated such polymorphisms with intelligence and cortical thickness, using socioeconomic status and environmental stress as covariates as a good proxy of the variables that determine intellectual abilities. Thirty-three children with a diagnosis of BIF were enrolled in the study. *SNAP-25* polymorphisms rs363050, rs363039, rs363043, rs3746544, and rs1051312 were analyzed by genotyping; cortical thickness was studied by MRI; intelligence was measured using the WISC-III/IV subscales; environmental stressors playing a role in neuropsychiatric development were considered as covariate factors. Results showed that BIF children carrying the rs363043(T) minor allele represented by (CT + TT) genotypes were characterized by lower performance Perceptual Reasoning Index and lower full-scale IQ scores (p = 0.04) compared to those carrying the (CC) genotype. This association was correlated with a reduced thickness of the left inferior parietal cortex (direct effect = 0.44) and of the left supramarginal gyrus (direct effect = 0.56). These results suggest a link between *SNAP-25* polymorphism and intelligence with the mediation role of brain morphological features in children with BIF.

Keywords: genetics, brain imaging, learning disabilities, neural plasticity, rehabilitation, child psychiatry

OPEN ACCESS

Edited by:
Noriyoshi Usui,
Osaka University, Japan

Reviewed by:
Henrik Rasmussen,
Sankt Hans Hospital, Denmark
Guang-Zhong Wang,
Shanghai Institutes for Biological Sciences (CAS), China

****Correspondence:***
Mario Clerici
mclerici@dongnocchi.it

† These authors have contributed equally to this work and share last authorship

Specialty section:
This article was submitted to Neurogenomics, a section of the journal Frontiers in Neuroscience

Received: *26 May 2021*
Accepted: *04 August 2021*
Published: *26 August 2021*

Citation:
Blasi V, Bolognesi E, Ricci C, Baglio G, Zanzottera M, Canevini MP, Walder M, Cabinio M, Zanette M, Baglio F, Clerici M and Guerini FR (2021) SNAP-25 Single Nucleotide Polymorphisms, Brain Morphology and Intelligence in Children With Borderline Intellectual Functioning: A Mediation Analysis. Front. Neurosci. 15:715048. doi: 10.3389/fnins.2021.715048

INTRODUCTION

Borderline intellectual functioning (BIF) is a condition characterized by a mental ability at the border between normal intellectual functioning and intellectual disability, with an Intellectual Quotient (IQ) within 1 and 2 standard deviations below the mean of the normal curve of the distribution of intelligence that impacts on adaptive abilities (Salvador-Carulla et al., 2013; Peltopuro et al., 2014). In primary school age, children with BIF are burdened with difficulties in school achievements due to learning difficulties in more than one executive functions domain, such as attention, concentration, planning, and inhibition of impulsive responses, as well as memory and motor skill limitations (Alloway, 2010; Vuijk et al., 2010; Salvador-Carulla et al., 2013; Peltopuro et al., 2014; Contena and Taddei, 2017). Furthermore, limitations in social skills, emotional competencies, and behavioral problems affect the social participation of these children (Baglio et al., 2016; Predescu et al., 2020). Children with BIF are thus at high risk of school failure and dropout (Fernell and Ek, 2010), and are more likely to develop psychiatric problems in adulthood (Douma et al., 2007; Emerson et al., 2010; Gigi et al., 2014; Hassiotis, 2015; Hassiotis et al., 2019). Potential risk factors for BIF include low weight at birth, low socioeconomic status, maltreatment, and high levels of maternal stress. However, the negative social condition does not explain all the BIF cases and their development across the life span.

Intelligence is one of the most heritable behavioral traits (Deary et al., 2009). Intelligence is nevertheless also a malleable entity under the influence of environmental conditions (Sauce and Matzel, 2018). As a logical consequence of this, intellectual disability, as well as the development of psychiatric disorders were suggested to be the result of an interaction between social environment and genetic background (Rizzi et al., 2012). Finally, a multifactorial and multigenic set may be responsible for BIF development (Ropers, 2008).

An important role in intelligence is likely played by the synaptosomal-associated protein of 25 kD *(SNAP-25)* gene, which is located on chromosome 20p12-p11.2, an area of previous suggestive linkage to intelligence (Posthuma et al., 2005). SNAP-25 protein takes part in the regulation of calcium-dependent synaptic vesicles exocytosis, ensuring the efficient release of neurotransmitters and the propagation of action potentials. The key role of SNAP-25 is to initiate exocytosis through the formation of a SNARE complex (Südhof, 2015). The SNARE complex is therefore involved in the processes of learning, locomotion, memory formation, and ultimately the normal functioning of the brain as a whole. *SNAP-25* single nucleotide polymorphisms (SNPs) were associated with variation of performance IQ in non-clinical, population based samples (Gosso et al., 2006, 2008). Interestingly, polymorphisms in the *SNAP-25* gene, as well as an altered expression of the SNAP-25 protein, are also associated with abnormal behavioral phenotype both in humans (Thompson et al., 2003; Guerini et al., 2011; Braida et al., 2015; Liu et al., 2017) and in animal models (Bruno et al., 2006; Gunn et al., 2011). Finally, evidence derived from multiple organisms suggested that SNAP-25 is involved in the process of axonal growth and synaptic plasticity (Martinez-Arca et al., 2001). Therefore, any variation of SNAP-25 protein expression may interfere with neural maturation and neurotransmission, affecting intellectual functioning.

Neural plasticity during development was investigated with neuroimaging techniques that evaluated longitudinal changes in cortical thickness, a parameter influenced by genetics, which modulates intelligence (Brans et al., 2010). Notably, a number of results show how differences in a distributed network that include frontal and parietal cortices predict individual profiles in intelligence (Jung and Haier, 2007). Earlier data from our group, in particular, showed the presence of significant differences in cortical volume in areas belonging to this network in children with BIF and the relationship of this difference with intelligence (Baglio et al., 2014).

The aim of our work was to examine the complex relation between *SNAP-25* and cortical thickness in determining intelligence. To accomplish this aim, we selected four SNPs located in the intron region which were proved to be involved in both typical (Gosso et al., 2006, 2008) and atypical development (Barr et al., 2000; Guerini et al., 2011; Braida et al., 2015). We first identified the presence of possible correlations between the *SNAP-25* rs363050, rs363039, rs363043, rs3746544, and rs1051312 genetic polymorphisms with brain area morphology, and IQ scale in 33 children with BIF. Next, we conducted a mediation analysis in which genetic polymorphisms, brain area morphology and IQ scale were modeled in a comprehensive fashion. An association of the *SNAP-25* rs363043 polymorphism with PRI as well as with IQ scores was reported to be mediated by brain cortical thickness in the inferior parietal lobule.

MATERIALS AND METHODS

Patients Enrolled in the Study

Children were recruited from the Child and Adolescent Neuropsychiatry Unit of IRCCS Don Carlo Gnocchi Foundation and the ASST S. Paolo and S. Carlo Hospital; both in Milan, Italy. The sample included thirty-three children (6–11 years old) with BIF, i.e., a Full-Scale Intelligence Quotient (FSIQ) score in the borderline range, and clinical criteria, that attend primary mainstream school. The clinical evaluation consisted of a detailed medical history and social skills of the child and of his/her family and clinical observations reports.

Excluded criteria were: (1) ADHD, autism spectrum disorder, or other major neuropsychiatric disorders; (2) epilepsy, traumatic brain injury, brain malformation, infectious disease and other neurological conditions involving the central nervous system, and perinatal complications such as prematurity or other adverse events; (3) genetic syndromes such as Down syndrome or Fragile X syndrome and (4) systemic diseases such as diabetes or dysimmune disorders; and (5) current or past substance abuse (psychoactive drugs, psycho stimulants, neuroleptics, antidepressants, benzodiazepines, and antiepileptic drugs).

Informed consent was obtained from all parents/legal guardians prior to inclusion in the study. The study was conducted according to the guidelines of the Declaration of

Helsinki and was approved by the institutional review board of the Don Carlo Gnocchi ONLUS Foundation, Milan (Protocol nr: 06_18-05-2016).

Socioeconomic status was assessed by the SES questionnaire, an integrated measure of parent's education grade and occupation, widely used in research to identify the child/family social standing. The socio-cultural levels are low (range 8–19), middle-low (range 20–29), middle (range 30–39), middle-high (range 40–54) and high (range 55–66) (Hollingshead, 2011). Environmental stress was defined according to the ESCL, a list of V-codes from DSM-5, and Z-codes from ICD-10, to detect relational, neglect, physical, sexual and/or psychological abuse, educational and occupational, housing and economic, social exclusion or rejection problems, plus the presence of the following three conditions: social services intervention, major psychiatric diagnosis and/or substance abuse within the family members. The scoring is binary with a 0 (absence) or 1 (presence) attribution to each item, with a total score ranging from 0 to 24 (Blasi et al., 2020).

Neuropsychological Evaluation

The neuropsychological evaluation included: (1) the WISC –III (Orsini and Picone, 2006), with the exception of nine children evaluated with the WISC-IV (Orsini et al., 2012) that assess the global intellectual functioning and the cognitive profile; (2) the Socioeconomic Status (SES) (Hollingshead, 2011), to evaluate the family education level and financial well-being; (3) the Environmental Stress Check List (ESCL), a tool to detect all possible sources of environmental stress (Blasi et al., 2020) to which the children were exposed to.

The WISC-III provides three principal scores: the FSIQ, the Verbal IQ (VIQ), and the Performance (PIQ); in addition, to better describe the cognitive profile, it is possible to calculate four indices: the Verbal Comprehension Index (VCI), the Perceptual Organization Index (POI), the Freedom from Distractibility Index (FDI) and the Processing Speed Index (PSI). The WISC–IV provides an FSIQ and a four-index framework similar to that of the WISC III: the VCI, the Perceptual Reasoning Index (PRI), the Working Memory Index (WMI), and the PSI. The increased emphasis on fluid reasoning abilities and on working memory, with the introduction of new subtests, has resulted in the renaming of the POI as the Perceptual Reasoning Index (PRI) and the FDI as the Working Memory Index (WMI) respectively. Moreover, a high correlation between FSIQ, VCI, and PRI of both versions is demonstrated (FSIQ-FSIQ = 0.89; VCI-VCI = 0.88; POI-PRI = 0.72) (Flanagan and Kaufman, 2012). Finally, all indices are expressed in the standard score (Mean = 100; SD = 15). For the present study, we will refer to both POI and PRI indices with the acronym PRI and to both FDI and WMI as WMI. All the data were age-corrected when measured.

MRI Acquisition

All subjects underwent a magnetic resonance imaging (MRI) evaluation. MRI was performed on a 1.5 T Siemens Magnetom Avanto (Erlangen, Germany) scanner equipped with a 12-channels head coil. The acquisition included: (1) a 3D T1-weighted Magnetization Prepared Rapid Gradient-Echo (MPRAGE) image, (repetition time (TR)/echo time (TE) = 1900/3.37 ms, Filed of View (FoV) = 192 × 256 mm^2, voxel size = 1 mm isotropic, 176 axial slices); (2) two conventional anatomical sequences (axial PD/T2 and coronal FLAIR) to exclude gross brain abnormalities.

MRI Data Analysis

The 3D-T1 images were segmented and parcellated using FreeSurfer version 5.3[1] into 68 cortical areas (34 for each hemisphere) according to the Desikan atlas (Desikan et al., 2006). Furthermore, the FreeSurfer automatic labeling process was used to extract seven subcortical regions per hemisphere (thalamus, caudate, putamen, pallidum, and nucleus accumbens, amygdala, and hippocampus) and the brain stem for a total of 82 parcels. The quality of recon-all parcelation was assessed in each subject according to ENIGMA guidelines[2] for cortical and subcortical areas.

Mean thickness was then computed for each cortical area, and mean volume for each subcortical region.

Genetic Analyses

Single nucleotide polymorphisms typing: Three *SNAP-25* SNPs: rs363050, rs363039, and rs363043 located within intron 1, in a region of about 13.8 kb, known to affect transcription factor binding sites (Gosso et al., 2008) as well as two *SNAP-25* SNPs: rs3746544 and rs1051312 located in the 3′ untranslated region predicted as a binding site of miRNAs (endogenous non-coding RNA regulators of gene activity at the post-transcriptional level) (Ambros, 2004; Bartel, 2004) were investigated; these SNPs have previously been associated with ADHD (Barr et al., 2000). Genomic DNA was isolated from peripheral blood mononuclear cells by phenol-chloroform extraction. SNPs were typed using the Taqman SNP Genotyping Assays (Applied Biosystems by Life Technologies, Foster City, CA, United States) on an ABI PRISM 7000 Sequence Detection System. For rs363039, rs363043, rs363050, and rs3746544, respectively, the C_327976_10, C_2488346_10, C_329097_10 and C_27494002_10 Human Pre-Designed Assays (Applied Biosystems by Life Technologies) were used. The restriction enzyme polymorphism rs1051312 was genotyped by *Dde*I digestion as previously described (Barr et al., 2000).

Statistical Analysis

Age, socioeconomic status, environmental stress index, the total score, and the subscales of the Wechsler Intelligence Scale for Children were described by median and 5th to 95th centile range. *SNAP-25* polymorphisms were described by frequencies (**Table 1**).

Exact Hardy Weinberg analysis was applied to verify if *SNAP-25* SNPs genotype distribution among children with BIF were in Equilibrium (HWE).

SNAP-25 Linkage disequilibrium was calculated by SHEsis (Shi and He, 2005) by adding data from 615 healthy control

[1] https://surfer.nmr.mgh.harvard.edu

[2] http://enigma.ini.usc.edu/enigma-vis

TABLE 1 | Median, 5th–95th centiles of age, socioeconomic status, environmental stress and psychometric scores.

	Overall, *N* = 33	**Boys, *N* = 19 (57.6%)**	**Girls, *N* = 14 (42.4%)**
Age (years)	9.0 (6.0,10.0)	8.0 (6.0,10.1)	9.0 (6.0,10.0)
SES	22.0 (14.0,45.2)	22.0 (15.6,51.0)	22.0 (14.0,32.7)
ESCL	4.0 (0.6,8.0)	4.0 (1.0,8.2)	2.5 (0.0,8.0)
WISC-III-IV			
FSIQ	78.0 (62.8,85.4)	80.0 (69.1,86.2)	76.0 (62.3,85.0)
VCI	80.0 (57.0,94.8)	84.0 (68.2,94.4)	78.5 (57.3,89.5)
PRI	84.0 (77.2,104.2)	85.0 (77.8,103.8)	83.0 (74.9,98.9)
WMI	75.0 (63.0,92.2)	75.0 (61.8,94.6)	76.5 (63.0,91.0)
PSI	77.0 (60.8,95.2)	74.0 (58.7,94.6)	77.3 (64.0,95.0)
SNAP-25			
rs363039	GG (11), GA + AA (22)	GG (7), GA + AA (12)	GG (4), GA + AA (12)
rs363043	CC (16), CT + TT (17)	CC (8), CT + TT (11)	CC (8), CT + TT (6)
rs363050	AA (14), AG + GG (19)	AA (8), AG + GG (11)	AA (6), AG + GG (10)
rs3746544	TT (11), TG + GG (22)	TT (6), TG + GG (13)	TT (5), TG + GG (9)
rs1051312	TT (25), TC + CC (8)	TT (16), TC + CC (3)	TT (9), TC + CC (5)

Frequencies were reported for SNAP-25 polymorphisms.
SES, socioeconomic status; ESCL, environmental stress check list score; WISC-III-IV, Wechsler Intelligence Scale for Children; FSIQ, Full-Scale Intelligence Quotient; VCI, Verbal Comprehension Index; PRI, Perceptual Reasoning Index; WMI, Working Memory index; PSI, Processing Speed Index.

from a previous study (Guerini et al., 2014). Haplotype correlation with IQ profile was calculated by regression analysis, adjusting by gender, SES, and ESCL, using PLINK software (Purcell et al., 2007).

A causal network approach was applied to investigate the association between *SNAP-25* SNPs, MRI morphological data, and WISC-III-IV subscales (FSIQ, VCI, PRI, WMI, PSI) (Agler and De Boeck, 2017). Specifically, we considered a network in which *SNAP-25* SNPs may act on psychometric scores through a direct relation and by an indirect pathway in which morphological data, measured by MRI, may act as a mediator. Firstly, to reduce skewness, all outcome data were standardized and transformed in normal ranks using Blom's transformation (Gumbel, 1959). Afterward, models bearing the direct association (*SNAP-25* to WISC III-IV subscale) and two indirect associations (*SNAP-25* to brain morphology and brain morphology to WISC III-IV subscale), were applied to investigate the above causal pathway. Those models were based on a Kernel not parametric regression adjusted for sex, socioeconomic status, and Environmental Stress Check List score (ESCL). Regression coefficients were estimated and tested for significance by a procedure based on 5,000 bootstrap replications. To take into account numerous comparisons and to manage the related false discovery rate, the threshold *P*-value to detect significant associations was set according to the Benjamini–Hochberg procedure (Chen et al., 2017). Briefly, this method was chosen, instead of more conservative approaches, because of the small sample size and the need to reduce the false-negative rate (reduce the type-II error). Heat maps of statistically significant results were the graphical tool chosen to represent multiple associations between *SNAP-25* SNPs, MRI morphological data, and psychometric scores.

Afterward, according to the above explorative analyses, a mediation analysis was used to investigate the role of brain morphology in the association between *SNAP-25* SNPs and psychometric scores. In the mediation analyses, the direct and indirect effects were reported as standardized and rescaled regression coefficients. The total effect of *SNAP-25* SNPs on psychometric scores was computed as $a + b \times c$ and as $b \times c$ as the total and indirect effects respectively. Here the term "a" was the slope of the direct effect, while the terms "b" and "c" were the slopes of the two sides of the indirect effects, the association between single nucleotide polymorphism with MRI data, and the association between MRI data and the psychometric scores, respectively. Standardized coefficients were reported for all the associations. All statistical tests were two-tailed and the type-I error rate was set according to the Benjamini–Hochberg procedure for the single Kernel non-parametric models while an ordinary type-I error rate of 5% ($\alpha = 0.05$) was considered for the mediation analyses. The NP and the LAVAAN packages of the R software vers. 3.6. were used to conduct the kernel non-parametric regressions and the mediation analysis, respectively.

Given the small sample size, *a priori* and *a posteriori* power calculations were performed. In particular, the statistical power of Kernel non-parametric regression was investigated using the MultNonParam package of the R software vers. 3.6 while the statistical power of the mediation analysis was investigated using the pwr package of the R software vers. 3.6. According to this evaluation and considering the current sample size and type-I error rate used, medium to large standardized effect size in the range of 0.3–0.5, could be detected with a type-II error rate below 20% (Statistical power above 80%) for those two methods. According to statistical power, the current study could be defined as explorative.

RESULTS

SNAP-25 Polymorphisms Association With Neuropsychological Scores

The sample was composed of 19 boys and 14 girls with a median age of 9 years (5th to 95th centile 6–10 years old). Age, socioeconomic status, IQ evaluation scores, and *SNAP-25* polymorphisms were similar in boys and girls; the ESCL score, on the other hand, was lower in girls compared to boys, although not significantly ($p = 0.3964$). All WISC-III-IV scores had a median lower than 85, below 1 standard deviation with respect to the normal population (**Table 1**).

Initial results showed that *SNAP-25* rs363039, rs363043, rs363050, rs3746544, and rs1051312 SNPs genotype distribution was in HWE ($p = 0.96$; $p = 0.05$; $p = 0.07$; $p = 0.71$; $p = 0.57$ respectively) (**Figure 1**). The *SNAP-25* genetic patterns of distribution in BIF children, clustered into carriers of the minor allele (i.e., heterozygous + homozygous for minor) and carriers of the homozygote major allele, were analyzed next in relationship with FSIQ, VCI, PRI, WMI, and PSI scores (**Figure 1**).

Analysis of the relation between *SNAP-25* polymorphisms and IQ scores showed the presence of a significant association between the rs363043 (T) minor allele represented by (CT + TT)

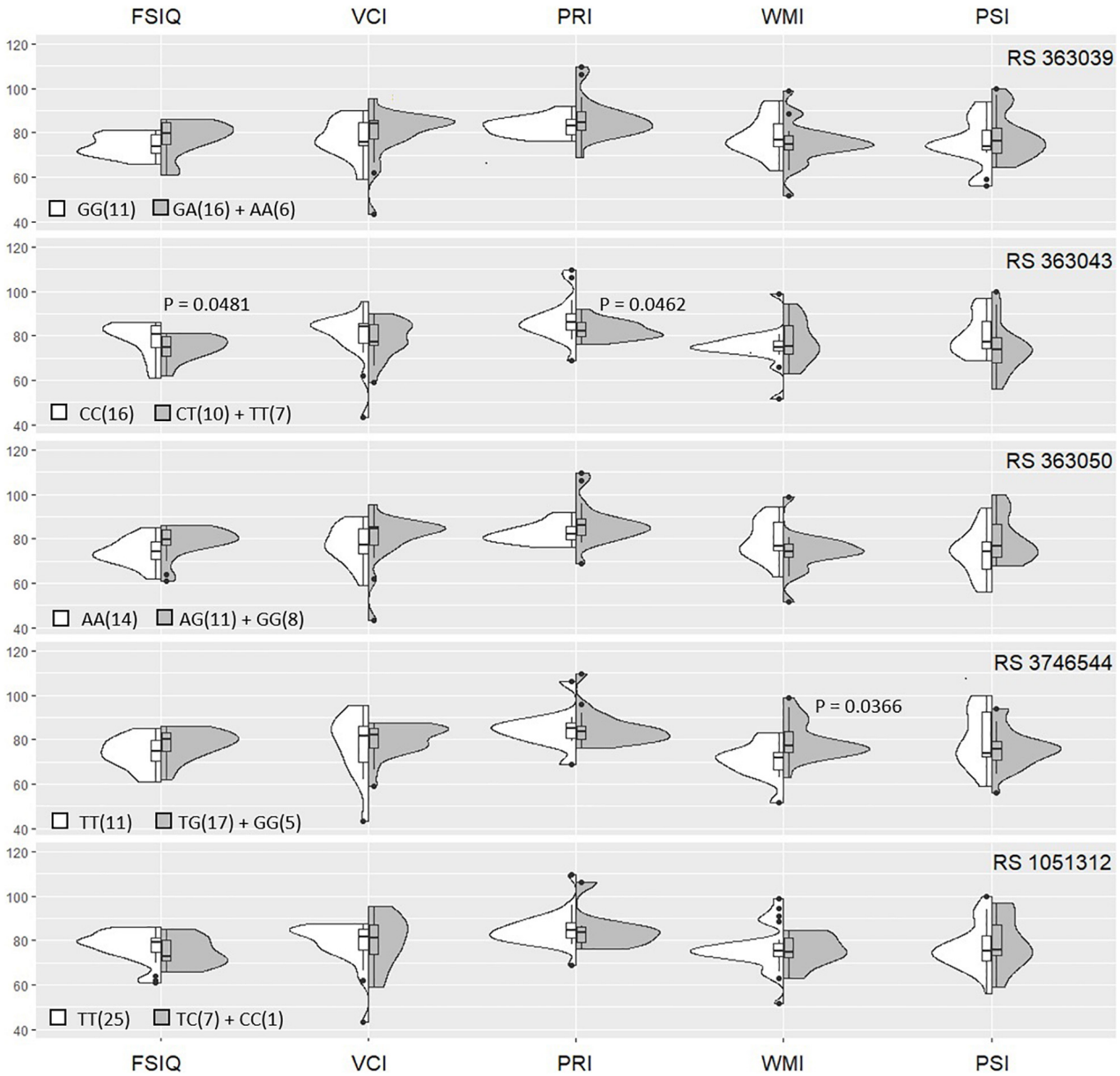

FIGURE 1 | Violin plots of Kernel's smoothed distributions of WISC-III/IV scores by *SNAP-25* genotypes. The box plots present the distribution of each IQ score (median and interquartile range) relatively to the genotype distribution. The "violin" area indicate the percentage of children with BIF for each allele (in gray the minor allele and white the major allele).

genotypes and lower FSIQ and PRI scores ($p = 0.04$). Notably, additional results showed that the rs3746544 (TT) genotype was also significantly associated with reduced WMI scores ($p = 0.04$) (**Figure 1**).

SNAP-25 Haplotype Linkage Analyses

Linkage haplotype analyses were used to evaluate the linkage disequilibrium between *SNAP-25* variants, as well as to verify the presence of an association between the different haplotypes and FSIQ, VCI, PRI, WMI, and PSI scores. Haplotype analysis evidenced, the presence of a linkage disequilibrium (LD) between: (1) rs363050 and rs363039 ($r2 > 0.3$); (2) rs363043 and rs363050 ($r2 = 0.24$); and (3) rs363043 and rs363039 ($r2 = 0.17$) and a linkage between rs3746544 and rs105312 polymorphisms ($r2 = 0.17$). Haplotype distributions were not significantly associated with IQ scores (data not shown).

MRI Parameters Mediators Between *SNAP-25* Polymorphisms and Intelligence

The relations between *SNAP-25* polymorphisms and MRI morphological data, along with the relations between MRI

morphological data from IQ evaluation were analyzed next. Results showed the presence of a number of associations between these features (**Supplementary Figures 1**, **2**). In particular, this exploratory association identified the cortical thickness in the left inferior parietal cortex as a possible mediator between rs363043 and PRI scores. Moreover, the thickness of the left supramarginal gyrus was suggested to act as a possible mediator between rs363043 and FSIQ. Finally, when considering the relation between the PRI score with the left inferior parietal cortex a significant variance of 21% was observed, whereas the relation between FSIQ with the left supramarginal gyrus resulted in an explained variance of 24%.

According to our mediation analyses, the association of the rs363043 polymorphism influenced the PRI score with a direct effect of 0.44. This association was mediated by a cortical thickness of the left inferior parietal by 3.1%. This means that a lower score of PRI associated with rs363043 (CT + TT) genotypes is directly related to a reduced cortical thickness. Similarly, the association of the rs363043 polymorphism with the FSIQ score had a direct effect of 0.56 and a mediated indirect effect of the cortical thickness of the left supramarginal gyrus of 3.5%. This means that the lower FSIQ score associated with the rs363043 (CT + TT) genotypes is directly related to a reduced cortical thickness of the left supramarginal gyrus. Results of the mediation analyses are presented in **Figure 2**.

DISCUSSION

In the present study, we show that *SNAP-25* rs363043(T) minor allele represented by (CT + TT) genotypes are associated with lower PRI scores in children with BIF; such association was found to be mediated by the left inferior parietal cortex thickness: lower thickness mediates lower PRI scores. Notably, the same children carrying the rs363043 (CT) or (TT) genotypes showed a lower full-scale IQ score, and this association was mediated by the cortical thickness in the left supramarginal gyrus.

The *SNAP-25* SNP rs363043, along with other polymorphisms on the *SNAP-25* gene, has previously been associated with intelligence in a normal population of Dutch children, adolescents, and adults (Gosso et al., 2006, 2008). In that case, though, the rs363043 (T) allele was associated with higher Verbal and performance IQ. Differences in the populations that have been analyzed, as well as in environmental components, might explain these discrepant results. Specifically, in the previous work (Gosso et al., 2008) the authors studied a population with an average IQ while we analyzed a group of BIF children belonging to a low socioeconomic status; importantly, the effect of several environmental stressors was considered as well in our analyses.

The interplay between genetic and environmental factors is complex and most likely both these factors have an important impact on individual differences in IQ (Sauce and Matzel, 2018). In the attempt to consider both aspects, we designed a model that includes the socioeconomic status and environmental stress as covariates; we believe this approach to be a good proxy of the diverse variables that determine intellectual abilities.

The *SNAP-25* rs363043 polymorphism herein reported is a (non) coding variant within the intron 1 of the *SNAP-25* gene that was shown to be involved in the regulation of SNAP-25 protein expression (Gosso et al., 2006). SNAP-25 protein is differentially expressed in the brain and is primarily present in the cerebral cortex, cerebellum, hippocampus, and caudate[3]. Notably, chronic reduction of SNAP-25 expression was shown to affect behavior in animal models. Thus, the coloboma mouse model, characterized by halved SNAP-25 levels (Hess et al., 1992), displays a hyperactive phenotype (Hess et al., 1992), associated with abnormal thalamic spike-wave discharges (Hess et al., 1995; Zhang et al., 2004; Faraone et al., 2005; Russell, 2007). Similarly, juvenile SNAP-25 heterozygous mice display moderate hyperactivity, which disappears in the adult animals, as well as impaired associative learning and memory, which persist in adulthood (Corradini et al., 2014).

Multiple studies have shown that different *SNAP-25* SNPs are associated with related traits of autism (Guerini et al., 2011) and ADHD (Forero et al., 2009; Braida et al., 2015), as well as with working memory ability (Söderqvist et al., 2010; Gao et al., 2015), short-/long-term memory and visual attention (Golimbet et al., 2010), and intellectual disability (Rizzi et al., 2012), These observations can be explained by the fact that the markers studied here are located close to a locus linked with behavioral and cognitive functions. A genetic linkage disequilibrium effect, which would explain the involvement of different SNPs in the same *SNAP-25* genetic locus cannot be excluded either in our cohort of BIF children.

In the attempt to find an explanation for our results, we investigated if *SNAP-25* SNPs could influence differences in brain morphology, thus explaining the connection between genetics and IQ scores. Results showed the involvement of different areas in the left hemisphere. In particular, the left inferior parietal cortex and the left supramarginal gyrus were found to mediate between genetics and the PRI and the FSIQ respectively. The PRI is a measure of the non-verbal components of intelligence such as visuospatial and visuomotor abilities involved in the reasoning and solving of new problems, while FSIQ is a composite measure derived by all IQ scores relative to verbal and non-verbal abilities. Interestingly, we observed that the relationship between PRI and FSIQ and genetics was mediated by the inferior parietal cortex and the supramarginal gyrus, which are both parts of the inferior parietal lobule (IPL), a multimodal region, considered a hub for its great interconnectivity with several areas in the brain (Igelström and Graziano, 2017). Our results are in line with previous evidence showing how the IPL has a relevant role in multimodal information integration for higher-order cognitive functions such as abstraction and symbolization (Igelström and Graziano, 2017). Moreover, the IPL is part of the mirror neuron system (Rizzolatti and Craighero, 2004), which is involved in the visuomotor integration processing of gestures, relevant not only for action understanding but also for learning. In support of these data, previous results showed how multimodal rehabilitation interventions to improve the intellectual abilities

[3]https://www.proteinatlas.org/ENSG00000132639-SNAP25/tissue#top

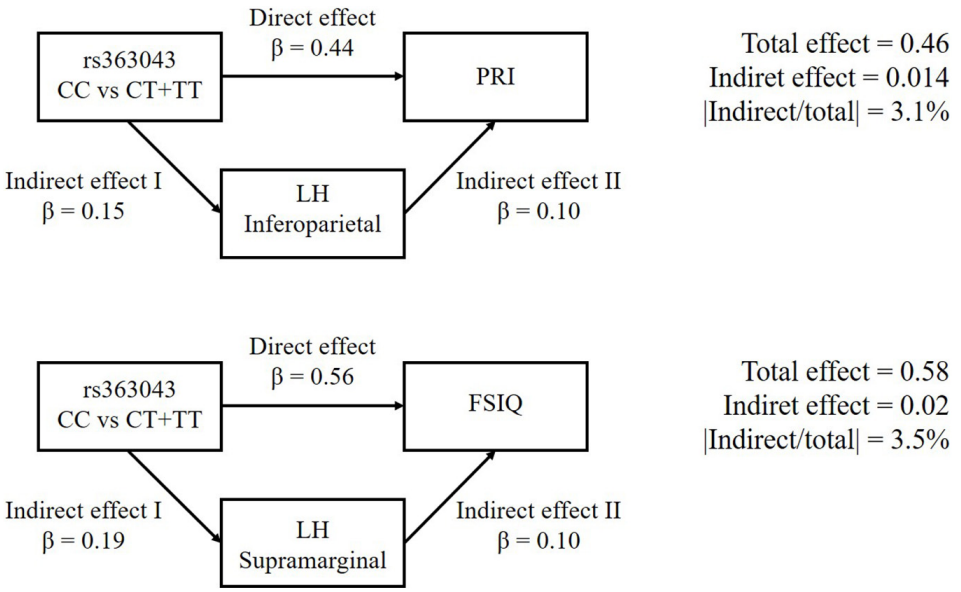

FIGURE 2 | Causal mediation analyses of *SNAP-25* rs363043 on PRI and FSIQ scores of the WISC-III/IV. The Left inferoparietal and supramarginal cortex thickness as the mediators for PRI and FSIQ, respectively. The Left inferior parietal and supramarginal cortex thickness were observed to be the mediators for PRI and FSIQ, respectively. The upper part of the figure shows the association of the rs363043 polymorphism with PRI score (direct effect = 0.44; contribution of the left inferior parietal = 3.1%). The lower part of the figure shows the association of the rs363043 polymorphism with FSIQ score (direct effect = 0.56; contribution of the left Supramarginal gyrus = 3.5%).

of children with BIF were more effective than single domain treatment (Blasi et al., 2020). Notably, our results can be seen in the light of previous studies showing how the variation in the cortical thickness of a distributed network comprising the dorsolateral prefrontal cortex, the inferior and superior parietal lobule, the anterior cingulate, and regions within the temporal and occipital lobes, predicts individual differences in the g-factor of intelligence (Jung and Haier, 2007). Specifically, a positive correlation between intelligence and cortical thickness in the IPL has been demonstrated in both children and adults (Menary et al., 2013).

Results herein are in line with previous studies showing that individual differences in frontal and parietal cortical thickness are strongly influenced by genetic components (Posthuma et al., 2002). The interplay between genetic and environment is complex and most likely both these factors have an important impact on individual differences in IQ (Sauce and Matzel, 2018). In our study, all children belonged to high-risk environments, had a medium to low SES, and were undergoing the effect of environmental stressors, all factors indirectly associated with low thickness in the frontoparietal network (Rosen et al., 2018). Our data suggest that the genetic background interacts with environmental factors in shaping brain configuration, thus determining the outcome of BIF.

Strength and Limitations

The current work has remarkable strengths. Firstly, we investigated determinants of intelligence in a sample of children with borderline intellectual functioning, a population of great clinical interest. Secondly, we adopted a rigorous research methodology resulting in reliable genetic polymorphisms, measures of intelligence, and brain morphology. Moreover, we used a comprehensive approach that included genetic, brain morphology, and intelligence outcomes as a whole, in an integrated analytical framework in which the issue of false discovery rate given by the limited sample size and large numbers of comparisons were taken into account using the appropriate statistical approaches. Finally, we would like to underline that this is the first study conducted in children with BIF that describes a multimodal association between *SNAP-25* polymorphisms, intelligence, and brain morphological features.

As usually is the case, though, this work also has limitations. Firstly, results were drawn from analyses performed in a limited number of children which could result in false-negative results. Moreover, the lack of a deeper analysis of the *SNAP-25* gene by next generation sequencing does not allow us to exclude that other polymorphisms could also be involved in shaping the intellectual functioning of children with BIF. Future studies evaluating the rs363043 polymorphism regulatory ability in larger cohorts of patients as well as an expression analysis of *SNAP-25* gene would be necessary.

Further, the observational nature of the study, the reduced sample size, and the skewness of the outcomes considered led to the use of non-parametric multivariate-adjusted models; this might have reduced the statistical power of statistical analyses. The use of Benjamini–Hochberg procedure to adjust for multiple comparisons and the use of bootstrap, nevertheless likely took care of this issue. Finally, without a control group, our study could be defined just as an explorative attempt. More rigorous observational studies, with larger sample size and possibly based

on a matched case-control design, should be performed to validate our results.

DATA AVAILABILITY STATEMENT

The data presented in this study are available on request from the corresponding author. The data are not publicly available due to privacy concerns.

ETHICS STATEMENT

The studies involving human participants were reviewed and approved by the Ethics Committees of the Don Gnocchi Foundation. Written informed consent to participate in this study was provided by the participants' legal guardian/next of kin.

AUTHOR CONTRIBUTIONS

FG, VB, MaC, and EB: conceptualization. FG, VB, CR, and EB: methodology. EB, MilZ, GB, and MoC: formal analysis. FG, VB, FB, EB, CR, MoC, and GB: investigation. FG and VB: data curation, writing—original draft preparation, and project administration. MPC, MW, and MicZ: resources. FG, VB, CR, and MaC: writing—review and editing. FG, VB, MaC, and FB: funding acquisition. All authors have read and agreed to the published version of the manuscript.

FUNDING

This study was funded by the Ministry of Health (Ricerca Corrente). The funder did not have any influence in the design, implementation, analysis or interpretation of the data in this study.

SUPPLEMENTARY MATERIAL

The Supplementary Material for this article can be found online at: https://www.frontiersin.org/articles/10.3389/fnins.2021.715048/full#supplementary-material

Supplementary Figure 1 | Association Heatmaps between *SNAP-25* genotypes and morphological brain features. Dark areas represents significant associations according to the Benjamini–Hochberg procedure. "All statistical significances are in the range between 0.05 and 0.01."

Supplementary Figure 2 | Association Heatmaps between WISC-III scores and morphological brain features. Dark areas represents significant associations according to the Benjamini–Hochberg procedure. "All statistical significances are in the range between 0.05 and 0.01."

REFERENCES

Agler, R., and De Boeck, P. (2017). On the interpretation and use of mediation: multiple perspectives on mediation analysis. *Front. Psychol.* 15:1984. doi: 10.3389/fpsyg.2017.01984

Alloway, T. P. (2010). Working memory and executive function profiles of individuals with borderline intellectual functioning. *J. Intellect. Disabil. Res.* 54, 448–456. doi: 10.1111/j.1365-2788.2010.01281.x

Ambros, V. (2004). The functions of animal microRNAs. *Nature* 431, 350–355. doi: 10.1038/nature02871

Baglio, F., Cabinio, M., Ricci, C., Baglio, G., Lipari, S., Griffanti, L., et al. (2014). Abnormal development of sensory-motor, visual temporal and parahippocampal cortex in children with learning disabilities and borderline intellectual functioning. *Front. Hum. Neurosci.* 8:806. doi: 10.3389/fnhum.2014.00806

Baglio, G., Blasi, V., Sangiuliano Intra, F., Castelli, I., Massaro, D., Baglio, F., et al. (2016). Social competence in children with borderline intellectual functioning: delayed development of theory of mind across all complexity levels. *Front. Psychol.* 7:1604. doi: 10.3389/fpsyg.2016.01604

Barr, C. L., Feng, Y., Wigg, K., Bloom, S., Roberts, W., Malone, M., et al. (2000). Identification of DNA variants in the SNAP-25 gene and linkage study of these polymorphisms and attention-deficit hyperactivity disorder. *Mol. Psychiatry.* 5, 405–409. doi: 10.1038/sj.mp.4000733

Bartel, D. P. (2004). MicroRNAs: genomics, biogenesis, mechanism, and function. *Cell* 116, 281–297. doi: 10.1016/s0092-8674(04)00045-5

Blasi, V., Pirastru, A., Cabinio, M., Di Tella, S., Laganà, M. M., Giangiacomo, A., et al. (2020). Early life adversities and borderline intellectual functioning negatively impact limbic system connectivity in childhood: a connectomics-based study. *Front. Psychiatry.* 11:497116. doi: 10.3389/fpsyt.2020.497116

Braida, D., Guerini, F. R., Ponzoni, L., Corradini, I., De Astis, S., Pattini, L., et al. (2015). Association between SNAP-25 gene polymorphisms and cognition in autism: functional consequences and potential therapeutic strategies. *Transl. Psychiatry* 5:e500. doi: 10.1038/tp.2014.136

Brans, R. G., Kahn, R. S., Schnack, H. G., van Baal, G. C., Posthuma, D., van Haren, N. E., et al. (2010). Brain plasticity and intellectual ability are influenced by shared genes. *J. Neurosci.* 30, 5519–5524. doi: 10.1523/JNEUROSCI.5841-09.2010

Bruno, K. J., Freet, C. S., Twining, R. C., Egami, K., Grigson, P. S., and Hess, E. J. (2006). Abnormal latent inhibition and impulsivity in coloboma mice, a model of ADHD. *Neurobiol Dis.* 25, 206–216. doi: 10.1016/j.nbd.2006.09.009

Chen, S. Y., Feng, Z., and Yi, X. (2017). A general introduction to adjustment for multiple comparisons. *J. Thorac. Dis.* 9, 1725–1729. doi: 10.21037/jtd.2017.05.34

Contena, B., and Taddei, S. (2017). Psychological and cognitive aspects of borderline intellectual functioning. *Eur. Psychol.* 22, 159–166. doi: 10.1027/1016-9040/a000293

Corradini, I., Donzelli, A., Antonucci, F., Welzl, H., Loos, M., Martucci, R., et al. (2014). Epileptiform activity and cognitive deficits in SNAP-25(±) mice are normalized by antiepileptic drugs. *Cereb. Cortex.* 24, 364–376. doi: 10.1093/cercor/bhs316

Deary, I. J., Johnson, W., and Houlihan, L. M. (2009). Genetic foundations of human intelligence. *Hum. Genet.* 126, 215–232. doi: 10.1007/s00439-009-0655-4

Desikan, R. S., Ségonne, F., Fischl, B., Quinn, B. T., Dickerson, B. C., Blacker, D., et al. (2006). An automated labeling system for subdividing the human cerebral cortex on MRI scans into gyral based regions of interest. *Neuroimage* 31, 968–980. doi: 10.1016/j.neuroimage.2006.01.021

Douma, J. C., Dekker, M. C., de Ruiter, K. P., Tick, N. T., and Koot, H. M. (2007). Antisocial and delinquent behaviors in youths with mild or borderline disabilities. *Am. J. Ment. Retard.* 112, 207–220. doi: 10.1352/0895-8017(2007)112[207:aadbiy]2.0.co;2

Emerson, E., Einfeld, S., and Stancliffe, R. J. (2010). The mental health of young children with intellectual disabilities or borderline intellectual functioning. *Soc. Psychiatr. Psychiatr. Epidemiol.* 45, 579–587. doi: 10.1007/s00127-009-0100-y

Faraone, S. V., Perlis, R. H., Doyle, A. E., Smoller, J. W., Goralnick, J. J., Holmgren, M. A., et al. (2005). Molecular genetics of attention-deficit/hyperactivity disorder. *Biol. Psychiatry* 57, 1313–1323. doi: 10.1016/j.biopsych.2004.11.024

Fernell, E., and Ek, U. (2010). Borderline intellectual functioning in children and adolescents – insufficiently recognized difficulties. *Acta Paediatr*. 99, 748–753. doi: 10.1111/j.1651-2227.2010.01707.x

Flanagan, D. P., and Kaufman, A. S. (2012). *Fondamenti per l'assessment con la WISC-IV*. Firenze: Giunti OS Organizzazioni speciali.

Forero, D. A., Arboleda, G. H., Vasquez, R., and Arboleda, H. (2009). Candidate genes involved in neural plasticity and the risk for attention-deficit hyperactivity disorder: a meta-analysis of 8 common variants. *J. Psychiatry Neurosci.* 34, 361–366.

Gao, Q., Liu, L., Chen, Y., Li, H., Yang, L., Wang, Y., et al. (2015). Synaptosome-related (SNARE) genes and their interactions contribute to the susceptibility and working memory of attention-deficit/hyperactivity disorder in males. *Prog. Neuropsychopharmacol. Biol. Psychiatry* 57, 132–139. doi: 10.1016/j.pnpbp.2014.11.001

Gigi, K., Werbeloff, N., Goldberg, S., Portuguese, S., Reichenberg, A., Fruchter, E., et al. (2014). Borderline intellectual functioning is associated with poor social functioning, increased rates of psychiatric diagnosis and drug use–a cross sectional population based study. *Eur. Neuropsychopharmacol.* 24, 1793–1797. doi: 10.1016/j.euroneuro.2014.07.016

Golimbet, V. E., Alfimova, M. V., Gritsenko, I. K., Lezheiko, T. V., Lavrushina, O. M., Abramova, L. I., et al. (2010). Association between a synaptosomal protein (SNAP-25) gene polymorphism and verbal memory and attention in patients with endogenous psychoses and mentally healthy subjects. *Neurosci. Behav. Physiol.* 40, 461–465. doi: 10.1007/s11055-010-9280-x

Gosso, M. F., de Geus, E. J., Polderman, T. J., Boomsma, D. I., Heutink, P., and Posthuma, D. (2008). Common variants underlying cognitive ability: further evidence for association between the SNAP-25 gene and cognition using a family-based study in two independent Dutch cohorts. *Genes Brain Behav*. 7, 355–364. doi: 10.1111/j.1601-183X.2007.00359.x

Gosso, M. F., de Geus, E. J., van Belzen, M. J., Polderman, T. J., Heutink, P., Boomsma, D. I., et al. (2006). The SNAP-25 gene is associated with cognitive ability: evidence from a family-based study in two independent Dutch cohorts. *Mol. Psychiatry* 11, 878–886. doi: 10.1038/sj.mp.4001868

Guerini, F. R., Agliardi, C., Sironi, M., Arosio, B., Calabrese, E., Zanzottera, M., et al. (2014). Possible association between SNAP-25 single nucleotide polymorphisms and alterations of categorical fluency and functional MRI parameters in Alzheimer's disease. *J. Alzheimers Dis*. 42, 1015–1028. doi: 10.3233/JAD-140057

Guerini, F. R., Bolognesi, E., Chiappedi, M., Manca, S., Ghezzo, A., Agliardi, C., et al. (2011). SNAP-25 single nucleotide polymorphisms are associated with hyperactivity in autism spectrum disorders. *Pharmacol. Res.* 64, 283–288. doi: 10.1016/j.phrs.2011.03.015

Gumbel, E. (1959). Statistical estimates and transformed beta-variables, by Gunnar Blom. *Can. Math. Bull*. 3, 201–202. doi: 10.1017/s0008439500025571

Gunn, R. K., Keenan, M. E., and Brown, R. E. (2011). Analysis of sensory, motor and cognitive functions of the coloboma (C3Sn.Cg-Cm/J) mutant mouse. *Genes Brain Behav.* 10, 579–588. doi: 10.1111/j.1601-183X.2011.00697.x

Hassiotis, A. (2015). Borderline intellectual functioning and neurodevelopmental disorders: prevalence, comorbidities and treatment approaches. *Adv. Mental Health Intellect. Disabil*. 9:28. doi: 10.1108/AMHID-06-2015-0028

Hassiotis, A., Brown, E., Harris, J., Helm, D., Munir, K., Salvador-Carulla, L., et al. (2019). Association of borderline intellectual functioning and adverse childhood experience with adult psychiatric morbidity. Findings from a British birth cohort. *BMC Psychiatry* 19:387. doi: 10.1186/s12888-019-2376-0

Hess, E. J., Jinnah, H. A., Kozak, C. A., and Wilson, M. C. (1992). Spontaneous locomotor hyperactivity in a mouse mutant with a deletion including the Snap gene on chromosome 2. *J. Neurosci*. 12, 2865–2874. doi: 10.1523/JNEUROSCI.12-07-02865.1992

Hess, E. J., Rogan, P. K., Domoto, M., Tinker, D. E., Ladda, R. L., and Ramer, J. C. (1995). Absence of linkage of apparently single gene mediated ADHD with the human syntenic region of the mouse mutant Coloboma. *Am. J. Med. Genet.* 60, 573–579. doi: 10.1002/ajmg.1320600619

Hollingshead, A. B. (2011). Four factor index of social status. *Yale J. Sociol.* 8, 21–53.

Igelström, K. M., and Graziano, M. S. A. (2017). The inferior parietal lobule and temporoparietal junction: a network perspective. *Neuropsychologia* 105, 70–83. doi: 10.1016/j.neuropsychologia.2017.01.001

Jung, R. E., and Haier, R. J. (2007). The Parieto-Frontal Integration Theory (P-FIT) of intelligence: converging neuroimaging evidence. *Behav Brain Sci.* 30, 135–154.doi: 10.1017/s0140525x07001185

Liu, Y. S., Dai, X., Wu, W., Yuan, F. F., Gu, X., Chen, J. G., et al. (2017). The association of SNAP25 gene polymorphisms in attention deficit/hyperactivity disorder: a systematic review and meta-analysis. *Mol. Neurobiol*. 54, 2189–2200. doi: 10.1007/s12035-016-9810-9

Martinez-Arca, S., Coco, S., Mainguy, G., Schenk, U., Alberts, P., Bouillé, P., et al. (2001). A common exocytotic mechanism mediates axonal and dendritic outgrowth. *J. Neurosci*. 1, 3830–3838. doi: 10.1523/JNEUROSCI.21-11-03830.2001

Menary, K., Collins, P. F., Porter, J. N., Muetzel, R., Olson, E. A., Kumar, V., et al. (2013). Associations between cortical thickness and general intelligence in children, adolescents and young adults. *Intelligence* 41, 597–606. doi: 10.1016/j.intell.2013.07.010

Orsini, A., and Picone, L. (2006). *Wechsler Intelligence scale for Children. Adattamento italiano*. Florence: Giunti OS.

Orsini, A., Pezzuti, L., and Picone, L. (2012). *Contributo alla Taratura Italiana [WISC-IV Italian Edition]*. Florence: Giunti OS.

Peltopuro, M., Ahonen, T., Kaartinen, J., Seppälä, H., and Närhi, V. (2014). Borderline intellectual functioning: a systematic literature review. *Intellect. Dev. Disabil.* 52, 419–443. doi: 10.1352/1934-9556-52.6.419

Posthuma, D., De Geus, E. J., Baaré, W. F., Hulshoff Pol, H. E., Kahn, R. S., and Boomsma, D. I. (2002). The association between brain volume and intelligence is of genetic origin. *Nat. Neurosci.* 5, 83–84. doi: 10.1038/nn0202-83

Posthuma, D., Luciano, M., Geus, E. J., Wright, M. J., Slagboom, P. E., Montgomery, G. W., et al. (2005). A genomewide scan for intelligence identifies quantitative trait loci on 2q and 6p. *Am. J. Hum. Genet*. 77, 318–326. doi: 10.1086/432647

Predescu, E., Sipos, R., Costescu, C. A., Ciocan, A., and Rus, D. I. (2020). Executive functions and emotion regulation in attention-deficit/hyperactivity disorder and borderline intellectual disability. *J. Clin. Med*. 9:986. doi: 10.3390/jcm9040986

Purcell, S., Neale, B., Todd-Brown, K., Thomas, L., Ferreira, M. A., Bender, D., et al. (2007). PLINK: a tool set for whole-genome association and population-based linkage analyses. *Am. J. Hum. Genet*. 81, 559–575. doi: 10.1086/519795

Rizzi, T. S., Beunders, G., Rizzu, P., Sistermans, E., Twisk, J. W., van Mechelen, W., et al. (2012). Supporting the generalist genes hypothesis for intellectual ability/disability: the case of SNAP25. *Genes Brain Behav*. 11, 767–771. doi: 10.1111/j.1601-183X.2012.00819.x

Rizzolatti, G., and Craighero, L. (2004). The mirror-neuron system. *Annu. Rev. Neurosci*. 27, 169–192. doi: 10.1146/annurev.neuro.27.070203.144230

Ropers, H. H. (2008). Genetics of intellectual disability. *Curr. Opin. Genet. Dev*. 18, 241–250. doi: 10.1016/j.gde.2008.07.008

Rosen, M. L., Sheridan, M. A., Sambrook, K. A., Meltzoff, A. N., and McLaughlin, K. A. (2018). Socioeconomic disparities in academic achievement: a multi-modal investigation of neural mechanisms in children and adolescents. *Neuroimage* 173, 298–310. doi: 10.1016/j.neuroimage.2018.02.043

Russell, V. A. (2007). Neurobiology of animal models of attention-deficit hyperactivity disorder. *J. Neurosci. Methods* 161, 185–198. doi: 10.1016/j.jneumeth.2006.12.005

Salvador-Carulla, L., García-Gutiérrez, J. C., Ruiz Gutiérrez-Colosía, M., Artigas-Pallarès, J., García Ibáñez, J., and González Pérez, J. (2013). Borderline intellectual functioning: consensus and good practice guidelines. *Rev. Psiquiatr. Salud Ment.* 6, 109–120. doi: 10.1016/j.rpsm.2012.12.001

Sauce, B., and Matzel, L. D. (2018). The paradox of intelligence: heritability and malleability coexist in hidden gene-environment interplay. *Psychol. Bull*. 144, 26–47. doi: 10.1037/bul0000131

Shi, Y. Y., and He, L. (2005). SHEsis, a powerful software platform for analyses of linkage disequilibrium, haplotype construction, and genetic association at polymorphism loci. *Cell Res*. 15, 97–98. doi: 10.1038/sj.cr.7290272

Söderqvist, S., McNab, F., Peyrard-Janvid, M., Matsson, H., Humphreys, K., Kere, J., et al. (2010). The SNAP25 gene is linked to working memory capacity and

maturation of the posterior cingulate cortex during childhood. *Biol. Psychiatry* 68, 1120–1125. doi: 10.1016/j.biopsych.2010.07.036

Südhof, T. C. (2015). La machinerie moléculaire de sécrétion des neurotransmetteurs [The molecular machinery of neurotransmitter secretion]. *Biol. Aujourdhui* 209, 3–33. doi: 10.1051/jbio/2015012

Thompson, P. M., Egbufoama, S., and Vawter, M. P. (2003). SNAP-25 reduction in the hippocampus of patients with schizophrenia. *Prog. Neuropsychopharmacol. Biol. Psychiatry* 27, 411–417. doi: 10.1016/S0278-5846(03)00027-7

Vuijk, P. J., Hartman, E., Scherder, E., and Visscher, C. (2010). Motor performance of children with mild intellectual disability and borderline intellectual functioning. *J. Intellect. Disabil. Res.* 54, 955–965. doi: 10.1111/j.1365-2788.2010.01318.x

Zhang, Y., Vilaythong, A. P., Yoshor, D., and Noebels, J. L. (2004). Elevated thalamic low-voltage-activated currents precede the onset of absence epilepsy in the SNAP25-deficient mouse mutant coloboma. *J. Neurosci.* 24, 5239–5248. doi: 10.1523/JNEUROSCI.0992-04.2004

Conflict of Interest: The authors declare that the research was conducted in the absence of any commercial or financial relationships that could be construed as a potential conflict of interest.

frontiers in Neuroscience

ORIGINAL RESEARCH
published: 22 September 2021
doi: 10.3389/fnins.2021.749230

Association Between Genetic Risks for Obesity and Working Memory in Children

*Nagahide Takahashi[1,2,3], Tomoko Nishimura[2,3], Taeko Harada[2,3], Akemi Okumura[2,3], Toshiki Iwabuchi[2,3], Md. Shafiur Rahman[2,3], Hitoshi Kuwabara[4], Shu Takagai[5], Yoko Nomura[6], Nori Takei[2,3] and Kenji J. Tsuchiya[2,3]**

[1] Department of Child and Adolescent Psychiatry, Nagoya University Graduate School of Medicine, Nagoya, Japan, [2] Research Center for Child Mental Development, Hamamatsu University School of Medicine, Hamamatsu, Japan, [3] United Graduate School of Child Development, Hamamatsu University School of Medicine, Hamamatsu, Japan, [4] Department of Psychiatry, Hamamatsu University School of Medicine, Hamamatsu, Japan, [5] Department of Child and Adolescent Psychiatry, Hamamatsu University School of Medicine, Hamamatsu, Japan, [6] Queens College and Graduate Center, City University of New York, New York, NY, United States

OPEN ACCESS

Edited by:
Stefano Berto,
University of Texas Southwestern Medical Center, United States

Reviewed by:
Yunpeng Wang,
University of Oslo, Norway
Kazutaka Ohi,
Gifu University, Japan

***Correspondence:**
Kenji J. Tsuchiya
tsuchiya@hama-med.ac.jp

Specialty section:
This article was submitted to Neurogenomics, a section of the journal Frontiers in Neuroscience

Received: 29 July 2021
Accepted: 26 August 2021
Published: 22 September 2021

Citation:
Takahashi N, Nishimura T, Harada T, Okumura A, Iwabuchi T, Rahman MS, Kuwabara H, Takagai S, Nomura Y, Takei N and Tsuchiya KJ (2021) Association Between Genetic Risks for Obesity and Working Memory in Children. Front. Neurosci. 15:749230. doi: 10.3389/fnins.2021.749230

Introduction: Obesity is highly heritable, and recent evidence demonstrates that obesity is associated with cognitive deficits, specifically working memory. However, the relationship between genetic risks for obesity and working memory is not clear. In addition, whether the effect of these genetic risks on working memory in children is mediated by increased body mass index (BMI) has not been elucidated.

Methods: In order to test whether the polygenic risk score (PRS) for obesity in adulthood (adulthood-BMI-PRS) is associated with working memory at 8 years of age, and whether the effect is mediated by childhood BMI, in children from the general population, participants in the Hamamatsu Birth Cohort for Mothers and Children (HBC) study in Hamamatsu, Japan, underwent testing for association of adulthood-BMI-PRS with working memory. HBC data collection began in December 2007 and is ongoing. Adulthood-BMI-PRS values were generated using summary data from the recent genome-wide association study (GWAS) undertaken in Japan, and the significance of thresholds was calculated for each outcome. Outcomes measured included the working memory index (WMI) of Weschler Intelligence Scale-4 (WISC-IV) scores and the BMI at 8 years of age. Gene-set enrichment analysis was conducted to clarify the molecular basis common to adulthood-BMI and childhood-WMI. Mediation analysis was performed to assess whether childhood-BMI of children mediated the association between adulthood-BMI-PRS and working memory.

Results: A total of 734 participants (377 males, 357 females) were analyzed. Adulthood-BMI-PRS was associated with lower childhood-WMI (β[SE], −1.807 [0.668]; p = 0.010, corrected) of WISC-IV. Gene-set enrichment analyses found that regulation of neurotrophin Trk receptor signaling (β[SE], −2.020 [6.39]; p = 0.002, corrected),

negative regulation of GTPase activity (β[SE], 2.001 [0.630]; $p = 0.002$, corrected), and regulation of gene expression epigenetic (β[SE], −2.119 [0.664]; $p = 0.002$, corrected) were enriched in BMI in adulthood and WMI in childhood. Mediation analysis showed that there is no mediation effect of childhood-BMI between the adulthood-BMI-PRS and working memory deficits in children.

Conclusion: Adulthood-BMI-PRS was associated with working memory among children in the general population. These genetic risks were not mediated by the childhood-BMI itself and were directly associated with working memory deficits.

Keywords: polygenic risk score, obesity, cognition, GWAS, child development

INTRODUCTION

Accumulating evidence shows that obesity is associated with deficits in neurocognitive functioning, such as deficits in working memory in children (Smith et al., 2011; Cornier et al., 2013; Crone and Steinbeis, 2017). Obesity is associated with adiposity, cellular stress, and excessive inflammation, all of which can lead to insulin resistance and cerebral structural alteration (Unamuno et al., 2018). Numerous neuroimaging studies have found structural alterations in obese children (Maayan et al., 2011; Veit et al., 2014; Sharkey et al., 2015; Saute et al., 2018); however, due to the limited sample size and methodological difference, results regarding the relationship between obesity, cortical thickness, and cognitive deficits have been inconsistent (Maayan et al., 2011; Sharkey et al., 2015; Saute et al., 2018). A recent large neuroimaging study reported that higher body mass index (BMI) was associated with lower working memory, and this association was mediated by reduced prefrontal cortex thickness in children (Laurent et al., 2019).

Although obesity is a complex phenotype, the role of genetic factors in the development of obesity remains undisputed. Additionally, a recent genome-wide association study (GWAS) identified 85 loci associated with BMI in adults from the Japanese general population (Akiyama et al., 2017). Furthermore, a previous study showed that BMI was genetically correlated with general cognitive function in adults using LD score regression analysis ($r_g = 0.51$) (Marioni et al., 2016). However, Riggs et al. found that alteration in working memory is antecedent to weight gain in children, suggesting the possibility that cortical thickness or subsequent cognitive dysfunctions cause obesity (Riggs et al., 2010; Groppe and Elsner, 2017). Together, it is reasonable to hypothesize that children with genetic risks for obesity might have a higher risk for neurocognitive deficits compared to those with low genetic risks for obesity and the genetic risks for obesity potentially directly affect working memory without mediation of BMI.

As such, we examined (1) whether polygenic risk scores (PRSs) for BMI in adulthood (adulthood-BMI-PRS) are associated with deficits in working memory, leveraged on our birth cohort, composed of representative samples of Japanese, and (2) whether childhood-BMI mediated the association between adulthood-BMI-PRS and working memory.

MATERIALS AND METHODS

Participants

Participants included infants ($n = 832$; 426 boys, 406 girls) born in Japan between December 2007 and June 2011. The recruitment procedures are described in detail in our previous study (Takagai et al., 2016). The study procedures were approved by the ethical committee. Written informed consent was obtained from each mother for the participation of her infant. Participants with parents of non-Japanese descent were excluded from the study ($n = 8$). No other screening, such as neurodevelopmental disorders or psychiatric disorders was conducted for the analysis. Hamamatsu University School of Medicine and the University Hospital Ethics Committee accepted the study methods.

Measurement

Working memory was assessed, using the working memory index (WMI) of the Wechsler Intelligence Scale for Children-4 (WISC-IV) when the children became 8 years of age. Information pertaining to BMI was obtained on the same day when the WISC-IV assessments were carried out.

Genotyping, Quality Control, and Imputation

Genotyping was conducted using the Japonica array designed specifically for single-nucleotide polymorphism (SNP) genotyping for a Japanese population (Kawai et al., 2015). The quality controls retaining SNPs and subjects were as follows: missing data for SNP < 0.02, Pi-hat calculated by identity-by-descent analysis < 0.2, SNP Hardy-Weinberg equilibrium of $p > 10^{-6}$, and minor allele frequency > 0.01. Genotyping imputation was performed using BEAGLE 5.0 (Browning et al., 2018) to the Japanese reference panel phase 3 of 1000 Genome Project. SNPs with an imputation INFO score < 0.8 were excluded. We also excluded SNPs located within the MHC region, because of high linkage disequilibrium (LD) in this region. The number of SNPs analyzed for PRS was 5,606,655.

TABLE 1 | Sample characteristics: participating children and their parents.

	Mean (*SD*)
Birthweight (g)	2935.1 (444.3)
Gestational age at birth (weeks)	38.9 (1.6)
Paternal age at birth (years)	33.5 (5.7)
Maternal age at birth (years)	29.3(5.2)
Household income (million JPY)	6.1 (2.7)
BMI	16.2 (2.4)
Gender	*n* (%)
Male	439 (50.1)
Female	437 (49.9)
Ethnicity	
Japanese	868
Mixed (Caucasian)	5
Mixed (Latino)	3
Small for gestational age	
<10th percentile	785 (89.6)
10th–100th percentile	91 (10.4)
Placenta-to-birthweight ratio (twin excluded)	
<10th percentile	164 (18.7)
10th–100th percentile	712 (81.3)
Paternal education	
<12 years	65 (7.4)
12years and longer	811 (92.6)
Maternal education	
<12 years	38 (4.3)

SD, standard deviation; BMI, body mass index.

STATISTICAL ANALYSIS

Polygenic Risk Score Analysis

PRS was generated by PRSice-2 (Choi and O'Reilly, 2019) using a recent BMI-GWAS in the Japanese adult population as a discovery cohort[1] (Akiyama et al., 2017). Four main components calculated with PLINK 1.9 (Chang et al., 2015) were used to account for population stratification. The criterion for SNP clumping was pairwise linkage disequilibrium of $r^2 < 0.1$ within a 1-Mb window. PRSs were calculated with different *p*-value thresholds: 0.05, 0.1, 0.2, 0.3, 0.4, and 0.5. Standardized PRS scores (mean = 0; standard deviation = 1) were used for the analyses. *p*-values for WMI were corrected using 10,000 permutation tests. Sex and small-for-gestational-age (SGA) were included as covariates. The statistical power of the PRS at each *p*-value threshold was calculated using the AVENGEME R-package (Dudbridge et al., 2018). Since SNP-based heritability (h^2 SNP) estimated from the original BMI study was 0.29812, all generated PRSs showed adequate power between 90 and 100%.

Gene-set enrichment analyses were conducted using PRSet (Choi et al., 2021) to identify gene sets that contain SNPs associated with both BMI in adulthood and WMI in childhood. Gene ontology (GO) sets (c5: biological process) were obtained from the MSigDB database[2] and used for the analyses by PRSice-2 (Choi and O'Reilly, 2019). The *p*-value threshold for PRSet was set at 1, since gene-set PRSs containing a small portion of SNPs may be unrepresentative of the entire gene set (Fanelli et al., 2020). The *p*-values for PRSet were corrected by 10,000 permutation tests.

Mediation Analysis

Mediation analysis was performed to assess whether childhood-BMI mediated the association between adulthood-BMI-PRS and working memory. Best-fit PRSs computed with highest R^2, obtained from linear regression analyses, were used for the medication analysis. The R package "lavaan" was used, and the significance of indirect effect of childhood-BMI was assessed by 1,000 bootstrap at a 95% confidential interval (Rosseel, 2012). The data were tested for normal distribution by a Shapiro–Wilk test.

RESULTS

Association Between Adulthood-Body Mass Index-Polygenic Risk Score and Childhood-Working Memory Index

Participant characteristics are summarized in **Table 1**. Genotyping quality control and identity-by-decent analysis were used to remove 98 individuals from the analysis, resulting in a total of 726 participants (373 males, 353 females) for further analysis. The adulthood-BMI-PRS was significantly

[1]https://humandbs.biosciencedbc.jp/hum0014-v23

[2]https://www.gsea-msigdb.org/gsea/msigdb/index.jsp

TABLE 2 | Association between BMI PRS and WMI of WISC-IV.

WISC items	*p*-value threshold	R^2	β	SE	*p*-values*
WMI	0.05	0.023	−1.416	0.675	0.129
	0.1	0.024	−1.470	0.687	0.099
	0.2	0.028	−1.713	0.674	**0.030**
	0.3	0.030	−1.807	0.668	**0.010**
	0.4	0.028	−1.691	0.664	**0.020**
	0.5	0.027	−1.616	0.667	**0.040**

BMI, body mass index; PRS, polygenic risk score; WISC-IV, Wechsler Intelligence Scale for Children-4; SNP, single-nucleotide polymorphism; WMI, working memory index.

The number of SNPs used to calculate PRSs were 22,093 ($p < 0.05$), 33,299 ($p < 0.1$), 50,147 ($p < 0.2$), 63,106 ($p < 0.3$), 73,554 ($p < 0.4$), and 82,278 ($p < 0.5$).

**p-values were corrected for 10,000 permutation tests. Statistically significant p-values were shown in bold.*

TABLE 3 | Top 20 gene sets significantly enriched for WMI and BMI.

Gene-sets	R^2	β	SE	Number of SNP	*p*-value
Regulation of neurotrophin Trk receptor signaling pathway	0.036	−2.020	0.639	99	0.002
Negative regulation of GTPase activity	0.036	2.001	0.630	320	0.002
Regulation of gene expression epigenetic	0.036	−2.119	0.664	1,360	0.002
DNA synthesis involved in DNA repair	0.036	2.029	0.636	221	0.003
Histone H3 K9 demethylation	0.032	1.893	0.658	105	0.004
Glutathione derivative biosynthetic process	0.031	−1.802	0.639	61	0.005
Negative regulation of bmp signaling pathway	0.033	−1.914	0.650	241	0.005
Positive regulation of neuron death	0.031	−1.914	0.681	400	0.006
Nucleoside diphosphate biosynthetic process	0.030	−1.905	0.694	45	0.006
Oligodendrocyte progenitor proliferation	0.030	−1.709	0.634	60	0.006
Layer formation in cerebral cortex	0.030	−1.788	0.662	92	0.007
Endoplasmic reticulum mannose trimming	0.029	1.711	0.643	84	0.008
Positive regulation of tor signaling	0.030	−1.822	0.661	172	0.008
Negative regulation of histone methylation	0.029	1.703	0.647	146	0.010
Canonical wnt signaling pathway	0.029	1.819	0.680	1,811	0.011
Negative regulation of RNA metabolic process	0.029	−1.723	0.649	171	0.011
Cellular response to brain derived neurotrophic factor stimulus	0.027	−1.717	0.700	62	0.015
Lateral ventricle development	0.027	1.631	0.667	96	0.016
Regulation of snare complex assembly	0.027	−1.576	0.650	62	0.016
Postsynaptic cytoskeleton organization	0.026	1.563	0.652	55	0.017

WMI, working memory index; BMI, body mass index; SNP, single-nucleotide polymorphism; SE, standard error.
p-values were corrected for 10,000 permutation tests.

associated with lower WMI of WISC-IV at various *p*-value thresholds (**Table 2**).

Gene-Set Enrichment Analysis of Adulthood-Body Mass Index-Polygenic Risk Score and Childhood-Working Memory Index

Gene-set enrichment analysis identified that several gene ontologies, such as regulation of neurotrophin Trk receptor signaling (β[SE], −2.020 [6.39]; $p = 0.002$, corrected), negative regulation of GTPase activity (β[SE], 2.001 [0.630]; $p = 0.002$, corrected), and regulation of gene expression epigenetic (β[SE], −2.119 [0.664]; $p = 0.002$, corrected), were enriched in BMI in adulthood and WMI in children (**Table 3**).

Mediation Analysis of Adulthood- Body Mass Index-Polygenic Risk Score, Childhood-Body Mass Index, and Childhood-Working Memory Index

All data including adulthood-BMI-PRS, childhood-BMI, and childhood-WMI were normally distributed by a Shapiro–Wilk test ($p > 0.05$). Mediation analysis was conducted for BMI-PRS (best fit *p*-value threshold at 0.319), childhood-BMI, and childhood-WMI. Analysis revealed that although there was a significant total effect of BMI-PRS on WMI (β[SE], −1.874 [0.633]; $p = 0.004$), no indirect effect of childhood-BMI (β[SE], 0.110 [0.102]; $p = .280$) was observed, indicating that most of the effect originated from the direct effect of BMI-PRS (β[SE], −1.736 [0.638]; $p = 0.006$) (**Figure 1**). Furthermore, regression analysis showed that there is no association between adulthood-BMI-PRS and childhood-BMI in the present study (β[SE], −0.185 [0.130]; $p = 0.156$).

FIGURE 1 | Mediation analysis of Adulthood-BMI-PRS, Childhood-BMI, and Childhood-Working memory. The solid line indicates the path that was statistically significant and the dashed lines indicate those that were estimated but not statistically significant. BMI, body mass index; PRS, polygenic risk score. $^{**}p < 0.01$.

DISCUSSION

We report that genetic risks for obesity are linked to working memory deficits in children. This finding partially supports the previous report (Laurent et al., 2019); however, we found that the effect of BMI-PRS on WMI was not mediated by childhood-BMI, indicating that childhood-BMI itself does not affect this cognitive domain directly, but the genes involved in adulthood-BMI are

responsible for these functions in the brain. This finding is also consistent with a previous study showing strong genetic correlation between BMI and general cognitive functions in adults using LD score regression analysis (Marioni et al., 2016).

Multiple reasons could be considered for the lack of association between adulthood-BMI-PRS and childhood-BMI itself in our study population. First, as we targeted 8-year-old children, it might be too early to detect the effect of genes related to adulthood-BMI on BMI in children. Second, there is a possibility that genes related to adulthood-BMI are different between children and adults.

In accordance with the previous GWAS results (Akiyama et al., 2017), GO sets commonly enriched in adulthood-BMI and childhood-WMI have been reported to be involved in the brain cortical maturation (Anton-Fernandez et al., 2015; Budday et al., 2015; Lian and Sheen, 2015). For example, genes in oligodendrocyte progenitor proliferation or layer formation in cerebral cortex have been reported to be expressed in the brain from the early postnatal period.[3] Among these GOs, it is noteworthy that regulation of gene expression epigenetic was identified, since a recent GWAS demonstrated that a SNP on the HDAC4 gene was associated with selective attention (Pinar et al., 2018). Taken together, it can be considered that these genes are involved in brain maturation and working memory directly, without mediation of body weight.

LIMITATIONS

There are a few limitations in our study. First, compared to the previous study (Laurent et al., 2019), the average childhood-BMI [mean (SD), 18.64 (3.9) in the previous study vs. 16.2 (2.4) in this study] was lower in our cohort; thus, there is a possibility that we did not target a population with a broad range of BMI and, thus, could not detect an effect of adulthood-BMI-PRS on childhood-BMI in this study. Incidence of children classified as overweight (i.e., 85–95%) in this study was 9.68%, compared to 13.4% in the previous study. Similarly, the incidence of children classified as obese (i.e., > 95%) was 6.98% in this study, compared to 15.4% in the previous study (Laurent et al., 2019). Second, as BMI does not always reflect obesity, more sophisticated measurement to evaluate obesity, such as body fat percentage, is needed (Nickerson et al., 2018).

CONCLUSION

In this study, the adulthood-BMI-PRS was associated with working memory among children in the general population. These genetic risks were directly associated with working memory deficits, and not mediated by children's BMI. Future studies are warranted in order to replicate these findings.

[3] informatics.jax.org

DATA AVAILABILITY STATEMENT

The data generated for this study is subject to the following licenses/restrictions: Privacy and Confidentiality of Participants. Requests to access these datasets should be directed to KT, tsuchiya@hama-med.ac.jp.

ETHICS STATEMENT

The studies involving human participants were reviewed and approved by Hamamatsu University School of Medicine and the University Hospital Ethics Committee. Written informed consent to participate in this study was provided by the participants' legal guardian/next of kin.

AUTHOR CONTRIBUTIONS

NaT had full access to all the data used in the study and takes responsibility for the integrity of the data and accuracy of the data analysis, and statistical analysis. NaT, NoT, and KT study concept and design. NaT and KT drafting the manuscript. NoT and KT study supervision. TH, TN, and AO administrative, technical, and material support. All authors contributed significantly to the study and the creation of this manuscript, acquisition, analysis, interpretation of data, and critical revision of the manuscript for important intellectual content.

FUNDING

This work was supported by grants from the Ministry of Education, Culture, Sports, Science, and Technology in Japan (Grant No. 19H03582 to KT).

ACKNOWLEDGMENTS

We are grateful to the individuals who participated in the study. We would like to thank Ms. Chikako Nakayasu, Ms. Yuko Anma, and Ms. Haruka Suzuki for data collection, and Ms. Noriko Kodera and Ms. Emi Higashimoto for administration. This is a short text to acknowledge the contributions of specific colleagues, institutions, or agencies that aided the efforts of the authors.

REFERENCES

Akiyama, M., Okada, Y., Kanai, M., Takahashi, A., Momozawa, Y., Ikeda, M., et al. (2017). Genome-wide association study identifies 112 new loci for body mass index in the Japanese population. *Nat. Genet.* 49, 1458–1467. doi: 10.1038/ng.3951

Anton-Fernandez, A., Leon-Espinosa, G., DeFelipe, J., and Munoz, A. (2015). Changes in the golgi apparatus of neocortical and hippocampal neurons in the hibernating hamster. *Front. Neuroanat.* 9:157. doi: 10.3389/fnana.2015.00157

Browning, B. L., Zhou, Y., and Browning, S. R. (2018). A one-penny imputed genome from next-generation reference panels. *Am. J. Hum. Genet.* 103, 338–348. doi: 10.1016/j.ajhg.2018.07.015

Budday, S., Steinmann, P., and Kuhl, E. (2015). Physical biology of human brain development. *Front. Cell. Neurosci.* 9:257. doi: 10.3389/fncel.2015.00257

Chang, C. C., Chow, C. C., Tellier, L. C., Vattikuti, S., Purcell, S. M., and Lee, J. J. (2015). Second-generation PLINK: rising to the challenge of larger and richer datasets. *Gigascience* 4:7. doi: 10.1186/s13742-015-0047-8

Choi, S. W., Garcia-Gonzalez, J., Ruan, Y., Wu, H. M., Johnson, J., O'Reilly, P., et al. (2021). *The Power of Pathway-Based Polygenic Risk Scores*. doi: 10.21203/rs.3.rs-643696/v1

Choi, S. W., and O'Reilly, P. F. (2019). PRSice-2: polygenic risk score software for biobank-scale data. *Gigascience* 8:giz082. doi: 10.1093/gigascience/giz082

Cornier, M. A., McFadden, K. L., Thomas, E. A., Bechtell, J. L., Eichman, L. S., Bessesen, D. H., et al. (2013). Differences in the neuronal response to food in obesity-resistant as compared to obesity-prone individuals. *Physiol. Behav.* 110–111, 122–128. doi: 10.1016/j.physbeh.2013.01.002

Crone, E. A., and Steinbeis, N. (2017). Neural perspectives on cognitive control development during childhood and adolescence. *Trends Cogn. Sci.* 21, 205–215. doi: 10.1016/j.tics.2017.01.003

Dudbridge, F., Pashayan, N., and Yang, J. (2018). Predictive accuracy of combined genetic and environmental risk scores. *Genet. Epidemiol.* 42, 4–19. doi: 10.1002/gepi.22092

Fanelli, G., Benedetti, F., Kasper, S., Kautzky, A., Zohar, J., Souery, D., et al. (2020). Higher polygenic risk scores for schizophrenia may be suggestive of treatment non-response in major depressive disorder. *medRxiv* [Preprint] doi: 10.1101/2020.01.15.20017699

Groppe, K., and Elsner, B. (2017). Executive function and weight status in children: a one-year longitudinal perspective. *Child Neuropsychol.* 23, 129–147. doi: 10.1080/09297049.2015.1089981

Kawai, Y., Mimori, T., Kojima, K., Nariai, N., Danjoh, I., Saito, R., et al. (2015). Japonica array: improved genotype imputation by designing a population-specific SNP array with 1070 Japanese individuals. *J. Hum. Genet.* 60, 581–587. doi: 10.1038/jhg.2015.68

Laurent, J. S., Watts, R., Adise, S., Allgaier, N., Chaarani, B., Garavan, H., et al. (2019). Associations among body mass index, cortical thickness, and executive function in children. *JAMA Pediatr.* 174, 170–177. doi: 10.1001/jamapediatrics.2019.4708

Lian, G., and Sheen, V. L. (2015). Cytoskeletal proteins in cortical development and disease: actin associated proteins in periventricular heterotopia. *Front. Cell. Neurosci.* 9:99. doi: 10.3389/fncel.2015.00099

Maayan, L., Hoogendoorn, C., Sweat, V., and Convit, A. (2011). Disinhibited eating in obese adolescents is associated with orbitofrontal volume reductions and executive dysfunction. *Obesity (Silver Spring)* 19, 1382–1387. doi: 10.1038/oby.2011.15

Marioni, R. E., Yang, J., Dykiert, D., Mottus, R., Campbell, A., Group, C. C. W., et al. (2016). Assessing the genetic overlap between BMI and cognitive function. *Mol. Psychiatry* 21, 1477–1482. doi: 10.1038/mp.2015.205

Nickerson, B. S., Esco, M. R., Bishop, P. A., Fedewa, M. V., Snarr, R. L., Kliszczewicz, B. M., et al. (2018). Validity of BMI-based body fat equations in men and women: a 4-compartment model comparison. *J. Strength Cond. Res.* 32, 121–129. doi: 10.1519/JSC.0000000000001774

Pinar, A., Hawi, Z., Cummins, T., Johnson, B., Pauper, M., Tong, J., et al. (2018). Genome-wide association study reveals novel genetic locus associated with intra-individual variability in response time. *Transl. Psychiatry* 8:207. doi: 10.1038/s41398-018-0262-z

Riggs, N., Chou, C. P., Spruijt-Metz, D., and Pentz, M. A. (2010). Executive cognitive function as a correlate and predictor of child food intake and physical activity. *Child Neuropsychol.* 16, 279–292. doi: 10.1080/09297041003601488

Rosseel, Y. (2012). lavaan: an R package for structural equation modeling. *J. Stat. Softw.* 48:36. doi: 10.18637/jss.v048.i02

Saute, R. L., Soder, R. B., Alves Filho, J. O., Baldisserotto, M., and Franco, A. R. (2018). Increased brain cortical thickness associated with visceral fat in adolescents. *Pediatr. Obes.* 13, 74–77. doi: 10.1111/ijpo.12190

Sharkey, R. J., Karama, S., and Dagher, A. (2015). Overweight is not associated with cortical thickness alterations in children. *Front. Neurosci.* 9:24. doi: 10.3389/fnins.2015.00024

Smith, E., Hay, P., Campbell, L., and Trollor, J. N. (2011). A review of the association between obesity and cognitive function across the lifespan: implications for novel approaches to prevention and treatment. *Obes. Rev.* 12, 740–755. doi: 10.1111/j.1467-789X.2011.00920.x

Takagai, S., Tsuchiya, K. J., Itoh, H., Kanayama, N., Mori, N., Takei, N., et al. (2016). Cohort profile: Hamamatsu birth cohort for mothers and children (HBC Study). *Int. J. Epidemiol.* 45, 333–342. doi: 10.1093/ije/dyv290

Unamuno, X., Gomez-Ambrosi, J., Rodriguez, A., Becerril, S., Fruhbeck, G., and Catalan, V. (2018). , Adipokine dysregulation and adipose tissue inflammation in human obesity. *Eur. J. Clin. Invest.* 48:e12997. doi: 10.1111/eci.12997

Veit, R., Kullmann, S., Heni, M., Machann, J., Haring, H. U., Fritsche, A., et al. (2014). Reduced cortical thickness associated with visceral fat and BMI. *Neuroimage Clin.* 6, 307–311. doi: 10.1016/j.nicl.2014.09.013

Conflict of Interest: The authors declare that the research was conducted in the absence of any commercial or financial relationships that could be construed as a potential conflict of interest.

Publisher's Note: All claims expressed in this article are solely those of the authors and do not necessarily represent those of their affiliated organizations, or those of the publisher, the editors and the reviewers. Any product that may be evaluated in this article, or claim that may be made by its manufacturer, is not guaranteed or endorsed by the publisher.

frontiers in Genetics

ORIGINAL RESEARCH
published: 20 October 2021
doi: 10.3389/fgene.2021.748627

Autistic-Like Behavior and Impairment of Serotonin Transporter and AMPA Receptor Trafficking in *N*-Ethylmaleimide Sensitive Factor Gene-Deficient Mice

Min-Jue Xie[1,2,3†], *Keiko Iwata*[1,2,3†], *Yasuyuki Ishikawa*[4], *Yuki Nomura*[5], *Tomomi Tani*[5], *Koshi Murata*[6], *Yugo Fukazawa*[1,2,6] *and Hideo Matsuzaki*[1,2,3*]

[1]Division of Development of Mental Functions, Research Center for Child Mental Development, University of Fukui, Fukui, Japan, [2]Life Science Innovation Center, University of Fukui, Fukui, Japan, [3]United Graduate School of Child Development, Osaka University, Kanazawa University, Hamamatsu University School of Medicine, Chiba University and University of Fukui, Osaka University, Osaka, Japan, [4]Department of Systems Life Engineering, Maebashi Institute of Technology, Maebashi, Japan, [5]School of Medicine, Faculty of Medical Sciences, University of Fukui, Fukui, Japan, [6]Division of Brain Structures and Function, Department of Morphological and Physiological Sciences, Faculty of Medical Sciences, University of Fukui, Fukui, Japan

OPEN ACCESS

Edited by:
Kazuya Toriumi,
Tokyo Metropolitan Institute of Medical Science, Japan

Reviewed by:
Akihiro Mouri,
Fujita Health University, Japan
Sandra Jurado,
Institute of Neurosciences of Alicante, Spain

***Correspondence:**
Hideo Matsuzaki
matsuzah@u-fukui.ac.jp

[†]These authors have contributed equally to this work and share first authorship

Specialty section:
This article was submitted to Neurogenomics, a section of the journal Frontiers in Genetics

Received: 28 July 2021
Accepted: 04 October 2021
Published: 20 October 2021

Citation:
Xie M-J, Iwata K, Ishikawa Y, Nomura Y, Tani T, Murata K, Fukazawa Y and Matsuzaki H (2021) Autistic-Like Behavior and Impairment of Serotonin Transporter and AMPA Receptor Trafficking in N-Ethylmaleimide Sensitive Factor Gene-Deficient Mice. Front. Genet. 12:748627. doi: 10.3389/fgene.2021.748627

Autism spectrum disorder (ASD), characterized by profound impairment in social interactions and communication skills, is the most common neurodevelopmental disorder. Many studies on the mechanisms underlying the development of ASD have focused on the serotonergic system; however, these studies have failed to completely elucidate the mechanisms. We previously identified *N*-ethylmaleimide-sensitive factor (NSF) as a new serotonin transporter (SERT)-binding protein and described its importance in SERT membrane trafficking and uptake *in vitro*. In the present study, we generated *Nsf*$^{+/-}$ mice and investigated their behavioral, neurotransmitter, and neurophysiological phenotypes *in vivo*. *Nsf*$^{+/-}$ mice exhibited abnormalities in sociability, communication, repetitiveness, and anxiety. Additionally, *Nsf* loss led to a decrease in membrane SERT expression in the raphe and accumulation of glutamate alpha-amino-3-hydroxy-5-methyl-4-isoxazole propionic acid receptors at the synaptic membrane surface in the hippocampal CA1 region. We found that postsynaptic density and long-term depression were impaired in the hippocampal CA1 region of *Nsf*$^{+/-}$ mice. Taken together, these findings demonstrate that NSF plays a role in synaptic plasticity and glutamatergic and serotonergic systems, suggesting a possible mechanism by which the gene is linked to the pathophysiology of autistic behaviors.

Keywords: serotonin transporer, N-ethylmaleimide-sensitive factor, autism spectrum disorder, AMPA receptor, behavior

INTRODUCTION

Autism spectrum disorder (ASD) is a neurodevelopmental disorder characterized by severe and sustained impairment of social interaction and communication and restricted or stereotyped patterns of behavior and interest. Multiple risk factors, comprising both genetic and environmental factors, are known to be associated with the onset of ASD, indicating the

complex etiology of this disorder. Research focusing on neurotransmitters has been conducted, and accumulating evidence suggests that both serotonin (5-HT) and glutamine (Glu) neurotransmitter systems are implicated in the onset and progression of ASD (Eissa et al., 2018).

5-HT signaling facilitates several neural processes, including neurogenesis, cell migration and survival, synaptogenesis, and synaptic plasticity. Previous studies have consistently found elevated serotonin levels in whole blood cells and platelets of patients with autism (Schain, 1961; Hanley et al., 1977; Ciaranello, 1982; Anderson et al., 1987; Cook et al., 1988) and their relatives (Abramson et al., 1989; Cook et al., 1990; Cross et al., 2008). Short-term dietary tryptophan (precursor of 5-HT) depletion has been shown to exacerbate repetitive behavior and elevate anxiety and feelings of unhappiness in adults with autism (McDougle et al., 1996). A single-photon emission computed tomography study revealed that children with autism have reduced serotonin transporter (SERT) binding in the medial frontal cortex, midbrain, and temporal lobe (Makkonen et al., 2008). SERT is an integral plasma membrane glycoprotein that regulates neurotransmission through the reuptake of 5-HT from the synaptic cleft. Importantly, SERT expression, determined using radioligand binding assay results, has been reported to be significantly lower throughout the brain in individuals with autism than in controls (Nakamura et al., 2010). In contrast, *SERT* mRNA expression has not been found to significantly change in brain samples and lymphocytes of patients with ASD (Iwata et al., 2014). These findings suggest that SERT expression at the membrane surface and 5-HT transport capacity are decreased in the brains of ASD patients.

Increased levels of Glu have been found in the blood samples of children and adults with ASD (Moreno et al., 1992; Moreno-Fuenmayor et al., 1996; Aldred et al., 2003; Shinohe et al., 2006; Shimmura et al., 2011; Tirouvanziam et al., 2012). Glu levels in the brain have been assessed *in vivo* using proton magnetic resonance spectroscopy. Several groups have reported significantly increased Glu levels in several brain regions, including the anterior cingulate gyrus (Bejjani et al., 2012; Joshi et al., 2013) and the auditory cortex (Brown et al., 2013). Alpha-amino-3-hydroxy-5-methyl-4-isoxazole propionic acid (AMPA) receptors, which are tetrameric (GluA1–GluA4) and cation-permeable ionotropic glutamate receptors, are expressed throughout the brain (Beneyto and Meador-Woodruff, 2004). Intriguingly, receptor autoradiography results have revealed that the AMPA receptor density is slightly decreased, while post-mortem studies have revealed that *GluA1-GluA3* mRNA levels are significantly increased in the brains of ASD individuals (Purcell et al., 2001b). These findings suggest that AMPA receptor expression at the membrane surface and its function are impaired in the brains of ASD patients.

N-ethylmaleimide-sensitive factor (NSF) is a homohexameric ATPase (Hanson et al., 1997; Fleming et al., 1998) that is an essential component of the protein machinery responsible for various membrane fusion events, including intercisternal Golgi protein transport and synaptic vesicle exocytosis (Rothman, 1994). NSF binds to soluble NSF attachment protein (SNAP)-receptor (SNARE) complexes and mediates the recycling of spent SNARE complexes for subsequent rounds of membrane fusion (Rothman, 1994; Hay and Scheller, 1997). While this is a major function of NSF, it also interacts with neurotransmitter receptors, such as AMPA receptors, and regulates their trafficking patterns or recycling (Nishimune et al., 1998; Osten et al., 1998; Song et al., 1998; Hanley et al., 2002; Evers et al., 2010). In addition to neurotransmitter receptors, we recently reported that NSF interacts with SERT under physiological conditions and is required for SERT membrane trafficking and its uptake function (Iwata et al., 2014). Notably, *NSF* mRNA expression is reduced in lymphocytes of ASD patients and is significantly correlated with the severity of clinical symptoms (Iwata et al., 2014).

Therefore, we hypothesized that NSF contributes to ASD pathophysiology through interactions with SERT and AMPA receptors and controls the trafficking and functions of these molecules. To test this hypothesis, we generated and evaluated Nsf heterozygous knockout ($Nsf^{+/-}$) mice by gene targeting. $Nsf^{+/-}$ mice exhibited a significant decrease in membrane SERT expression in the raphe and postsynaptic expression of AMPA receptors in the hippocampal CA1 region. We also found that $Nsf^{+/-}$ mice showed core ASD symptoms, such as abnormal sociability and communication, repetitiveness, and anxiety. In addition, $Nsf^{+/-}$ mice showed decreased postsynaptic density (PSD) areas and abnormal synaptic plasticity.

MATERIALS AND METHODS

Animals

Four-week-old male mice were used for all experiments, except for the ultrasonic vocalization test (male pups at postnatal day 6). All experimental procedures were approved by the Animal Research Committee, University of Fukui, and the Institutional Animal Care and Use Committee of the Maebashi Institute of Technology. All experiments were conducted in compliance with institutional guidelines and regulations. All efforts were made to minimize the number of animals used and their suffering.

Generation of *Nsf* Knockout Mice

To generate *Nsf* knockout (KO) mice, we used C57BL/6N-background embryonic stem cells, EGR-101, carrying a "knockout first" (Testa et al., 2004) targeted *Nsf* allele obtained from the KOMP Repository (Vector ID: PG00174_Z_5_D06), which contains flippase recombination target-flanked *lacZ* and neomycin resistance (*Neo*) cassettes in front of a loxP-flanked (floxed) *Nsf* exon 6 (**Figure 1A**). The targeted *Nsf* allele was designed to be a knockout by splicing the cDNA into a *lacZ-neo* cassette. The cassette was then inserted upstream of a critical exon for *Nsf*, exon 6, to create a null allele of the gene. Embryonic stem cells were injected into eight-cell Institute for Cancer Research (ICR) mouse embryos, and chimeric blastocysts were transferred into the uteri of pseudo-pregnant ICR female mice (Fujihara et al., 2013). The resultant chimeric mice were bred to C57BL/6N

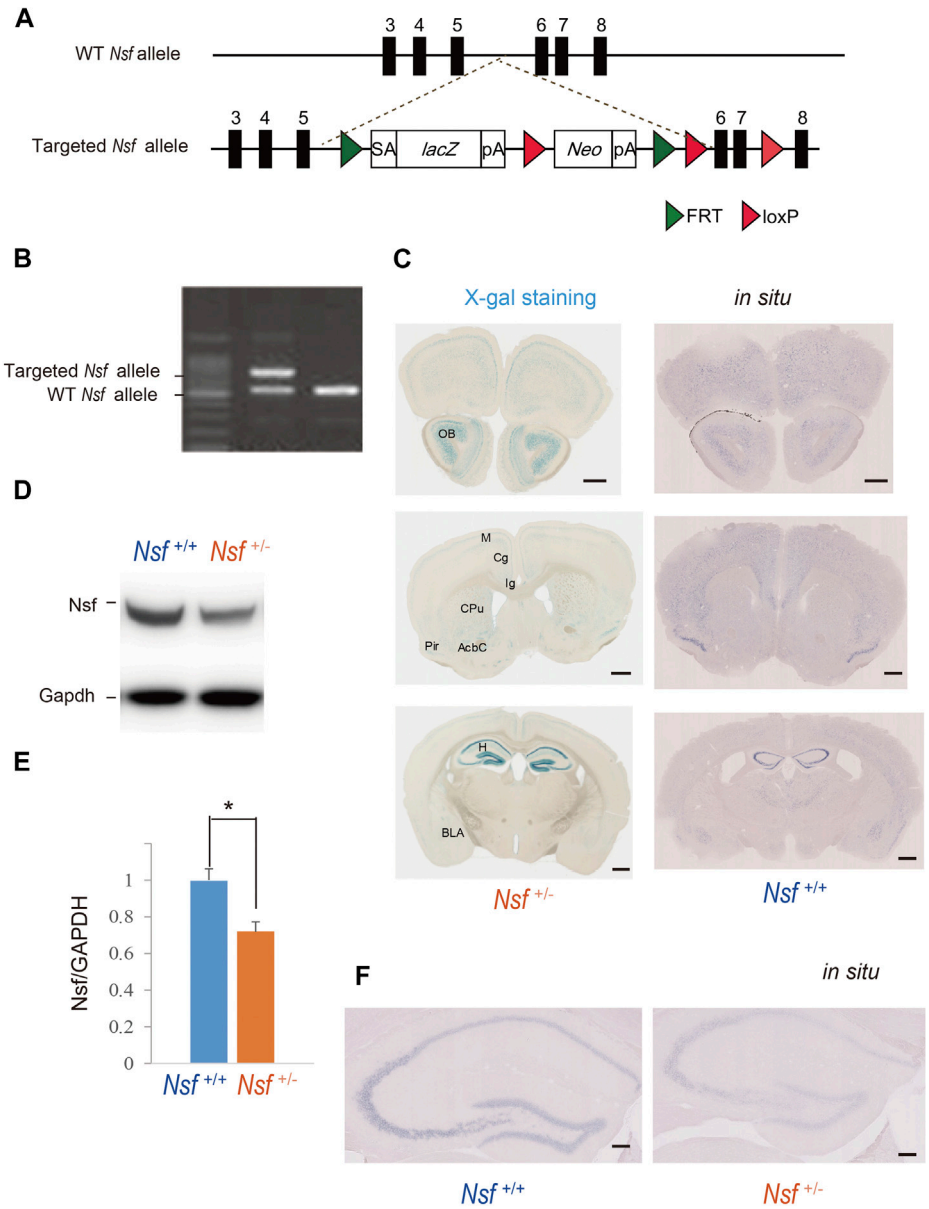

FIGURE 1 | Generation of Nsf knockout mice **(A)** Schematic representation of the genomic structure of the relevant part of the *Nsf* wild-type (WT) allele and the targeted allele construct with splice acceptor (SA) sequence, *IRES* followed by *lacZ* (fusion of β-gal gene and neomycin phosphotransferase gene), and a polyadenylation signal sequence (pA). Exons 5 and 6 of *Nsf* are flanked by *lacZ* and neomycin resistance (*Neo*) cassettes. **(B)** WT alleles and targeted alleles were detected using genomic PCR. The WT and mutant alleles are shown as 504 and 737 bp fragments, respectively. **(C)** X-gal staining (left panels) and *in situ* hybridization of *Nsf* (right panels) in *Nsf* $^{+/-}$ mouse brains. H, hippocampus; M, motor cortex; Cg, cingulate cortex; Ig, indusium griseum; Cpu, caudate putamen; Pir, piriform cortex; Acb, accumbens nucleus; Bla, basolateral amygdala. Scale bar represents 500 μm. **(D)** Nsf protein expression in the hippocampus from *Nsf*$^{+/+}$ and *Nsf* $^{+/-}$ mice was detected by western blotting (upper panel). The blots were subsequently probed with an anti-Gapdh antibody as a protein loading control (lower panel). **(E)** Relative band densities of Nsf were quantified using scanning densitometry ($n = 4$ for each genotype; mean ± SEM. Student's *t*-test, $^{*}p < 0.05$). **(F)** *In situ* hybridization of Nsf in the hippocampus of *Nsf*$^{+/+}$ mice (right panel) and *Nsf*$^{+/-}$ mice (left panel). Scale bar represents 2.5 mm.

background, and germline transmission was verified by conventional polymerase chain reaction (PCR) with the following primers for the wild-type allele, with a 504 bp fragment, (F: 5′-CCCAGCATCCTGAAGGGA-3′ in exon 6) and (R: 5′-CGATAAGATTGAGCGACGAATTTT-3′ in exon 7), and the targeted allele, with a 737 bp fragment, (F: 5′-CCC AGCATCCTGAAGGGA-3′ in exon 6) and (R: 5′-ACTGAT GGCGAGCTCAGACC-3′ in loxP), in F1 heterozygous KO mice (*Nsf*$^{+/-}$; **Figure 1B**). The mice were housed under specific pathogen-free conditions *and controlled laboratory conditions under an inverse 12 h light/dark cycle* (lights on at 7:00 am), *with ad libitum access to food and water.*

X-gal Staining

Mice were transcardially perfused for 1 min with phosphate-buffered saline, followed by 12 min of perfusion with 0.1 M phosphate buffer containing 4% paraformaldehyde at a rate of 5 ml/min. After rapid removal of the brains from the skull, they were fixed in 4% paraformaldehyde overnight. Following a buffer change with 0.1 M phosphate buffer, the brain was sliced (100 μm thick) on a vibratome (Dosaka, Kyoto, Japan). After the brain tissue sections were immersed in NP40 deoxycholate solution (0.02% NP40, 0.01% deoxycholate) for 15 min, X-gal staining was performed by incubating the samples overnight at 37°C in X-gal solution (20 mg/ml X-gal/dimethylformamide [Sigma-Aldrich, MO, United States], 5 mM $K_3Fe(CN)_6$, 5 mM $K_4Fe(CN)_6$, 2 mM $MgCl_2$, 0.02% NP-40, 0.01% sodium deoxycholate, 5 mM EDTA, and 1 × phosphate-buffered saline). The targeted vector included the bacterial beta-galactosidase reporter gene (*lacZ*) *sequence* and used the artificial substrate *X-gal*, which turns blue when cleaved by β-*galactosidase*. Nuclei were counterstained with Nuclear Fast Red (Sigma-Aldrich).

Immunohistochemistry and Western Blotting

Experiments were performed according to a previously described method (Xie et al., 2019). Mouse anti-Nsf (123011 and 123002, Synaptic Systems, Göttingen, Germany), rabbit anti-HRP-Gapdh (M171-7, MBL, MA, United States), mouse anti-SERT (SC-1458, Santa Cruz Biotechnology, TX, United States), rabbit anti-GluA2 (MAB397, Millipore, MA, United States) and GluA1-3 antibodies were used (Xie et al., 2019).

In Situ Hybridization

To confirm the expression pattern of *Nsf* in the mouse brain, we performed *in situ* hybridization using digoxigenin-labeled antisense RNA probes. The *Nsf* plasmid was prepared by pGEM-t kit PCR with the following primers: 5'-CGTGAA GTGTCCGCCTCT-TAGGCAAACCACCCTCCA-3' and 5-CTTGTCTTTAGCTTCAATGATAA-CGATAAGATTGAGCG ACGAA-3'. The subsequent experiments were performed according to previously described methods (Murata et al., 2020).

Three-Chamber Test

The three-chamber testing apparatus consisted of a rectangular, three-chambered box and a lid with an infrared video camera (TimeCSI2; Ohara & Co., Tokyo, Japan). Each chamber was 20 cm × 40 cm × 22 cm, and the dividing walls were made of acrylic partitions, with small rectangular openings (5 × 3 cm) allowing access into each chamber. Small wire cages (9 cm radius × 22 cm height) were placed in both corners of the three-chambered box and illuminated at 50 lx. The wire cage consisted of vertical bars, allowing minimal contact among the mice to prevent fighting. The test was performed in six sessions (Tochitani et al., 2016). In session I, the subject mouse was placed in the middle chamber of an empty cage to habituate and freely investigate for 5 min. In session II, an unfamiliar C57BL/6N female mouse (stranger 1) was placed in one of the cages, and the subject mouse was allowed to explore the three chambers without restrictions for 5 min. In sessions III-V, the stranger 1 mouse was kept in the same cage, and unrestricted exploration by the subject mouse was allowed for 5 min. In session VI, a second unfamiliar C57BL/6N female mouse (stranger 2) was placed in the same cage, and the subject mouse was placed in the middle chamber and allowed to explore the chambers without restrictions for 5 min. Each mouse was used once per day. The movement of the subject mouse was recorded with an infrared video camera, and the time spent in close interaction in each wire cage was analyzed with ImageJ CSI software (Ohara & Co). The time spent in close interaction in each wire cage was converted into a preference index. The preference index in the sociability test was calculated as follows: ([time spent exploring the stranger mouse] − [time spent exploring the empty cage])/[total time spent exploring both targets] × 100 (Hisaoka et al., 2018).

Ultrasonic Vocalization Task

Mouse pups ($n = 26$ in $Nsf^{+/+}$ mice and $n = 20$ in $Nsf^{+/-}$ mice) from different litters at postnatal day 6 were placed in an empty glass beaker in a sound attenuation recording chamber with an ultrasonic microphone (W500 × D350 × H350 mm). The frequency of the vocal sounds was observed using MKSPL software (Muromachi Kikai Co., Tokyo, Japan). Ultrasonic vocalizations from individual pups were recorded and analyzed for a period of 10 min using the Vocalization Analyzer software (Muromachi Kikai Co.). The same program was used to count all the calls above 30 kHZ.

Open-Field Test

The open-field test was used to assess locomotor activity and repetitive behavior in a relatively large novel environment in a square arena (48 cm × 48 cm) (MELQUEST Co., Toyama, Japan; Tochitani et al., 2016). Mice were placed in the right-front corner of the open-field arena and allowed free movement for 30 min while being tracked by the SCANET MV-40 (Noldus Information Technology, Wageningen, Netherlands) automated tracking system. The total distance and vertical activity were automatically collected and analyzed using this system.

Light/Dark Transition Test

The apparatus used for the light/dark transition test consisted of two boxes (15 cm × 15 cm × 15 cm), light and dark, each with a door (MELQUEST Co.). The light box illumination was 390 lx, whereas the dark box illumination was 2 lx. Mice were placed in the dark box, and the door was opened after initiating the test. The mice were allowed to move freely between the two chambers with the door open for 10 min.

Slice Biotinylation

Slice biotinylation was performed as previously described (Gill et al., 2011). Mouse hippocampal and midbrain slices (400 μm in thickness) were incubated in slicing buffer (124 mM NaCl, 26 mM $NaHCO_3$, 3 mM KCl, 10 mM glucose, 0.5 mM $CaCl_2$, and 4 mM $MgCl_2$) for 30 min and then recovered in biotinylation

solution (124 mM NaCl, 26 mM $NaHCO_3$, 3 mM KCl, 10 mM glucose, 2.3 mM $CaCl_2$, and 1.3 mM $MgCl_2$) for 30 min at 20–25°C. Slices were then preincubated in ice-cold biotinylation solution for 1 min. Surface proteins of the dissected tissue were labeled with sulfo-NHS-SS-biotin (1.5 mg/ml; Pierce) for 30 min on ice, and the reaction was quenched with biotinylation solution with 50 mM glycine three times. Slices were homogenized with Tris buffer (50 mM Tris, pH 7.4, 2 mM EGTA) and then sonicated. To isolate the membrane fraction, homogenates were centrifuged at 100,000 × *g* for 20 min, and the pellet was resuspended in RIPA buffer (50 mM Tris, pH 7.4, 1 mM EDTA, 2 mM EGTA, 150 mM NaCl, 1% NP40, and 0.5% DOC) for 30 min. The lysate was cleared by centrifugation at 100,000 × g for 20 min. High-capacity streptavidin agarose resins (Roche, Basel, Switzerland) were added and incubated at 4°C for 2 h. Non-bound internal protein solution was removed. Beads were washed with RIPA buffer and biotinylated surface proteins were eluted by boiling for 10 min in Laemmli buffer containing dithiothreitol (7.7 mg/ml). Eluted and internal proteins were detected using western blotting. Western blots were carried out using 10% Tris-glycine extended Stain-Free gradient gels (Bio-Rad, CA, United States) and subsequently transferred to nitrocellulose membranes (Bio-Rad). Gels were activated by UV exposure for 2 min using a ChemiDoc™ MP imager (Bio-Rad). The membranes were imaged for Stain-Free staining, and total protein was quantified using ImageLab 5.2.1 (Bio-Rad).

SDS-Digested Freeze-Fracture Replica Immunolabeling

"Brain slices (130 μm) were prepared from the hippocampi of post-natal day 28 mice for FRIL. Mice were perfused transcardially for 1 min with PBS, followed by 12 min of perfusion with 0.1 M PB containing 2% paraformaldehyde and 15% saturated picric acid solution at a rate of 5 ml/min. The brains were quickly removed from the skull and sliced (130 μm thick) on a vibratome (Dosaka, Kyoto, Japan). Hippocampal slices were cryoprotected in 30% glycerol in 0.1 M PB and high-pressure frozen using HPM010 machine (Bal-Tec, Balzers, Liechtenstein). The frozen slices were then freeze fractured at −130°C and replicated with an initial carbon layer (5 nm), shadowed unidirectionally with platinum (2 nm), and strengthened with a second carbon layer (15 nm) in a BAF060 freeze-etching machine (Bal-Tec). After thawing, the tissue attached to the replicas was solubilized by shaking at 80°C for 18 h in the following solubilisation solution: 15 mM Tris [hydroxymethyl]-aminomethane, 20% sucrose, and 2.5% sodium dodecyl sulfate, pH 8.3. Immunolabelling of replicas was carried out according to previously published procedures with minor modifications46. Blocking was performed with a solution consisting of 5% bovine serum albumin and 0.1% TWEEN 20 in TBS (pH 7.4). The replicas were incubated in primary antibodies (anti-GluA1-3 or anti-GluA1 antibodies, both generated in horse against synthetic peptides deduced from the common and unique aa sequences of the extracellular portion of GluA1, respectively) at 15°C for 3 days. The specificity of these antibodies in FRIL analysis was confirmed by the absence of labelling in parallel fibre-Purkinje cell synapses of GluA2/3 knock-out mice and hippocampal synapses of GluA1 knock-out mice. Following extensive washing with unbound primary antibody, the replicas were incubated with gold-conjugated anti-rabbit secondary antibodies (British Biocell International, Cardiff, United Kingdom; 5 nm), overnight at 15°C. To mark IMP clusters on exoplasmic-face derived from excitatory synapses, NMDA receptor labelling was carried out simultaneously with the secondary antibody incubation by adding mouse anti-NR1 antibody (clone 54.1, 1:100, Millipore), which was then detected by incubation with anti-mouse secondary antibodies (British Biocell International; 10 nm) at room temperature for 1 h. The replicas were then mounted on pioloform-coated copper mesh grids and examined at 80 kV acceleration voltage in an H-7650 transmission electron microscope equipped with a CCD camera (Hitachi High-Technologies Corporation, Tokyo, Japan). Electron micrographs captured at 400,00x were analysed with the program ImageJ (Rasband, W.S., ImageJ, U.S. National Institutes of Health, Bethesda, MA, http://imagej.nih.gov/ij/, 1997–2015) for measurement of synaptic area and quantification of immunogold particles within individual synapses. (Xie et al., 2019)."

Ultrastructural Reconstructions

Experiments were performed according to our previously described methods (Xie et al., 2019). PSD area was identified as the membrane facing PSD which is clearly identified as an electron-dense thickening in dendritic spines. Independent traces were drawn for the entire spine structure and PSD and three-dimensional area were obtained. Three-dimensional reconstruction of dendritic spines was carried out with the aid of reconstruct software (Reconstruct 1.1.0.0, available from https://synapseweb.clm.utexas.edu).

Electrophysiology

A glass microelectrode (Narishige, Tokyo, Japan) filled with artificial cerebrospinal fluid (ACSF, 2–4 MΩ electrical resistance) was used. Field excitatory postsynaptic potentials (fEPSPs) were recorded in the CA1 stratum radiatum with the glass microelectrode. For experiment of input-output relationship, the input-output curve of fEPSP slope (mV/ms) versus presynaptic fiber volleys (FV; mV) at the Schaffer collateral pathway was observed in slices. Paired-pulse facilitation, the short-term enhancement of synaptic efficacy following delivery of two closely spaced stimuli (inter-pulse interval; 25–500 ms), was also assessed. We induced long-term potentiation (LTP) with 100 pulses applied at a rate of 100 Hz for 1 s and long-term depression (LTD) with 900 pulses applied at a rate of 1 Hz for 15 min (Ishikawa et al., 2011). Hippocampal slice preparation and electrophysiology were performed according to our previously described methods (Xie et al., 2019).

Statistical Analysis

For All statistical analyses were performed using IBM SPSS Statistics 23 and JMP Pro 14. Pairwise comparisons

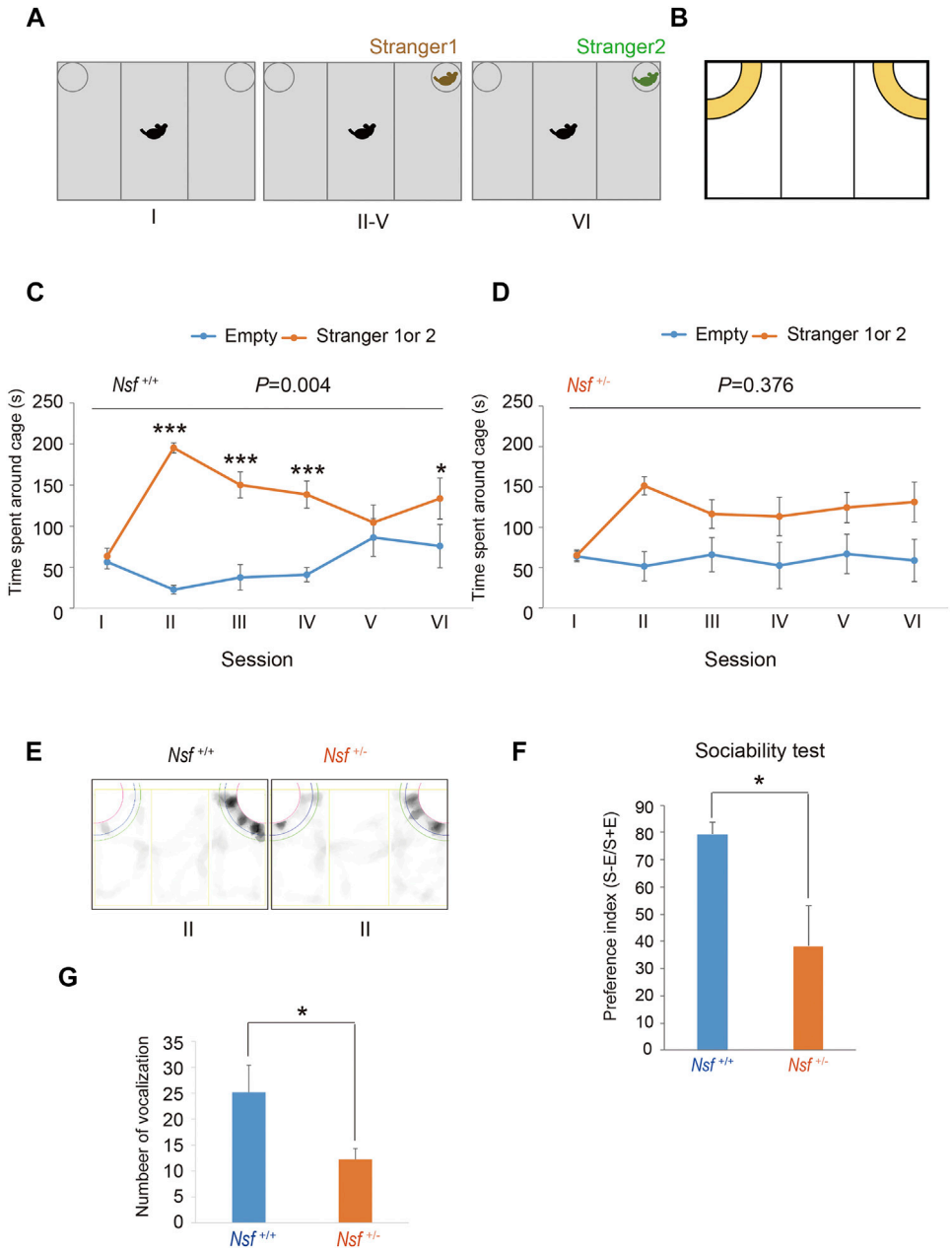

FIGURE 2 | Deficits in social interaction and communication in $Nsf^{+/-}$ mice. **(A)** Schematic representation of three-chamber social interaction tests. Session I: the subject mouse was placed in the middle chamber without any stimulants. Session II–V: stranger 1 was placed inside a cage located in one of the chambers. Then, the subject mouse was placed at the center of the middle chamber. The subject mouse investigated the same stimulant (stranger) mouse during each of the four sessions (II–V). Session VI: stranger 2, instead of stranger 1, was placed inside the same cage as session II-V. Then, the subject mouse was placed at the center of the middle chamber. The subject mouse moved freely in the three chambers for 5 min for each session. **(B)** Yellow represents the virtual interaction areas near cages. **(C)** Time spent around cages with "stranger 1 or 2" or "Empty" by $Nsf^{+/+}$ mice during sessions I–IV (n = 13, mean ± SEM. Two-way repeated measures ANOVA, p = 0.004, Tukey's post hoc test, ***p < 0.001, *p < 0.05). **(D)** Time spent around cages with "stranger 1 or 2" or "Empty" by $Nsf^{+/-}$ mice during sessions I–IV (n = 13, Mean ± SEM. Two-way repeated measures ANOVA, p = 0.376). **(E)** Representative mount-graph of each genotype during session II. **(F)** The preference index of the sociability (n = 13 for each genotype, mean ± SEM. Wilcoxon/Kruskal-Wallis test, *p < 0.05). **(G)** Number of ultrasonic vocalizations emitted by postnatal day 6 pups of each genotype during a 10 min separation from their mother (n = 26 in $Nsf^{+/+}$ mice and n = 20 in $Nsf^{+/-}$ mice, mean ± SEM. Spearman's rank-order test, *p < 0.05).

between groups were conducted using the two-tailed Student's *t*-test or Mann–Whitney *U test*, and correlations were tested for statistical significance using Pearson's correlation test or Spearman's rank-order test. A two-way repeated-measures ANOVA with Tukey's *post hoc* test was used for the analysis of data from the social interaction test. The null hypothesis was rejected at $p < 0.05$.

RESULTS

Generation of *Nsf* KO Mice

To elucidate NSF involvement in the onset and/or pathophysiology of ASD, we generated *Nsf* KO mice using the International Knockout Mouse Consortium targeting vector inserted between exons 5 and 6 of *Nsf* (**Figure 1A**). The targeted *Nsf* allele was designed to be a KO by splicing the cDNA into the *lacZ-neo* cassette, which was inserted upstream of a critical exon for *Nsf*, i.e., exon 6 (**Figure 1A**). The targeted allele of the founder ($Nsf^{+/-}$ mice) was confirmed by PCR (**Figure 1B**). Because of the *lacZ* cassette in the targeted allele, cells with the targeted allele were detected by X-gal staining (West et al., 2015). We found strong lacZ expression in the olfactory bulb and hippocampus and moderate expression in the cortex, striatum, and amygdala in $Nsf^{+/-}$ mice (**Figure 1C**, left panels). In contrast, no signals were detected in $Nsf^{+/+}$ mice (**Supplementary Figure S1A**). The X-gal staining patterns were identical to endogenous *Nsf* expression patterns confirmed by *in situ* hybridization (**Figure 1C**, right panels), indicating that the $Nsf^{+/-}$ mouse model was successfully established. Since homozygous KO mice ($Nsf^{-/-}$) caused early embryonic lethality, we used heterozygous KO mice ($Nsf^{+/-}$) in all experiments in this study. $Nsf^{+/-}$ mice were born in good health and grew into adulthood. There were no notable differences in body and brain weights between $Nsf^{+/+}$ and $Nsf^{+/-}$ mice (**Supplementary Figure S2**). In $Nsf^{+/-}$mouse brains, Nsf expression decreased by an average of 72% compared with that of $Nsf^{+/+}$ mouse brains ($Nsf^{+/+}$ mice, 1.00 ± 0.07; $Nsf^{+/-}$ mice, 0.72 ± 0.05, $^*p = 0.03$, Student's *t*-test) (**Figures 1D,E**). We examined the expression pattern of Nsf in $Nsf^{+/-}$mice using immunofluorescence. In support of the western blotting results, Nsf expression was decreased without changing the expression pattern itself (**Figure 1F** and **Supplementary Figure S1B**).

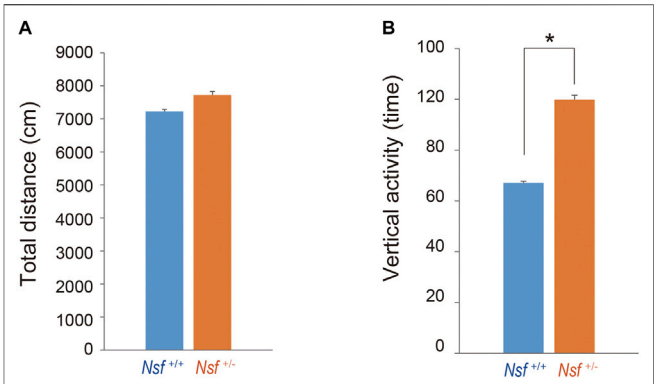

FIGURE 3 | Increase in repetitive behavior of $Nsf^{+/-}$ mice in the open field. **(A)** Total distance (locomotor activity) and **(B)** vertical activity (repetitive behavior) of $Nsf^{+/+}$ and $Nsf^{+/-}$ mice. ($Nsf^{+/-}$ mice, $n = 13$, $Nsf^{+/+}$ mice, $n = 11$, mean ± SEM. Student's t-test.$^*p < 0.05$).

$Nsf^{+/-}$ Mice Showed Abnormalities in Social Interaction and Communication

We evaluated the effect of *Nsf* downregulation on mouse behavior. First, social interaction was assessed by a three-chamber test with six sessions (Tochitani et al., 2016). Following habituation (session I), mice were introduced into the center of the box, which contained a cage with a stranger (stimulus) mouse in a corner (session II), and the session was repeated three times with the same stimulus mouse (session III-V; **Figure 2A**). In session VI, we introduced the stranger mouse to a new stimulus mouse (**Figure 2A**). $Nsf^{+/+}$ mice spent significantly more time around the cage containing a stranger mouse than around the empty cage in sessions II, III, and IV ($p < 0.01$, two-way repeated measures ANOVA; session I, $p = 0.776$; sessions II, III, and IV, $p < 0.001$; session V, $p = 0.453$, Tukey's post hoc test; **Figures 2B,C**). In session V, $Nsf^{+/+}$ mice showed a decline in the time spent around the cage containing a stranger mouse because stimuli became familiar, and the presentation of an unfamiliar mouse in session VI resulted in significantly more time spent around the cage containing a stranger mouse than around the empty cage (session VI, $p = 0.020$, Tukey's post hoc test; **Figure 2C**). In contrast, $Nsf^{+/-}$ mice did not show a preference for social targets throughout testing ($p = 0.376$, two-way repeated measures ANOVA; **Figure 2D**). In addition, $Nsf^{+/-}$ mice showed significantly less interaction with the stranger than $Nsf^{+/+}$ mice during session II ($Nsf^{+/-}$ mice, 38.3 ± 14.7; $Nsf^{+/+}$ mice, 79.4 ± 4.5, Wilcoxon/Kruskal-Wallis test, $^*p = 0.02$; **Figures 2E,F**). Separation-induced ultrasonic vocalizations were measured to evaluate the communication abilities of $Nsf^{+/-}$ mice. Ultrasonic calls are important for mother–infant social interactions (Smotherman et al., 1974) and represent important neurobehavioral development markers (Branchi et al., 1998). At postnatal day 6, $Nsf^{+/-}$ pups emitted significantly fewer calls than $Nsf^{+/+}$ pups ($Nsf^{+/+}$ mice, 25.2 ± 12.3; $Nsf^{+/-}$ mice, 12.3 ± 2.1, $^*p = 0.04$. Spearman's rank-order test; **Figure 2G**).

$Nsf^{+/-}$ Mice Showed Increased Repetitive Behavior and Anxiety

We measured the locomotor activity and relative behavior of $Nsf^{+/-}$ mice in a novel environment using an open-field test. There was no significant between-group difference in the total distance ($Nsf^{+/+}$ mice, 7,226.3 ± 444.6; $Nsf^{+/-}$ mice 7,719.6 ± 310.5, $p = 0.37$, Student's *t*-test; **Figure 3A**). In contrast, vertical activity (that is, repetitive behavior) were significantly increased in $Nsf^{+/-}$ mice compared with $Nsf^{+/+}$ mice ($Nsf^{+/+}$ mice, 67.1 ± 10.7; $Nsf^{+/-}$ mice 99.9 ± 8.8, $^*p = 0.04$, Student's *t*-test; **Figure 3B**). Next, to assess anxiety behavior, we conducted a light/dark box test. The latency to enter the light chamber served as an anxiety index, and $Nsf^{+/-}$ mice exhibited a longer latency to enter the light box than $Nsf^{+/+}$ mice ($Nsf^{+/+}$ mice, 324.0 ± 54.3; $Nsf^{+/-}$ mice, 878.8 ± 205.8; Student's *t*-test, $^*p = 0.02$; **Figure 4A**). The distance (dark box: $Nsf^{+/+}$ mice, 796.9 ± 59.8; $Nsf^{+/-}$ mice, 869.3 ± 64.7, $p = 0.44$. light box: $Nsf^{+/+}$ mice, 560.9 ± 71.59; $Nsf^{+/-}$ mice, 438.4 ± 56.3, $p = 0.21$, Student's *t*-test; **Figure 4B**) and duration (dark box: $Nsf^{+/+}$ mice, 4,052.5 ± 355.3; $Nsf^{+/-}$ mice, 4,538.3 ± 244.7, $p = 0.30$. light box: $Nsf^{+/+}$ mice, 1,932.1 ± 355.0; $Nsf^{+/-}$ mice, 1,449.8 ± 246.0, $p = 0.30$,

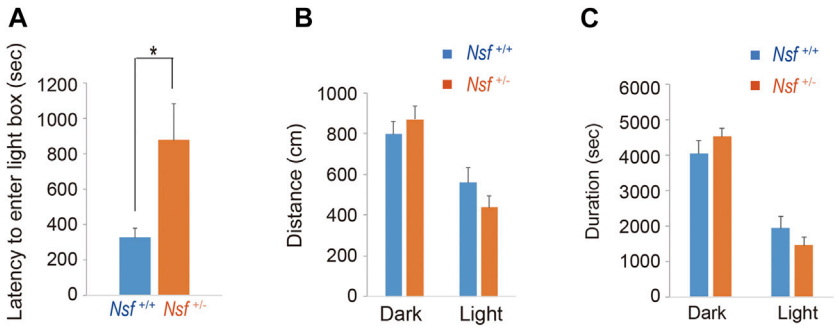

FIGURE 4 | *Nsf*$^{+/-}$ mice show anxiety in the light/dark box test. **(A)** The latency to the first entry of the light box. **(B)** The total distance between the light and dark boxes. **(C)** The time spent in the light and dark boxes. (n = 11 for each genotype, mean ± SEM. Student's t-test. *p < 0.05).

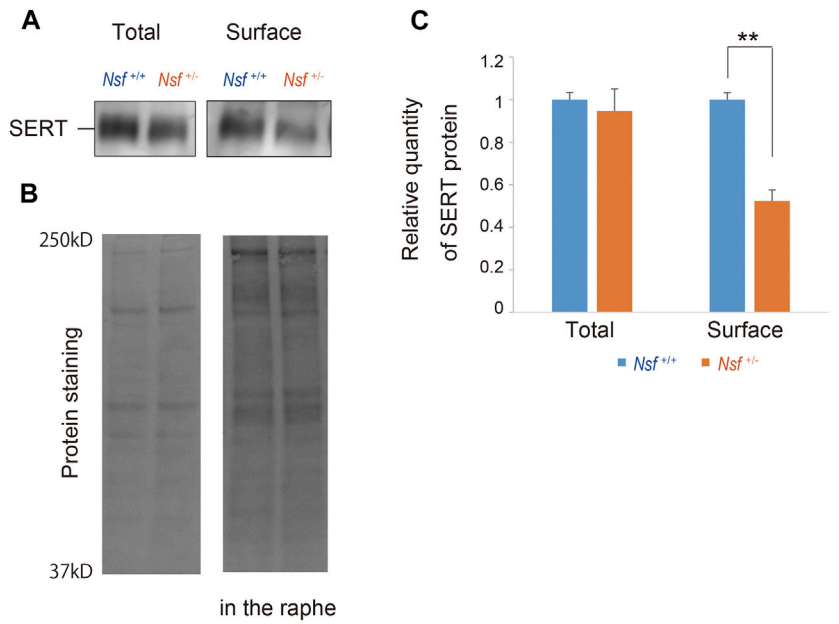

FIGURE 5 | Decrease in serotonin transporter (SERT) expression at the membrane surface in *Nsf*$^{+/-}$ mice. **(A)** Total and biotinylated membrane protein levels in the raphe of mouse of each genotype were analyzed by immunoblotting using an anti-SERT antibody. **(B)** Stain-Free gels were activated by UV exposure and imaged using a ChemiDocTM MP imager as protein loading control. **(C)** Relative band densities of SERT were quantified using scanning densitometry and normalized to protein loading control Results are expressed as a ratio of *Nsf*$^{+/+}$ mice expression, resulting in a *Nsf*$^{+/+}$ mice ratio of 1. (n = 4 for each genotype, mean ± SEM. Student's t-test, **p < 0.01).

Student's t-test; **Figure 4C**) in the dark and light boxes were not significantly different for either mouse.

Decrease in Serotonin Transporter Surface Expression in the Raphe of *Nsf*$^{+/-}$ Mice

We previously demonstrated that Nsf bound to SERT *in vitro* and vivo (Iwata et al., 2014). In addition, Nsf co-localized with SERT in the raphe of *Nsf*$^{+/+}$ mice (**Supplementary Figure S3**). Our previous study also demonstrated that Nsf was important for SERT membrane trafficking *in vitro* (Iwata et al., 2014). To confirm this *in vivo*, we compared SERT surface levels in the raphe from *Nsf*$^{+/+}$ and *Nsf*$^{+/-}$ mice using a cell-impermeant biotinylation reagent. In support of our *in vitro* data, SERT surface expression was decreased by an average of 48% in the raphe of *Nsf*$^{+/-}$ mice compared with that of *Nsf*$^{+/+}$ mice, despite the total SERT expression remaining unchanged (SERT surface expression: *Nsf*$^{+/+}$ mice, 0.31 ± 0.02; *Nsf*$^{+/-}$ mice, 0.15 ± 0.02, **p = 0.004. Total SERT expression: *Nsf*$^{+/+}$ mice, 1.29 ± 0.04; *Nsf*$^{+/-}$ mice, 1.22 ± 0.13, p = 0.690, Student's t-test; **Figures 5A,C**). As a protein loading control, Stain-Free gels were activated by UV exposure and imaged using a ChemiDoc™ MP imager (**Figure 5B**).

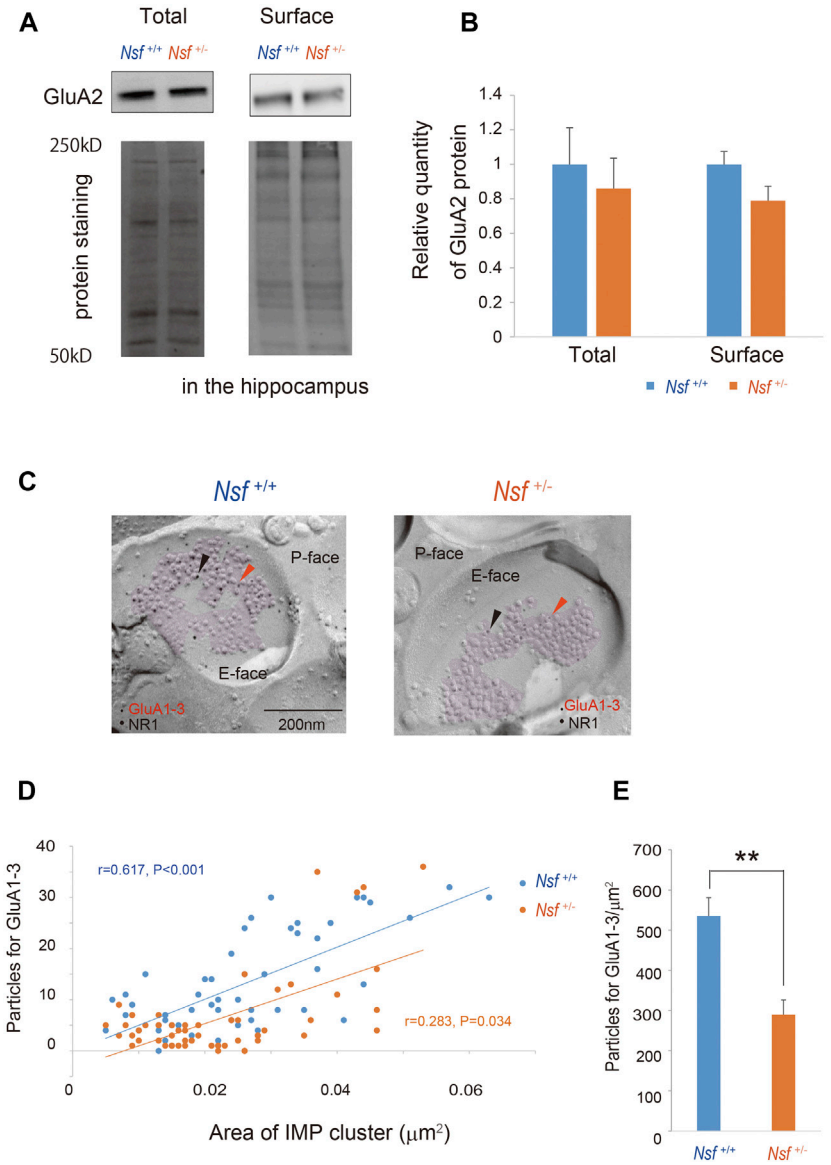

FIGURE 6 | Decrease in alpha-amino-3-hydroxy-5-methyl-4-isoxazole propionic acid (AMPA) receptor expression in postsynaptic membrane in *Nsf*$^{+/-}$ mice. **(A)** Total and biotinylated membrane protein levels in the hippocampus of mice of each genotype were analyzed by immunoblotting using anti-AMPA receptor (GluA) 2 antibody. Stain-Free gels were activated by UV exposure and imaged using a ChemiDocTM MP imager as a protein loading control. **(B)** Relative band densities of GluA2 were quantified using scanning densitometry. and normalized to protein loading control Results are expressed as a ratio of *Nsf*$^{+/+}$ mice expression, resulting in a *Nsf*$^{+/+}$ mice ratio of 1. (n = 4 for each genotype, mean ± SEM. Student's t-test). **(C)** Replicas were prepared from the hippocampal CA1 region. Using a transmission electron microscope, postsynaptic membrane specializations of excitatory synapses in replicas were identified in the exoplasmic (E)-face of the plasma membrane by clusters of intra-membrane particles (IMP clusters, purple). Immunoreactivity for GluA1-3 was visualized with 5 nm immunogold particles (orange arrowheads). Immunolabeling for the NR1 subunit was visualized with 10 nm immunogold particles (black arrowheads) to confirm the IMP cluster areas. **(D)** The numbers of immunoparticles for GluA1-3 in individual IMP clusters were plotted against the IMP cluster areas. Correlation between the GluA1-3 labeling number and synaptic area in mice of each genotype (Spearman's rank-order test: the *Nsf*$^{+/+}$ mice, n = 56 synapses, r = 0.617, p < 0.001; the *Nsf*$^{+/-}$ mice, n = 56 synapses, r = 0.283, $^{*}p$ = 0.034). **(E)** The average labeling particles for synaptic GluA1-3 in *Nsf*$^{+/-}$ and *Nsf*$^{+/+}$ mice (mean ± SEM. Spearman's rank-order test, $^{**}p$ < 0.01).

Nsf Contributes to GluA1-3 Accumulation at the Synaptic Membrane Surface

We focused on the hippocampus in the central nervous system because Nsf expression is the highest in this brain region (Puschel et al., 1994; **Figure 1C**). Indeed, *in vitro* studies have shown that Nsf interacts with GluA2 and regulates the surface expression of GluA2-containing AMPA receptors in hippocampal neurons (Nishimune et al., 1998; Noel et al., 1999; Lu et al., 2014). Here, we examined whether *Nsf* haploinsufficiency changed GluA2 membrane expression *in vivo*. Using a cell-impermeant

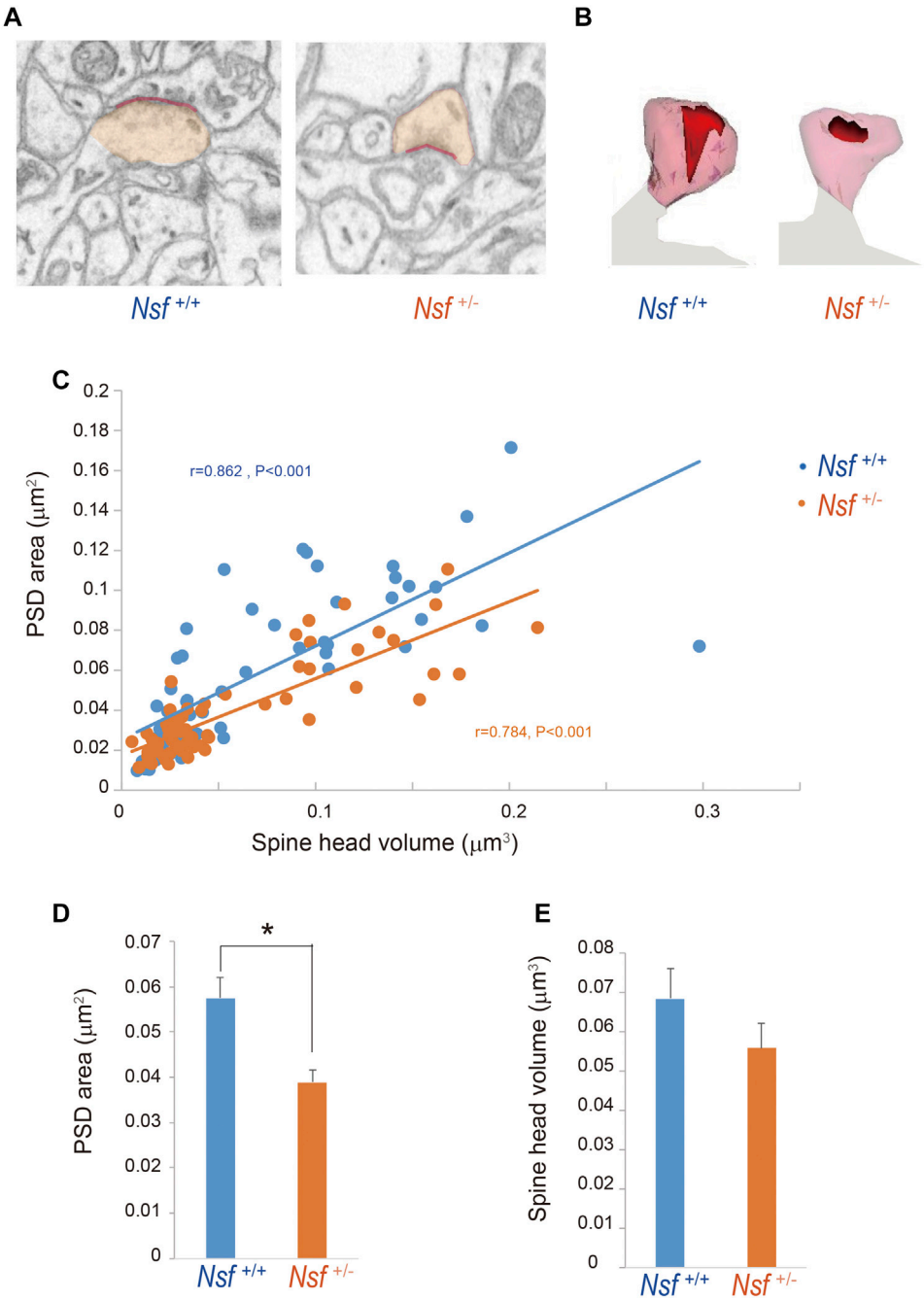

FIGURE 7 | Decrease in postsynaptic density (PSD) area in postsynaptic membrane in *Nsf*$^{+/-}$ mice. Reconstruction of dendritic spines from serial FIB-SEM images. PSD was defined as postsynaptic membrane specialization. **(A)** Representative FIB-SEM images of the hippocampal CA1 region of *Nsf*$^{+/+}$ and *Nsf*$^{+/-}$ mice (spine head in orange and PSD in red). **(B)** Examples of 3D-reconstructed spines from *Nsf*$^{+/+}$ and *Nsf*$^{+/-}$ mice (head in transparent orange and PSD in red). **(C)** Correlation between the PSD area and spine head volume in mice of each genotype (Spearman's rank-order test: *Nsf*$^{+/+}$ mice, $n = 58$ synapses, $r = 0.862$, $p < 0.001$; *Nsf*$^{+/-}$ mice, $n = 65$ synapses, $r = 0.784$, $p < 0.001$). **(D)** The average PSD areas and **(E)** head volumes in the hippocampus of *Nsf*$^{+/+}$ and *Nsf*$^{+/-}$ mice (mean ± SEM. Spearman's rank-order test, $p = 0.074$).

biotinylation reagent, we compared GluA2 surface levels in the hippocampus of *Nsf*$^{+/+}$ and *Nsf*$^{+/-}$ mice. Total GluA2 was not changed, and unexpectedly, GluA2 surface expression was not changed significantly in *Nsf*$^{+/-}$ mice (total expression: *Nsf*$^{+/+}$ mice, 0.07 ± 0.01; *Nsf*$^{+/-}$ mice, 0.06 ± 0.01, $p = 0.673$. GluA2 surface expression: *Nsf*$^{+/+}$ mice, 0.14 ± 0.02; *Nsf*$^{+/-}$ mice, 0.11 ± 0.02, $p = 0.336$. Student's *t*-test; **Figures 6A,B**). Nsf has been previously reported to be highly expressed in the PSD (Walsh and Kuruc,

1992). Therefore, we examined whether a decrease in Nsf levels affected AMPA receptor expression, including GluA2, at the postsynaptic membrane. Using the FRIL technique (Xie et al., 2019), we monitored endogenous AMPA receptor (GluA1-3) expression at the surfaces of the stratum radiatum spines of the hippocampal CA1 region. We could not measure GluA2 levels specifically, as there was no appropriate anti-GluA2 antibody available for this technique. The subcellular localization of the postsynaptic membrane area in a dendritic spine was identified in the exoplasmic face of the replicas as an area accompanied by clustered intramembrane particles (IMP) labeled for the NR1 subunit of the NMDA receptor (**Figure 6C**). The number of immunogold particles for GluA1-3 in individual IMP cluster areas was proportional to the area of the IMP clusters in both $Nsf^{+/+}$ and $Nsf^{+/-}$ mice ($Nsf^{+/+}$ mice, $r = 0.617$, $p < 0.001$; r = 0.283, $Nsf^{+/-}$ mice, $p = 0.034$, Spearman's rank-order test; **Figure 6D**). In contrast, a significant reduction of 54% in the labeling density for synaptic GluA1-3 was observed in $Nsf^{+/-}$ mice compared with $Nsf^{+/+}$ mice ($Nsf^{+/+}$ mice, 535.5 ± 45.5, gold particles/μm^2; $Nsf^{+/-}$ mice, 289.7 ± 36.8, gold particles/μm^2, Spearman's rank-order test, $^{**}p = 0.005$; **Figure 6E**).

Postsynaptic Density Areas Are Decreased in $Nsf^{+/-}$ Mice

To investigate whether the decrease in GluA1-3 levels at the synaptic membrane surface of $Nsf^{+/-}$ mice was due to an enlargement of PSD areas in the mutant mice, we reconstructed spines from serial electron micrographs captured using a focused ion beam scanning electron microscope (FIB-SEM). PSDs were observed as electron-dense thickenings of the postsynaptic plasma membrane, which was similar to their appearance in conventional transmission electron microscopy (**Figure 7A**). The PSD region was traced with a red line in individual images, and the entire area of the postsynaptic membrane specialization as well as the spine head (orange) was reconstructed (**Figures 7A,B**). The area of the PSD was proportional to the volume of the spine head in both genotypes ($r = 0.862$, $p < 0.001$ for $Nsf^{+/+}$ mice and $r = 0.784$, $p < 0.001$ for $Nsf^{+/-}$ mice; **Figure 7C**). The average PSD areas were decreased in $Nsf^{+/-}$ mice (0.057 ± 0.004 μm^2 for $Nsf^{+/+}$ mice and 0.039 ± 0.001 μm^2 for $Nsf^{+/-}$ mice, Spearman's rank-order test, $^{*}p = 0.049$; **Figure 7D**), whereas there was no significant difference between the two genotypes in spine head volumes (0.068 ± 0.008 μm^3 for $Nsf^{+/+}$ mice and 0.056 ± 0.006 μm^3 for $Nsf^{+/-}$ mice, Spearman's rank-order test, $p = 0.074$; **Figure 7E**).

Nsf Is Required for Normal Induction of Synaptic Plasticity Long-Term Depression but Not Long-Term Potentiation Induction

Synaptic AMPA receptors have been suggested to be important for synaptic plasticity, such as LTP and LTD (Luscher et al., 2000; Carroll et al., 2001; Sheng and Lee, 2001; Malenka, 2003). Therefore, we examined whether LTP and LTD induction were influenced by decreased levels of AMPA receptors in $Nsf^{+/-}$ mice. LTD was induced in hippocampal CA1 neurons

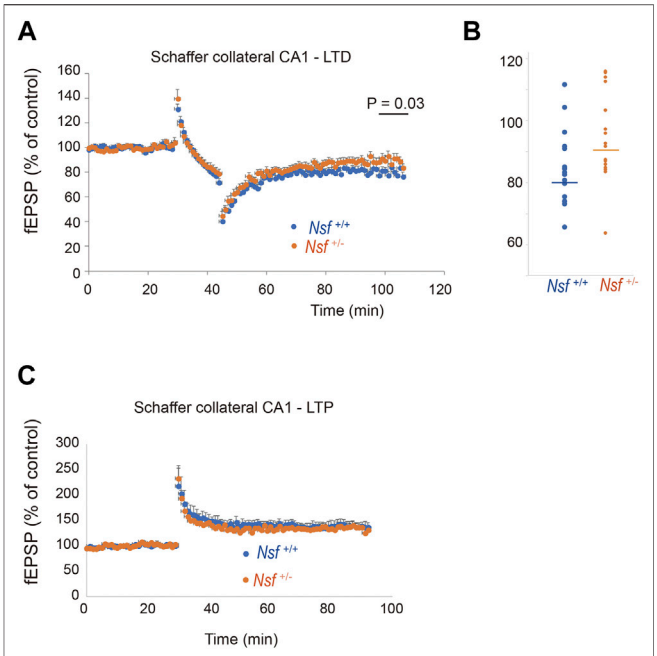

FIGURE 8 | Nsf is required for normal induction of long-term depression (LTD). **(A)** Electrophysiological analyses of the effects of Nsf on hippocampal LTD. LTD was induced by low-frequency stimulation (LFS; 1 Hz; 900 pulses, 15 min) of the Schaffer collaterals in hippocampus slices from $Nsf^{+/-}$ and $Nsf^{+/+}$ mice (n = 17 slices for each mouse. Mean ± SEM. Mann–Whitney U test, $p = 0.031$ at the boxed time points, 97–106 min). A value of 100% corresponds to the pre-LFS baseline. **(B)** The dispersion of individual fEPSP data for $Nsf^{+/+}$ and $Nsf^{+/-}$ mice at the significant time point (97–106 min) in **(A)**. **(C)** Electrophysiological analyses of the effects of Nsf on hippocampal long-term potentiation (LTP). LTP was induced by high-frequency stimulation (HFS) (100 Hz; 100 pulses, 1 s) of the Schaffer collaterals from $Nsf^{+/-}$ and $Nsf^{+/+}$ mice ($n = 6$ slices for $Nsf^{+/-}$ mice and $n = 9$ slices for $Nsf^{+/-}$ mice. Mean ± SEM. Student's t-test, $p = 0.77$). A value of 100% corresponds to the pre-LFS baseline.

by low-frequency stimulation of Schaffer collaterals. Expectedly, elevation of recorded fEPSPs was decreased in $Nsf^{+/-}$ mice compared to $Nsf^{+/+}$ mice at the indicated time points (97–106 min). (Mann–Whitney U test, $^{*}p = 0.031$; **Figures 8A,B**). We also induced LTP by high-frequency stimulation of Schaffer collaterals in both mice and observed no change in the fEPSPs (**Figure 8C**). In addition, we analysed input-output relationship and paired-pulse facilitation (PPF) to assess the strength of basal synaptic transmission and the presynaptically mediated form of potentiation, respectively. No significant difference was observed in terms of basal synaptic function between the $Nsf^{+/+}$ mice and the $Nsf^{+/-}$ mice (**Supplementary Figures S4A,B**).

DISCUSSION

A decrease in NSF expression has been suggested in individuals with ASD (Iwata et al., 2014); however, causality between NSF expression and the onset and/or pathophysiology of ASD remains unclear. In this study, we first generated $Nsf^{+/-}$ mice and found

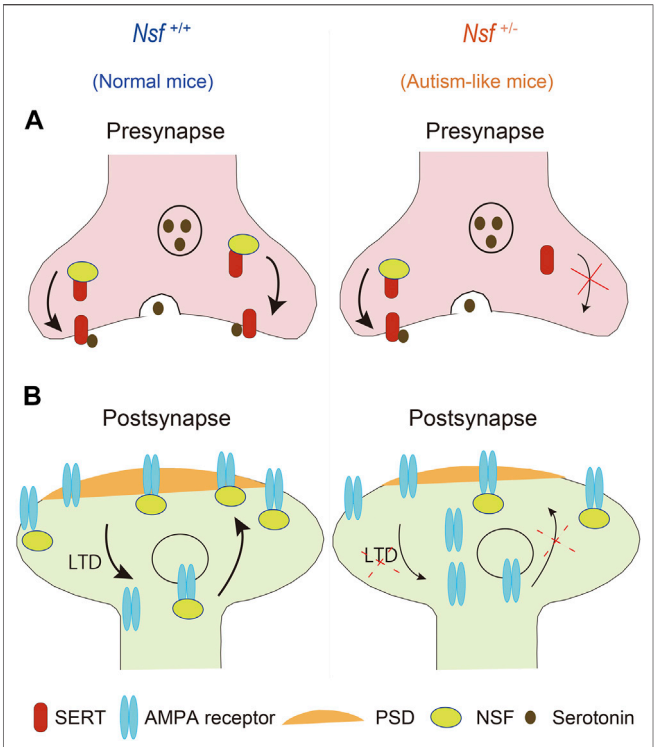

FIGURE 9 | Schematic representation of possible mechanisms through which haploinsufficiency of Nsf causes neurophysiological and behavioral phenotypes similar to autism spectrum disorder via defective membrane trafficking of serotonin transporter (SERT) and alpha-amino-3-hydroxy-5-methyl-4-isoxazole propionic acid (AMPA) receptor in mice.

that the mice showed core ASD symptoms, such as abnormal sociability and communication, repetitiveness, and anxiety. Additionally, these mice showed decreased membrane expression of SERT and AMPA receptors in the brain, which were hound in ASD patients (Purcell et al., 2001a; Nakamura et al., 2010; Iwata et al., 2014). The mice also showed impaired PSD and LTD in the hippocampal CA1 region.

Decrease in Membrane Expression of Serotonin Transporter and Alpha-Amino-3-Hydroxy-5-Methyl-4-Isoxazole Propionic Acid Receptors in *Nsf* $^{+/-}$ Mice

Previous *in vitro* studies have shown the importance of NSF in serotonergic and glutaminergic systems. We have previously reported that NSF interacts with SERT and traffics it to the plasma membrane *in vitro* (Iwata et al., 2014). To the best of our knowledge, the present study is the first to show that haploinsufficiency of *Nsf* leads to a significant decrease in the membrane expression of SERT *in vivo*. *Nsf* also interacts with GluA2 and regulates the surface expression of GluA2-containing AMPA receptors in hippocampal neurons (Nishimune et al., 1998; Noel et al., 1999). In the present study, our results showed that membrane GluA2 expression does not change in the hippocampus of *Nsf*$^{+/-}$ mice. This may be due to haploinsufficiency of *Nsf* in our mice (that is, not homozygous KO mice) and/or the whole membrane fraction was corrected instead of correcting the synaptic membrane where *Nsf* is enriched (Walsh and Kuruc, 1992). Indeed, when we measured AMPA receptor levels (GluA1-3) in the postsynaptic membrane using the FRIL technique, a significant reduction in the labeling density for synaptic GluA1-3 receptors was observed in *Nsf*$^{+/-}$ mice compared with *Nsf*$^{+/+}$ mice (**Figure 6E**). With this technique, we could not measure GluA2 specifically because there was no appropriate anti-GluA2 antibody available. In the forebrain, including the hippocampus and cerebral neocortex, the predominantly expressed subunits are GluA1 and GluA2, and the major neuronal population expresses AMPA receptors primarily composed of heterotetramers of GluA1 and GluA2 (Isaac et al., 2007), and NSF does not interact with GluA1 (Song et al., 1998). Therefore, a decrease in the synaptic GluA1-3 receptor density may reflect a reduction in GluA2 levels in the postsynaptic membrane. In ASD patients, partial loss of *NSF* transcription and reduced SERT and GluA2 expression at the membrane surface without a decrease in their expression at the mRNA level have been reported (Purcell et al., 2001a; Nakamura et al., 2010; Iwata et al., 2014). The *Nsf*$^{+/-}$ mouse is a unique model that recapitulates the molecular abnormalities observed in ASD patients.

Haploinsufficiency of *Nsf* Leads to Autism Spectrum Disorder-like Abnormal Behaviors

Notably, most behavioral alterations in *Nsf* $^{+/-}$ mice we report here are relevant to core ASD symptoms. While SERT and GluA2 are implicated in the pathology of ASD, behavioral abnormalities of SERT or GluA2 homozygous KO mice are inconsistent with ASD-like behaviors. SERT homozygous KO mice show impaired locomotor function, increased anxiety, and reduced aggression and depression-like behaviors (Holmes et al., 2002; Wellman et al., 2007; Murphy et al., 2008; Bartolomucci et al., 2010). GluA2 homozygous KO mice show decreased object exploration, rearing, grooming, locomotion in a novel environment, and abnormal motor coordination and learning (Jia et al., 1996; Gerlai et al., 1998). Notably, both SERT and GluA2 heterozygous KO mice appeared to be normal (Gerlai et al., 1998; Bartolomucci et al., 2010). Interestingly, *Pten*$^{+/-}$ mice show impaired social interactions, and this phenotype is exacerbated by crossing with SERT$^{+/-}$ mice (Page et al., 2009). Moreover, tryptophan depletion has been shown to exacerbate repetitive behavior and elevate anxiety in adults with autism (McDougle et al., 1996). These reports suggest that a decrease in SERT expression could increase vulnerability to ASD-like behaviors. It is possible that a modest decrease in membrane expression of SERT (48% of control) and AMPA receptors (54% of control) due to haploinsufficiency of *Nsf* may lead to ASD-like behaviors in a combined manner. Alternatively, NSF has been reported to interact with β2 adrenergic receptors and $GABA_A$ receptors and is thought to affect their trafficking patterns or recycling (Cong et al., 2001; Kittler et al., 2001; Leil et al., 2004). Therefore, it is possible that membrane expression of these receptors might

be altered in *Nsf*$^{+/-}$ mice, which may affect mouse behavior. The mechanisms underlying the behavioral abnormalities in *Nsf* $^{+/-}$ mice will be a subject for future investigation.

Abnormal Postsynaptic Density in *Nsf* $^{+/+}$ Mice

PSD is an electron-dense structure beneath the postsynaptic membrane of excitatory synapses and is usually located at the dendritic spine tip. PSD is composed of proteins, including neurotransmitter receptors, cell adhesion molecules, scaffold proteins, signaling enzymes, cytoskeleton proteins, and membrane trafficking proteins (Sheng and Hoogenraad, 2007; Kaizuka and Takumi, 2018). Many of the glutamate receptor proteins, including AMPA receptors, are concentrated in the PSD (Dosemeci et al., 2016). PSD protein mutations, including AMPA receptors, are associated with neurodevelopmental disorders, such as ASD and schizophrenia (Coley and Gao, 2018; Kaizuka and Takumi, 2018). In the current study, *Nsf* $^{+/-}$ mice exhibited decreased PSD areas. One explanation for this reduction is decreased AMPA receptor levels in the IMP in *Nsf* $^{+/-}$ mice. However, there is a possibility that the membrane expression of other proteins localized at the PSD also decreases. Further investigation is needed to assess the reasons for the reduction in PSD areas in *Nsf* $^{+/+}$ mice.

Long-Term Depression Impairment in *Nsf* $^{+/-}$ Mice

Synaptic AMPA receptors have been suggested to be important for synaptic plasticity, such as LTP and LTD (Luscher et al., 2000; Carroll et al., 2001; Sheng and Lee, 2001; Malenka, 2003). A previous study revealed that blockade of the NSF–GluA2 interaction by a specific peptide introduced into neurons prevented homosynaptic LTD in the hippocampal CA1 region (Luthi et al., 1999). In contrast, another study reported that AP2, a clathrin adaptor, binds to GluA2 with the same binding site as with NSF and that AP2-GluA2 binding is essential for hippocampal LTD, while NSF function is needed to maintain synaptic AMPA receptor responses but is not directly required for LTD (Lee et al., 2002). Here, we showed that LTD was impaired in the hippocampal CA1 region in *Nsf* $^{+/-}$ mice. Our results support those of a previous study suggesting that the interaction between NSF and GluA2 is important for LTD expression (Luthi et al., 1999). LTD dysregulation has been observed in several mouse models of ASD (Piochon et al., 2016). In the hippocampus, enhanced LTD has been reported in Fmr1$^{-/-}$ mice (Huber et al., 2002) and Mecp2$^{-/-}$ mice (Asaka et al., 2006), and reduced LTD has been reported in *Tsc2*$^{+/-}$ (Auerbach et al., 2011) and Syngap$^{+/-}$ mice (Barnes et al., 2015). To date, the direct link between LTD deregulation and phenotypes has not been clarified in ASD patients. However, LTD-like processes are involved in synaptic pruning; therefore, LTD dysregulation in ASD may primarily manifest as deficits in developmental synaptic pruning and the optimization of connectivity in the brain (Hansel, 2019).

CONCLUSION

This study revealed that defective membrane trafficking of SERT and GluA2 due to haploinsufficiency of *Nsf* causes neurophysiological and behavioral phenotypes similar to ASD in mice (**Figure 9**). Although ASD showed abnormal membrane expression of many neurotransmitter receptors and transporters, including SERT and AMPA receptors, the involvement of these receptors and transporters in ASD has never been investigated simultaneously. The idea that these transmitter abnormalities have an upstream cause has not yet been discussed. To the best of our knowledge, the present study is the first to demonstrate that haploinsufficiency of *Nsf* leads to defects in the membrane expression of both SERT and AMPA receptors and causes ASD-like behavioral deficits. Notably, haploinsufficiency of *Nsf* was sufficient to develop abnormalities similar to ASD phenotypes in mice. This suggests that there may be a type of ASD with neurotransmitter and behavioral abnormalities whose root cause is the downregulation of NSF expression. Additionally, *Nsf* $^{+/-}$ mice provide new opportunities to explore ASD pathophysiology as a model that has neurotransmitter, neurophysiological, and behavioral phenotypes similar to ASD.

DATA AVAILABILITY STATEMENT

The original contributions presented in the study are included in the article/**Supplementary Material**, further inquiries can be directed to the corresponding author.

ETHICS STATEMENT

The animal study was reviewed and approved by the Animal Research Committee, University of Fukui, and the Institutional Animal Care and Use Committee of the Maebashi Institute of Technology.

AUTHOR CONTRIBUTIONS

M-JX performed almost all experiments, including electron microscope experiments. KI generated *Nsf* knockout mice and wrote the manuscript together with M-JX. YI performed all electrophysiological experiments. YN performed behavior experiments. TT performed behavior experiments and analyzed the SDS-FRIL experiments. KM performed *in situ* hybridization experiments. YF advised and performed certain SDS-FRIL and FIB-SEM experiments and wrote those sections in the manuscript. HM conceived the project, directed the research, and wrote the manuscript together with M-JX. All listed members provided invaluable comments on the article and contributed to the final version of the manuscript.

FUNDING

This work was supported, in part, by KAKENHI from the Ministry of Education, Culture, Sports, Science and Technology of Japan (16H05373 and 19H03581 to HM, 21K06752 to M-JX, and 19K08041 to KI). This work was also supported, in part, by Takeda Science Foundation.

ACKNOWLEDGMENTS

We are grateful to Y. Sasaki, S. Kanae, I. Kumano, Y. Ishii, S. Shimizu, K. Tamai, M. Murasima, and N. Kasahara for technical assistance and T. Taniguchi for secretarial assistance. We also thank NPO Biotechnology Research and Development for technical assistance. We thank Gioavnni Piccoli for the information about Nsf antibody (123002, Synaptic Systems, Göttingen, Germany).

SUPPLEMENTARY MATERIAL

The Supplementary Material for this article can be found online at: https://www.frontiersin.org/articles/10.3389/fgene.2021.748627/full#supplementary-material

REFERENCES

Abramson, R. K., Wright, H. H., Carpenter, R., Brennan, W., Lumpuy, O., and Cole, E. (1989). Elevated blood serotonin in autistic probands and their first-degree relatives. *J. Autism Dev. Disord.* 19, 397–407. doi:10.1007/BF02212938

Aldred, S., Moore, K. M., Fitzgerald, M., and Waring, R. H. (2003). Plasma amino acid levels in children with autism and their families. *J. Autism Dev. Disord.* 33, 93–97. doi:10.1023/a:1022238706604

Anderson, G. M., Freedman, D. X., Cohen, D. J., Volkmar, F. R., Hoder, E. L., Mcphedran, P., et al. (1987). Whole blood serotonin in autistic and normal subjects. *J. Child. Psychol. Psychiatry* 28, 885–900. doi:10.1023/a:1022238706604

Asaka, Y., Jugloff, D. G. M., Zhang, L. A., Eubanks, J. H., and Fitzsimonds, R. M. (2006). Hippocampal synaptic plasticity is impaired in the Mecp2-null mouse model of Rett syndrome. *Neurobiol. Dis.* 21, 217–227. doi:10.1023/a:1022238706604

Auerbach, B. D., Osterweil, E. K., and Bear, M. F. (2011). Mutations causing syndromic autism define an axis of synaptic pathophysiology. *Nature* 480, 63–68. doi:10.1038/nature10658

Barnes, S. A., Wijetunge, L. S., Jackson, A. D., Katsanevaki, D., Osterweil, E. K., Komiyama, N. H., et al. (2015). Convergence of Hippocampal Pathophysiology in Syngap+/- and Fmr1-/y Mice. *J. Neurosci.* 35, 15073–15081. doi:10.1523/JNEUROSCI.1087-15.2015

Bartolomucci, A., Carola, V., Pascucci, T., Puglisi-Allegra, S., Cabib, S., Lesch, K. P., et al. (2010). Increased vulnerability to psychosocial stress in heterozygous serotonin transporter knockout mice. *Dis. Models Mech.* 3, 459–470. doi:10.1523/JNEUROSCI.1087-15.201510.1242/dmm.004614

Bejjani, A., O'neill, J., Kim, J. A., Frew, A. J., Yee, V. W., Ly, R., et al. (2012). Elevated glutamatergic compounds in pregenual anterior cingulate in pediatric autism spectrum disorder demonstrated by 1H MRS and 1H MRSI. *PLoS One* 7, e38786. doi:10.1371/journal.pone.0038786

Beneyto, M., and Meador-Woodruff, J. H. (2004). Expression of transcripts encoding AMPA receptor subunits and associated postsynaptic proteins in the macaque brain. *J. Comp. Neurol.* 468, 530–554. doi:10.1002/cne.10981

Branchi, I., Santucci, D., Vitale, A., and Alleva, E. (1998). Ultrasonic vocalizations by infant laboratory mice: a preliminary spectrographic characterization under different conditions. *Dev. Psychobiol.* 33, 249–256. doi:10.1002/(sici)1098-2302(199811)33:3<249:aid-dev5>3.0.co;2-r

Brown, M. S., Singel, D., Hepburn, S., and Rojas, D. C. (2013). Increased glutamate concentration in the auditory cortex of persons with autism and first-degree relatives: a (1)H-MRS study. *Autism Res.* 6, 1–10. doi:10.1002/aur.1260

Carroll, R. C., Beattie, E. C., Von Zastrow, M., and Malenka, R. C. (2001). Role of AMPA receptor endocytosis in synaptic plasticity. *Nat. Rev. Neurosci.* 2, 315–324. doi:10.1038/35072500

Ciaranello, R. D. (1982). Hyperserotonemia and early infantile autism. *N. Engl. J. Med.* 307, 181–183. doi:10.1056/NEJM198207153070310

Coley, A. A., and Gao, W. J. (2018). PSD95: A synaptic protein implicated in schizophrenia or autism. *Prog. Neuropsychopharmacol. Biol. Psychiatry* 82, 187–194. doi:10.1016/j.pnpbp.2017.11.016

Cong, M., Perry, S. J., Hu, L. A., Hanson, P. I., Claing, A., and Lefkowitz, R. J. (2001). Binding of the beta2 adrenergic receptor to N-ethylmaleimide-sensitive factor regulates receptor recycling. *J. Biol. Chem.* 276, 45145–45152. doi:10.1074/jbc.M106087200

Cook, E. H., Jr., Leventhal, B. L., and Freedman, D. X. (1988). Serotonin and measured intelligence. *J. Autism Dev. Disord.* 18, 553–559. doi:10.1007/BF02211873

Cook, E. H., Jr., Leventhal, B. L., Heller, W., Metz, J., Wainwright, M., and Freedman, D. X. (1990). Autistic children and their first-degree relatives: relationships between serotonin and norepinephrine levels and intelligence. *J. Neuropsychiatry Clin. Neurosci.* 2, 268–274. doi:10.1176/jnp.2.3.268

Cross, S., Kim, S. J., Weiss, L. A., Delahanty, R. J., Sutcliffe, J. S., Leventhal, B. L., et al. (2008). Molecular genetics of the platelet serotonin system in first-degree relatives of patients with autism. *Neuropsychopharmacology* 33, 353–360. doi:10.1038/sj.npp.1301406

Dosemeci, A., Weinberg, R. J., Reese, T. S., and Tao-Cheng, J. H. (2016). The Postsynaptic Density: There Is More than Meets the Eye. *Front. Synaptic Neurosci.* 8, 23. doi:10.3389/fnsyn.2016.00023

Eissa, N., Al-Houqani, M., Sadeq, A., Ojha, S. K., Sasse, A., and Sadek, B. (2018). Current Enlightenment About Etiology and Pharmacological Treatment of Autism Spectrum Disorder. *Front. Neurosci.* 12, 304. doi:10.3389/fnins.2018.00304

Evers, D. M., Matta, J. A., Hoe, H. S., Zarkowsky, D., Lee, S. H., Isaac, J. T., et al. (2010). Plk2 attachment to NSF induces homeostatic removal of GluA2 during chronic overexcitation. *Nat. Neurosci.* 13, 1199–1207. doi:10.1038/nn.2624

Fleming, K. G., Hohl, T. M., Yu, R. C., Muller, S. A., Wolpensinger, B., Engel, A., et al. (1998). A revised model for the oligomeric state of the N-ethylmaleimide-sensitive fusion protein. *NSF. J. Biol. Chem.* 273, 15675–15681. doi:10.1074/jbc.273.25.15675

Fujihara, Y., Kaseda, K., Inoue, N., Ikawa, M., and Okabe, M. (2013). Production of mouse pups from germline transmission-failed knockout chimeras. *Transgenic Res.* 22, 195–200. doi:10.1007/s11248-012-9635-x

Gerlai, R., Henderson, J. T., Roder, J. C., and Jia, Z. (1998). Multiple behavioral anomalies in GluR2 mutant mice exhibiting enhanced LTP. *Behav. Brain Res.* 95, 37–45. doi:10.1016/s0166-4328(98)00002-3

Gill, M. B., Kato, A. S., Roberts, M. F., Yu, H., Wang, H., Tomita, S., et al. (2011). Cornichon-2 modulates AMPA receptor-transmembrane AMPA receptor regulatory protein assembly to dictate gating and pharmacology. *J. Neurosci.* 31, 6928–6938. doi:10.1523/JNEUROSCI.6271-10.2011

Hanley, H. G., Stahl, S. M., and Freedman, D. X. (1977). Hyperserotonemia and amine metabolites in autistic and retarded children. *Arch. Gen. Psychiatry* 34, 521–531. doi:10.1001/archpsyc.1977.01770170031002

Hanley, J. G., Khatri, L., Hanson, P. I., and Ziff, E. B. (2002). NSF ATPase and alpha-/beta-SNAPs disassemble the AMPA receptor-PICK1 complex. *Neuron* 34, 53–67. doi:10.1016/s0896-6273(02)00638-4

Hansel, C. (2019). Deregulation of synaptic plasticity in autism. *Neurosci. Lett.* 688, 58–61. doi:10.1016/j.neulet.2018.02.003

Hanson, P. I., Roth, R., Morisaki, H., Jahn, R., and Heuser, J. E. (1997). Structure and conformational changes in NSF and its membrane receptor complexes visualized by quick-freeze/deep-etch electron microscopy. *Cell* 90, 523–535. S0092-8674(00)80512-7.

Hay, J. C., and Scheller, R. H. (1997). SNAREs and NSF in targeted membrane fusion. *Curr. Opin. Cel Biol.* 9, 505–512. doi:10.1016/s0955-0674(97)80026-9

Hisaoka, T., Komori, T., Kitamura, T., and Morikawa, Y. (2018). Abnormal behaviours relevant to neurodevelopmental disorders in Kirrel3-knockout mice. *Sci. Rep.* 8, 1408. doi:10.1038/s41598-018-19844-7

Holmes, A., Murphy, D. L., and Crawley, J. N. (2002). Reduced aggression in mice lacking the serotonin transporter. *Psychopharmacology (Berl)* 161, 160–167. doi:10.1007/s00213-002-1024-3

Huber, K. M., Gallagher, S. M., Warren, S. T., and Bear, M. F. (2002). Altered synaptic plasticity in a mouse model of fragile X mental retardation. *Proc. Natl. Acad. Sci. U S A.* 99, 7746–7750. doi:10.1073/pnas.122205699

Isaac, J. T., Ashby, M. C., and Mcbain, C. J. (2007). The role of the GluR2 subunit in AMPA receptor function and synaptic plasticity. *Neuron* 54, 859–871. doi:10.1016/j.neuron.2007.06.001

Ishikawa, Y., Tamura, H., and Shiosaka, S. (2011). Diversity of neuropsin (KLK8)-dependent synaptic associativity in the hippocampal pyramidal neuron. *J. Physiol.* 589, 3559–3573. doi:10.1113/jphysiol.2011.206169

Iwata, K., Matsuzaki, H., Tachibana, T., Ohno, K., Yoshimura, S., Takamura, H., et al. (2014). N-ethylmaleimide-sensitive factor interacts with the serotonin transporter and modulates its trafficking: implications for pathophysiology in autism. *Mol. Autism* 5, 33. doi:10.1186/2040-2392-5-33

Jia, Z., Agopyan, N., Miu, P., Xiong, Z., Henderson, J., Gerlai, R., et al. (1996). Enhanced LTP in mice deficient in the AMPA receptor GluR2. *Neuron* 17, 945–956. doi:10.1016/s0896-6273(00)80225-1

Joshi, G., Biederman, J., Wozniak, J., Goldin, R. L., Crowley, D., Furtak, S., et al. (2013). Magnetic resonance spectroscopy study of the glutamatergic system in adolescent males with high-functioning autistic disorder: a pilot study at 4T. *Eur. Arch. Psychiatry Clin. Neurosci.* 263, 379–384. doi:10.1007/s00406-012-0369-9

Kaizuka, T., and Takumi, T. (2018). Postsynaptic density proteins and their involvement in neurodevelopmental disorders. *J. Bioche.* 163, 447–455. doi:10.1093/jb/mvy022

Kittler, J. T., Rostaing, P., Schiavo, G., Fritschy, J. M., Olsen, R., Triller, A., et al. (2001). The subcellular distribution of GABARAP and its ability to interact with NSF suggest a role for this protein in the intracellular transport of GABA(A) receptors. *Mol. Cel Neurosci.* 18, 13–25. doi:10.1006/mcne.2001.1005

Lee, S. H., Liu, L. D., Wang, Y. T., and Sheng, M. (2002). Clathrin adaptor AP2 and NSF interact with overlapping sites of GluR2 and play distinct roles in AMPA receptor trafficking and hippocampal LTD. *Neuron* 36, 661–674. doi:10.1016/S0896-6273(02)01024-3

Leil, T. A., Chen, Z. W., Chang, C. S., and Olsen, R. W. (2004). GABAA receptor-associated protein traffics GABAA receptors to the plasma membrane in neurons. *J. Neurosci.* 24, 11429–11438. doi:10.1523/JNEUROSCI.3355-04.2004

Lu, H. F., Wu, P. F., Yang, Y. J., Xiao, W., Fan, J., Liu, J., et al. (2014). Interactions between N-ethylmaleimide-sensitive factor and GluR2 in the nucleus accumbens contribute to the expression of locomotor sensitization to cocaine. *J. Neurosci.* 34, 3493–3508. doi:10.1523/JNEUROSCI.2594-13.2014

Luscher, C., Nicoll, R. A., Malenka, R. C., and Muller, D. (2000). Synaptic plasticity and dynamic modulation of the postsynaptic membrane. *Nat. Neurosci.* 3, 545–550. doi:10.1038/75714

Luthi, A., Chittajallu, R., Duprat, F., Palmer, M. J., Benke, T. A., Kidd, F. L., et al. (1999). Hippocampal LTD expression involves a pool of AMPARs regulated by the NSF-GluR2 interaction. *Neuron* 24, 389–399. doi:10.1016/S0896-6273(00)80852-1

Makkonen, I., Riikonen, R., Kokki, H., Airaksinen, M. M., and Kuikka, J. T. (2008). Serotonin and dopamine transporter binding in children with autism determined by SPECT. *Dev. Med. Child. Neurol.* 50, 593–597. doi:10.1111/j.1469-8749.2008.03027.x

Malenka, R. C. (2003). Synaptic plasticity and AMPA receptor trafficking. *An.n N. Y. Acad. Sci.* 1003, 1–11. doi:10.1196/annals.1300.001

Mcdougle, C. J., Naylor, S. T., Cohen, D. J., Aghajanian, G. K., Heninger, G. R., and Price, L. H. (1996). Effects of tryptophan depletion in drug-free adults with autistic disorder. *Arch. Gen. Psychiatry* 53, 993–1000. doi:10.1001/archpsyc.1996.01830110029004

Moreno, H., Borjas, L., Arrieta, A., Saez, L., Prassad, A., Estevez, J., et al. (1992). Clinical heterogeneity of the autistic syndrome: a study of 60 families. *Invest. Clin.* 33, 13–31.

Moreno-Fuenmayor, H., Borjas, L., Arrieta, A., Valera, V., and Socorro-Candanoza, L. (1996). Plasma excitatory amino acids in autism. *Invest. Clin.* 37, 113–128.

Murata, K., Kinoshita, T., Ishikawa, T., Kuroda, K., Hoshi, M., and Fukazawa, Y. (2020). Region- and neuronal-subtype-specific expression of Na,K-ATPase alpha and beta subunit isoforms in the mouse brain. *J. Comp. Neurol.* 528, 2654–2678. doi:10.1002/cne.24924

Murphy, D. L., Fox, M. A., Timpano, K. R., Moya, P. R., Ren-Patterson, R., Andrews, A. M., et al. (2008). How the serotonin story is being rewritten by new gene-based discoveries principally related to SLC6A4, the serotonin transporter gene, which functions to influence all cellular serotonin systems. *Neuropharmacology* 55, 932–960. doi:10.1016/j.neuropharm.2008.08.034

Nakamura, K., Sekine, Y., Ouchi, Y., Tsujii, M., Yoshikawa, E., Futatsubashi, M., et al. (2010). Brain serotonin and dopamine transporter bindings in adults with high-functioning autism. *Arch. Gen. Psychiatry* 67, 59–68. doi:10.1001/archgenpsychiatry.2009.137

Nishimune, A., Isaac, J. T., Molnar, E., Noel, J., Nash, S. R., Tagaya, M., et al. (1998). NSF binding to GluR2 regulates synaptic transmission. *Neuron* 21, 87–97. S0896-6273(00)80517-6.

Noel, J., Ralph, G. S., Pickard, L., Williams, J., Molnar, E., Uney, J. B., et al. (1999). Surface expression of AMPA receptors in hippocampal neurons is regulated by an NSF-dependent mechanism. *Neuron* 23, 365–376. doi:10.1016/S0896-6273(00)80786-2

Osten, P., Srivastava, S., Inman, G. J., Vilim, F. S., Khatri, L., Lee, L. M., et al. (1998). The AMPA receptor GluR2 C terminus can mediate a reversible, ATP-dependent interaction with NSF and alpha- and beta-SNAPs. *Neuron* 21, 99–110. S0896-6273(00)80518-8.. doi:10.1016/s0896-6273(00)80518-8

Page, D. T., Kuti, O. J., Prestia, C., and Sur, M. (2009). Haploinsufficiency for Pten and Serotonin transporter cooperatively influences brain size and social behavior. *Proc. Natl. Acad. Sci. U S A.* 106, 1989–1994. doi:10.1073/pnas.0804428106

Piochon, C., Kano, M., and Hansel, C. (2016). LTD-like molecular pathways in developmental synaptic pruning. *Nat. Neurosci.* 19, 1299–1310. doi:10.1038/nn.4389

Purcell, A. E., Jeon, O. H., and Pevsner, J. (2001a). The abnormal regulation of gene expression in autistic brain tissue. *J. Autism Dev. Disord.* 31, 545–549. doi:10.1023/a:1013290826504

Purcell, A. E., Jeon, O. H., Zimmerman, A. W., Blue, M. E., and Pevsner, J. (2001b). Postmortem brain abnormalities of the glutamate neurotransmitter system in autism. *Neurology* 57, 1618–1628. doi:10.1212/wnl.57.9.1618

Puschel, A. W., O'connor, V., and Betz, H. (1994). The N-ethylmaleimide-sensitive fusion protein (NSF) is preferentially expressed in the nervous system. *FEBS Lett.* 347, 55–58. doi:10.1016/0014-5793(94)00505-2

Rothman, J. E. (1994). Mechanisms of intracellular protein transport. *Nature* 372, 55–63. doi:10.1038/372055a0

Schain, R. J. (1961). Effects of 5-hydroxytryptamine on the dorsal muscle of the leech (Hirudo medicinalis). *Br. J. Pharmacol. Chemother.* 16, 257–261. doi:10.1111/j.1476-5381.1961.tb01085.x

Sheng, M., and Hoogenraad, C. C. (2007). The postsynaptic architecture of excitatory synapses: a more quantitative view. *Annu. Rev. Biochem.* 76, 823–847. doi:10.1146/annurev.biochem.76.060805.160029

Sheng, M., and Lee, S. H. (2001). AMPA receptor trafficking and the control of synaptic transmission. *Cell* 105, 825–828. doi:10.1016/s0092-8674(01)00406-8

Shimmura, C., Suda, S., Tsuchiya, K. J., Hashimoto, K., Ohno, K., Matsuzaki, H., et al. (2011). Alteration of plasma glutamate and glutamine levels in children with high-functioning autism. *PLoS One* 6, e25340. doi:10.1371/journal.pone.0025340

Shinohe, A., Hashimoto, K., Nakamura, K., Tsujii, M., Iwata, Y., Tsuchiya, K. J., et al. (2006). Increased serum levels of glutamate in adult patients with autism. *Prog. Neuropsychopharmacol. Biol. Psychiatry* 30, 1472–1477. doi:10.1016/j.pnpbp.2006.06.013

Smotherman, W. P., Bell, R. W., Starzec, J., Elias, J., and Zachman, T. A. (1974). Maternal responses to infant vocalizations and olfactory cues in rats and mice. *Behav. Biol.* 12, 55–66. doi:10.1016/s0091-6773(74)91026-8

Song, I., Kamboj, S., Xia, J., Dong, H., Liao, D., and Huganir, R. L. (1998). Interaction of the N-ethylmaleimide-sensitive factor with AMPA receptors. *Neuron* 21, 393–400. S0896-6273(00)80548-6.

Testa, G., Schaft, J., Van Der Hoeven, F., Glaser, S., Anastassiadis, K., Zhang, Y., et al. (2004). A reliable lacZ expression reporter cassette for multipurpose, knockout-first alleles. *Genesis* 38, 151–158. doi:10.1002/gene.20012

Tirouvanziam, R., Obukhanych, T. V., Laval, J., Aronov, P. A., Libove, R., Banerjee, A. G., et al. (2012). Distinct plasma profile of polar neutral amino acids, leucine, and glutamate in children with Autism Spectrum Disorders. *J. Autism Dev. Disord.* 42, 827–836. doi:10.1007/s10803-011-1314-x

Tochitani, S., Ikeno, T., Ito, T., Sakurai, A., Yamauchi, T., and Matsuzaki, H. (2016). Administration of Non-Absorbable Antibiotics to Pregnant Mice to Perturb the Maternal Gut Microbiota Is Associated with Alterations in Offspring Behavior. *PLoS One* 11, e0138293. doi:10.1371/journal.pone.0138293

Walsh, M. J., and Kuruc, N. (1992). The postsynaptic density: constituent and associated proteins characterized by electrophoresis, immunoblotting, and peptide sequencing. *J. Neurochem.* 59, 667–678. doi:10.1111/j.1471-4159.1992.tb09421.x

Wellman, C. L., Izquierdo, A., Garrett, J. E., Martin, K. P., Carroll, J., Millstein, R., et al. (2007). Impaired stress-coping and fear extinction and abnormal corticolimbic morphology in serotonin transporter knock-out mice. *J. Neurosc.i* 27, 684–691. doi:10.1523/JNEUROSCI.4595-06.2007

West, D. B., Pasumarthi, R. K., Baridon, B., Djan, E., Trainor, A., Griffey, S. M., et al. (2015). A lacZ reporter gene expression atlas for 313 adult KOMP mutant mouse lines. *Genome Res.* 25, 598–607. doi:10.1101/gr.184184.114

Xie, M. J., Ishikawa, Y., Yagi, H., Iguchi, T., Oka, Y., Kuroda, K., et al. (2019). PIP_3-Phldb2 is crucial for LTP regulating synaptic NMDA and AMPA receptor density and PSD95 turnover. *Sci. Rep.* 9, 4305. doi:10.1038/s41598-019-40838-6

Conflict of Interest: The authors declare that the research was conducted in the absence of any commercial or financial relationships that could be construed as a potential conflict of interest.

Publisher's Note: All claims expressed in this article are solely those of the authors and do not necessarily represent those of their affiliated organizations, or those of the publisher, the editors and the reviewers. Any product that may be evaluated in this article, or claim that may be made by its manufacturer, is not guaranteed or endorsed by the publisher.

frontiers in Genetics

BRIEF RESEARCH REPORT
published: 21 October 2021
doi: 10.3389/fgene.2021.741175

Identifying New COVID-19 Receptor Neuropilin-1 in Severe Alzheimer's Disease Patients Group Brain Using Genome-Wide Association Study Approach

*Key-Hwan Lim†, Sumin Yang†, Sung-Hyun Kim and Jae-Yeol Joo**

Neurodegenerative Disease Research Group, Korea Brain Research Institute, Daegu, South Korea

OPEN ACCESS

Edited by:
Noriyoshi Usui, Osaka University, Japan

Reviewed by:
Kazuya Toriumi, Tokyo Metropolitan Institute of Medical Science, Japan
Sangwon Byun, Korea Research Institute of Bioscience and Biotechnology (KRIBB), South Korea

***Correspondence:**
Jae-Yeol Joo
joojy@kbri.re.kr

† These authors have contributed equally to this work

Specialty section:
This article was submitted to Neurogenomics, a section of the journal Frontiers in Genetics

Received: *14 July 2021*
Accepted: *02 August 2021*
Published: *21 October 2021*

Citation:
Lim K-H, Yang S, Kim S-H and Joo J-Y (2021) Identifying New COVID-19 Receptor Neuropilin-1 in Severe Alzheimer's Disease Patients Group Brain Using Genome-Wide Association Study Approach. Front. Genet. 12:741175. doi: 10.3389/fgene.2021.741175

Recent preclinical studies show that Neuropilin-1 (NRP1), which is a transmembrane protein with roles in neuronal development, axonal outgrowth, and angiogenesis, also plays a role in the infectivity of severe acute respiratory syndrome coronavirus 2 (SARS-CoV-2). Thus, we hypothesize that NRP1 may be upregulated in Alzheimer's disease (AD) patients and that a correlation between AD and SARS-CoV-2 NRP1-mediated infectivity may exist as angiotensin converting enzyme 2 (ACE2). We used an AD mouse model that mimics AD and performed high-throughput total RNA-seq with brain tissue and whole blood. For quantification of NRP1 in AD, brain tissues and blood were subjected to Western blotting and real-time quantitative PCR (RT-qPCR) analysis. *In silico* analysis for NRP1 expression in AD patients has been performed on human hippocampus data sets. Many cases of severe symptoms of COVID-19 are concentrated in an elderly group with complications such as diabetes, degenerative disease, and brain disorders. Total RNA-seq analysis showed that the *Nrp1* gene was commonly overexpressed in the AD model. Similar to ACE2, the NRP1 protein is also strongly expressed in AD brain tissues. Interestingly, *in silico* analysis revealed that the level of expression for NRP1 was distinct at age and AD progression. Given that NRP1 is highly expressed in AD, it is important to understand and predict that NRP1 may be a risk factor for SARS-CoV-2 infection in AD patients. This supports the development of potential therapeutic drugs to reduce SARS-CoV-2 transmission.

Keywords: SARS-CoV-2, Neuropilin-1, Alzheimer's disease, genome-wide association study (GWAS), gene expression

INTRODUCTION

Severe acute respiratory syndrome coronavirus 2 (SARS-CoV-2) is being evaluated as a third-high-risk contagious infection (Hu et al., 2020). People are still highly vulnerable to the ongoing and life-threatening COVID-19 pandemic, as FDA-authorized vaccines or beneficial treatments remain unavailable (Singh et al., 2020). The risk of severe complications that are eventually

associated with high mortality is indicated in older people (Carstensen et al., 2020). Moreover, a bidirectional interrelation between neurological complications and COVID-19 is extensively reported (Verkhratsky et al., 2020).

Age-dependent vulnerability to SARS-CoV-2 has been associated with concomitant symptomatic infections (Liu et al., 2020; Wu et al., 2020). Alzheimer's disease (AD) is a highly destructive neurodegenerative disorder that mostly affects the elderly and is characterized by a progressive cognitive decline (Masters et al., 2015). Although various hypotheses have been proposed to explain its multifactorial properties (Liu et al., 2019), the exact mechanism and related features of AD remain obscure. An analysis of 627 patients suggests that AD is a risk factor for SARS-CoV-2 infection (Bianchetti et al., 2020).

Angiotensin converting enzyme 2 (ACE2) is required for SARS-CoV-2 infection. Recently, it is reported that the *Ace2* gene and protein expression are elevated in AD patients compared with in normal elderly individuals (Ding et al., 2020; Lim et al., 2020; Rahman et al., 2020). Consistent with these results, an increase in ACE2 expression results in an increased susceptibility to SARS-CoV-2 infection in elderly patients with AD. Furthermore, a recent study suggests that the transmembrane protein Neuropilin-1 (NRP1) also plays a role in SARS-CoV-2 infection (Daly et al., 2020; Mayi et al., 2021). Biochemical experiments and X-ray crystallography show that NRP1 strongly interacts with a polybasic sequence on the spike protein of SARS-CoV-2, which fits the C-end rule region (CendR) required for NRP1-peptide interaction (Daly et al., 2020; Song et al., 2020). NRP1 depletion with RNAi targeting Nrp1 mRNA inhibits the binding of the SARS-CoV-2 spike protein to NRP1 and, consequently, decreases the rate of viral infection (Daly et al., 2020; Song et al., 2020). In addition, a monoclonal antibody against the b1b2 domain of NRP1 reduces the infectivity of SARS-CoV-2 lentiviral pseudo-particles (Cantuti-Castelvetri et al., 2020). NRP1 is a neuronal receptor associated with the regulation of neurite outgrowth through the binding of vascular endothelial growth factor (VEGF) (Abdullah et al., 2020). When NRP1 is activated by CendR, which is a peptide R/KXXR/K motif contained within C-terminal domains, it enables cells to internalize ligands, such as viruses, containing the motif (Teesalu et al., 2009). Furthermore, NRP1 is expressed in the central nervous system, including the brain olfactory-related regions in which SARS-CoV-2 entry may occur, thereby facilitating COVID-19 infection (Davies et al., 2020).

Thus, we hypothesize that, in addition to ACE2, NRP1 expression might be upregulated in the brains of elderly AD patients. In this study, molecular characterization via high-throughput analysis and biochemical assays reveals that NRP1 is highly expressed in AD, which suggests that NRP1 may be a potential genetic therapy target in AD patients with COVID-19.

MATERIALS AND METHODS

Animals

Five × FAD transgenic mice were purchased from the Jackson Laboratory. All animal experiments performed in this study were reviewed and approved by the IACUC committee at the Korea Brain Research Institute (IACUC-20-00018).

Total RNA Sequencing and Human *in silico* Analysis

The data analysis of total RNA-seq from the mouse cortex was performed as previously described in Lim and Joo (2020). Briefly, the brain was extracted from 6-month-old wild-type (WT) and 5×FAD mice and cortex isolated to prepare the pure RNA and total RNA-seq library. RNA-seq libraries were prepared using the TruSeq Stranded Total RNA LT Sample Prep Kit (Illumina Sample Preparation Guide) from isolated mRNA. To profile the insert length of libraries, we used the Agilent 2100 Bioanalyzer, and constructed libraries were sequenced from HiSeq^{TM}4000 platform (Illumina, United States). Then, converted nucleotide sequences using HiSeq^{TM}4000 were sorted and the dirty reads filtered from the raw reads. RNA-seq data was accessible using Gene Expression Omnibus (GEO) accession number GSE147792. *In silico* data analysis was performed using the Affymetrix Human Genome U133 Plus 2.0 Array (Lim et al., 2020). The GSE1297 data sets were derived from human hippocampus and GSE4226 data sets were derived from human peripheral blood mononuclear cells (PBMCs) in normal and AD patients.

RNA Isolation

Total RNA isolation was performed with the mouse cortex according to TRIzol using the commercial protocol. First, phenol-based TRIzol (Invitrogen) is added in the cortex tissue tube for homogenizing. Then, it is separated into three phases by chloroform for the collect only RNA dissolved aqueous phase except the DNA and protein precipitated phases. An equal volume of isopropanol was used to precipitate RNA. After centrifugation, supernatant was discarded, and it was washed with prechilled 75% ethanol once. RNA was dehydrated and crystalized without organic compound contamination and eluted with nuclease-free water. RNA was then denatured in the 65°C heat block for 10 min. The procedure was performed without RNase contamination.

Complementary DNA Synthesis

Isolated total RNA was synthesized into complementary DNA (cDNA) following the manufacturer's protocol of High-Capacity cDNA Reverse Transcription Kits (Applied Biosystems). Template RNA (2 μg) was prepared to synthesize a single reaction, and reverse transcription kit components were premixed. The premixture contains 10 × RT buffer, 25 × dNTP mix (4 mM), 10 × RT Random Primers, MultiScribe Reverse Transcriptase (50 U), RNase inhibitor, and nuclease-free water for adjusting the total volume for the reaction. Gently mixed template RNA and an equal volume of premixture was placed in the thermal cycler. The condition for reverse transcription was suggested as optimized temperature and time: 25°C for 10 min, 37°C for 120 min, and 85°C for 5 min.

Real-Time Quantitative PCR

Real-time quantitative PCR (RT-qPCR) was performed according to commercial protocol using SYBR Green PCR Master Mix (Applied Biosystems). Primers employed were *Nrp1* forward, 5′ CCTCACATTGGGCGTTATTG 3′, reverse, 5′ CACTGTAGTTGGCTGAGAAAC 3′; *Gapdh* forward, 5′ AGGTCGGTGTGAACGGATTT 3′, reverse, 5′ TGTAGACCATGTAGTTGAGG 3′. Each reaction contains SYBR Green PCR Master Mix, Template cDNA, and forward and reverse primer and is adjusted with nuclease-free water.

Western Blot

Protein was extracted from the mouse cortex and mixed with sample buffer (5% 2-mercaptoethanol) and boiled at 100°C for

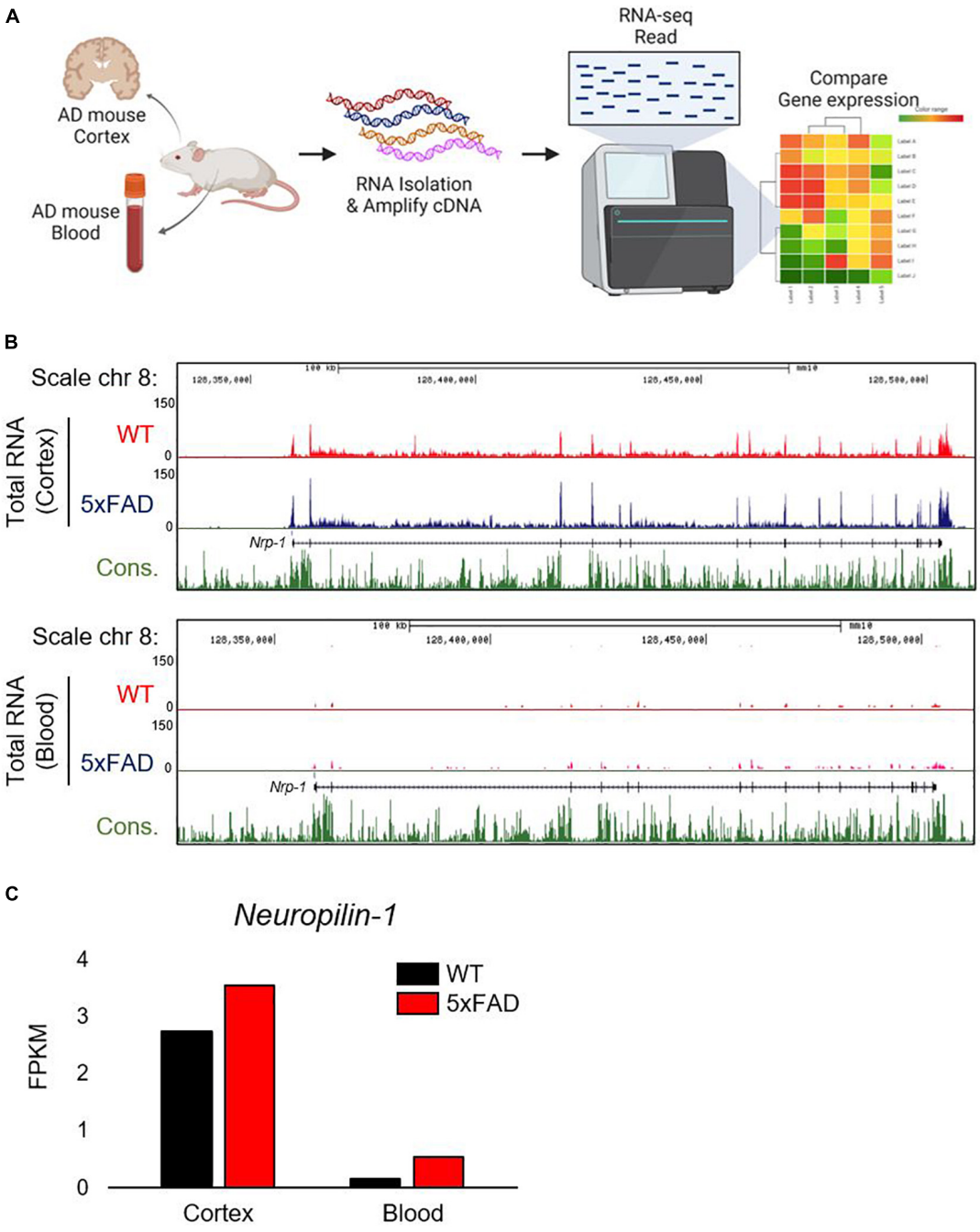

FIGURE 1 | Correlation between *Nrp1* gene and protein expression in AD brain. **(A)** Graphic representation of *Nrp1* gene expression in the cortex of five familial AD mutations (5×FAD) mice, which are used as a murine model of AD. **(B)** The representation is shown on the UCSC genome browser following total RNA-seq. **(C)** *Nrp1* gene expression levels are increased by 129% in 5×FAD cortex compared with control WT cortex.

denaturation. Protein samples were loaded on 4–15% gradient gel (Bio-Rad) to separate by size through the vertical SDS-PAGE system. Antibodies used for immune-blot analysis were anti-Neuropilin-1 (abcam, 1:1000) and anti-β-actin (BETHYL, 1:10000). Images were acquired by ChemiDoc MP imaging system (Bio-Rad).

RESULTS

High-Throughput Analysis of *Nrp1* Expression in Alzheimer's Disease

Given that the gene expression of ACE2 is upregulated in the brains of patients with AD and may be associated with the mortality rate from COVID-19 in the elderly (Fu et al., 2020; Lim et al., 2020), we hypothesize that NRP1, which codes for a newly recognized SARS-CoV-2 spike receptor, may be also increased in AD patients. To assess *Nrp1* gene expression in AD, we first used a murine model that mimics AD and performed total RNA-seq using mouse brain tissue and whole blood. Total RNA-seq was analyzed by the HiSeq^{TM}4000 platform (Illumina, United States) (**Figure 1A**). We applied the *Nrp1* gene expression level in the brain and blood from AD and WT and then mapped the sequencing reads (**Figure 1B**). The track of *Nrp1* gene was displayed with University of California, Santa Cruz (USCS) genome browser (**Figure 1B**). Interestingly, total RNA-seq analysis revealed upregulation of *Nrp1* gene expression in the brain of the AD model compared to WT (**Figure 1B**), and *Nrp1* fragments per kb per million reads values are increased in the AD model brain as well (**Figure 1C**). Although *Nrp1* gene expression was increased by 319% in AD blood compared with WT blood, the endogenous expression levels of *Nrp1* in the blood were significantly lower than those in the brain (**Figures 1B,C**). Collectively, our total RNA-seq results show that

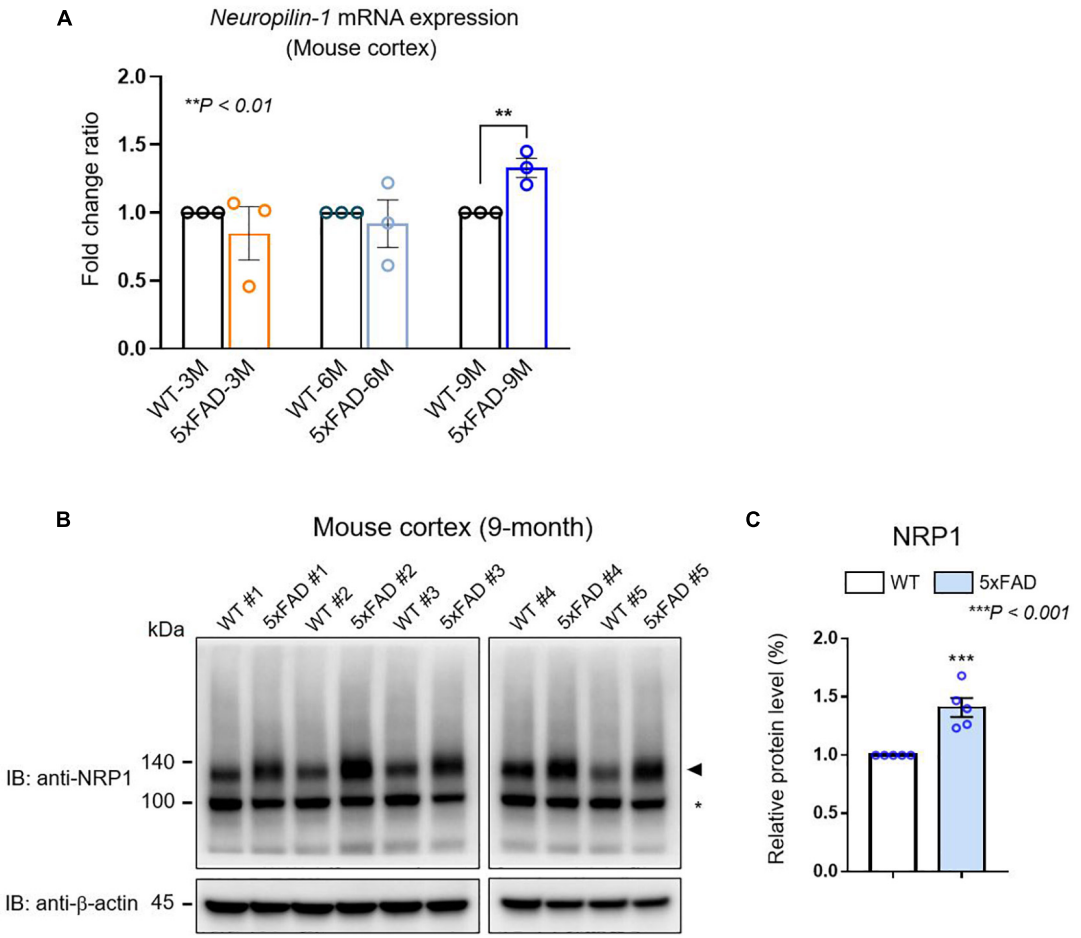

FIGURE 2 | The expression of NRP1 in mouse AD brain. **(A)** RT-qPCR analysis showing the *Nrp1* mRNA expression levels in the cortex of WT and 5×FAD mice. *Nrp1* mRNA expression is significantly increased in 9-month-old 5×FAD cortex compared with that in WT cortex. No significant differences are observed in the early disease stages of 5×FAD mice (3 and 6 months). The data are shown as the mean ± standard error of the mean (SEM) from $n = 3$ mice per group; statistical differences were assessed using unpaired *t*-test. **(B)** Representative Western blot analyzing the NRP1 protein levels in 5×FAD brains. Endogenous NRP1 is highly expressed in 9-month-old 5×FAD brains compared with that in the WT brain. β-actin was used as a loading control. The arrowhead indicates the NRP1 protein, and the asterisk indicates a non-specific band ($n = 5$ mice per group). **(C)** NRP1 Western blot band intensity measured by ImageJ 1.50i software ($n = 5$ mice per group). Statistical differences were assessed using unpaired *t*-test.

Nrp1 is preferentially expressed in the brain and upregulated in the brains of AD mice.

Nrp1 Is Upregulated in Alzheimer's Disease Brain

Nrp1 is abundantly expressed in the neurons and plays an important role for axon guidance, regeneration, neuronal plasticity, or various human diseases, such as epilepsy and seizure (Kumanogoh and Kikutani, 2013).

We confirmed *Nrp1* gene expression in both WT and AD model mouse brains through the total RNA-seq (**Figure 1**). To further analyze *Nrp1* expression during AD progression, we measured the Nrp1 mRNA levels in 3- to 9-month-old AD brains. RT-qPCR revealed an approximately 145% increase in *Nrp1* mRNA expression in 9-month-old AD brains compared with that in WT brains (**Figure 2A**). In addition, NRP1 protein expression was also significantly increased in 9-month-old AD brains compared with that in the WT (**Figures 2B,C**). Taken together, these findings indicate that *NRP1* gene and protein expression levels are significantly increased in the brains of aged AD mice.

Severe Alzheimer's Disease Patients Are Highly Expressed With *Nrp1*

Having found increased *Nrp1* gene expression in the brains of AD mice, we next performed *Nrp1* gene expression profiling of brains and PBMCs from human patients with different stages of AD (**Supplementary Table 1**). To identify the fold change of the ratio for *Nrp1* gene from AD patients, we performed *in silico* analysis

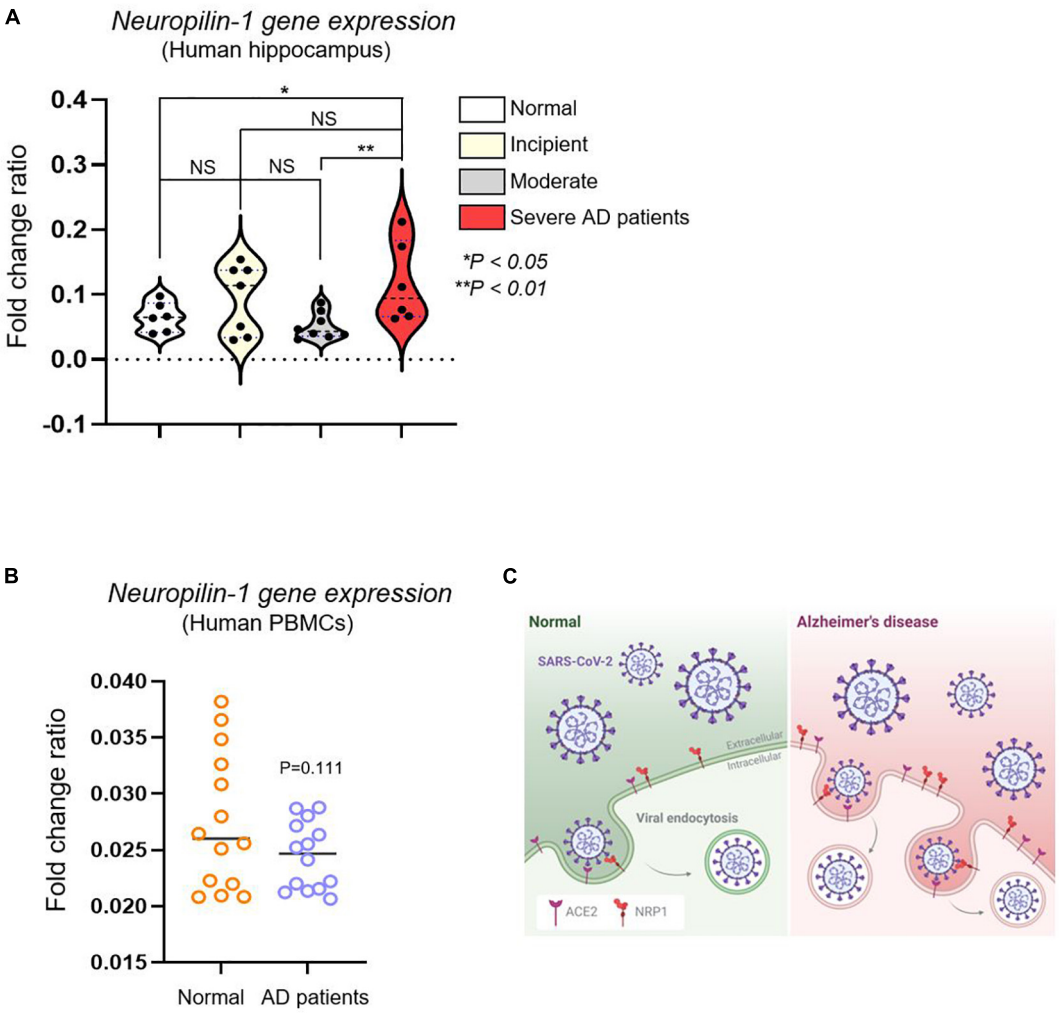

FIGURE 3 | *In silico* analysis of *Nrp1* gene expression in human hippocampus and PBMCs from AD patients. **(A)** *Nrp1* expression is significantly increased in the human hippocampus of severe AD patients compared with that in the control group (179%). No statistical difference is observed when WT is compared to incipient and moderate AD patients. Normal control group $n = 6$, incipient group $n = 7$, moderate group $n = 8$, and severe group $n = 6$. Statistical differences were assessed using *post hoc* test after one-way ANOVA. **(B)** *Nrp1* expression in PBMCs from AD patients is not statistically different from that in the control group. Normal elderly control, female $n = 7$ and male $n = 7$; AD patient group, female $n = 7$ and male $n = 7$. Statistical differences were assessed using unpaired *t*-test. **(C)** Schematic model of NRP1- and ACE2-mediated SARS-CoV-2 infection in AD. NRP1 and ACE2 mediate SARS-CoV-2 binding to the cell membrane and, consequently, infection. Because these two receptors are highly expressed in AD patients, these individuals may be more sensitive to SARS-CoV-2 infection.

using the GSE1297 and GSE4296 microarray data set. Patients with severe AD showed significantly upregulated *Nrp1* gene expression (179%) compared with the control group (individuals without AD), whereas incipient and moderate AD patients did not show increases in brain *Nrp1* gene expression (**Figure 3A**). Interestingly, we did not find differences in PBMC *Nrp1* gene expression between any of the groups (**Figure 3B**). These data correlate with results from the AD murine model. Together, the results demonstrate that NRP1 mRNA and protein expression is significantly elevated in the brains of late-stage AD patients.

DISCUSSION

Since the beginning of the COVID-19 pandemic, there have been significant efforts to identify unique SARS-CoV-2–associated proteins that could serve as targets for novel vaccines or therapeutic agents. Despite notable studies suggesting the possibility of developing other COVID-19-targeted drugs, the first-generation drugs have mostly focused on the viral spike protein receptor ACE2 (Yin et al., 2020). As high-throughput genomic studies begin to define the abnormal expression of individual DNA in particular diseases, it may become possible to rationally determine disease-specific gene expression and, thus, establish biomarkers for risk prediction in older people with complications, such as AD. Recently, we showed the increase of ACE2 expression in an elderly group with AD; therefore, our *in silico* analysis accurately predicts high risk for SARS-CoV-2 infection in elderly patients with AD (Lim et al., 2020). In addition, our research scheme may be useful for predicting the risk of AD in patients with SARS-CoV-2 infection.

Our findings have implications for the prevention and treatment of SARS-CoV-2 infection in elderly patients with AD. First, both *Ace2* and *Nrp1* are preferentially expressed in the brain, and their expression level may determine the sensitivity to SARS-CoV-2 infection (**Figure 3C**). Interestingly, it was recently suggested that differences in cytokines, such as IL-1β and TNF-α, are less pronounced in peripheral blood in SARS-CoV-2 infection (Totura and Baric, 2012; Tincati et al., 2020). Second, in addition to *Ace2*, *Nrp1* expression was also upregulated in patients with severe AD. Although predictive immune biomarkers are suggested for the clinical treatment of COVID-19 (Fouladseresht et al., 2020), our high-throughput analysis–based approach would probably provide an accurate prediction of SARS-CoV-2 risk in elderly AD patients. Notably, *Ace2* gene expression gradually increased with the severity of AD symptoms (from incipient to severe stage) (Lim et al., 2020), whereas elevated *Nrp1* gene expression was only present in the severe AD patient group (**Figures 1B,C**). This result indicates that ACE2 may be a more fundamental gene for SARS-CoV-2 infection compared with NRP1.

Recently, the spread of SARS-CoV-2 infection has accelerated worldwide. Efforts on the clinical treatment of SARS-CoV-2 infection are concentrated on the development of vaccines and drugs, including gene therapy (Chugh et al., 2020). To our knowledge, this is the first study examining NRP1 expression in AD patients and reporting its higher expression these individuals. Moreover, it reveals the importance of determining SARS-CoV-2 spike protein receptor gene expression. Our gene profiling could potentially be used to predict the risk for SARS-CoV-2 infection in elderly AD patients.

DATA AVAILABILITY STATEMENT

The datasets presented in this study can be found in online repositories. The names of the repository/repositories and accession number(s) can be found in the article/**Supplementary Material**.

ETHICS STATEMENT

All animal experiments performed in this study were reviewed and approved by the IACUC Committee at Korea Brain Research Institute (IACUC-20-00018). Written informed consent was obtained from the owners for the participation of their animals in this study. Written informed consent was obtained from the individual(s) for the publication of any potentially identifiable images or data included in this article.

AUTHOR CONTRIBUTIONS

J-YJ and K-HL designed the research. K-HL, SY, S-HK, and J-YJ wrote the manuscript, performed the research, discussed the results, and commented on the manuscript. All authors contributed to the article and approved the submitted version.

FUNDING

This work was supported by Korea Brain Research Institute (KBRI) basic research program through KBRI funded by the Ministry of Science and ICT (21-BR-02-09, 21-BR-02-21), and Basic Science Research Program through the National Research Foundation of Korea (NRF) funded by the Ministry of Education (2019R1F1A1059595).

ACKNOWLEDGMENTS

We would like to thank Sun-Woo Lee for assistance of bioinformatics analysis. 5×FAD (9-month) mice were kindly provided by Sungkun Chun at Jeonbuk National University Medicine School. A graphic figure was made with biorender.com. We would also like to thank Editage for English language editing.

SUPPLEMENTARY MATERIAL

The Supplementary Material for this article can be found online at: https://www.frontiersin.org/articles/10.3389/fgene.2021.741175/full#supplementary-material

REFERENCES

Abdullah, A., Akhand, S. S., Paez, J. S. P., Brown, W., Pan, L., Libring, S., et al. (2020). Epigenetic targeting of neuropilin-1 prevents bypass signaling in drug-resistant breast cancer. *Oncogene* 40, 322–333. doi: 10.1038/s41388-020-01530-6

Bianchetti, A., Rozzini, R., Guerini, F., Boffelli, S., Ranieri, P., Minelli, G., et al. (2020). Clinical presentation of COVID19 in dementia patients. *J. Nutr. Health Aging* 24, 560–562. doi: 10.1007/s12603-020-1389-1

Cantuti-Castelvetri, L., Ojha, R., Pedro, L. D., Djannatian, M., Franz, J., Kuivanen, S., et al. (2020). Neuropilin-1 facilitates SARS-CoV-2 cell entry and infectivity. *Science* 370, 856–860. doi: 10.1126/science.abd2985

Carstensen, L. L., Shavit, Y. Z., and Barnes, J. T. (2020). Age advantages in emotional experience persist even under threat from the COVID-19 pandemic. *Psychol. Sci.* 31, 1374–1385. doi: 10.1177/0956797620967261

Chugh, H., Awasthi, A., Agarwal, Y., Gaur, R. K., Dhawan, G., and Chandra, R. (2020). A comprehensive review on potential therapeutics interventions for COVID-19. *Eur. J. Pharmacol.* 890, 173741. doi: 10.1016/j.ejphar.2020.173741

Daly, J. L., Simonetti, B., Klein, K., Chen, K. E., Williamson, M. K., Anton-Plagaro, C., et al. (2020). Neuropilin-1 is a host factor for SARS-CoV-2 infection. *Science* 370, 861–865. doi: 10.1126/science.abd3072

Davies, J., Randeva, H. S., Chatha, K., Hall, M., Spandidos, D. A., Karteris, E., et al. (2020). Neuropilin-1 as a new potential SARS-CoV-2 infection mediator implicated in the neurologic features and central nervous system involvement of COVID-19. *Mol. Med. Rep.* 22, 4221–4226. doi: 10.3892/mmr.2020.11510

Ding, Q., Shults, N. V., Harris, B. T., and Suzuki, Y. J. (2020). Angiotensin-converting enzyme 2 (ACE2) is upregulated in Alzheimer's disease brain. *bioRxiv* [Preprint]. doi: 10.1101/2020.10.08.331157

Fouladseresht, H., Doroudchi, M., Rokhtabnak, N., Abdolrahimzadehfard, H., Roudgari, A., Sabetian, G., et al. (2020). Predictive monitoring and therapeutic immune biomarkers in the management of clinical complications of COVID-19. *Cytokine Growth Factor Rev.* 58, 32–48. doi: 10.1016/j.cytogfr.2020.10.002

Fu, L., Wang, B., Yuan, T., Chen, X., Ao, Y., Fitzpatrick, T., et al. (2020). Clinical characteristics of coronavirus disease 2019 (COVID-19) in China: a systematic review and meta-analysis. *J. Infect.* 80, 656–665. doi: 10.1016/j.jinf.2020.03.041

Hu, B., Guo, H., Zhou, P., and Shi, Z.-L. (2020). Characteristics of SARS-CoV-2 and COVID-19. *Nat. Rev. Microbiol.* 19, 141–154. doi: 10.1038/s41579-020-00459-7

Kumanogoh, A., and Kikutani, H. (2013). Immunological functions of the neuropilins and plexins as receptors for semaphorins. *Nat. Rev. Immunol.* 13, 802–814. doi: 10.1038/nri3545

Lim, K. H., and Joo, J. Y. (2020). Predictive potential of circulating Ube2h mRNA as an E2 ubiquitin-conjugating enzyme for diagnosis or treatment of Alzheimer's disease. *Int. J. Mol. Sci.* 21:3398. doi: 10.3390/ijms21093398

Lim, K. H., Yang, S., Kim, S. H., and Joo, J. Y. (2020). Elevation of ACE2 as a SARS-CoV-2 entry receptor gene expression in Alzheimer's disease. *J. Infect.* 81, e33–e34. doi: 10.1016/j.jinf.2020.06.072

Liu, K., Chen, Y., Lin, R., and Han, K. (2020). Clinical features of COVID-19 in elderly patients: a comparison with young and middle-aged patients. *J. Infect.* 80, e14–e18. doi: 10.1016/j.jinf.2020.03.005

Liu, P.-P., Xie, Y., Meng, X.-Y., and Kang, J.-S. (2019). History and progress of hypotheses and clinical trials for Alzheimer's disease. *Signal Trans. Targeted Ther.* 4:29. doi: 10.1038/s41392-019-0063-8

Masters, C. L., Bateman, R., Blennow, K., Rowe, C. C., Sperling, R. A., and Cummings, J. L. (2015). Alzheimer's disease. *Nat. Rev. Dis. Primers* 1:15056. doi: 10.1038/nrdp.2015.56

Mayi, B. S., Leibowitz, J. A., Woods, A. T., Ammon, K. A., Liu, A. E., and Raja, A. (2021). The role of Neuropilin-1 in COVID-19. *PLoS Pathog.* 17:e1009153. doi: 10.1371/journal.ppat.1009153

Rahman, M. A., Islam, K., Rahman, S., and Alamin, M. (2020). Neurobiochemical cross-talk between COVID-19 and Alzheimer's disease. *Mol. Neurobiol.* 58, 1017–1023. doi: 10.1007/s12035-020-02177-w

Singh, D. D., Han, I., Choi, E.-H., and Yadav, D. K. (2020). Recent advances in pathophysiology, drug development and future perspectives of SARS-CoV-2. *Front. Cell Dev. Biol.* 8:580202. doi: 10.3389/fcell.2020.580202

Song, E., Zhang, C., Israelow, B., Lu-Culligan, A., Prado, A. V., Skriabine, S., et al. (2020). Neuroinvasion of SARS-CoV-2 in human and mouse brain. *bioRxiv* [Preprint]. doi: 10.1084/jem.20202135

Teesalu, T., Sugahara, K. N., Kotamraju, V. R., and Ruoslahti, E. (2009). C-end rule peptides mediate neuropilin-1-dependent cell, vascular, and tissue penetration. *Proc. Natl. Acad. Sci. U.S.A.* 106, 16157–16162. doi: 10.1073/pnas.0908201106

Tincati, C., Cannizzo, E. S., Giacomelli, M., Badolato, R., D'arminio Monforte, A., and Marchetti, G. (2020). Heightened circulating interferon-inducible chemokines, and activated pro-cytolytic Th1-cell phenotype features Covid-19 aggravation in the second week of illness. *Front. Immunol.* 11:580987. doi: 10.3389/fimmu.2020.580987

Totura, A. L., and Baric, R. S. (2012). SARS coronavirus pathogenesis: host innate immune responses and viral antagonism of interferon. *Curr. Opin. Virol.* 2, 264–275. doi: 10.1016/j.coviro.2012.04.004

Verkhratsky, A., Li, Q., Melino, S., Melino, G., and Shi, Y. (2020). Can COVID-19 pandemic boost the epidemic of neurodegenerative diseases? *Biol. Direct* 15:28. doi: 10.1186/s13062-020-00282-3

Wu, J. T., Leung, K., Bushman, M., Kishore, N., Niehus, R., De Salazar, P. M., et al. (2020). Estimating clinical severity of COVID-19 from the transmission dynamics in Wuhan. China. *Nat. Med.* 26, 506–510. doi: 10.1038/s41591-020-0822-7

Yin, S., Tong, X., Huang, A., Shen, H., Li, Y., Liu, Y., et al. (2020). Longitudinal anti-SARS-CoV-2 antibody profile and neutralization activity of a COVID-19 patient. *J. Infect.* 81, e31–e32. doi: 10.1016/j.jinf.2020.06.076

Conflict of Interest: The authors declare that the research was conducted in the absence of any commercial or financial relationships that could be construed as a potential conflict of interest.

Publisher's Note: All claims expressed in this article are solely those of the authors and do not necessarily represent those of their affiliated organizations, or those of the publisher, the editors and the reviewers. Any product that may be evaluated in this article, or claim that may be made by its manufacturer, is not guaranteed or endorsed by the publisher.

frontiers in Genetics

ORIGINAL RESEARCH
published: 02 November 2021
doi: 10.3389/fgene.2021.754198

Early Life Stress Alters Gene Expression and Cytoarchitecture in the Prefrontal Cortex Leading to Social Impairment and Increased Anxiety

Noriyoshi Usui[1,2,3,4,5]*, *Yuta Ono*[5], *Ryoko Aramaki*[5], *Stefano Berto*[6], *Genevieve Konopka*[7], *Hideo Matsuzaki*[2,5,8†] and *Shoichi Shimada*[1,2,4†]

[1]Department of Neuroscience and Cell Biology, Graduate School of Medicine, Osaka University, Suita, Japan, [2]United Graduate School of Child Development, Osaka University, Suita, Japan, [3]Global Center for Medical Engineering and Informatics, Osaka University, Suita, Japan, [4]Addiction Research Unit, Osaka Psychiatric Research Center, Osaka Psychiatric Medical Center, Osaka, Japan, [5]Division of Development of Mental Functions, Research Center for Child Mental Development, University of Fukui, Fukui, Japan, [6]Department of Neuroscience, Medical University of South Carolina, Charleston, SC, United States, [7]Department of Neuroscience, University of Texas Southwestern Medical Center, Dallas, TX, United States, [8]Life Science Innovation Center, University of Fukui, Fukui, Japan

OPEN ACCESS

Edited by:
Silvia Pellegrini,
University of Pisa, Italy

Reviewed by:
Bryan Kolb,
University of Lethbridge, Canada
David G. Ashbrook,
University of Tennessee Health Science Center (UTHSC), United States

***Correspondence:**
Noriyoshi Usui
usui@anat1.med.osaka-u.ac.jp

†These authors have contributed equally to this work

Specialty section:
This article was submitted to Neurogenomics, a section of the journal Frontiers in Genetics

Received: *06 August 2021*
Accepted: *11 October 2021*
Published: *02 November 2021*

Citation:
Usui N, Ono Y, Aramaki R, Berto S, Konopka G, Matsuzaki H and Shimada S (2021) Early Life Stress Alters Gene Expression and Cytoarchitecture in the Prefrontal Cortex Leading to Social Impairment and Increased Anxiety. Front. Genet. 12:754198. doi: 10.3389/fgene.2021.754198

Early life stress (ELS), such as abuse, neglect, and maltreatment, exhibits a strong impact on the brain and mental development of children. However, it is not fully understood how ELS affects social behaviors and social-associated behaviors as well as developing prefrontal cortex (PFC). In this study, we performed social isolation on weaned pre-adolescent mice until adolescence and investigated these behaviors and PFC characteristics in adolescent mice. We found the ELS induced social impairments in social novelty, social interaction, and social preference in adolescent mice. We also observed increases of anxiety-like behaviors in ELS mice. In histological analysis, we found a reduced number of neurons and an increased number of microglia in the PFC of ELS mice. To identify the gene associated with behavioral and histological features, we analyzed transcriptome in the PFC of ELS mice and identified 15 differentially expressed genes involved in transcriptional regulation, stress, and synaptic signaling. Our study demonstrates that ELS influences social behaviors, anxiety-like behaviors through cytoarchitectural and transcriptomic alterations in the PFC of adolescent mice.

Keywords: early life stress, social isolation, social behavior, anxiety, prefrontal cortex, transcriptome

INTRODUCTION

The environment is a crucial factor for providing optimal growth and health conditions for children, including social, cognitive, or immune system-related aspects (Ferguson et al., 2013; Sonuga-Barke et al., 2017; Consiglio and Brodin, 2020; Mackes et al., 2020). Particularly, childhood environments have great impacts on the brain architecture, synaptic plasticity, and mental development (Takesian and Hensch, 2013; Miguel et al., 2019).

For example, adverse childhood environments and experiences such as abuse, neglect, and maltreatment have profound effects on the brain and mental development, and constitutes major risk factors for brain structural changes and adult psychopathology (Teicher et al., 2016; Jaffee, 2017). Human brain imaging studies have reported that maltreatment reduces specific brain region volumes such as anterior cingulate cortex, ventromedial and dorsomedial PFC, hippocampus, and striatum,

and these brain regions are highly involved in emotional control and the reward system (Chugani et al., 2001; Cohen et al., 2006; Edmiston et al., 2011; Dannlowski et al., 2012; Teicher et al., 2012; Kelly et al., 2013; Teicher et al., 2016). Importantly, specific brain regions are affected by specific types of abuse, neglect or maltreatment. Exposure to harsh corporal punishment caused a reduced gray matter volume in the prefrontal cortex of young adults (Tomoda et al., 2009). In addition, exposure to parental verbal aggression in childhood reduced fractional anisotropy in the arcuate fasciculus, and affected the development of the auditory association cortex involved in language processing (Tomoda et al., 2011). The child brain development has plasticity, and the effects of the childhood environments and experiences lead to structural and functional changes in the brain, as well as behavioral alterations.

Social isolation, social defeat stress, and electric shock are widely used as animal models to reproduce ELS and traumatic experiences in childhood (Schöner et al., 2017; Aspesi and Pinna, 2019; Pinna, 2019). A previous study of animal models reported that socially isolated mice during postnatal days (P) 21–35 displayed reduced sociality, working memory, and myelination in the PFC (Makinodan et al., 2012). In addition, reduced synapses and endogenous excitatory subtypes of the layer 5 pyramidal neurons were reported in the PFC of mice socially isolated for the same period (Yamamuro et al., 2018). We have also reported that social isolation during P21–53 induced the alteration of gut microbiota in mice (Usui et al., 2021b). These studies indicate that social isolation causes a lack of social experience and isolation stress, resulting in serious impacts on both PFC architecture and physical health. However, it is not fully understood how ELS affects various social behaviors and its-associated behaviors as well as transcriptome in the PFC of stressed individuals.

To address these questions, we performed social isolation on weaned pre-adolescent mice until adolescence for analyzing the impacts of ELS. In this study, we investigated various social behaviors (interaction, novelty, and preference), anxiety-like behaviors as well as cytoarchitecture and gene expressions by RNA sequencing (RNA-seq) of the PFC in adolescent ELS mice.

MATERIALS AND METHODS

Mice

Wild-type C57BL/6N (Japan SLC Inc., Shizuoka, Japan) mouse was used. Mice were housed in the barrier facilities of University of Fukui under 50% humidity and a 12:12 h light:dark cycle (8:00 to 20:00) and given free access to water and food. Social isolation-induced ELS was performed as described previously (Usui et al., 2021b). Briefly, the used experimental and control mice came from the litters of the same mother. For ELS (*via* social isolation), male mice were individually housed using a filter cap (#CL-4150, CLEA Japan, Inc., Tokyo, Japan) immediately after the weaning at P21 until P50. For controls, 4 male mice were co-housed in the same cage without filter cap. Mice behaviors were assessed from P50 and kept in each housing condition until dissection at P67. A total of 39 mice were used in this study, using littermates that gave birth to 6 or more at a time. The number of mice used in each experiment is shown in corresponding figure legend. All procedures were performed according to the ARRIVE guidelines and relevant official guidelines under the approval (#27-010) of the Animal Research Committee of the University of Fukui. All behavioral tests were performed between 10am and 5pm. Experimenters blind to housing information performed all behavioral tests.

Three-Chamber Social Interaction Test

Three-chamber social interaction test was performed as described previously (Usui et al., 2021b). Sociability and social novelty behaviors were assessed using a three-chamber box (W610 × D400 × H220 mm) with an infrared video camera system (O'Hara & Co., Ltd, Tokyo, Japan) at P53 after collecting fecal samples. For the first trial, empty wired cages were placed into both chambers for habituation. For the second trial, a stranger male mouse (mouse A) was placed into a wired cage of the right chamber to examine the sociability. For the third trial, mouse A was kept in the same wired cage as a familiar mouse, and a novel stranger male mouse (mouse B) was placed into a wired cage of the left chamber to examine the social novelty. Each trial was examined for 5 min after which the interactions with the targets were scored using an infrared video camera system (O'Hara & Co., Ltd, Tokyo, Japan).

Social Interaction Test

Two mice were placed in the diagonal corners of a novel chamber (W480 × D480 × H330 mm) and allowed to examine the social interactions for 10 min. Time spent in social interaction was measured and tracked by digital counters with infrared sensors (SCANET MV-40, MELQUEST Ltd., Toyama, Japan).

Social Preference Test

Mice were placed in one of the corners of a novel chamber (W480 × D480 × H330 mm) and allowed to examine the social preference for 10 min. A stranger male mouse was placed into a wired cage (80 × 80 mm) of the center of arena to examine the social preference. Time spent around the wired cage area (250 × 250 mm) and locomotor activity were measured and tracked by digital counters with infrared sensors (SCANET MV-40, MELQUEST Ltd., Toyama, Japan).

Light-Dark Box Test

Mice were placed in the dark room of a light -dark box (W300 × D150 × H150 mm) and allowed to freely explore for 10 min. Time spent in each box (W150 × D150 × H150 mm), transition, and locomotor activity were measured and tracked by digital counters with infrared sensors (SCANET MV-40, MELQUEST Ltd., Toyama, Japan).

Open Field Test

Mice were placed in one of the corners of a novel chamber (W480 × D480 × H330 mm) and allowed to freely explore for 120 min. Time spent in the center of arena (80 × 80 mm) and locomotor activity were measured and tracked by digital counters with

infrared sensors (SCANET MV-40, MELQUEST Ltd., Toyama, Japan).

Marble-Burying Test

Marble-burying test was performed as described previously (Usui et al., 2021a). Mice were placed in the corner of a novel home cage evenly placed eighteen marbles and allowed to freely explore for 20 min. After 20 min, the number of marbles buried was recorded. A marble was defined as buried when less than one-third of the marble was visible.

Immunohistochemistry

Immunohistochemistry was performed as described previously (Usui et al., 2021a). The mouse brain was fixed with 4% PFA in PBS overnight at 4°C, cryoprotected in 30% sucrose in PBS overnight at 4°C, and then embedded in Tissue-Tek O.C.T. Compound (#4583; Sakura Finetek Japan Co., Ltd., Osaka, Japan) for cryosectioning. Cryosections (20 μm thick) were placed in PBS and then permeabilized in PBS-T for 30 min at room temperature. Blocking was performed using 10% goat serum and 1% BSA in PBS-T for 1 h at room temperature. Sections were stained with the following established primary antibodies overnight at 4°C: mouse monoclonal anti-NeuN (1: 200, #MAB377, Millipore, Billerica, MA), rabbit polyclonal anti-Iba1 (1:1000, #019-19741, FUJIFILM Wako pure chemical corporation, Osaka, Japan). Sections were washed three times with PBS-T, incubated with species-specific antibodies conjugated to Alexa Fluor 488 (1:2,000; Invitrogen, Carlsbad, CA, United States) for 1 h at room temperature, and then washed 3 times with PBS-T. Cover glasses were mounted with Fluoromount/Plus (#K048; Diagnostic BioSystems, Pleasanton, CA, United States) or ProLong Diamond Antifade Mountant with DAPI (#P-36931 or #P36971, Thermo Fisher Scientific, Waltham, MA, United States) for nuclear staining. DAPI (#11034-56; Nacalai Tesque, Kyoto, Japan) was also used to stain nuclei. Images were collected using an all-in-one fluorescence microscope (BZ-X700, KEYENCE Corporation). Immunopositive cells in the PFC (cingulate and prelimbic cortical regions) were manually quantified within the area (4.8×10^5 μm) at bregma 1.98 to 1.78 by an experimenter blind to housing information.

RNA-Sequencing

RNA-seq was performed as a service by Bioengineering Lab. Co., Ltd. (Kanagawa, Japan). Briefly, total RNA was extracted with the AllPrep DNA/RNA Mini Kit (#80204, Qiagen, Hilden, Germany) according to the manufacturer's instruction. RNA integrity number (RIN) of total RNA was quantified by Agilent 2100 Bioanalyzer using Agilent RNA 6000 Pico Kit (#5067-1513, Agilent, Santa Clara, CA). Total RNA with RIN values of ≥8.8 were used for RNA-seq library preparation. mRNA was purified from 500 ng total RNA by KAPA mRNA Capture Kit (#KK8440, Kapa Biosystems, Boston, MA), and subjected to cDNA library making (fragmentation, first and second strand syntheses, adenylation, ligation and amplification) using KAPA Stranded mRNA-Seq Kit (#KK8400, Kapa Biosystems, Boston, MA) according to the manufacturer's instruction. cDNA library quality was quantified by 2100 Bioanalyzer using Agilent High Sensitivity DNA Kit (#5067-4626, Agilent, Santa Clara, CA). Library was sequenced as 151 bp paired-end on Illumina NextSeq 500.

RNA-Seq Data Analysis

RNA-seq data analysis was performed as described previously (Usui et al., 2017a). Raw reads were first filtered for quality and trimmed for adapters using FASQC (http://www.bioinformatics.babraham.ac.uk/projects/fastqc) and Trimmomatic (Bolger et al., 2014). Filtered reads were then aligned to the mouse genome mm10 (https://genome.ucsc.edu) using STAR v2.5.2b (Dobin et al., 2013) allowing three mismatches. Uniquely mapped reads (bam flag NH:i:1) were used to obtain the gene counts using HTSeq package (Anders et al., 2015), and the read counts were normalized to the CPM (counts per million) implemented in the edgeR package (Robinson et al., 2010; McCarthy et al., 2012). For further analysis, we performed a sample-specific CPM filtering considering genes with CPM values of 1 in all replicates for treatments or controls. DESeq (Anders and Huber, 2010; Love et al., 2014) was then used to detect the differentially expressed genes (DEGs). We applied a filter of FDR (adjusted p-value) of <0.05 and absolute log fold change of >0.3 to identify significantly changed genes. Gene ontology (GO) analysis with the significant DEGs was carried out using ToppGene (https://toppgene.cchmc.org), and these GO terms were consolidated using REVIGO (Supek et al., 2011). The list of autism spectrum disorder (ASD) genes was derived from the SFARI database (1010 genes; https://gene.sfari.org/database/human-gene). The NCBI Gene Expression Omnibus (GEO) accession number for the RNA-seq data reported in this manuscript is GSE180055 (token: ivureikyjdwthuf).

Quantitative Real-Time PCR

qPCR was performed as described previously (Usui et al., 2017b). Total RNA was extracted from the mouse PFC using the miRNeasy Mini Kit (#217004; Qiagen, Hilden, Germany) according to the manufacturer's instructions. Single-stranded cDNA was prepared using DNaseI, Amplification grade (#18068015; Thermo Fisher Scientific) and SuperScript III First-Strand Synthesis SuperMix (#18080400; Thermo Fisher Scientific) and amplified by PCR according to the manufacturer's instructions. qRT-PCR was performed using PowerUp SYBR Green Master Mix (#A25742; Thermo Fisher Scientific) and a QuantStudio 7 Flex Real-Time PCR System (Thermo Fisher Scientific). Each biological sample had four technical replicates for qPCR, and the number of biological replicates for each experiment is indicated in each figure legend. *18S* rRNA was used as a reference for normalization. Data were analyzed by the ΔΔCq method using QuantStudio 7 Flex Real-Time PCR System software (Thermo Fisher Scientific). The following primers were used: *18S rRNA*, F-5′-GAGGGAGCCTGAGAAACGG-3′, R-5′-GTCGGGAGTGGGTAATTTGC-3′; *mZbtb16*, F-5′-AGGGAGCTGTTCAGCAAGC-3′, R-5′-TCATCCCACTGTGCAGTTTC-3′; *mBanp*, F-5′-GTGGTTCAGATTGCAGTGGA-3′, R-5′-TCAAGGCAGGTT

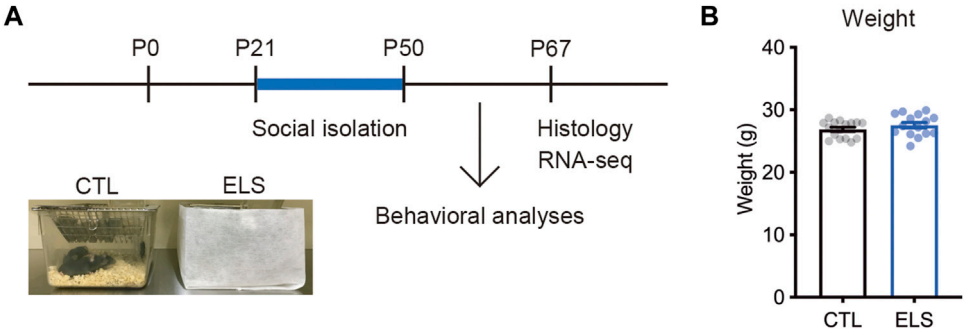

FIGURE 1 | Experimental scheme. **(A)** Experimental design and time course of early life stress (ELS). In ELS mice, male mice were individually housed after the weaning at postnatal days 21 (P21) until P50. In control mice, 4 male mice were co-housed in the same cage after the weaning at P21. Mouse behaviors, brain, and gene expression were analyzed at P50 and P67, respectively. **(B)** No significant difference in the weight after social isolation. Data are presented as means (±SEM), unpaired *t*-test, *n* = 15–16/condition. CTL, control mice; ELS, early life stressed mice.

CATCATCA-3′; *mHif3a*, F-5′-GAGTGGAACCAGGTGGAAAA-3′, R-5′-TCTTGGTCACAGGGATGGAT-3′; *mNr4a1*, F-5′-CAATGCTTCGTGTCAGCACT-3′, R-5′-TGGCGCTTTTCTGTACTGTG-3′; *mPer2*, F-5′-GCGGTCACGTTTTCCACTAT-3′, R-5′-CTTGGGGAGAAGTCCACGTA-3′; *mFos*, F-5′-ATGGGCTCTCCTGTCAACAC-3′, R-5′-TGTCACCGTGGGGATAAAGT-3′; *mMcf2l*, F-5′-TGGCCCTAGAAGAAATGGTG-3′, R-5′-TTCTTCAGCTGCTCCTGGAT-3′; *mTsc22d3*, F-5′-GGTGGCCCTAGACAACAAGA-3′, R-5′-TCTTCTCAAGCAGCTCACGA-3′; *mLrfn2*, F-5′-GGTCAAGTGGTCTGTCAGCA-3′, R-5′-TAGCCAGTACGCACAAGTCG-3′; *mOsbpl3*, F-5′-GGAATACAGCGAGCTTCTGG-3′, R-5′-TGCATTCGTACGTTTCTCCA-3′; *mFkbp5*, F-5′-CCCCAATGCTGAGCTTATGT-3′, R-5′-TCCCTTCTCTTTCACGATGG-3′; *mSh2d3c*, F-5′-GGCGAAGCATTACCATGACT-3′, R-5′-TGGAGATCTGGGATCTGGTC-3′; *mArc*, F-5′-AGCCAGGAGAATGACACCAG-3′, R-5′-CCAGGCACCTCCTCTCTGTA-3′; *mNpas4*, F-5′-GGACTTGGCCACCTATGAAA-3′, R-5′-GCTCCACGTCTTGATGACAA-3′; *mCys1*, F-5′-CTACGCCTGCTGGATCAGTT-3′, R-5′-ACAGCTGTCTTCAGGGTTGC-3′. Cycling conditions were 50°C for 2 min and 95°C for 2 min, followed by 40 cycles at 95°C for 1 s and 60°C for 30 s according to the manufacturer's instructions.

Statistical Analysis

All behavioral data are represented as the means of biologically independent experiments with ± standard errors of the mean (SEM). The statistical analyses (independent samples *t*-test and Pearson's r) were performed using the GraphPad Prism 9 software. Asterisks indicate *p*-values (****$p < 0.0001$, ***$p < 0.001$, **$p < 0.01$, *$p < 0.05$) with $p < 0.05$ being considered as the threshold of statistical significance.

RESULTS

ELS Caused Adolescent Social Impairments

To investigate the influence of ELS on behaviors, cytoarchitecture, and transcriptome in the PFC of adolescent mice, we performed social isolation immediately after the weaning (**Figure 1A**). After the social isolation period (P21–P50), we found that there was no difference in the weight between controls and ELS mice (control = 26.89 ± 0.34, ELS = 27.55 ± 0.45, 95 %Cl = −0.4800 to 1.786, $p = 0.25$) (**Figure 1B**).

We examined social behaviors by multiple evaluation tests. In the sociability trial of three-chamber social interaction test, control and ELS mice interacted with a social target (stranger 1) in approach (controls: empty = 3.00 ± 0.43, stranger 1 = 6.19 ± 0.44, 95 %Cl = 1.934 to 4.441, $p < 0.0001$; ELS mice: empty = 2.47 ± 0.64, stranger 1 = 4.20 ± 0.42, 95 %Cl = 0.1712 to 3.295, $p = 0.0309$) (**Figures 2A,B**), distance (controls: empty = 47.08 ± 9.68, stranger 1 = 233.50 ± 21.56, 95 %Cl = 138.2 to 234.7, $p < 0.0001$; ELS mice: empty = 47.18 ± 11.98, stranger 1 = 146.10 ± 23.30, 95 %Cl = 45.22 to 152.6, $p = 0.0008$) (**Figures 2E,F**), and time (controls: empty = 27.09 ± 5.97, stranger 1 = 153.20 ± 11.92, 95 %Cl = 98.90 to 153.4, $p < 0.0001$; ELS mice: empty = 24.17 ± 6.79, stranger 1 = 125.60 ± 18.37, 95 %Cl = 61.27 to 141.5, $p < 0.0001$) (**Figures 2I,J**). However, ELS mice showed fewer interactions compared with control mice (approach: 95 % Cl = −3.230 to −0.7452, $p = 0.0028$; distance: 95 %Cl = −152.3 to −22.63, $p = 0.0099$; time: 95 %Cl = −71.89 to 16.58, $p = 0.21$) (**Supplementary Figure S1**), indicating the reduction of sociability in ELS mice. In the social novelty trial, control mice displayed more interactions with stranger mouse (stranger 2) than familiar mouse in approach (familiar = 5.31 ± 0.47, stranger 2 = 5.44 ± 0.45, 95 %Cl = −1.202 to 1.452, $p = 0.85$) (**Figure 2C**), distance (familiar = 97.04 ± 9.61, stranger 2 = 159.5 ± 10.98, 95 %Cl = 32.68 to 92.29, $p = 0.0002$) (**Figure 2G**), and time (familiar = 59.63 ± 6.08, stranger 2 = 104.70 ± 6.86, 95 %Cl = 26.31 to 63.75, $p < 0.0001$) (**Figure 2K**). In contrast, ELS mice showed no different interactions between a stranger mouse and a familiar mouse in approach (familiar = 3.80 ± 0.73, stranger 2 = 3.33 ± 0.47, 95 %Cl = −2.242 to 1.309, $p = 0.59$) (**Figure 2D**), distance (familiar = 84.09 ± 20.02, stranger 2 = 104.80 ± 18.65, 95 %Cl = 35.30 to 76.80, $p = 0.46$) (**Figure 2H**), and time (familiar = 67.63 ± 19.05, stranger 2 = 87.20 ± 18.78, 95 %Cl = −35.22 to 74.35, $p = 0.47$) (**Figure 2L**). These results indicate that sociability and social novelty are both impaired in adolescent ELS mice.

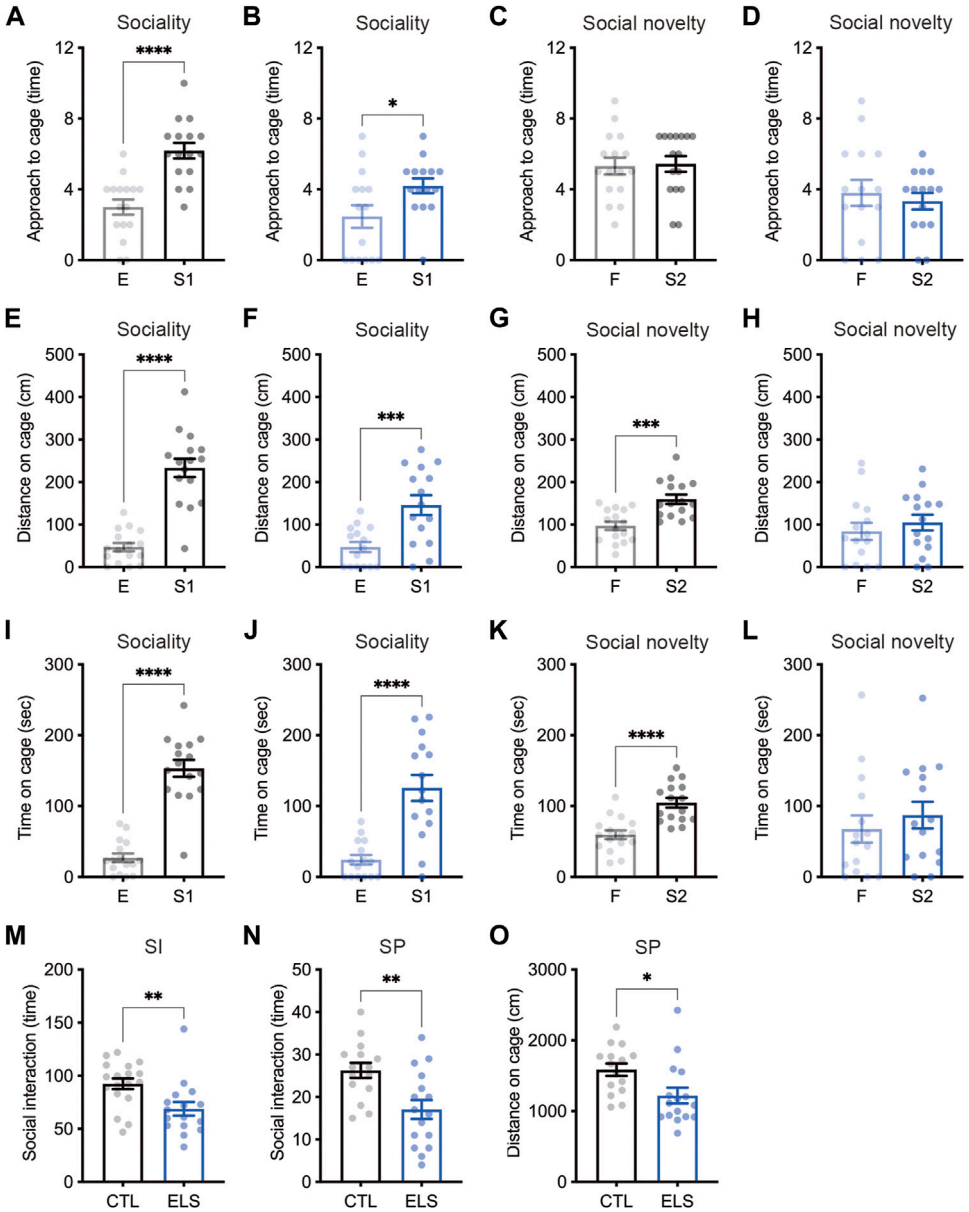

FIGURE 2 | Social impairments induced by ELS. **(A–L)** Quantifications of three-chamber social interaction test results. The numbers of approaches **(A–D)**, distance **(E–H)**, and time **(I–L)** were shown during the 2nd trial (sociability behavior) **(A, B, E, F, I, J)** and the 3rd trial (social novelty behavior) **(C, D, G, H, K, L)** of three-chamber social interaction test (3CSI), respectively. Sociability and social novelty were impaired in adolescent ELS mice. CTL was shown in black, and the ELS was shown in blue. E, empty; S1, stranger mouse 1; S2, stranger mouse 2; SI, social interaction test. **(M)** Reduced number of social interactions in adolescent ELS mice. **(N, O)** Quantifications of social preference in ELS mice. The number of interaction **(N)** and distance **(O)** were reduced in ELS mice. SP, social preference test. Data are presented as means (±SEM). Asterisks indicate ****p < 0.0001, ***p < 0.001, **p < 0.01, *p < 0.05, unpaired t-test, n = 15–16/condition for 3CSI and SP, n = 16–18/condition for SI.

We next examined social interaction under the free moving condition in the chamber, and found the reduced social interaction events in ELS mice (control = 92.44 ± 5.05, ELS = 68.88 ± 6.39, 95 %CI = −39.99 to −7.145, p = 0.0063) (**Figure 2M**). We also found that the reductions of social interaction events (control = 26.27 ± 1.78, ELS = 17.06 ± 2.23, 95 %CI = −15.09 to −3.314, p = 0.0034) (**Figure 2N**) and distance around social target (control = 1586 ± 87.56, ELS = 1219 ± 111.1, 95 %CI = −659.0 to −75.29, p = 0.0155) (**Figure 2O**) in ELS mice by social preference test. Together, these results demonstrate that various social behaviors are impaired in adolescent ELS mice.

Anxiety-Like Behavior Induced by ELS

Since the ELS mice showed impaired social behaviors, we investigated anxiety-like behaviors as social-associated behaviors. In light-dark box test, we found that decreased

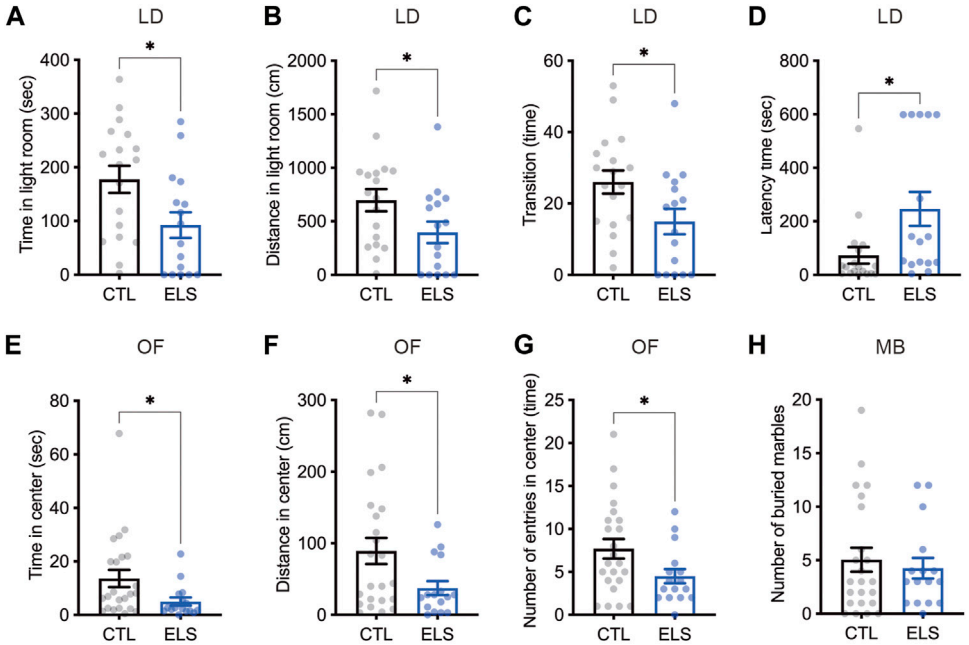

FIGURE 3 | Increased anxiety-like behaviors in ELS mice. **(A–D)** Quantifications of light-dark box test result. Significant reductions of time **(A)** and distance **(B)** in light room, the transition number between the rooms **(C)**, and latency time to enter the light room **(D)** were observed in adolescent ELS mice. LD, light-dark box test. **(E–G)** Quantifications of open field test result. Significant reductions of time **(E)**, distance **(F)**, and the number of entries **(G)** in center were observed in adolescent ELS mice. **(H)** Quantification of the number of buried marbles. There was no difference in the repetitive behavior in adolescent ELS mice. MB, marble-burying test; OF, open field test. Data are presented as means (±SEM). Asterisk indicates *p < 0.05, unpaired *t*-test, *n* = 16–18/condition for LD, *n* = 16–23/condition for OF, *n* = 16–23/condition for MB.

time (control = 177.50 ± 25.29, ELS = 92.46 ± 23.84, 95 %Cl = −156.4 to −13.75, p = 0.0209) (**Figure 3A**) and distance (control = 696.90 ± 104.00, ELS = 397.10 ± 100.10, 95 %Cl = −595.7 to −4.104, p = 0.0471) (**Figure 3B**) of the light room in ELS mice. We also found that decreased the number of transitions between the rooms (control = 26.00 ± 3.26, ELS = 14.94 ± 3.53, 95 %Cl = −20.84 to −1.285, p = 0.0278) (**Figure 3C**) and increased latency time (control = 73.24 ± 30.97, ELS = 246.2 ± 63.68, 95 %Cl = 33.67 to 312.2, p = 0.0166) (**Figure 3D**) in ELS mice. In addition, decreased time (control = 13.63 ± 3.22, ELS = 4.99 ± 1.50, 95 %Cl = −16.90 to −0.3771, p = 0.0409) (**Figure 3E**) and distance (control = 89.2 ± 18.19, ELS = 37.4 ± 9.68, 95 %Cl = −99.05 to −4.552, p = 0.0325) (**Figure 3F**) in the center area of open field test, and the number of entries to the center area (control = 7.70 ± 1.14, ELS = 4.50 ± 0.82, 95 %Cl = −6.291 to −0.1001, p = 0.0434) (**Figure 3G**) were observed in ELS mice. We also examined repetitive behavior of ELS mice by marble-burying test, however there was no difference (control = 5.04 ± 1.11, ELS = 4.25 ± 0.96, 95 %Cl = −3.951 to 2.364, p = 0.61) (**Figure 3H**). These results indicate that anxiety-like behavior is increased in ELS mice.

Neuronal Loss and Microglia Increase by ELS

Next, we examined how ELS affects the PFC cytoarchitecture. We found a slight reduction of the number of NeuN+ mature neurons in the PFC of ELS mice (control = 358.00 ± 6.89, ELS = 329.80 ± 9.95, 95 %Cl = −56.12 to −0.2850, p = 0.0482) (**Figures 4A,C,D**). We found a slight increase of the number of Iba1+ microglia in the PFC of ELS mice (control = 103.20 ± 2.44, ELS = 115.00 ± 4.18, 95 %Cl = 0.6355 to 22.96, p = 0.0407) (**Figures 4B,C,E**). These results indicate that ELS caused a decrease in the number of neurons and an increase in the number of microglia in the PFC of adolescent ELS mice.

ELS Altered PFC Transcriptome

To understand the molecular mechanisms underlying behavioral and histological phenotypes, we characterized the transcriptome in the PFC of ELS mice by RNA-seq. Transcriptome profiles were clearly separated between control and ELS mice (**Figure 5A**). Differential expression analysis of the RNA-seq data uncovered 15 DEGs (FDR < 0.05) in PFC of ELS mice compared to control mice (**Figure 5B**, **Supplementary Table S1**). GO analysis for the DEGs highlighted functions involved in regulation of transcription by RNA polymerase II, positive regulation of transcription, positive regulation of RNA metabolic process, response to corticosterone, response to mineralocorticoid, and trans−synaptic signaling (**Figure 5C**, **Supplementary Table S2**). DEGs were also involved in the pathway in glucocorticoid receptor regulatory network, and diseases such as sleep disorders, *Clostridium difficile*, glucocorticoid receptor deficiency, substance withdrawal syndrome, and stress, psychological (**Figure 5C**, **Supplementary Table S2**). The

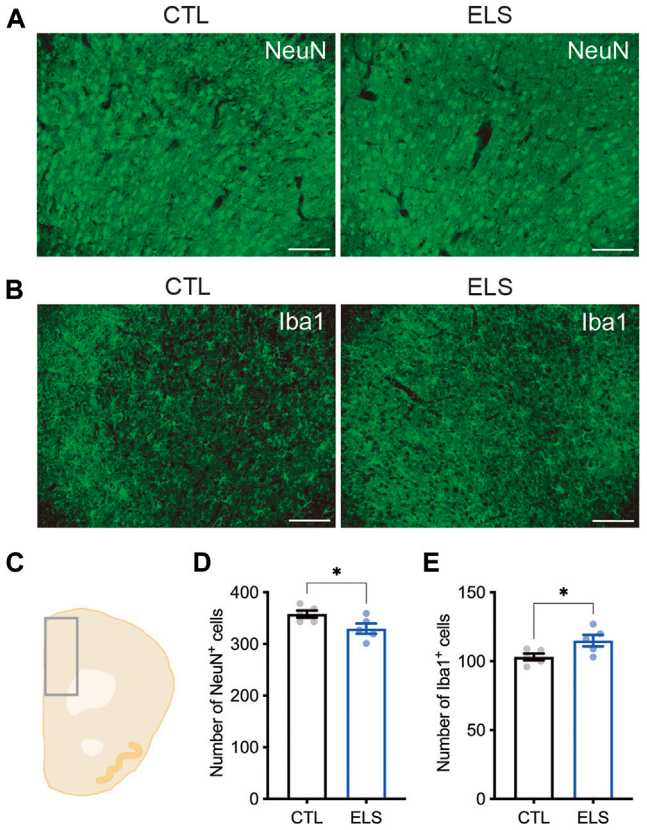

FIGURE 4 | Neuronal loss and microglia increase in the PFC of ELS mice. **(A, B)** Representative fluorescent images of NeuN+ neuron **(A)** and Iba1+ microglia **(B)**. **(C)** Schematic diagram of mouse cortex analyzed at bregma 1.94. **(D, E)** Quantifications of NeuN+ neuron **(D)** and Iba1+ microglia **(E)** in the PFC. Decreased NeuN+ neurons and increased Iba1+ microglia were observed in the PFC of adolescent ELS mice. Data are presented as means (±SEM). Asterisk indicates $^*p < 0.05$, unpaired *t*-test, n = 5/condition. Scale bars: 100 μm.

expressions of DEGs were confirmed in the PFC of ELS mice by qPCR (**Figure 5D**). Since ELS mice exhibited social impairments, we overlapped the DEGs with the gene list of ASD, a developmental disorder that shows impairments in social communication. Then, we found that 3 DEGs (*Zbtb16*, *Per2*, *Lrfn2*) overlapped with SFARI ASD genes (**Figure 5E**). Together, these results indicate that ELS affected genes are involved in transcriptional regulation, stress signaling, and sleep disorders. Our results also suggest that 3 DEGs (*Zbtb16*, *Per2*, *Lrfn2*) are involved in sociality.

DISCUSSION

In this study, we demonstrate that ELS causes the impairments of social behaviors (sociality, social novelty, and social preference) and an increased anxiety-like behavior in adolescent mice. ELS induced neuronal loss and microglia increase in the PFC of adolescent mice. As the ELS-affected genes, we identified 15 DEGs involved in transcriptional regulation, stress signaling, and sleep disorders in the PFC of adolescent mice.

Previous studies have reported that social isolation at pre-adolescent period caused the reduction of sociality in mice (Makinodan et al., 2012; Usui et al., 2021b). Here we showed that various social impairments and increased anxiety-like behaviors in ELS mice (**Figures 2**, **3**). Social isolation during adulthood has been used as a well-known method of generating depression models, and such mice show increased anxiety-like behaviors (Du Preez et al., 2020). In fact, increased anxiety-like behavior, repetitive behavior, memory impairment, and depression-like behavior have been reported in mice that were socially isolated earlier (P14–50) than our condition (Niwa et al., 2011). Sociality and anxiety are closely related and are controlled by neural circuits centered on PFC and amygdala (Stein and Stein, 2008; Penninx et al., 2021). These two brain regions have been reported as ones of corresponding regions involved in social behaviors (Amaral et al., 2008), and are also known as the brain regions impaired by neglect and maltreatment (Teicher et al., 2016). In the PFC of ELS mice, we observed slight changes in the numbers of NeuN+ mature neurons and Iba1+ microglia (**Figure 4**). This result suggests the possibility that ELS may cause inflammation and results neuronal cell death in the brain. To support this idea, previous studies have reported neuronal cell death due to chronic stress (Bachis et al., 2008; Natarajan et al., 2017). Moreover, chronic stress has been reported to increase blood corticosterone and induce an increase in microglia (Du Preez et al., 2020). It will be interesting to analyze the effects of ELS on the amygdala as a future study.

In terms of gene expression in the PFC of ELS mice, we identify total 15 DEGs involved in transcriptional regulation, stress signaling, and sleep disorders (**Figures 5B,C**). It was reasonable that there were changes in the genes related to such GOs due to ELS. Among those DEGs, there were many transcription factors, suggesting ELS causes functional changes in PFC. The alterations of genes involved in stress signals were presumed to be the effects of chronic stress due to social isolation. It is known that sleep disorders coexist in social withdrawal (Rubin et al., 2009) and psychiatric disorders such as major depressive disorder (Goldstein and Walker, 2014; Otte et al., 2016). Our data suggests that the alterations of genes associated with circadian rhythm such as *Per2* and *Npas4* due to the influences of ELS may trigger sleep disorders.

In order to explore the gene involved in sociality, we overwrapped the DEGs with SFARI ASD gene list, and identified *Zbtb16*, *Per2*, and *Lrfn2* (**Figure 5E**). Zbtb16 (Plzf) is known as a transcription factor playing key roles in many biological processes such as stem cell proliferation, differentiation, apoptosis, chromatin remodeling, metabolism and immunity (Suliman et al., 2012; Šeda et al., 2017). *ZBTB16* is associated with ASD (Bacchelli et al., 2019) and skeletal defects, genital hypoplasia, and mental retardation (SGYMR) (Wieczorek et al., 2002; Fischer et al., 2008). *Zbtb16* KO mice displayed ASD-like behaviors such as social impairment and increased repetitive behaviors as well as cognitive impairment (Usui et al., 2021a). However, *Zbtb16* KO mice

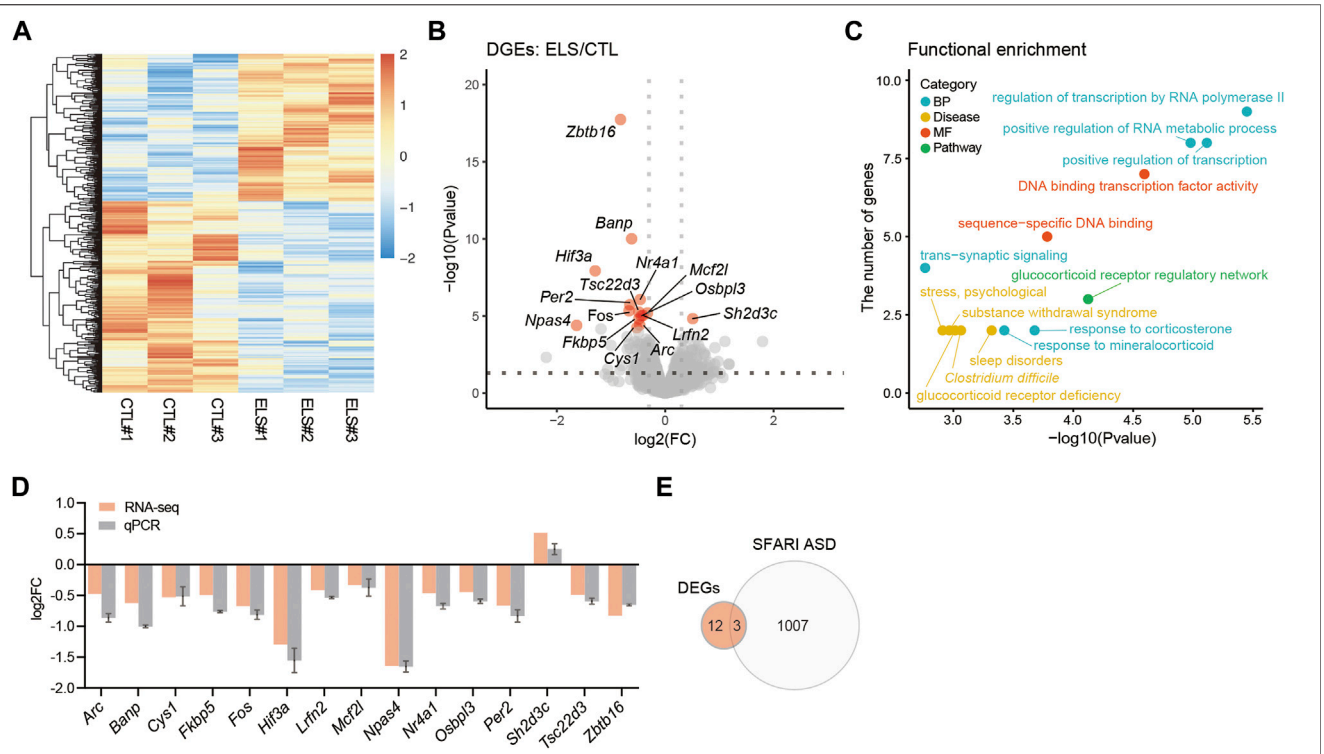

FIGURE 5 | Transcriptomic alteration in the PFC of ELS mice. **(A)** Heatmap of gene expressions in the PFC. **(B)** Volcano plots showing ELS differentially expressed genes (DEGs). FDR < 0.05. X-axis = –log10(Pvalue), Y-axis = log2(FC). FC, fold change. **(C)** Scatter plots represent functional enrichment of ELS DEGs in biological process (BP), disease, molecular function (MF), and pathway. X-axis = –log10(Pvalue), Y-axis = the number of genes. *p*-Values reported by FDR < 0.05 threshold. **(D)** qPCR confirmation of ELS DEGs expressions in the PFC. **(E)** Venn diagram of ELS DEGs overlapping with SFARI autism spectrum disorder (ASD) genes. The overlapping 3 genes are *Zbtb16, Per2,* and *Lrfn2*. *n* = 3/condition for RNA-seq.

showed antianxiety-like (risk-taking) behaviors (Usui et al., 2021a). Per2 is known as a clock gene of Period family and controls circadian rhythm under the CLOCK/ARNTL regulation (Takahashi, 2017; Rijo-Ferreira and Takahashi, 2019). *PER2* is also associated with ASD (Iossifov et al., 2014; RK et al., 2017), and sleep problem has been reported to coexist in developmental disorders such as ASD (Couturier et al., 2005; Krakowiak et al., 2008; Souders et al., 2009; Mazurek and Sohl, 2016). Moreover, it has been reported that *Per2* expression was altered by social defeat stress (Moravcová et al., 2021). Lrfn2 (SALM1) is known as a synapse adhesion molecule interacting with PSD-95 (Ko et al., 2006). *LRFN2* is associated with ASD (Voineagu et al., 2011), learning disabilities (Thevenon et al., 2016), and antisocial personality disorder (Rautiainen et al., 2016). *Lrfn2* KO mice also displayed ASD-like behaviors such as social withdrawal, decreased vocal communications, increased repetitive behaviors and prepulse inhibition deficits, but not anxiety-like behaviors (Morimura et al., 2017). *Lrfn2* KO mice also displayed synaptic morphological abnormalities in the CA1 hippocampal neurons, resulting LTP enhancement (Morimura et al., 2017). Together, these findings suggest that *Zbtb16*, *Per2*, and *Lrfn2* are the genes involved in sociality.

We acknowledge that our study has several limitations. Since only male mice are used in this study, caution must be taken in interpreting the results of behavioral analysis. In addition, despite the analysis of the effects of environmental factors, the sample size in transcriptome analysis was small and the *p* value in gene expressions was not significant, thus only few genes were identified as DEGs. It is expected that increasing the sample size will lead to the identification of more genes affected by ELS. Furthermore, it is also important to understand the maternal gestational stress as a one of ELS, which is known to affect the brain development and behavior of the offspring. Previous studies have reported that maternal gestational stress has an epigenetic alteration on offspring gene expression as well as impairments of motor and cognitive development, immune system, and adaptation to stress (Wadhwa et al., 2001; Kingston et al., 2012; Argyraki et al., 2019).

In conclusion, our results demonstrate that ELS impacts adolescent social behaviors, anxiety-like behaviors, and PFC characteristics in mice. Our study suggests that ELS causes the alterations in the cytoarchitecture and transcriptome of PFC, leading to social impairments and increased anxiety-like behaviors in adolescents.

DATA AVAILABILITY STATEMENT

The datasets presented in this study can be found in online repositories. The names of the repository/repositories and accession number(s) can be found in the article/**Supplementary Material**.

ETHICS STATEMENT

The animal study was reviewed and approved by the Animal Research Committee of the University of Fukui.

AUTHOR CONTRIBUTIONS

Conceptualization, NU; methodology, NU; validation, NU, GK, HM, and SS; formal analysis, NU, RA, YO, and SB; investigation, NU, RA, YO, and SB; resources, NU; writing—original draft preparation, NU; writing—review and editing, NU, SB, GK, HM, and SS; visualization, NU and SB; supervision, GK, HM, and SS; project administration, NU; funding acquisition, NU. All authors have read and agreed to the published version of the manuscript.

FUNDING

This work was supported by the Japan Society for the Promotion of Science (JSPS) Grant-in-Aid for Scientific Research (C) (20K06872) to NU; JSPS Grant-in-Aid for Early-Career Scientists (18K14814) to NU; Uehara Memorial Foundation to NU; Takeda Science Foundation to NU; SENSHIN Medical Research Foundation to NU; The Osaka Medical Research Foundation for Intractable Diseases to NU; Public Health Science Foundation to NU; Eli Lilly Japan Research Grant to NU; The Grant for Life Cycle Medicine from Faculty of Medical Sciences, University of Fukui to NU. This study was supported by Center for Medical Research and Education, Graduate School of Medicine, Osaka University, and CoMIT Omics Center, Graduate School of Medicine, Osaka University.

ACKNOWLEDGMENTS

We thank Yuuto Ohara, Yuuki Takaba, Xie Min-Jue, Yoko Sasaki, and Tomoko Taniguchi for their support.

SUPPLEMENTARY MATERIAL

The Supplementary Material for this article can be found online at: https://www.frontiersin.org/articles/10.3389/fgene.2021.754198/full#supplementary-material

Supplementary Figure S1 | An impairment of sociality in ELS mice.

Supplementary Table S1 | The list of DEGs in ELS mice.

Supplementary Table S2 | The list of ToppGene information of DEGs.

REFERENCES

Amaral, D. G., Schumann, C. M., and Nordahl, C. W. (2008). Neuroanatomy of Autism. *Trends Neurosciences* 31, 137–145. doi:10.1016/j.tins.2007.12.005

Anders, S., and Huber, W. (2010). Differential Expression Analysis for Sequence Count Data. *Genome Biol.* 11, R106. doi:10.1186/gb-2010-11-10-r106

Anders, S., Pyl, P. T., and Huber, W. (2015). HTSeq--a Python Framework to Work with High-Throughput Sequencing Data. *Bioinformatics* 31, 166–169. doi:10.1093/bioinformatics/btu638

Argyraki, M., Damdimopoulou, P., Chatzimeletiou, K., Grimbizis, G. F., Tarlatzis, B. C., Syrrou, M., et al. (2019). In-utero Stress and Mode of conception: Impact on Regulation of Imprinted Genes, Fetal Development and Future Health. *Hum. Reprod. Update* 25, 777–801. doi:10.1093/humupd/dmz025

Aspesi, D., and Pinna, G. (2019). Animal Models of post-traumatic Stress Disorder and Novel Treatment Targets. *Behav. Pharmacol.* 30, 130–150. doi:10.1097/fbp.0000000000000467

Bacchelli, E., Loi, E., Cameli, C., Moi, L., Vega Benedetti, A., Blois, S., et al. (2019). Analysis of a Sardinian Multiplex Family with Autism Spectrum Disorder Points to Post-Synaptic Density Gene Variants and Identifies CAPG as a Functionally Relevant Candidate Gene. *Jcm* 8, 212. doi:10.3390/jcm8020212

Bachis, A., Cruz, M. I., Nosheny, R. L., and Mocchetti, I. (2008). Chronic Unpredictable Stress Promotes Neuronal Apoptosis in the Cerebral Cortex. *Neurosci. Lett.* 442, 104–108. doi:10.1016/j.neulet.2008.06.081

Bolger, A. M., Lohse, M., and Usadel, B. (2014). Trimmomatic: a Flexible Trimmer for Illumina Sequence Data. *Bioinformatics* 30, 2114–2120. doi:10.1093/bioinformatics/btu170

Chugani, H. T., Behen, M. E., Muzik, O., Juhász, C., Nagy, F., and Chugani, D. C. (2001). Local Brain Functional Activity Following Early Deprivation: a Study of Postinstitutionalized Romanian Orphans. *NeuroImage* 14, 1290–1301. doi:10.1006/nimg.2001.0917

Cohen, R. A., Grieve, S., Hoth, K. F., Paul, R. H., Sweet, L., Tate, D., et al. (2006). Early Life Stress and Morphometry of the Adult Anterior Cingulate Cortex and Caudate Nuclei. *Biol. Psychiatry* 59, 975–982. doi:10.1016/j.biopsych.2005.12.016

Consiglio, C. R., and Brodin, P. (2020). Stressful Beginnings with Long-Term Consequences. *Cell* 180, 820–821. doi:10.1016/j.cell.2020.02.021

Couturier, J. L., Speechley, K. N., Steele, M., Norman, R., Stringer, B., and Nicolson, R. (2005). Parental Perception of Sleep Problems in Children of normal Intelligence with Pervasive Developmental Disorders: Prevalence, Severity, and Pattern. *J. Am. Acad. Child Adolesc. Psychiatry* 44, 815–822. doi:10.1097/01.chi.0000166377.22651.87

Dannlowski, U., Stuhrmann, A., Beutelmann, V., Zwanzger, P., Lenzen, T., Grotegerd, D., et al. (2012). Limbic Scars: Long-Term Consequences of Childhood Maltreatment Revealed by Functional and Structural Magnetic Resonance Imaging. *Biol. Psychiatry* 71, 286–293. doi:10.1016/j.biopsych.2011.10.021

Dobin, A., Davis, C. A., Schlesinger, F., Drenkow, J., Zaleski, C., Jha, S., et al. (2013). STAR: Ultrafast Universal RNA-Seq Aligner. *Bioinformatics* 29, 15–21. doi:10.1093/bioinformatics/bts635

Du Preez, A., Law, T., Onorato, D., Lim, Y. M., Eiben, P., Musaelyan, K., et al. (2020). The Type of Stress Matters: Repeated Injection and Permanent Social Isolation Stress in Male Mice Have a Differential Effect on Anxiety- and Depressive-like Behaviours, and Associated Biological Alterations. *Transl Psychiatry* 10, 325. doi:10.1038/s41398-020-01000-3

Edmiston, E. E., Wang, F., Mazure, C. M., Guiney, J., Sinha, R., Mayes, L. C., et al. (2011). Corticostriatal-limbic gray Matter Morphology in Adolescents with Self-Reported Exposure to Childhood Maltreatment. *Arch. Pediatr. Adolesc. Med.* 165, 1069–1077. doi:10.1001/archpediatrics.2011.565

Ferguson, K. T., Cassells, R. C., MacAllister, J. W., and Evans, G. W. (2013). The Physical Environment and Child Development: an International Review. *Int. J. Psychol.* 48, 437–468. doi:10.1080/00207594.2013.804190

Fischer, S., Kohlhase, J., Böhm, D., Schweiger, B., Hoffmann, D., Heitmann, M., et al. (2008). Biallelic Loss of Function of the Promyelocytic Leukaemia Zinc finger (PLZF) Gene Causes Severe Skeletal Defects and Genital Hypoplasia. *J. Med. Genet.* 45, 731–737. doi:10.1136/jmg.2008.059451

Goldstein, A. N., and Walker, M. P. (2014). The Role of Sleep in Emotional Brain Function. *Annu. Rev. Clin. Psychol.* 10, 679–708. doi:10.1146/annurev-clinpsy-032813-153716

Iossifov, I., O'Roak, B. J., Sanders, S. J., Ronemus, M., Krumm, N., Levy, D., et al. (2014). The Contribution of De Novo Coding Mutations to Autism Spectrum Disorder. *Nature* 515, 216–221. doi:10.1038/nature13908

Jaffee, S. R. (2017). Child Maltreatment and Risk for Psychopathology in Childhood and Adulthood. *Annu. Rev. Clin. Psychol.* 13, 525–551. doi:10.1146/annurev-clinpsy-032816-045005

Kelly, P. A., Viding, E., Wallace, G. L., Schaer, M., De Brito, S. A., Robustelli, B., et al. (2013). Cortical Thickness, Surface Area, and Gyrification Abnormalities in Children Exposed to Maltreatment: Neural Markers of Vulnerability? *Biol. Psychiatry* 74, 845–852. doi:10.1016/j.biopsych.2013.06.020

Kingston, D., Tough, S., and Whitfield, H. (2012). Prenatal and Postpartum Maternal Psychological Distress and Infant Development: a Systematic Review. *Child. Psychiatry Hum. Dev.* 43, 683–714. doi:10.1007/s10578-012-0291-4

Ko, J., Kim, S., Chung, H. S., Kim, K., Han, K., Kim, H., et al. (2006). SALM Synaptic Cell Adhesion-like Molecules Regulate the Differentiation of Excitatory Synapses. *Neuron* 50, 233–245. doi:10.1016/j.neuron.2006.04.005

Krakowiak, P., Goodlin-Jones, B., Hertz-Picciotto, I., Croen, L. A., and Hansen, R. L. (2008). Sleep Problems in Children with Autism Spectrum Disorders, Developmental Delays, and Typical Development: a Population-Based Study. *J. Sleep Res.* 17, 197–206. doi:10.1111/j.1365-2869.2008.00650.x

Love, M. I., Huber, W., and Anders, S. (2014). Moderated Estimation of Fold Change and Dispersion for RNA-Seq Data with DESeq2. *Genome Biol.* 15, 550. doi:10.1186/s13059-014-0550-8

Mackes, N. K., Golm, D., Sarkar, S., Kumsta, R., Rutter, M., Fairchild, G., et al. (2020). Early Childhood Deprivation Is Associated with Alterations in Adult Brain Structure Despite Subsequent Environmental Enrichment. *Proc. Natl. Acad. Sci. USA* 117, 641–649. doi:10.1073/pnas.1911264116

Makinodan, M., Rosen, K. M., Ito, S., and Corfas, G. (2012). A Critical Period for Social Experience-dependent Oligodendrocyte Maturation and Myelination. *Science* 337, 1357–1360. doi:10.1126/science.1220845

Mazurek, M. O., and Sohl, K. (2016). Sleep and Behavioral Problems in Children with Autism Spectrum Disorder. *J. Autism Dev. Disord.* 46, 1906–1915. doi:10.1007/s10803-016-2723-7

McCarthy, D. J., Chen, Y., and Smyth, G. K. (2012). Differential Expression Analysis of Multifactor RNA-Seq Experiments with Respect to Biological Variation. *Nucleic Acids Res.* 40, 4288–4297. doi:10.1093/nar/gks042

Miguel, P. M., Pereira, L. O., Silveira, P. P., and Meaney, M. J. (2019). Early Environmental Influences on the Development of Children's Brain Structure and Function. *Dev. Med. Child. Neurol.* 61, 1127–1133. doi:10.1111/dmcn.14182

Moravcová, S., Červená, K., Míková, H., Pačesová, D., Pallag, G., Novotný, J., et al. (2021). Social Defeat Stress Affects Resident's Clock Gene and Bdnf Expression in the Brain. *Stress* 24, 206–212. doi:10.1080/10253890.2020.1759548

Morimura, N., Yasuda, H., Yamaguchi, K., Katayama, K.-i., Hatayama, M., Tomioka, N. H., et al. (2017). Autism-like Behaviours and Enhanced Memory Formation and Synaptic Plasticity in Lrfn2/SALM1-Deficient Mice. *Nat. Commun.* 8, 15800. doi:10.1038/ncomms15800

Natarajan, R., Forrester, L., Chiaia, N. L., and Yamamoto, B. K. (2017). Chronic-Stress-Induced Behavioral Changes Associated with Subregion-Selective Serotonin Cell Death in the Dorsal Raphe. *J. Neurosci.* 37, 6214–6223. doi:10.1523/jneurosci.3781-16.2017

Niwa, M., Matsumoto, Y., Mouri, A., Ozaki, N., and Nabeshima, T. (2011). Vulnerability in Early Life to Changes in the Rearing Environment Plays a Crucial Role in the Aetiopathology of Psychiatric Disorders. *Int. J. Neuropsychopharm.* 14, 459–477. doi:10.1017/s1461145710001239

Otte, C., Gold, S. M., Penninx, B. W., Pariante, C. M., Etkin, A., Fava, M., et al. (2016). Major Depressive Disorder. *Nat. Rev. Dis. Primers* 2, 16065. doi:10.1038/nrdp.2016.65

Penninx, B. W., Pine, D. S., Holmes, E. A., and Reif, A. (2021). Anxiety Disorders. *The Lancet* 397, 914–927. doi:10.1016/s0140-6736(21)00359-7

Pinna, G. (2019). Animal Models of PTSD: The Socially Isolated Mouse and the Biomarker Role of Allopregnanolone. *Front. Behav. Neurosci.* 13, 114. doi:10.3389/fnbeh.2019.00114

Rautiainen, M.-R., Paunio, T., Repo-Tiihonen, E., Virkkunen, M., Ollila, H. M., Sulkava, S., et al. (2016). Genome-wide Association Study of Antisocial Personality Disorder. *Transl Psychiatry* 6, e883. doi:10.1038/tp.2016.155

Rijo-Ferreira, F., and Takahashi, J. S. (2019). Genomics of Circadian Rhythms in Health and Disease. *Genome Med.* 11, 82. doi:10.1186/s13073-019-0704-0

Rk, C. Y., Merico, D., Bookman, M., J, L. H., Thiruvahindrapuram, B., Patel, R. V., et al. (2017). Whole Genome Sequencing Resource Identifies 18 New Candidate Genes for Autism Spectrum Disorder. *Nat. Neurosci.* 20, 602–611. doi:10.1038/nn.4524

Robinson, M. D., McCarthy, D. J., and Smyth, G. K. (2010). edgeR: a Bioconductor Package for Differential Expression Analysis of Digital Gene Expression Data. *Bioinformatics* 26, 139–140. doi:10.1093/bioinformatics/btp616

Rubin, K. H., Coplan, R. J., and Bowker, J. C. (2009). Social Withdrawal in Childhood. *Annu. Rev. Psychol.* 60, 141–171. doi:10.1146/annurev.psych.60.110707.163642

Schöner, J., Heinz, A., Endres, M., Gertz, K., and Kronenberg, G. (2017). Post-traumatic Stress Disorder and beyond: an Overview of Rodent Stress Models. *J. Cel. Mol. Med.* 21, 2248–2256. doi:10.1111/jcmm.13161

Šeda, O., Šedová, L., Včelák, J., Vaňková, M., Liška, F., and Bendlová, B. (2017). ZBTB16 and Metabolic Syndrome: a Network Perspective. *Physiol. Res.* 66, S357–s365. doi:10.33549/physiolres.933730

Sonuga-Barke, E. J. S., Kennedy, M., Kumsta, R., Knights, N., Golm, D., Rutter, M., et al. (2017). Child-to-adult Neurodevelopmental and Mental Health Trajectories after Early Life Deprivation: the Young Adult Follow-Up of the Longitudinal English and Romanian Adoptees Study. *The Lancet* 389, 1539–1548. doi:10.1016/s0140-6736(17)30045-4

Souders, M. C., Mason, T. B. A., Valladares, O., Bucan, M., Levy, S. E., Mandell, D. S., et al. (2009). Sleep Behaviors and Sleep Quality in Children with Autism Spectrum Disorders. *Sleep* 32, 1566–1578. doi:10.1093/sleep/32.12.1566

Stein, M. B., and Stein, D. J. (2008). Social Anxiety Disorder. *The Lancet* 371, 1115–1125. doi:10.1016/s0140-6736(08)60488-2

Suliman, B. A., Xu, D., and Williams, B. R. G. (2012). The Promyelocytic Leukemia Zinc finger Protein: Two Decades of Molecular Oncology. *Front. Oncol.* 2, 74. doi:10.3389/fonc.2012.00074

Supek, F., Bošnjak, M., Škunca, N., and Šmuc, T. (2011). REVIGO Summarizes and Visualizes Long Lists of Gene Ontology Terms. *PloS one* 6, e21800. doi:10.1371/journal.pone.0021800

Takahashi, J. S. (2017). Transcriptional Architecture of the Mammalian Circadian Clock. *Nat. Rev. Genet.* 18, 164–179. doi:10.1038/nrg.2016.150

Takesian, A. E., and Hensch, T. K. (2013). Balancing Plasticity/stability across Brain Development. *Prog. Brain Res.* 207, 3–34. doi:10.1016/b978-0-444-63327-9.00001-1

Teicher, M. H., Anderson, C. M., and Polcari, A. (2012). Childhood Maltreatment Is Associated with Reduced Volume in the Hippocampal Subfields CA3, Dentate Gyrus, and Subiculum. *Proc. Natl. Acad. Sci.* 109, E563–E572. doi:10.1073/pnas.1115396109

Teicher, M. H., Samson, J. A., Anderson, C. M., and Ohashi, K. (2016). The Effects of Childhood Maltreatment on Brain Structure, Function and Connectivity. *Nat. Rev. Neurosci.* 17, 652–666. doi:10.1038/nrn.2016.111

Thevenon, J., Souchay, C., Seabold, G. K., Dygai-Cochet, I., Callier, P., Gay, S., et al. (2016). Heterozygous Deletion of the LRFN2 Gene Is Associated with Working Memory Deficits. *Eur. J. Hum. Genet.* 24, 911–918. doi:10.1038/ejhg.2015.221

Tomoda, A., Sheu, Y.-S., Rabi, K., Suzuki, H., Navalta, C. P., Polcari, A., et al. (2011). Exposure to Parental Verbal Abuse Is Associated with Increased gray Matter Volume in superior Temporal Gyrus. *NeuroImage* 54 (Suppl. 1), S280–S286. doi:10.1016/j.neuroimage.2010.05.027

Tomoda, A., Suzuki, H., Rabi, K., Sheu, Y.-S., Polcari, A., and Teicher, M. H. (2009). Reduced Prefrontal Cortical gray Matter Volume in Young Adults Exposed to Harsh Corporal Punishment. *NeuroImage* 47 (Suppl. 2), T66–T71. doi:10.1016/j.neuroimage.2009.03.005

Usui, N., Araujo, D. J., Kulkarni, A., Co, M., Ellegood, J., Harper, M., et al. (2017a). Foxp1 Regulation of Neonatal Vocalizations via Cortical Development. *Genes Dev.* 31, 2039–2055. doi:10.1101/gad.305037.117

Usui, N., Berto, S., Konishi, A., Kondo, M., Konopka, G., Matsuzaki, H., et al. (2021a). Zbtb16 Regulates Social Cognitive Behaviors and Neocortical Development. *Transl Psychiatry* 11, 242. doi:10.1038/s41398-021-01358-y

Usui, N., Co, M., Harper, M., Rieger, M. A., Dougherty, J. D., and Konopka, G. (2017b). Sumoylation of FOXP2 Regulates Motor Function and Vocal Communication through Purkinje Cell Development. *Biol. Psychiatry* 81, 220–230. doi:10.1016/j.biopsych.2016.02.008

Usui, N., Matsuzaki, H., and Shimada, S. (2021b). Characterization of Early Life Stress-Affected Gut Microbiota. *Brain Sci.* 11, 913. doi:10.3390/brainsci11070913

Voineagu, I., Wang, X., Johnston, P., Lowe, J. K., Tian, Y., Horvath, S., et al. (2011). Transcriptomic Analysis of Autistic Brain Reveals Convergent Molecular Pathology. *Nature* 474, 380–384. doi:10.1038/nature10110

Wadhwa, P. D., Sandman, C. A., and Garite, T. J. (2001). Chapter 9 the Neurobiology of Stress in Human Pregnancy: Implications for Prematurity and Development of the Fetal central Nervous System. *Prog. Brain Res.* 133, 131–142. doi:10.1016/s0079-6123(01)33010-8

Wieczorek, D., Köster, B., and Gillessen-Kaesbach, G. (2002). Absence of Thumbs, A/hypoplasia of Radius, Hypoplasia of Ulnae, Retarded Bone Age, Short Stature, Microcephaly, Hypoplastic Genitalia, and Mental Retardation. *Am. J. Med. Genet.* 108, 209–213. doi:10.1002/ajmg.10271

Yamamuro, K., Yoshino, H., Ogawa, Y., Makinodan, M., Toritsuka, M., Yamashita, M., et al. (2018). Social Isolation during the Critical Period Reduces Synaptic and Intrinsic Excitability of a Subtype of Pyramidal Cell in Mouse Prefrontal Cortex. *Cereb. Cortex* 28, 998–1010. doi:10.1093/cercor/bhx010

Conflict of Interest: The authors declare that the research was conducted in the absence of any commercial or financial relationships that could be construed as a potential conflict of interest.

Publisher's Note: All claims expressed in this article are solely those of the authors and do not necessarily represent those of their affiliated organizations, or those of the publisher, the editors and the reviewers. Any product that may be evaluated in this article, or claim that may be made by its manufacturer, is not guaranteed or endorsed by the publisher.

frontiers in Genetics

ORIGINAL RESEARCH
published: 06 December 2021
doi: 10.3389/fgene.2021.762999

AKR1A1 Variant Associated With Schizophrenia Causes Exon Skipping, Leading to Loss of Enzymatic Activity

*Kyoka Iino[1†], Kazuya Toriumi[1†], Riko Agarie[1], Mitsuhiro Miyashita[1,2,3], Kazuhiro Suzuki[1,4], Yasue Horiuchi[1], Kazuhiro Niizato[2], Kenichi Oshima[2], Atsushi Imai[2], Yukihiro Nagase[3], Itaru Kushima[5,6], Shinsuke Koike[7], Tempei Ikegame[7], Seiichiro Jinde[7], Eiichiro Nagata[8], Shinsuke Washizuka[4], Toshio Miyata[9], Shunya Takizawa[8], Ryota Hashimoto[10], Kiyoto Kasai[7,11], Norio Ozaki[5], Masanari Itokawa[1,2] and Makoto Arai[1]**

[1]*Schizophrenia Research Project, Department of Psychiatry and Behavioral Sciences, Tokyo Metropolitan Institute of Medical Science, Tokyo, Japan,* [2]*Department of Psychiatry, Tokyo Metropolitan Matsuzawa Hospital, Tokyo, Japan,* [3]*Department of Psychiatry, Takatsuki Hospital, Hachioji, Tokyo, Japan,* [4]*Department of Psychiatry, Graduate School of Medicine, Shinshu University, Nagano, Japan,* [5]*Department of Psychiatry, Nagoya University Graduate School of Medicine, Nagoya, Japan,* [6]*Medical Genomics Center, Nagoya University Hospital, Nagoya, Japan,* [7]*Department of Neuropsychiatry, Graduate School of Medicine, The University of Tokyo, Tokyo, Japan,* [8]*Department of Neurology, Tokai University School of Medicine, Isehara, Japan,* [9]*Division of Molecular Medicine and Therapy, Tohoku University Graduate School of Medicine, Sendai, Japan,* [10]*Department of Pathology of Mental Diseases, National Institute of Mental Health, National Center of Neurology and Psychiatry, Kodaira, Japan,* [11]*The International Research Center for Neurointelligence (WPI-IRCN) at The University of Tokyo Institutes for Advanced Study (UTIAS), Aoba-ku, Sendai, Japan*

OPEN ACCESS

Edited by:
Ruth Luthi-Carter, University of Leicester, United Kingdom

Reviewed by:
Estela Maria Bruxel, State University of Campinas, Brazil
Jiuyong Xie, University of Manitoba, Canada

***Correspondence:**
Makoto Arai
arai-mk@igakuken.or.jp

[†]These authors have contributed equally to this work

Specialty section:
This article was submitted to Neurogenomics, a section of the journal Frontiers in Genetics

Received: *23 August 2021*
Accepted: *10 November 2021*
Published: *06 December 2021*

Citation:
Iino K, Toriumi K, Agarie R, Miyashita M, Suzuki K, Horiuchi Y, Niizato K, Oshima K, Imai A, Nagase Y, Kushima I, Koike S, Ikegame T, Jinde S, Nagata E, Washizuka S, Miyata T, Takizawa S, Hashimoto R, Kasai K, Ozaki N, Itokawa M and Arai M (2021) AKR1A1 *Variant Associated With Schizophrenia Causes Exon Skipping, Leading to Loss of Enzymatic Activity. Front. Genet. 12:762999. doi: 10.3389/fgene.2021.762999*

Schizophrenia is a heterogeneous psychiatric disorder characterized by positive symptoms such as hallucinations and delusions, negative symptoms such as anhedonia and flat affect, and cognitive impairment. Recently, glucuronate (GlucA) levels were reported to be significantly higher in serum of patients with schizophrenia than those in healthy controls. The accumulation of GlucA is known to be related to treatment-resistant schizophrenia, since GlucA is known to promote drug excretion by forming conjugates with drugs. However, the cause of GlucA accumulation remains unclear. Aldo-keto reductase family one member A1 (AKR1A1) is an oxidoreductase that catalyzes the reduction of GlucA. Genetic loss of AKR1A1 function is known to result in the accumulation of GlucA in rodents. Here, we aimed to explore genetic defects in *AKR1A1* in patients with schizophrenia, which may result in the accumulation of GlucA. We identified 28 variants of *AKR1A1* in patients with schizophrenia and control subjects. In particular, we identified a silent c.753G > A (rs745484618, p. Arg251Arg) variant located at the first position of exon 8 to be associated with schizophrenia. Using a minigene assay, we found that the c.753G > A variant induced exon 8 skipping in AKR1A1, resulting in a frameshift mutation, which in turn led to truncation of the AKR1A1 protein. Using the recombinant protein, we demonstrated that the truncated AKR1A1 completely lost its activity. Furthermore, we showed that *AKR1A1* mRNA expression in the whole blood cells of individuals with the c.753G > A variant tended to be lower than that in those without the variants, leading to lower AKR activity. Our findings suggest that *AKR1A1* carrying the c.753G > A variant induces exon skipping, leading to a loss of gene expression and enzymatic activity. Thus, GlucA patients with schizophrenia with the c.753G > A variant

may show higher GlucA levels, leading to drug-resistant schizophrenia, since drug excretion by GlucA is enhanced.

Keywords: aldo-keto reductase family 1 member A1, treatment-resistant schizophrenia, single nucleotide variant (SNV), exon skipping, frameshift mutation, glucuronate

INTRODUCTION

Schizophrenia is a complex and heterogeneous psychiatric disorder caused by genetic and environmental factors with a worldwide prevalence of approximately 1% (Owen et al., 2016). Recently, it has been reported that unmedicated patients with schizophrenia show increased levels of glucuronate (GlucA) in the peripheral blood compared with those in healthy controls, which can be improved by treatment with risperidone (Xuan et al., 2011). These findings suggest that GlucA in the blood might be useful as a metabolic biomarker for schizophrenia. Moreover, the accumulation of GlucA might be related to drug-resistant schizophrenia, since GlucA is known to promote drug excretion by forming conjugates with drugs (Mazerska et al., 2016). However, little is known about the molecular mechanisms underlying GlucA accumulation in patients with schizophrenia.

Aldo-keto reductase family one member A1 (AKR1A1) is an approximately 40 kDa monomeric oxidoreductase that is ubiquitously expressed throughout the body, especially in the kidneys and liver. AKR1A1 displays a broad spectrum of substrate activity and detoxifies aldehyde and carbonyl compounds such as methylglyoxal and 3-deoxyglucosone in a nicotinamide adenine dinucleotide phosphate (NADPH)-dependent manner (Petrash and Srivastava, 1982; Bohren et al., 1989; Spite et al., 2007; Kurahashi et al., 2014; Fujii et al., 2021). Furthermore, AKR1A1 catalyzes the reduction of GlucA in the biosynthesis of ascorbic acid in rodents (Gabbay et al., 2010; Takahashi et al., 2012). Inhibition of AKR1A1 in mice increases urinary output of GlucA (Barski et al., 2005). These findings suggest that AKR1A1 dysfunction leads accumulation of GlucA.

In the present study, we aimed to analyze genetic defects in *AKR1A1* in patients with schizophrenia and identify the molecular mechanisms that cause the accumulation of GlucA.

MATERIALS AND METHODS

Human Subjects

Blood samples were obtained from 808 patients with schizophrenia (mean age: 49.0 years [standard deviation [SD]: 14.2 years]) and 636 healthy control subjects (mean age: 40.6 years [SD: 13.0 years]) for genome resequencing of *AKR1A1*. Patients were randomly recruited inpatients and outpatients. The cases included 437 men (mean age: 48.5 years [SD: 14.0 years]) and 417 women (mean age: 49.5 years [SD: 14.5 years]). Control subjects comprised 283 men (mean age: 41.5 years [SD: 13.6 years]) and 424 women (mean age: 40.1 years [SD: 12.5 years]). We did not assess the association between common variants and schizophrenia as the aim of this study was to focus on rare variations to reveal large biological effects, thus enabling clarification of pathophysiology in rare cases of schizophrenia. Therefore, these samples were not matched for age or sex. Schizophrenia was diagnosed according to the Diagnostic and Statistical Manual of Mental Disorders, fourth edition (4th ed., text rev.; DSM–IV–TR; American Psychiatric Association, 2000) to obtain a best-estimate lifetime psychiatric diagnosis, with consensus from at least two experienced psychiatrists. No structured interviews were conducted. The available medical records and family informant reports were also taken into consideration. Peripheral blood cells were obtained from patients with schizophrenia with/without the c.753G > A variant (n = 6) and two healthy controls among the subjects included in the genetic study. All participants provided written informed consent, and the study protocols were approved by the ethics committees of the Tokyo Metropolitan Institute of Medical Science (approval no. 20-17) and Tokyo Metropolitan Matsuzawa Hospital (approval no. 2018-8).

Sequencing

Genome was purified from whole blood by SRL (Tokyo, Japan), which is a private clinical laboratory test company. Polymerase chain reaction (PCR) amplification was performed using the primer sets and PCR kits (**Supplementary Table S1**) as per the manufacturer's instructions. All coding regions, exon–intron boundaries, 5′ untranslated region (UTR), and 3′ UTR of *AKR1A1* were examined by directly sequencing the PCR products using BigDye Terminator Cycle Sequencing Kit (Applied Biosystems, Foster City, CA, United States) and ABI PRISM 3130/3500 Genetic Analyzer (Applied Biosystems). We read both strands when an inserted or deleted nucleotide yielded dual signals derived from the wild-type (WT) and mutant strands. *AKR1A1* sequence analysis was performed based on RefSeq NM_006066. Variant data we found are deposited in the NCBI dbSNP: NCBI_subsnp# are 2137544288 and 5316170415–5316170441.

Minigene Constructs

The exons 7–9 and the internal introns in *AKR1A1* gene were amplified from the human genome using the *AKR1A1*_ex7-9_fw and *AKR1A1*_ex7-9_rv primers (**Supplementary Table S2**) and inserted into the pTA2 cloning vector. Then, the *AKR1A1* minigene in the pTA2 vector was cut using HindIII and PstI enzymes and transferred into the pAcGFP1-C1 vector at the same site.

A c.753G > A mutant at the first position of exon 8 was produced using the KOD-plus- Mutagenesis Kit (Toyobo, Tokyo, Japan). For mutagenesis, *AKR1A1*_ex7-9_c.753_fw and *AKR1A1*_ex7-9_c.753_rv primers were used (**Supplementary Table S2**).

Cell Culture and Transfection

HEK293, SH-SY5Y, and 1321N1 cells were maintained in Dulbecco's modified Eagle's medium (Gibco, Waltham, MA, United States) with 10% fetal bovine serum (Life Technologies, Carlsbad, CA, United States), 100 U/ml penicillin, and 100 μg/ml streptomycin (Gibco). At ~80% confluency in a 10 cm dish, 5 μg of DNA constructs were transfected using FuGENE6 transfection reagent (Promega, Madison, WI, United States) according to the manufacturer's protocol. The cells were collected 48 h after transfection.

RNA Extraction and Reverse Transcription-PCR

Total RNA was extracted from HEK293, SH-SY5Y, and 1321N1 cells using the SV Total RNA Isolation System (Promega) and the extracted RNA was purified using the RNeasy MinElute Cleanup Kit (QIAGEN, Hilden, Germany) according to the manufacturer's protocol. The obtained RNA was quantified using NanoDrop spectrophotometer (Thermo Fisher Scientific, Waltham, MA, United States), and 500 ng of the purified RNA was used as a template for complementary DNA (cDNA) synthesis using ReverTra Ace qPCR RT Kit (Toyobo). To investigate exon skipping, 10% of the synthesized cDNA was amplified using the pAcGFP1-C1_fw and AKex9_PstI_rv primers (**Supplementary Table S2**).

Cloning and Mutagenesis

Total RNA derived from a human postmortem brain tissues was prepared using the SV Total RNA Isolation System (Promega), cleaned with an RNeasy MinElute Cleanup Kit (QIAGEN, Hilden, Germany) according to the manufacturer's protocol. A High-Capacity cDNA Archive Kit (Applied Biosystems, Foster City, California) was used for reverse transcription of total RNA to first-strand cDNA synthesis according to the supplier's protocols.

Full-length *AKR1A1* was cloned from the cDNA library using h*AKR1A1*_fw and h*AKR1A1*_rv primers (**Supplementary Table S2**). The amplified products were inserted into the pTA2 vector using TArget Clone (Toyobo). *AKR1A1* mutants, c.753G > A and c.264delC, were produced using pTA2_*AKR1A1* as a template with the KOD-plus-Mutagenesis Kit (Toyobo). *AKR1A1*_c.753_fw1 and rv1 primers were used for the c.753G > A mutant, and *AKR1A1*_c.264_fw1 and rv1 primers were used for the c.264delC mutant (**Supplementary Table S2**). Moreover, to delete the extra sequence below the new termination codon caused by the frameshift mutation, the c.753G > A and c.264delC mutants were amplified using the primer sets *AKR1A1*_c.753/c.264_fw2 and *AKR1A1*_c.753_rv2 and *AKR1A1*_c.264_rv2, respectively, and then self-ligated.

Construction of the Recombinant Plasmid and Purification of the GST Fusion Protein

pTA2_*AKR1A1*_WT, pTA2_*AKR1A1*_c.753, and pTA2_*AKR1A1*_c.264 were used as templates for amplification of *AKR1A1* with EcoRI and SalI restriction enzyme cut sites at the 5′ and 3′ termini, respectively. The EcoRI_*AKR1A1*_fw and *AKR1A1*_SalI_WT_rv primers for the amplification of *AKR1A1* WT, *AKR1A1*_SalI_c.753_rv primer for the amplification of *AKR1A1* c.753, and *AKR1A1*_SalI_c.264_rv primer were employed for the amplification of *AKR1A1* c.264 (**Supplementary Table S2**). After amplification of *AKR1A1* with EcoRI and SalI restriction enzyme cut sites, the products were cut with EcoRI and SalI enzymes. The pGEX-4T-2 plasmid was cut with EcoRI and XhoI enzymes and ligated together to make the plasmid pGEX-4T-2_*AKR1A1*. The sequence of pGEX-4T-2_*AKR1A1* was confirmed using the pGEX_fw and pGEX_rv primers (**Supplementary Table S2**).

BL21 *Escherichia coli* transformed with pGEX-4T-2_*AKR1A1* was added to 3 ml of Luria Bertani medium containing 100 μg/ml ampicillin and incubated at 37°C with shaking. After 12–24 h, the optical density at 600 nm (OD_{600}) was measured with GloMax Explorer Multimode Microplate Reader (Promega). The culture was diluted to OD = 0.4–0.5 with Luria Bertani medium containing 100 μg/ml ampicillin and incubated at 37°C with shaking. After 1 h, the culture was induced with 30 μl of 100 mM isopropyl β-D-1-thiogalactopyranoside and incubated at 37°C with shaking for 3 h. Cells were harvested by centrifugation at 20,400 × *g* for 1 min.

Glutathione-S-transferase (GST) fusion AKR1A1 from BL21 *E. coli* transformed with pGEX-4T-2_AKR1A1 was purified using the MagneGST Protein Purification System (Promega) according to the manufacturer's protocols. Protein concentrations were determined using the bicinchoninic acid protein assay with GloMax Explorer Multimode Microplate Reader (Promega). Finally, we verified the purification of GST-AKR1A1 proteins using sodium dodecyl sulfate polyacrylamide gel electrophoresis (SDS-PAGE).

Cell Sample Preparation and Enzymatic Activity Assay

A total of 150 μl of cOmplete Lysis-M (Merck, Darmstadt, Germany) was added to the pellet of HEK293, SH-SY5Y, and 1321N1 cells or human red blood cells. The mixture was sonicated, followed by centrifugation at 20,400 × *g* for 15 min. The supernatant was then collected from the cell lysate.

The activity of AKR1A1 was measured by monitoring NADPH consumption. The reaction mixture contained 100 mM HEPES (pH 7.4), 0.1 mM NADPH, and 10 mM GlucA. Reactions were monitored by assessing the decrease in absorbance at 340 nm using an Epoch Microplate Spectrophotometer (BioTek Instruments, Winooski, VT, United States) at 37°C. The enzyme activity was defined as the amount of enzyme that catalyzes the oxidation of 1 μmol of NADPH per min.

RNA Extraction and Quantitative PCR

Total RNA was extracted from whole blood cell in using the NucleoSpin RNA Blood kit (NucleoSpin, MACHEREY-NAGEL, Duren, Germany) and the extracted RNA was purified using the RNeasy MinElute Cleanup Kit (QIAGEN, Hilden, Germany) according to the manufacturer's protocol. The obtained RNA

TABLE 1 | Genotype and allele frequency of variants detected in *AKR1A1*.

	Nucleotide change, effect on protein (rs number)	gnomAD ID	Exon		N	Genotype counts (frequency)			*p* value	Effect size (Cramer's V)	Allele counts (frequency)[b]		p value[c]	Effect size (Φ)
V1[a]	c.264 del C	1-45566924AC-A	Exon5			II	ID	DD			I	D		
				SCZ	758	757 (0.999)	1 (0.001)	0 (0)			1,515 (0.999)	1 (0.001)		
				CON	617	617 (1)	0 (0)	0 (0)	>0.999	0.024	1,234 (1)	0 (0)	> 0.999	0.017
				East Asian	2,588	2,587 (1)	1 (0)	0 (0)	0.402	0.016	5,175 (1)	1 (0)	0.402	0.011
				Total	76,027	76,026 (1)	1 (0)	0 (0)	0.020*	0.025	1,52,053 (1)	1 (0)	0.020*	0.018
V2	c.474 G>A Ala158Ala (rs147059021)	1-45568099G-A	Exon6			GG	GA	AA			G	A		
				SCZ	638	638 (1)	0 (0)	0 (0)			1,276 (1)	0 (0)		
				CON	549	548 (0.998)	1 (0.002)	0 (0)	0.464	0.031	1097 (0.999)	1 (0.001)	0.463	0.022
				East Asian	2,589	2,589 (1)	0 (0)	0 (0)	>0.999	0.000	5,178 (1)	0 (0)	> 0.999	0.000
				Total	76,047	75,999 (0.999)	48(0.001)	0 (0)	>0.999	0.002	1,52,046 (1)	48 (0)	> 0.999	0.002
V3	c.753 G>A Arg251Arg (rs745484618)	1-45568927G-A	Exon8			GG	GA	AA			G	A		
				SCZ	745	731 (0.981)	13 (0.017)	1 (0.001)			1,475 (0.99)	15 (0.01)		
				CON	617	612 (0.992)	5 (0.008)	0 (0)	0.191	0.048	1,229 (0.996)	5 (0.004)	0.074	0.035
				East Asian	2,600	2,591 (0.997)	9 (0.003)	0 (0)	<0.001***	0.079	5,191 (0.998)	9 (0.002)	<0.001***	0.058
				Total	76,076	76,067 (1)	9 (0)	0 (0)	<0.001***	0.107	1,52,143 (1)	9 (0)	<0.001***	0.078
V4	c.911 C > T Thr304Met (rs150392728)	1-45569228C-T	Exon9			CC	CT	TT			C	T		
				SCZ	745	743 (0.997)	2 (0.003)	0 (0)			1,488 (0.999)	2 (0.001)		
				CON	617	617 (1)	0 (0)	0 (0)	0.504	0.035	1,234 (1)	0 (0)	0.504	0.029
				East Asian	2,595	2,584 (0.996)	11 (0.004)	0 (0)	0.745	0.010	5,179 (0.998)	11 (0.002)	0.745	0.007
				Total	76,063	76,015 (0.999)	48 (0.001)	0 (0)	0.085	0.008	1,52,078 (1)	48 (0)	0.085	0.006

[a]*The variants detected in the coding region are described using gene region, genotype counts, and allele counts.*

[b]*Allele frequencies of East Asian and Total groups (including African/African-American, Amish, Ashkenazi Jewish, East Asian, Finnish, non-Finnish European, Latino/Admixed American, Middle Eastern, Other, and South Asian) based on Genome Aggregation Database (gnomAD) were also used as controls. GRCh38 was used as a reference genome.*

[c]*The chi-squared test was used for statistical analysis when all cells had an expected value of more than 5. Fisher's exact test was used when one or more cells had an expected value of 5 or less.* *p < *0.05*, ***p < *0.001 versus control.*

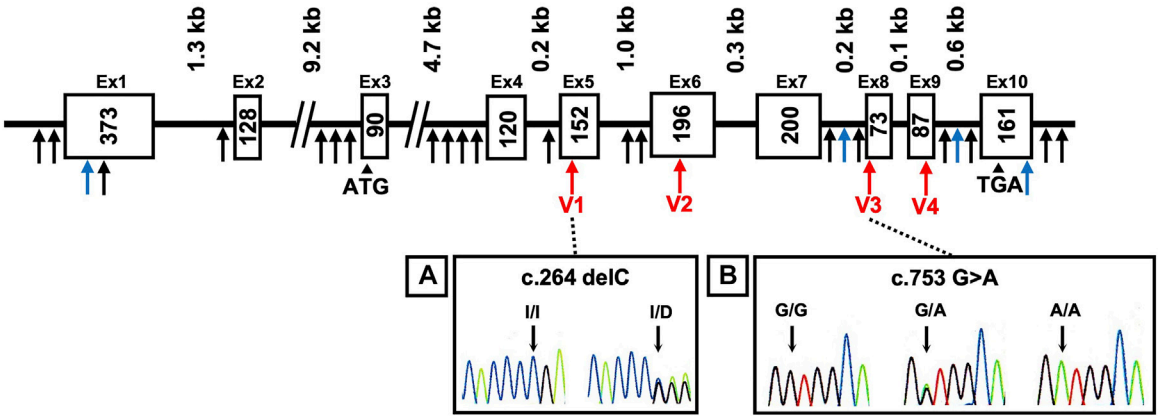

FIGURE 1 | DNA sequence chromatograms showing frameshift mutation and variants. Novel variants (blue arrows), variants in coding regions shown in **Table 1** (V1–V4 variants: red arrows), and others (black arrows) are shown. Heterozygous sequence traces derived from individuals carrying **(A)** a cytosine deletion within exon 5 (V1 variant) and **(B)** a mutation from guanine to adenine at the first position of exon 8 (V3 variant). Sequencing analyses revealed normal (denoted I/I or G/G) and mutant (denoted delC or G > A) sequences; kb indicates the kilobase pairs. WT, wild-type.

was quantified using NanoDrop spectrophotometer (Thermo Fisher Scientific, Waltham, MA, United States), and 500 ng of the purified RNA was used as a template for cDNA synthesis using ReverTra Ace qPCR RT Kit (Toyobo).

The qPCR assay was performed using Power SYBR Green PCR Master Mix (ThermoFisher Scientific). AKR1A1_qPCR_fw primer, AKR1A1_qPCR_rv primer, GAPDH_qPCR_fw primer and GAPDH_qPCR_rv primer were used (**Supplementary Table S2**). The qPCR protocol was as below: at 95°C for 10 min, followed by 40 cycles of 95°C for 15 s, 56°C for 30 s and 72°C for 30 s. For relative expression, each expression was normalized to average of two subjects without c.753G > A variant using the $\Delta\Delta C_T$ calculation.

Statistical Analysis

The statistical tests were performed using GraphPad Prism version 9.0. Results are expressed as mean ± standard deviation (SD) or standard error of mean (SEM). Comparisons between groups were performed using two-way analysis of variance (ANOVA) or one-way ANOVA followed by Bonferroni's multiple comparison test. Statistical significance was set at $p < 0.05$.

RESULTS

Genetic Analysis of *AKR1A1*

The *AKR1A1* sequence was analyzed in patients with schizophrenia (n = 808) and control subjects (n = 636), and 28 variants were identified as a result (**Supplementary Table S3**). Among them, four were novel variants: g.-403_-397 del AAGTTC, g.753-62_65 delC, g.913-114 C > A, and *85 G > C. The other variants have already been registered with the single nucleotide polymorphism database dbSNP (https://www.ncbi.nlm.nih.gov/snp/). In addition, four variants were found in the coding region: c.264 delC (rs755292778, p.Glu89ArgfsTer23), c.474 G > A (rs147059021, p.Ala158Ala), c.753 G > A (rs745484618, p.Arg251Arg), and c.911 C > T (rs150392728, p.Thr304Met), although the frequencies of the genotypes and alleles in the four variants did not noticeably differ between patients with schizophrenia and healthy controls (**Table 1**; **Figure 1**).

The c.753G > A variant is a silent mutation. This variant was identified in 14 cases in the schizophrenia patient group (including 13 heterozygous and one homozygous) and five subjects in the healthy group, but no remarkable difference in genotype ($p = 0.191$) or allele frequency ($p = 0.074$) was observed. Next, we applied the frequency of the variants to "East Asian" and "Total groups (including African/African-American, Amish, Ashkenazi Jewish, East Asian, Finnish, non-Finnish European, Latino/Admixed American, Middle Eastern, Other, and South Asian)" obtained from Genome Aggregation Database (gnomAD) v3.1.1, a public database containing human genome data, as the frequency of control. The results showed that the frequency of genotypes GA and AA was significantly higher in patients than that in "East Asian" and "Total groups." In addition, the frequency of allele A in patients was significantly higher than that in "East Asian" and "Total groups."

The c.264delC variant was identified as a deletion-type mutation, which can have a significant impact on the expression product. This was observed in only one patient with schizophrenia in our sequence analysis. There was no significant difference in the genotype and allele frequencies between patients and controls in our dataset. However, further analysis using the database gnomAD showed that the frequency of genotype ID and allele D in patients was significantly higher than that in "Total groups," but not "East Asian."

The c.474G > A variant is a silent mutation without amino acid substitution. It was only found in one healthy person. In addition, the c.911C > T variant was identified in two patients in the schizophrenia patient group (heterozygous), and it was not identified in the healthy group. Regarding these variants, there

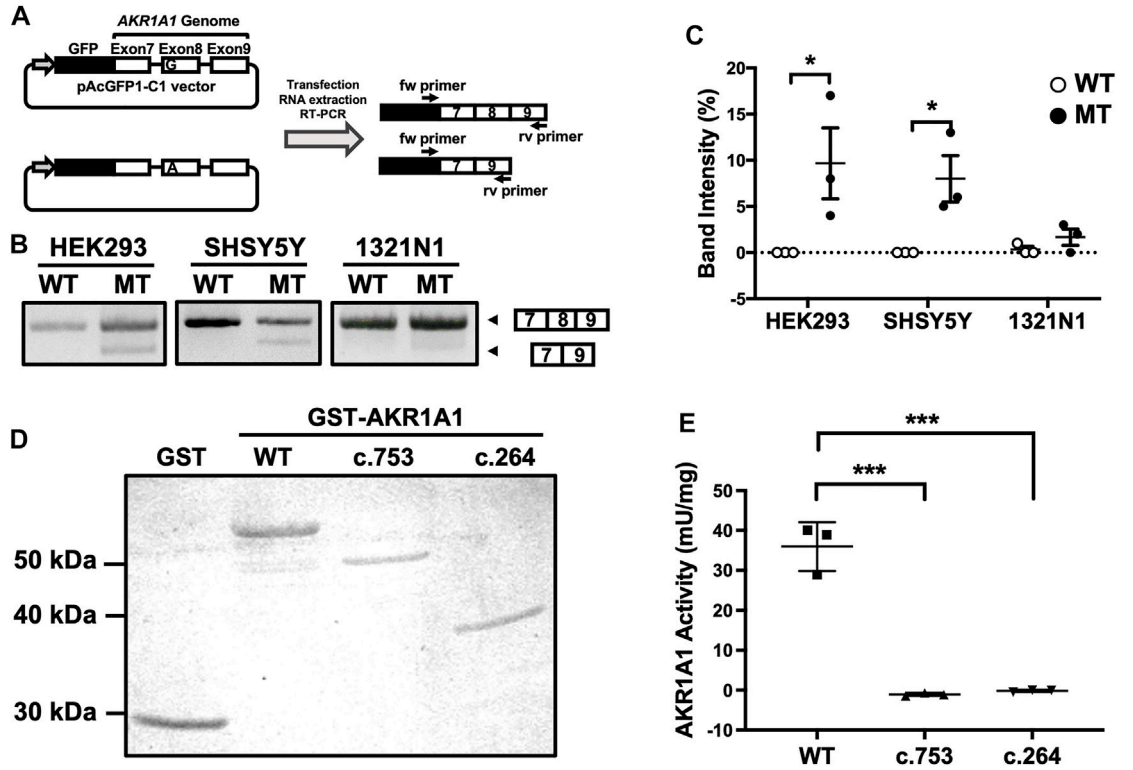

FIGURE 2 | Exon skipping induced by the c.753G > A variant in *AKR1A1*. **(A)** An outline of the splicing assay is shown. Exon 8 skipping was confirmed using cDNA generated from HEK293, SH-SY5Y, and 1321N1 cells expressing minigenes for WT or c.753G > A variant (mutant [MT]). **(B)** The results of the splicing assay are shown. The upper band indicates products including exons 7–9, whereas the lower band shows exon 8 skipping products, including only exons 7 and 9. **(C)** Data represent the mean of three independent experiments for the splicing assay. Two-way analysis of variance: $F_{Interaction(2,12)} = 2.65$, $p > 0.05$; $F_{Cell(2,12)} = 2.21$, $p > 0.05$; $F_{Variant(1,12)} = 16.4$, $p < 0.01$. **(D)** GST and GST-AKR1A1s were purified and separated by sodium dodecyl sulfate polyacrylamide gel electrophoresis. **(E)** AKR1A1 activity of the purified GST-AKR1A1s was determined. Data represent the mean ± standard error of mean. $^{*}p < 0.05$, $^{***}p < 0.001$ versus WT. AKR1A1, aldo-keto reductase family one member A1; WT, wild-type; GST, glutathione-S-transferase.

was no significant difference in the frequency of the genotype and allele between patients and controls both in our dataset and gnomAD.

Effect of the Mutation at the First Position of *AKR1A1* Exon on Exon Skipping and Decrease in Enzymatic Activity

A mutation at the first position of an exon has been reported to cause exon skipping by alternative splicing (Fu et al., 2011). To address whether the variant c.753G > A located at the first position of exon 8 in the *AKR1A1* gene results in exon skipping, a minigene assay was performed. We constructed minigenes by inserting *AKR1A1* exons 7, 8, and 9 and the internal introns into the pAc-GFP1-C1 vector and by introducing the G > A mutation at the first position of exon 8 (**Figure 2A**). The minigenes were transfected into HEK293, SH-SY5Y, and 1321N1 cells, and their products were confirmed by PCR. The results showed that exon 8 skipping occurred in the A allele minigene (mutant [MT]) but not in the G allele (WT) in any cell type (**Figure 2B**). In HEK293 and SH-SY5Y cells, MT considerably increased the frequency of exon skipping compared to WT (**Figure 2C**). These findings suggest that the variant c.753G > A in the *AKR1A1* gene induced the skipping of exon 8.

The skipping of exon 8 causes a frameshift mutation and may result in the decreased enzymatic activity of AKR1A1 due to the c.753G > A variant, even though it is a silent mutation. To confirm this, we purified the AKR1A1 mutant recombinant protein produced by exon skipping and evaluated its activity (**Figure 2D**). We found that AKR1A1 produced by the c.753G > A variant exhibited no activity, which was significantly lower than that of the WT AKR1A1 (**Figure 2E**). Furthermore, c.264 delC mutation, which cause a frameshift mutation, also resulted in a complete loss of AKR1A1 enzymatic activity.

Effect of the Mutation at the First Position of Exon in *AKR1A1* on Enzymatic Activity in Human Red Blood Cells

To investigate the effect of the c.753G > A variant on AKR1A1 enzymatic activity in patients with schizophrenia, AKR enzymatic activity in red blood cells from six patients with schizophrenia and two control subjects was measured

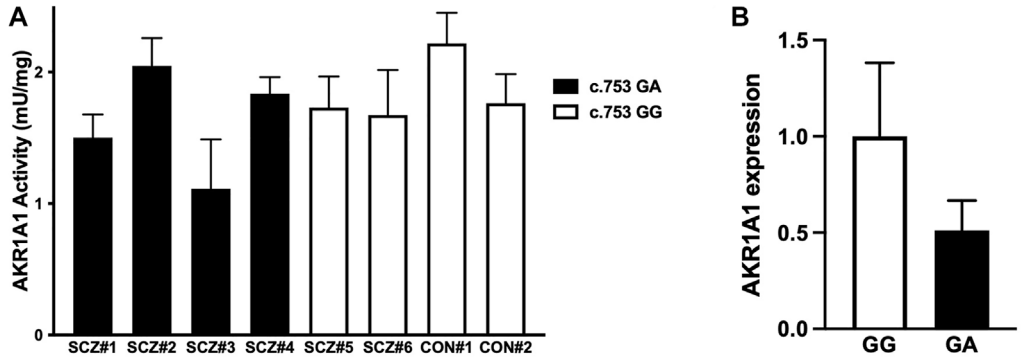

FIGURE 3 | AKR enzymatic activity and *AKR1A1* gene expression in human. **(A)** The enzymatic activities of AKR in the red blood cells of six patients with schizophrenia (SCZ#1 to #4 with the c.753G > A variant and SCZ#5 and #6 without the variant) and two control subjects (CON#1 and #2 without the variant) were examined. Data represent mean ± SD of three independent experiments. **(B)** The *AKR1A1* mRNA expression in five subjects (SCZ#1, SCZ#3, SCZ#4, SCZ#6, and CON#2) was quantified by qPCR. For relative expression, each expression was normalized to average of SCZ#6 and CON#2 with GG alleles using the $\Delta\Delta C_T$ calculation. Data represent mean ± SD.

(**Figure 3A**). Two out of four patients who were heterozygous at the c.753G > A variant exhibited lower enzymatic activity (patients with schizophrenia [SCZ]#1: 1.50 mU/mg protein, SCZ#3: 1.11 mU/mg protein), and a slight decrease was observed in patients with the variant compared to those without it (SCZ/GA: 1.62 ± 0.41 mU/mg protein; SCZ/GG: 1.70 ± 0.04 mU/mg protein). In addition, the enzymatic activity in four patients with GA was slightly lower than that in four subjects with GG (GA: 1.62 ± 0.41 mU/mg, GG: 1.85 ± 0.25 mU/mg). Furthermore, the enzymatic activity in patients with schizophrenia was slightly lower than that in control subjects (SCZ: 1.65 ± 0.32 mU/mg protein; control: 1.99 ± 0.32 mU/mg protein). Although there was no significant difference between any of the groups due to the small number of subjects, these results suggest that the c.753G > A variant of *AKR1A1* may reduce the enzymatic activity of AKR1A1.

Finally, to investigate the effect of the c.753G > A variant on *AKR1A1* expression, we quantified mRNA level in the whole blood cells obtained from five subjects (CON#2 and SCZ#6 with c.753 GG alleles, and SCZ#1, SCZ#2, and SCZ#4 with c.753 GA alleles), since unfortunately we were unable to collect peripheral blood from three individuals whose AKR activity we have measured. We found that mRNA expression of *AKR1A1* with c.753 GA alleles decreased to approximately 50% compared to that with c.753 GG (**Figure 3B**). These results suggest that the reduction of AKR activity in subjects with the variant may be caused from the reduction of gene expression.

DISCUSSION

In the present study, we identified 28 variants of the *AKR1A1* (**Figure 1**; **Supplementary Table S1**). Among them, we found that two variants in the coding region were significantly associated with schizophrenia using the database gnomAD: the frameshift mutation in exon 5 (c.264delC, p.Glu89ArgfsTer23) and the exon-skipping mutation in exon 8 (c.753 G > A, p.Arg251Arg). The c.264delC allele frequency in patients with schizophrenia was significantly higher than that in healthy controls in "Total groups" populations in the database gnomAD (**Table 1**; $p = 0.020$). According to the Japanese multi omics reference panel including 8380 healthy subjects (jMorp: https://jmorp.megabank.tohoku.ac.jp.), the c.264delC allele frequency in Japanese is 0.0001. As the c.264delC variant produces a termination codon in the middle of the gene due to a frameshift, its aberrant product may undergo degradation via a nonsense-mediated mRNA decay (NMD) mechanism (Kishor et al., 2019). In one heterozygous case with c.264delC, a decrease in expression and enzymatic activity of the AKR1A1 protein and the subsequent GlucA accumulation was expected, but it could not be confirmed because of difficulty in re-recruiting the subject.

The c.753 A allele frequency in patients with schizophrenia was significantly higher than that in healthy controls in "East Asian" and "Total groups" populations in the database gnomAD (**Table 1**; $p < 0.001$, $p < 0.001$, respectively). According to the jMorp, the c.753A allele frequency in Japanese was 0.0037, which means that it is relatively common among Japanese people compared to the world. Furthermore, three patients from the same family (mother and two identical sons) were found to possess the c.753G > A variant. These findings suggest that the c.753G > A variant may be one of the genetic factors related to schizophrenia.

The g.-275 T allele frequency in patients with schizophrenia was significantly higher than that in healthy controls in "East Asian" and "Total groups" populations in the database gnomAD (**Supplementary Table S3**; $p = 0.020$ and $p < 0.001$, respectively). It is located in untranslated region, but it has been reported that this variant is associated with negative symptoms of schizophrenia (Martinez-Magana et al., 2021).

It should be noted that the c.753G > A mutation is located at the first position of exon 8, although the variant itself is a silent mutation. We revealed that this variant led to exon 8 skipping using a splicing assay with minigenes (**Figures 2A–C**). In the splicing process, splicing factors $U2AF^{35}$ and $U2AF^{65}$ bind to the 5′ exon (3′ splice) site and the polypyrimidine tract in the intron, respectively

(Warnasooriya et al., 2020). When the polypyrimidine tract is sufficiently long (10–15 nt), $U2AF^{65}$ binds strongly and normal splicing occurs even without $U2AF^{35}$ binding. However, in cases where the polypyrimidine chain is short, the binding of $U2AF^{35}$ to the 5′ exon site is required for splicing. If the polypyrimidine chain is short and there is a mutation in the first position of the exon, both $U2AF^{65}$ and $U2AF^{35}$ cannot bind to the splicing site, resulting in exon skipping (Fu et al., 2011). Therefore, the exon-skipping frequency depends on the length of the polypyrimidine tract and the 5′ exon site. Our findings showing the c.753G > A mutation at the first position of exon 8 are consistent with the splicing mechanism because the polypyrimidine tract upstream of exon 8 in *AKR1A1* is as short as 6 nt. Furthermore, the c.753G > A variant induced exon skipping in HEK293 and SH-SY5Y cells, but not in 1321N cells (**Figures 2B,C**). This difference in the frequency of exon skipping among these cell types may be due to differences in the expression of splicing factors such as $U2AF^{35}$ and $U2AF^{65}$.

Exon 8 skipping in *AKR1A1* caused a frameshift mutation, resulting in a truncated AKR1A1 protein. The normal protein of AKR1A1 consists of 325 amino acids, but when the c.753G > A variant causes a frameshift, the first 88 amino acids from the N-terminus are the same as those in the normal protein, but the rest are lost, resulting in a truncated protein with ten extra amino acids (total of 261 amino acids). As for the c.264delC variant, the first 88 amino acids are the same as those in the normal protein, but the rest are lost, resulting in a truncated protein with 22 extra amino acids (total of 110 amino acids). Using the recombinant protein, we demonstrated that the truncated AKR1A1 proteins produced by c.753G > A and c.264delC variants completely lost their enzymatic activity (**Figures 2D,E**). These findings suggest that patients with c.753G > A and c.264delC variants in *AKR1A1* might show GlucA accumulation in the peripheral blood. Moreover, it is known that AKR1A1 is involved in the metabolism of the neurotransmitter noradrenaline and the carbonyl compound methylglyoxal (Sato et al., 1999; Vander Jagt et al., 1992). Noradrenaline levels are reduced in patients with schizophrenia, and negative symptoms are improved by inhibiting noradrenaline reuptake (Matthews et al., 2018; Catak et al., 2019). Therefore, the frameshift mutations in AKR1A1 might affect these metabolic processes, and thus may be related to the pathophysiology of schizophrenia.

Furthermore, we found that AKR activity tended to be lower in patients with the c.753G > A mutation than that in healthy controls (**Figure 3A**). Furthermore, *AKR1A1* mRNA expression in the whole blood cells of individuals with the c.753G > A variant tended to be lower than that in those without the variants, leading to lower AKR activity (**Figure 3B**). This is consistent with the findings of our *in vitro* analyses (**Figure 2**). These findings suggest that the aberrant product caused by c.753 G > A variants may undergo degradation probably via NMD, leading to decreased AKR activities. However, as seen in **Figure 2C**, the occurrence of exon skipping due to the allele A is about 10–20% at most, which is not very frequent. The result suggests the reduced expression of *AKR1A1* in patients with the c.753G > A variant is not entirely due to the variant. Perhaps an unknown molecular pathology present in schizophrenia patients is involved in the decreased expression of *AKR1A1*. Further studies with larger populations will be needed in the future to clarify this point.

A detailed clinical information of three (SCZ#1, SCZ#3 and SCZ#4) out of four patients harboring mutant type allele at c.753G > A revealed that all the patients exhibited treatment resistant (TR) phenotype. Of these patients, SCZ#1 and SCZ#3 showed marked and moderate reduction of enzymatic activity of AKR1A1 compared to that of patients with wild type allele, respectively. In particular, maintenance electroconvulsive therapy has been necessary for SCZ#3 to prevent the relapse because any therapeutic agents have no efficacy for the psychotic symptoms. Therefore, elevated GlucA may contribute to the pathophysiology of TR phenotype for these patients due to diminished enzymatic activity of AKR1A1 caused by mutation at c.753G > A. In contrast to these patients, AKR1A1 activity of SCZ#4 was comparable with that of patients with wild type. Thus, underlying mechanism of TR phenotype for SCZ#4 may be different from that of SCZ#3 and SCZ#1.

The enzymatic activity of patient SCZ#2 is not reduced, even though the patient has the variant (**Figure 3A**). However, due to the lack of detailed clinical information and difficulty in re-recruiting the patient SCZ#2, we were unable to conduct further analysis, including *AKR1A1* expression analysis. It is one of the limitations of this study, and we believe that the unaltered enzymatic activity of SCZ#2 may be due to epigenetic effects or other cofactors.

In addition, this study data has other notable limitations. First, the number of patients and healthy subjects whose AKR activity could be measured was extremely small. Second, we cannot measure the GlucA level in the blood of patients with the c.753G > A mutation, so we have not been able to evaluate the actual effect of the mutation on glucuronic acid accumulation. In the future, a higher number of patients must be considered for further investigation and the link between the frameshift mutations in AKR1A1 and the aforementioned metabolic processes and whether GlucA accumulation occurs in patients with these variants should be clarified.

Among the identified variants of *AKR1A1* related to schizophrenia, the c.753G > A variant caused exon skipping, leading to the production of a truncated AKR1A1 protein. We found that this truncated AKR1A1 protein lost its enzymatic activity, probably leading to the accumulation of GlucA. Notably, we revealed that AKR activity tends to be reduced in patients with the c.753G > A mutation compared with healthy controls, suggesting that patients with schizophrenia with the c.753G > A variant might show higher GlucA levels, leading to drug-resistant schizophrenia, since drug excretion by GlucA is enhanced.

DATA AVAILABILITY STATEMENT

The datasets presented in this study can be found in online repositories. The names of the repository/repositories and accession number(s) can be found in the article/ **Supplementary Material**.

ETHICS STATEMENT

The studies involving human participants were reviewed and approved by the Tokyo Metropolitan Institute of Medical Science

(approval no. 20-17) and Tokyo Metropolitan Matsuzawa Hospital (approval no. 2018-8). The patients/participants provided their written informed consent to participate in this study.

AUTHOR CONTRIBUTIONS

MA had full access to all the data in the study and take responsibility for the integrity of the data and the accuracy of the data analysis. Concept and design: KI, KT, and MA. Substantial contribution to acquisition, analysis, or interpretation of data: KI, KT, RA, MM, KS, YH, MI, and MA. Drafting of the manuscript: KI and KT. Critical revision of the manuscript for important intellectual content: KI, KT, MM, KS, YH, EN, SW, TM, ST, RH, KK, NO, MI, and MA. Statistical analysis: KI, KT, and MA. Obtained funding: KT, KO, IK, RH, KK, NO, MI, and MA. Administrative, technical, or material support: MM, KS, KN, KO, AI, YN, IK, SK, TI, SJ, RH, KK, NO, and MI. Substantial supervision: MI and MA. KI and KT. contributed equally to the manuscript.

FUNDING

This work was supported by the Japan Society for the Promotion of Science (JSPS) KAKENHI Grant Numbers (18K06977, KT; 20H03608, MA; 21K07543, 21H00194, 17H05090, 15K19720, IK; JP20H03596, 21H00451, KK), Japan Agency for Medical Research and Development (AMED) under Grant Numbers (JP20dm0107088, MI; JP21wm0425019, KO; JP21km0405216, JP21ek0109411, IK; JP21uk1024002,JP21dk0307103, RH; JP21wm0425007, JP21dm0207075, JP21dk0307103, NO; JP18dm0207004, JP21dm0207069, JP21dm0307001, JP21dm0307004, KK), the Kanae Foundation for the Promotion of Medical Science (KT), Takeda Science Foundation (KT), the Uehara Memorial Foundation (MA), and the Sumitomo Foundation (MA), SENSHIN Medical Research Foundation (KT, MA), Moonshot R&D (JPMJMS2021, KK), UTokyo Center for Integrative Science of Human Behavior (CiSHuB), the International Research Center for Neurointelligence (WPI-IRCN) at The University of Tokyo Institutes for Advanced Study (UTIAS).

ACKNOWLEDGMENTS

We thank the donors and their families for the samples used in these studies. We are grateful for the expert technical assistance of Izumi Nohara, Chikako Ishida, Yukiko Shimada, Emiko Hama, Nanako Obata, Mai Hatakenaka, and Ikuyo Kito.

SUPPLEMENTARY MATERIAL

The Supplementary Material for this article can be found online at: https://www.frontiersin.org/articles/10.3389/fgene.2021.762999/full#supplementary-material

REFERENCES

American Psychiatric Association (2000). *Diagnostic and Statistical Manual of Mental Disorders*. 4th ed. Washington DC: American Psychiatric Association Publishing.

Barski, O. A., Papusha, V. Z., Ivanova, M. M., Rudman, D. M., and Finegold, M. J. (2005). Developmental Expression and Function of Aldehyde Reductase in Proximal Tubules of the Kidney. *Am. J. Physiol. Ren. Physiol* 289, F200–F207. doi:10.1152/ajprenal.00411.2004

Bohren, K. M., Bullock, B., Wermuth, B., and Gabbay, K. H. (1989). The Aldo-Keto Reductase Superfamily. *J. Biol. Chem.* 264, 9547–9551. doi:10.1016/s0021-9258(18)60566-6

Catak, Z., Kocdemir, E., Ugur, K., Yardim, M., Sahin, İ., Kaya, H., et al. (2019). A Novel Biomarker Renalase and its Relationship with its Substrates in Schizophrenia. *J. Med. Biochem.* 38, 299–305. doi:10.2478/jomb-2018-0031

Fu, Y., Masuda, A., Ito, M., Shinmi, J., and Ohno, K. (2011). AG-dependent 3′-splice Sites Are Predisposed to Aberrant Splicing Due to a Mutation at the First Nucleotide of an Exon. *Nucleic Acids Res.* 39, 4396–4404. doi:10.1093/nar/gkr026

Fujii, J., Homma, T., Miyata, S., and Takahashi, M. (2021). Pleiotropic Actions of Aldehyde Reductase (AKR1A). *Metabolites* 11, 343. doi:10.3390/metabo11060343

Gabbay, K. H., Bohren, K. M., Morello, R., Bertin, T., Liu, J., and Vogel, P. (2010). Ascorbate Synthesis Pathway. *J. Biol. Chem.* 285, 19510–19520. doi:10.1074/jbc.m110.110247

Kishor, A., Fritz, S. E., and Hogg, J. R. (2019). Nonsense-mediated mRNA Decay: The challenge of Telling Right from Wrong in a Complex Transcriptome. *WIREs RNA* 10, e1548. doi:10.1002/wrna.1548

Kurahashi, T., Kwon, M., Homma, T., Saito, Y., Lee, J., Takahashi, M., et al. (2014). Reductive Detoxification of Acrolein as a Potential Role for Aldehyde Reductase (AKR1A) in Mammals. *Biochem. Biophysical Res. Commun.* 452, 136–141. doi:10.1016/j.bbrc.2014.08.072

Martínez-Magaña, J. J., Genis-Mendoza, A. D., González-Covarrubias, V., Juárez-Rojop, I. E., Tovilla-Zárate, C. A., Soberón, X., et al. (2021). Association of FAAH p.Pro129Thr and COMT p.Ala72Ser with Schizophrenia and Comorbid Substance Use through Next-Generation Sequencing: an Exploratory Analysis. *Braz. J. Psychiatry* 1, S1516–S44462021005016201. doi:10.1590/1516-4446-2020-1546

Matthews, P. R. L., Horder, J., and Pearce, M. (2018). Selective Noradrenaline Reuptake Inhibitors for Schizophrenia. *Cochrane Database Syst. Rev.* 2018, CD010219. doi:10.1002/14651858.CD010219.pub2

Mazerska, Z., Mróz, A., Pawłowska, M., and Augustin, E. (2016). The Role of Glucuronidation in Drug Resistance. *Pharmacol. Ther.* 159, 35–55. doi:10.1016/j.pharmthera.2016.01.009

Owen, M. J., Sawa, A., and Mortensen, P. B. (2016). Schizophrenia. *The Lancet* 388, 86–97. doi:10.1016/S0140-6736(15)01121-6

Petrash, J. M., and Srivastava, S. K. (1982). Purification and Properties of Human Liver Aldehyde Reductases. *Biochim. Biophys. Acta (Bba) - Protein Struct. Mol. Enzymol.* 707, 105–114. doi:10.1016/0167-4838(82)90402-2

Sato, S., Kawamura, M., Eisenhofer, G., Kopin, I. J., Fujisawa, S., Kador, P. F., et al. (1999). Aldo-Keto Reductases in Norepinephrine Metabolism. *Adv. Exp. Med. Biol.* 463, 459–463. doi:10.1007/978-1-4615-4735-8_57

Spite, M., Baba, S. P., Ahmed, Y., Barski, O. A., Nijhawan, K., Petrash, J. M., et al. (2007). Substrate Specificity and Catalytic Efficiency of Aldo-Keto Reductases with Phospholipid Aldehydes. *Biochem. J.* 405, 95–105. doi:10.1042/bj20061743

Takahashi, M., Miyata, S., Fujii, J., Inai, Y., Ueyama, S., Araki, M., et al. (2012). *In Vivo* role of Aldehyde Reductase. *Biochim. Biophys. Acta (Bba) - Gen. Subjects* 1820, 1787–1796. doi:10.1016/j.bbagen.2012.07.003

Vander Jagt, D. L., Robinson, B., Taylor, K. K., and Hunsaker, L. A. (1992). Reduction of Trioses by NADPH-dependent Aldo-Keto Reductases. Aldose Reductase, Methylglyoxal, and Diabetic Complications. *J. Biol. Chem.* 267, 4364–4369. doi:10.1016/s0021-9258(18)42844-x

Warnasooriya, C., Feeney, C. F., Laird, K. M., Ermolenko, D. N., and Kielkopf, C. L. (2020). A Splice Site-Sensing Conformational Switch in U2AF2 Is Modulated by U2AF1 and its Recurrent Myelodysplasia-Associated Mutation. *Nucleic Acids Res.* 48, 5695–5709. doi:10.1093/nar/gkaa293

Xuan, J., Pan, G., Qiu, Y., Yang, L., Su, M., Liu, Y., et al. (2011). Metabolomic Profiling to Identify Potential Serum Biomarkers for Schizophrenia and Risperidone Action. *J. Proteome Res.* 10, 5433–5443. doi:10.1021/pr2006796

Conflict of Interest: The authors declare that the research was conducted in the absence of any commercial or financial relationships that could be construed as a potential conflict of interest.

Publisher's Note: All claims expressed in this article are solely those of the authors and do not necessarily represent those of their affiliated organizations, or those of the publisher, the editors and the reviewers. Any product that may be evaluated in this article, or claim that may be made by its manufacturer, is not guaranteed or endorsed by the publisher.

frontiers in Genetics

ORIGINAL RESEARCH
published: 03 January 2022
doi: 10.3389/fgene.2021.783074

EDNRA Gene rs1878406 Polymorphism is Associated With Susceptibility to Large Artery Atherosclerotic Stroke

Wan Wei[1], Xianjun Xuan[2], Jiahui Zhu[3], Tianwen Chen[2], Yudan Fang[2], Jiao Ding[3], Danfei Ji[3], Guoyi Zhou[3], Bo Tang[2] and Xudong He[4]**

[1]Affiliated Hangzhou First People's Hospital, Zhejiang University School of Medicine, Hangzhou, China, [2]Department of Neurology, Hangzhou Ninth People's Hospital, Hangzhou, China, [3]Fourth Clinical Medical College of Zhejiang Chinese Medical University, Hangzhou, China, [4]Sir Run Xuedong Shaw Hospital, Hangzhou, China

Objective: We performed this study to investigate whether the EDNRA gene rs1878406 C > T polymorphism is associated with risk of large artery atherosclerosis (LAA) stroke in the Chinese Han population.

Methods: Genotyping of rs1878406 was performed in 1,112 LAA stroke patients and 1,192 healthy controls. Multivariate logistic regression analyses were applied to assess the effect of the rs1878406 C > T polymorphism on susceptibility to LAA stroke.

Results: A significant increase of LAA stroke risk was found in the recessive model (TT vs. CC/TC, OR = 1.74, 95% CI = 1.23–2.48, p = 0.002) and co-dominant model (TC vs. CC, OR = 1.06, 95% CI = 0.89–1.27, TT vs. CC, OR = 1.79, 95% CI = 1.25–2.55, p = 0.006). However, the interaction between age and genotypes of rs1878406 was not statistically significant, and no significant interactive effect was observed between the rs1878406 C > T polymorphism and sex (p > 0.05).

Conclusion: The rs1878406 C > T polymorphism is associated with increased risk of LAA stroke in the Chinese Han population.

Keywords: polymorphism, large artery atherosclerosis, genotype, stroke, rs1878406

OPEN ACCESS

Edited by:
Guang-Zhong Wang, Shanghai Institute of Nutrition and Health (CAS), China

Reviewed by:
Estela Maria Bruxel, State University of Campinas, Brazil
Kazuya Toriumi, Tokyo Metropolitan Institute of Medical Science, Japan

****Correspondence:***
Bo Tang
tangboo200909@163.com
Xudong He
hexudong_2000@163.com

Specialty section:
This article was submitted to Neurogenomics, a section of the journal Frontiers in Genetics

Received: *25 September 2021*
Accepted: *22 November 2021*
Published: *03 January 2022*

Citation:
Wei W, Xuan X, Zhu J, Chen T, Fang Y, Ding J, Ji D, Zhou G, Tang B and He X (2022) EDNRA Gene rs1878406 Polymorphism is Associated With Susceptibility to Large Artery Atherosclerotic Stroke. Front. Genet. 12:783074. doi: 10.3389/fgene.2021.783074

INTRODUCTION

Stroke has become the second leading cause of death and the third cause of disability in humans. Among them, ischemic stroke accounts for about 80% of all strokes (GBD 2015 DALYs and HALE Collaborators, 2016), and it is a major cause of mortality and disability worldwide (Mendis et al., 2015), loading heavy economic burden especially in low- and middle-income countries (Benjamin et al., 2017). The occurrence and development of stroke are related to endothelial injury, atherosclerosis (Hankey, 2017), and traditional risk factors including age, gender, hypertension, diabetes mellitus, hyperlipidemia, and smoking. Besides traditional risk factors, some specific gene locus polymorphisms have also been confirmed to be associated with LAA stroke (Bellenguez et al., 2012; Malik et al., 2018). In recent years, genome-wide association studies (GWAS) have become an important research method for finding complex disease-related susceptibility genes, and many

single-nucleotide polymorphisms (SNPs) related to LAA stroke have been discovered (Traylor et al., 2012). The interaction between gene and environmental factors has also received increasing attention.

Endothelin type A receptor (EDNRA) is a receptor for endothelin-1 (ET-1), a potent vasoconstrictor. *EDNRA* is expressed in vascular smooth muscle cells (Yu et al., 1995). ET-1, encoded by the *EDN1* gene located in chromosome 6p21-24, is a potent vasoconstrictor in the body. ET-1 is expressed in several tissues, including endothelial cells and cardiomyocytes (Brunner et al., 2006). After ET-1 being bounded firmly to EDNRA, it activates calcium channels and phospholipase activation pathway to play a long-lasting vasoconstriction effect (Kampoli et al., 2011). It can also promote the proliferation and migration of vascular smooth muscle cells, increasing the ratio of neointima and media, stimulating the production of cytokines and growth factors, and inducing the formation of extracellular matrix and fibers. Hyperplasia is involved in the occurrence and development of atherosclerosis through many ways (Dai and Dai, 2010; Li et al., 2015a). GWAS have identified that SNP rs1878406 C > T polymorphism in *EDNRA* gene is related to carotid plaque (Bis et al., 2011). A following study also associated rs1878406 with coronary artery disease (Hemerich et al., 2015). Therefore, we performed this study to investigate the association between the rs1878406 C > T polymorphism and LAA stroke risk in the Chinese Han population and test whether age or gender interacts rs1878406 to influence LAA stroke risk.

MATERIALS AND METHODS

Study Subjects

We consecutively recruited first-ever LAA stroke patients between January 2015 and December 2019 from the first hospital of Hangzhou Neurology Department. Ischemic stroke was defined as sudden focal neurological deficits lasting ≥24 h, with evidence of cerebral infarction in clinically relevant areas of the brain confirmed by computed tomography (CT) and/or magnetic resonance imaging (MRI). Patients were enrolled if they (1) were 18 years or older; (2) were of Chinese Han ethnicity; (3) had available blood samples; and (4) diagnosed with LAA stroke according to TOAST classification (Adams et al., 1993). Exclusion criteria included severe liver or kidney dysfunction, hematological diseases, malignancies, and autoimmune disorders. The non-stroke controls were recruited from local inhabitants during the same period and the inclusion criteria were as follows: (1) aged 18 years or older; (2) Chinese Han ethnicity; (3) had regular physical examination; (4) no history of transient ischemic attacks, cerebrovascular, cardiovascular, and atherosclerotic diseases; and (5) no history of severe liver or kidney dysfunction, hematological diseases, malignancies, and autoimmune disorders. The study was approved by the Ethical Review Board of the First Hospital of Hangzhou (Hangzhou, China).

TABLE1 | Baseline clinical and demographic characteristics of the LAA stroke patients and controls.

Characteristic	Case	Control	*p*
N	1,112 (48.26%)	1,192 (51.74%)	
Sex			
Female	290 (26%)	440 (37%)	< 0.001
Male	822 (74%)	752 (63%)	
Age	61.40 ± 10.31	57.42 ± 10.16	< 0.001
≤60	496 (45%)	810 (68%)	< 0.001
>60	616 (55%)	382 (32%)	
Hypertension			
No	292 (26%)	851 (71%)	< 0.001
Yes	820 (74%)	341 (29%)	
Diabetes mellitus			
No	740 (67%)	1,041 (87%)	< 0.001
Yes	372 (33%)	151 (13%)	
Hyperlipidemia			
No	677 (60.9%)	892 (74.8%)	< 0.001
Yes	435 (39.1%)	300 (25.2%)	
Smoker			
No	632 (57%)	823 (69%)	< 0.001
Yes	480 (43%)	369 (31%)	

Data Collection

Baseline characteristics included demographic information (age, gender, height, and weight), medical histories (hypertension, diabetes mellitus, hyperlipidemia, and smoking), and laboratory tests. Smokers were those who had smoked ≥100 cigarettes during their lifetime and currently smoke every day or some days (Loke et al., 2014). Routine laboratory investigations were performed after overnight fasting within 24 h of admission. The definition of hyperlipidemia is serum triglyceride ≥150 mg/dl, low-density lipoprotein cholesterol ≥130 mg/dl, high-density lipoprotein cholesterol ≤40 mg/dl in adult males and ≤50 mg/dl in adult females, any use of lipid-lowering drugs, or any self-reported history of hyperlipidemia (Wang et al., 2015).

Genotyping

All patients took 5 ml of fasting peripheral venous blood in the early morning and placed it in an *EDTA* anticoagulation tube. After centrifugation, the lower layer of blood cells was removed and stored in a refrigerator at −80°C. Genotyping was conducted by SNPscan technology, supported by the Center for Human Genetics Research, Genesky Biotechnology Co. Ltd. (Shanghai, China). About 5% of the samples were randomly selected and genotyped repeatedly to confirm the genotyping credibility, and the results were 100% consistent.

Statistical Analyses

Statistical analyses were performed with SPSS Statistics Version 22.0 (IBM, Armonk, NY, United States). Student's *t*-test was conducted for continuous variable. Categorical data were expressed as frequency and percentage. Categorical variables were compared using Chi-square test. The mean age of LAA stroke onset for three polymorphisms was compared using one-way ANOVA. Univariate and multivariate logistic regression

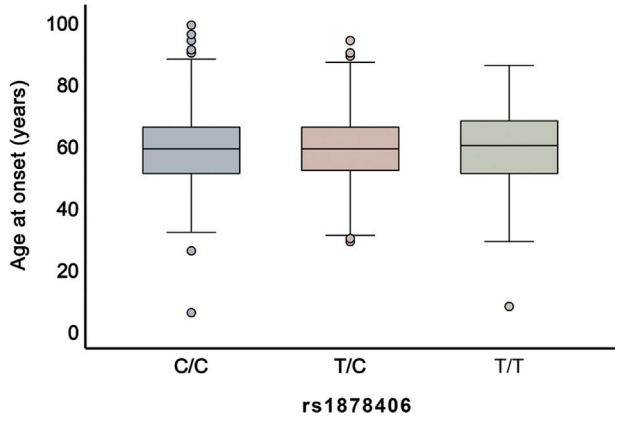

FIGURE 1 | Association between rs1878406 polymorphism and age at onset of LAA stroke. Box plot of age at LAA stroke onset for three different genotypes of patients with rs1878406.

analyses were performed to investigate the association of the rs1878406 C > T polymorphism with risk of LAA stroke. Akaike information criterion (AIC) was calculated for selecting the best model for the SNP. All statistical tests were two-sided and $p < 0.05$ was considered statistically significant.

In Silico Analysis

To provide function annotation for rs1878406 polymorphism in *EDNRA* gene, we performed *in silico* analysis using Haploreg v4.118 (https://pubs.broadinstitute.org/mammals/haploreg/haploreg.php).

RESULTS

Baseline Characteristics of the Subjects

A total of 1,112 LAA stroke patients and 1,192 healthy controls were recruited in this study. Baseline clinical and demographic characteristics are shown in **Table 1**. Compared with the controls, patients were older ($p < 0.001$) and had a higher proportion of male and traditional risk factors for ischemic stroke, such as history of hypertension, diabetes mellitus, hyperlipidemia, and smoking ($p < 0.001$).

Association of rs1878406 Polymorphism With Age of Onset of LAA Stroke

We first evaluated the correlation between the rs1878406 polymorphism and the age of onset of LAA stroke. As shown in **Figure 1**, these three polymorphisms were not significantly related to the age at onset of LAA stroke ($p > 0.05$).

Association of rs1878406 C > T Polymorphism With the Risk of LAA Stroke

The frequencies of CC, TC, and TT genotypes were 60.1%, 35.3%, and 4.5%, among the LAA stroke patients, respectively, and 56.8%, 35.5%, and 7.6%, among the controls, respectively. According to the AIC values, the recessive model is the best-fitting model. In the recessive model, compared with CC and TC genotype, TT genotype of the rs1878406 was associated with significantly increased risk of LAA stroke (OR = 1.74, 95% CI = 1.23–2.48, $p = 0.002$; **Table 2**). After adjustment for gender, age, hypertension, diabetes mellitus, hyperlipidemia, and smoking, the association remained significant (OR = 1.80, 95% CI = 1.19–2.73, $p = 0.005$ for CC/CT vs. TT). The rs1878406 C > T polymorphism also had a common effect on LAA stroke in the co-dominant model (TC vs. CC, OR = 1.06, 95% CI = 0.89–1.27; TT vs. CC, OR = 1.79, 95% CI = 1.25–2.55; $p = 0.006$). However, the risk effect was not statistically significant in the dominant model ($p = 0.137$). A dose–response relationship between the T allele and risk of LAA stroke was determined by the log-additive model (OR = 1.20, 95% CI = 1.03–1.41, $p = 0.022$; **Table 2**).

Subgroup Analysis and Interaction Analysis According to Age and Sex

Table 3 shows the effect of rs1878406 on the risk of LAA stratified by age. In adults aged ≤60 years, the T allele of rs1878406 showed significant association with risk of LAA stroke (CC/CT vs. TT, OR = 2.00, 95% CI = 1.16–3.45, $p = 0.013$). In adults aged

TABLE 2 | Association of the rs1878406 C > T polymorphism with risk of LAA stroke.

Genetic models	Genotype	Case	Control	Crude OR (95%CI)	Crude *p* value	AIC	Adjusted OR (95%CI)	*p*[a]
Codominant	C/C	717 (60.1%)	632 (56.8%)	1	0.006	3,186.9	1	0.016
	T/C	421 (35.3%)	395 (35.5%)	1.06 (0.89–1.27)			1.07 (0.87–1.32)	
	T/T	54 (4.5%)	85 (7.6%)	1.79 (1.25–2.55)			1.85 (1.21–2.83)	
Dominant	C/C	717 (60.1%)	632 (56.8%)	1	0.106	3192.6	1	0.137
	T/C-T/T	475 (39.9%)	480 (43.2%)	1.15 (0.97–1.35)			1.16 (0.95–1.41)	
Recessive	C/C-T/C	1,138 (95.5%)	1,027 (92.4%)	1	0.002	3,185.4	1	0.005
	T/T	54 (4.5%)	85 (7.6%)	1.74 (1.23–2.48)			1.80 (1.19–2.73)	
Log-additive	—	—	—	1.19 (1.04–1.36)	0.011	3,188.8	1.20 (1.03–1.41)	0.022

[a]*Adjusted for age, blood pressure, diabetes, hypertension, hyperlipidemia, and smoking.*

TABLE 3 | Age-stratified analysis of the association between the rs1878406 C > T polymorphism and risk of LAA stroke.

Genotypes	≤60				>60			
	Control	Case	OR (95% CI)	p^a	Control	Case	OR (95% CI)	p^a
C/C-T/C	775	458	1	0.013	363	569	1	0.248
T/T	35	38	2.00 (1.16–3.45)		19	47	1.44 (0.78–2.66)	

[a]*Adjusted for blood pressure, diabetes, hypertension, hyperlipidemia, and smoking.*

TABLE 4 | Sex-stratified analysis of the association between the rs1878406 C > T polymorphism and risk of LAA stroke.

Genotypes	Female				Male			
	Control	Case	OR (95% CI)	p^a	Control	Case	OR (95% CI)	p^a
C/C-T/C	418	270	1	0.308	720	757	1	0.011
T/T	22	20	1.43 (0.68–3.02)		32	65	1.89 (1.14–3.11)	

[a]*Adjusted for age, blood pressure, diabetes, hypertension, hyperlipidemia, and smoking.*

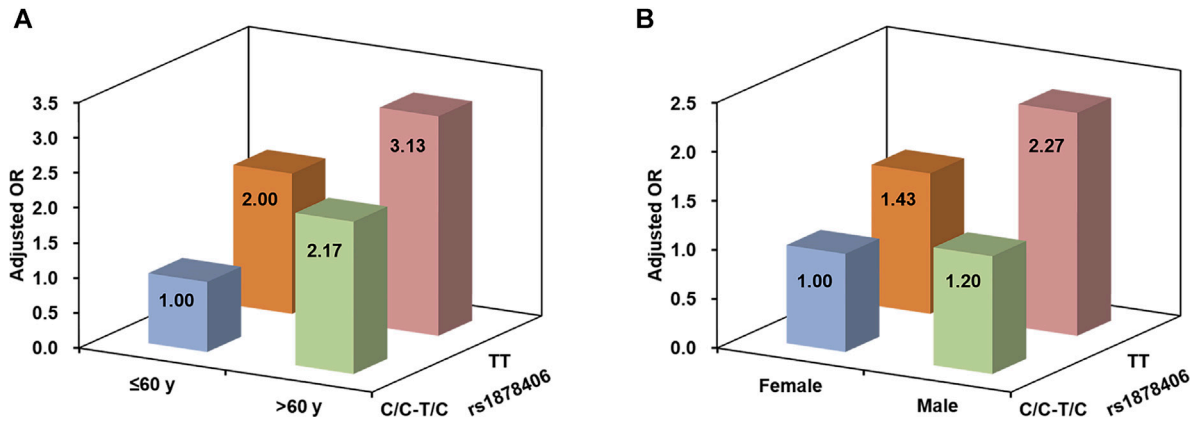

FIGURE 2 | (A) Adjusted OR of LAA stroke according to rs1878406 and age; the interaction between rs1878406 and age was non-significant ($p_{interaction}$ = 0.442). **(B)** Adjusted OR of LAA stroke according to rs1878406 and sex; the interaction between rs1878406 and sex was non-significant ($p_{interaction}$ = 0.553).

TABLE 5 | Regulatory motifs altered for rs1878406 based on HaploReg v4.1.

PWM ID	PWM match score		C Allele: TTATCTTCAGTCTCACCTCCGAATCCTGTCAGCTGTTATCTCGTATTTAGAGCTTACCA
	C Allele	T Allele	T Allele: TTATCTTCAGTCTCACCTCCGAATCCTGTTAGCTGTTATCTCGTATTTAGAGCTTACCA
GATA_known1	12	12.4	HBDHVDYTCTTATCTHYHHWHV
GATA_known4	12.9	12.6	NNHHBSTTATCWHBNDW
Myf_4	13.4	5.9	NDRVCAVCTGYYNNBB

PWM, Position Weight Matrix (Library from Kheradpour and Kellis, 2013).

>60 years, however, no significant association was found. In the stratified analysis by sex, the T allele of rs1878406 significantly increased the risk of LAA stroke in males (CC/CT vs. TT, OR = 1.89, 95% CI = 1.14–3.11, p = 0.011; **Table 4**). In females, however, we did not detect any significant association of rs1878406 with risk of LAA stroke. The results suggested potential interactions between rs1878406 polymorphism, age, and sex in the etiology of LAA stroke. However, the interaction between age and genotypes of rs1878406 was not statistically significant ($p_{interaction}$ = 0.442; **Figure 2A**). Similarly, there was no statistical evidence for interaction between these rs1878406 polymorphism and sex on the risk of LAA stroke ($p_{interaction}$ = 0.553; **Figure 2B**).

Functional Annotation

Bioinformatics analysis by HaploReg v4.1 indicated that rs1878406 could change the binding affinity of regulatory motifs Myf_4 (**Table 5**).

DISCUSSION

We confirmed that age, blood pressure, diabetes, hypertension, hyperlipidemia, and smoking were independent risk factors for cerebral infarction by comparing the general data of atherosclerotic cerebral infarction with those of normal controls, which were consistent with the results of previous studies. After adjusting for factors such as gender, age, and hypertension under the recessive model, it was shown that TT genotype at rs1878406 was a risk factor for susceptibility to cerebral infarction as compared with the CC/TC genotype. Under the recessive model, the interaction between age or gender and genotypes of rs1878406 C > T polymorphism was not statistically significant. Altogether, it is found that the T allele at *EDNRA* rs1878406 is a risk factor for cerebral infarction.

The *EDNRA* gene encodes ET-1 receptor A, which plays an important role in effective and durable vasoconstriction (Dai and Dai, 2010; Li et al., 2015a), and is widely distributed in the cardiovascular and central nervous system. Encoded by *EDN1*, ET-1 is a potent vasoconstrictor that is expressed in a variety of tissues, including endothelial cells and cardiomyocytes (Brunner et al., 2006). ET-1 is closely related to cardiovascular and cerebrovascular diseases, and endothelial dysfunction can be found in hypertension, atherosclerosis, diabetes, hyperlipidemia, and cerebrovascular spasm, with increased ET release (Balletshofer et al., 2000). In 1992, Zir et al. (Balletshofer et al., 2000) first confirmed the elevated plasma ET-1 level in patients with acute ischemic cerebral infarction. In recent years, the relationship between ET-1 and ischemic cerebrovascular disease has become a hot topic in basic and clinical medicine. ET-1 mediates endothelial dysfunction mainly by increasing fibroblasts and macrophages. Endothelial damage greatly enhances the sensitivity of blood vessels to ET-1, causing durable contraction of local blood vessels, and ischemia and hypoxia of brain tissue. In addition to its effect on blood vessels, ET-1 can also directly act on nerve cells, causing cell death, accelerating the death of neurons in the hypoxia area by promoting the release of excitatory amino acids (Lin et al., 1990). Studies have shown that ET-1 can bind to its receptor and activate the voltage-sensitive L-type calcium channel, causing extracellular calcium influx and intracellular calcium overload, thus aggravating the damage of nerve cells (Marsden et al., 1989). All the above lines of evidence provide us with the theoretical basis that the rs1878406 variant in *EDNRA* may be related to cerebral infarction.

Multiple previous studies have shown that the rs1878406 variant is associated with atherosclerosis and endothelial dysfunction. For example, in the 2011 meta-analysis by Bis et al. (2011), it was found that the C allele of rs1878406 was associated with lower risk of plaque. However, the T allele was associated with a 22% increased odds of the presence of plaque. These associations may provide important insights into the pathophysiological mechanisms relating the genes to atherosclerosis and subsequent artery disease. Another study (Li et al., 2015b) explored the potential relationship between EDNRA rs1878406 polymorphisms and the carotid intima-media thickness (IMT) levels, but no statistically significant differences were found when this polymorphism was assessed according to carotid IMT values. Instead, they identified a significant interaction of gender with this variant rs1878406 in the *EDNRA* gene. For gene–gender interaction on common carotid arteries IMT, the adjusted mean for men carrying the GA/GG genotype of *EDNRA* SNP rs1878406 was 1.18 times higher than that for men carrying the AA genotype. This may be due to the fact that the sample size of their study was relatively small. Zhang et al. (2017) found in their analysis of the Han population that the rs1878406 TT/TC genotype could be a significant risk factor for severe multiple coronary artery lesions. Moreover, our results indicated that rs1878406 could change the binding affinity of regulatory motifs Myf_4. The above results of previous studies are consistent with our studies, suggesting that the C→T mutation in the *EDNRA* gene rs1878406 may influence the function of ET-1, thereby affecting the occurrence of atherosclerosis.

Our study has some limitations. First of all, we only analyzed the Han population, which is not representative of other ethnic groups. More international institutions should further combine for sample collection, so that possible geographical and ethnic differences can be compared in the future. Secondly, the sample size of this study is relatively small, and further larger sample study is required. In addition, there is a lack of in-depth study on the related mechanism of rs1878406 polymorphism increasing the risk of cerebral infarction, and further functional verification can be conducted, including *in vivo* and *in vitro* experiments.

In conclusion, the results of this study suggest that individuals carrying the *EDNRA* rs1878406 TT genotype may be a risk factor against cerebral infarction. However, to explore the relationship between rs1878406 and pre-cerebral infarction, we need to conduct joint analysis on the basis of the largest sample size as possible, so as to provide a reliable theoretical basis for the early prevention and treatment of cerebral infarction.

DATA AVAILABILITY STATEMENT

The data presented in the study are deposited in the EMBL-EBI repository, accession number PRJEB48922.

ETHICS STATEMENT

The studies involving human participants were reviewed and approved by the Affiliated Hangzhou ninth People's Hospital, Zhejiang University School of Medicine. The patients/participants provided their written informed consent to participate in this study.

AUTHOR CONTRIBUTIONS

WW and XX contributed to conception and design of the study. WW, JZ, TC, YF, JD, DJ, and GZ organized the database. BT and XH performed the statistical analysis. WW wrote the first draft of the manuscript. WW and XH wrote the manuscript. All authors contributed to manuscript revision, read, and approved the submitted version.

REFERENCES

Adams, H. P., Bendixen, B. H., Kappelle, L. J., Biller, J., Love, B. B., Gordon, D. L., et al. (1993). Classification of Subtype of Acute Ischemic Stroke. Definitions for Use in a Multicenter Clinical Trial. TOAST. Trial of Org 10172 in Acute Stroke Treatment. *Stroke* 24, 35–41. doi:10.1161/01.str.24.1.35

Balletshofer, B. M., Rittig, K., Enderle, M. D., Volk, A., Maerker, E., Jacob, S., et al. (2000). Endothelial Dysfunction Is Detectable in Young Normotensive First-Degree Relatives of Subjects with Type 2 Diabetes in Association with Insulin Resistance. *Circulation* 101, 1780–1784. doi:10.1161/01.cir.101.15.1780

Bellenguez, C., Bevan, S., Bevan, S., Gschwendtner, A., Spencer, C. C. A., Burgess, A. I., et al. (2012). Genome-wide Association Study Identifies a Variant in HDAC9 Associated with Large Vessel Ischemic Stroke. *Nat. Genet.* 44, 328–333. doi:10.1038/ng.1081

Benjamin, E. J., Blaha, M. J., Chiuve, S. E., Cushman, M., Das, S. R., Deo, R., et al. (2017). Heart Disease and Stroke Statistics-2017 Update: A Report from the American Heart Association. *Circulation* 135, e146–603. doi:10.1161/CIR.0000000000000485

Bis, J. C., Kavousi, M., Kavousi, M., Franceschini, N., Isaacs, A., Abecasis, G. R., et al. (2011). Meta-analysis of Genome-wide Association Studies from the CHARGE Consortium Identifies Common Variants Associated with Carotid Intima media Thickness and Plaque. *Nat. Genet.* 43, 940–947. doi:10.1038/ng.920

Brunner, F., Brás-Silva, C., Cerdeira, A. S., and Leite-Moreira, A. F. (2006). Cardiovascular Endothelins: Essential Regulators of Cardiovascular Homeostasis. *Pharmacol. Ther.* 111, 508–531. doi:10.1016/j.pharmthera.2005.11.001

Dai, D.-Z., and Dai, Y. (2010). Role of Endothelin Receptor a and NADPH Oxidase in Vascular Abnormalities. *Vhrm* 6, 787–794. doi:10.2147/vhrm.s6556

GBD 2015 DALYs and HALE Collaborators (2016). Global, Regional, and National Disability-Adjusted Life-Years (DALYs) for 315 Diseases and Injuries and Healthy Life Expectancy (HALE), 1990-2015: a Systematic Analysis for the Global Burden of Disease Study 2015. *Lancet* 388, 1603–1658. doi:10.1016/S0140-6736(16)31460-X

Hankey, G. J. (2017). Stroke. *The Lancet* 389, 641–654. doi:10.1016/S0140-6736(16)30962-X

Hemerich, D., van der Laan, S. W., Tragante, V., den Ruijter, H. M., de Borst, G. J., Pasterkamp, G., et al. (2015). Impact of Carotid Atherosclerosis Loci on Cardiovascular Events. *Atherosclerosis* 243, 466–468. doi:10.1016/j.atherosclerosis.2015.10.017

Kampoli, A.-M., Tousoulis, D., Briasoulis, A., Latsios, G., Papageorgiou, N., and Stefanadis, C. (2011). Potential Pathogenic Inflammatory Mechanisms of Endothelial Dysfunction Induced by Type 2 Diabetes Mellitus. *Cpd* 17, 4147–4158. doi:10.2174/138161211798764825

Li, C., Chen, W., Jiang, F., Simino, J., Srinivasan, S. R., Berenson, G. S., et al. (2015). Genetic Association and Gene-Smoking Interaction Study of Carotid Intima-media Thickness at Five GWAS-Indicated Genes: The Bogalusa Heart Study. *Gene* 562, 226–231. doi:10.1016/j.gene.2015.02.078

Li, T.-C., Li, C.-I., Liao, L.-N., Liu, C.-S., Yang, C.-W., Lin, C.-H., et al. (2015). Associations of EDNRA and EDN1 Polymorphisms with Carotid Intima media Thickness through Interactions with Gender, Regular Exercise, and Obesity in Subjects in Taiwan: Taichung Community Health Study (TCHS). *BioMed* 5, 8. doi:10.7603/s40681-015-0008-7

Lin, W.-W., Lee, C. Y., and Chuang, D.-M. (1990). Endothelin-1 Stimulates the Release of Preloaded [3H]D-Aspartate from Cultured Cerebellar Granule Cells. *Biochem. Biophysical Res. Commun.* 167, 593–599. doi:10.1016/0006-291x(90)92066-9

Loke, W. M., Sing, K. L. M., Lee, C.-Y. J., Chong, W. L., Chew, S. E., Huang, H., et al. (2014). Cyclooxygenase-1 Mediated Platelet Reactivity in Young Male Smokers. *Clin. Appl. Thromb. Hemost.* 20, 371–377. doi:10.1177/1076029612466284

Malik, R., Chauhan, G., Traylor, M., Sargurupremraj, M., Okada, Y., Mishra, A., et al. (2018). Multiancestry Genome-wide Association Study of 520,000 Subjects Identifies 32 Loci Associated with Stroke and Stroke Subtypes. *Nat. Genet.* 50, 524–537. doi:10.1038/s41588-018-0058-3

Marsden, P. A., Raju Danthuluri, N., Brenner, B. M., Ballermann, B. J., and Brock, T. A. (1989). Endothelin Action on Vascular Smooth Muscle Involves Inositol Trisphosphate and Calcium Mobilization. *Biochem. Biophysical Res. Commun.* 158, 86–93. doi:10.1016/s0006-291x(89)80180-9

Mendis, S., Davis, S., and Norrving, B. (2015). Organizational Update. *Stroke* 46, e121. doi:10.1161/STROKEAHA.115.008097

Traylor, M., Farrall, M., Holliday, E. G., Sudlow, C., Hopewell, J. C., Cheng, Y.-C., et al. (2012). Genetic Risk Factors for Ischaemic Stroke and its Subtypes (The METASTROKE Collaboration): A Meta-Analysis of Genome-wide Association Studies. *Lancet Neurol.* 11, 951–962. doi:10.1016/S1474-4422(12)70234-X

Wang, X., Zhao, X., Johnston, S. C., Xian, Y., Hu, B., Wang, C., et al. (2015). Effect of Clopidogrel with Aspirin on Functional Outcome in TIA or Minor Stroke. *Neurology* 85, 573–579. doi:10.1212/WNL.0000000000001844

Yu, J. C. M., Pickard, J. D., and Davenport, A. P. (1995). Endothelin ETA Receptor Expression in Human Cerebrovascular Smooth Muscle Cells. *Br. J. Pharmacol.* 116, 2441–2446. doi:10.1111/j.1476-5381.1995.tb15093.x

Zhang, L., Chen, J., He, Q., Dai, R., and Chen, M. (2017). Association of Endotheline Receptor Gene Rs1878406 Polymorphism with Severe Multi-Vessel Coronary disease. *Zhonghua Yi Xue Yi Chuan Xue Za Zhi* 34, 597–601. doi:10.3760/cma.j.issn.1003-9406.2017.04.028

Conflict of Interest: The authors declare that the research was conducted in the absence of any commercial or financial relationships that could be construed as a potential conflict of interest.

frontiers in Neuroscience

ORIGINAL RESEARCH
published: 21 January 2022
doi: 10.3389/fnins.2021.799761

Association of Epigenetic Differences Screened in a Few Cases of Monozygotic Twins Discordant for Attention-Deficit Hyperactivity Disorder With Brain Structures

Takashi X. Fujisawa[1,2], Shota Nishitani[1,2], Kai Makita[1], Akiko Yao[1,2], Shinichiro Takiguchi[3], Shoko Hamamura[2,3], Koji Shimada[1,2,4], Hidehiko Okazawa[1,2,4], Hideo Matsuzaki[1,2,3] and Akemi Tomoda[1,2,3]**

[1] Research Center for Child Mental Development, University of Fukui, Fukui, Japan, [2] Division of Developmental Higher Brain Functions, United Graduate School of Child Development, Osaka University, Kanazawa University, Hamamatsu University School of Medicine, Chiba University, and University of Fukui, Osaka, Japan, [3] Department of Child and Adolescent Psychological Medicine, University of Fukui Hospital, Fukui, Japan, [4] Biomedical Imaging Research Center, University of Fukui, Fukui, Japan

OPEN ACCESS

Edited by:
Noriyoshi Usui,
Osaka University, Japan

Reviewed by:
Minyoung Jung,
Korea Brain Research Institute, South Korea
Esther Walton,
University of Bath, United Kingdom

***Correspondence:**
Takashi X. Fujisawa
tfuji@u-fukui.ac.jp
Akemi Tomoda
atomoda@u-fukui.ac.jp

Specialty section:
This article was submitted to Neurogenomics, a section of the journal Frontiers in Neuroscience

Received: 22 October 2021
Accepted: 16 December 2021
Published: 21 January 2022

Citation:
Fujisawa TX, Nishitani S, Makita K, Yao A, Takiguchi S, Hamamura S, Shimada K, Okazawa H, Matsuzaki H and Tomoda A (2022) Association of Epigenetic Differences Screened in a Few Cases of Monozygotic Twins Discordant for Attention-Deficit Hyperactivity Disorder With Brain Structures. Front. Neurosci. 15:799761. doi: 10.3389/fnins.2021.799761

The present study examined the relationship between DNA methylation differences and variations in brain structures involved in the development of attention-deficit hyperactivity disorder (ADHD). First, we used monozygotic (MZ) twins discordant (2 pairs of 4 individuals, 2 boys, mean age 12.5 years) for ADHD to identify candidate DNA methylation sites involved in the development of ADHD. Next, we tried to replicate these candidates in a case-control study (ADHD: *N* = 18, 15 boys, mean age 10.0 years; Controls: *N* = 62, 40 boys, mean age 13.9 years). Finally, we examined how methylation rates at those sites relate to the degree of local structural alterations where significant differences were observed between cases and controls. As a result, we identified 61 candidate DNA methylation sites involved in ADHD development in two pairs of discordant MZ twins, among which elevated methylation at a site in the sortilin-related Vps10p domain containing receptor 2 (*SorCS2*) gene was replicated in the case-control study. We also observed that the ADHD group had significantly reduced gray matter volume (GMV) in the precentral and posterior orbital gyri compared to the control group and that this volume reduction was positively associated with *SorCS2* methylation. Furthermore, the reduced GMV regions in children with ADHD are involved in language processing and emotional control, while *SorCS2* methylation is also negatively associated with emotional behavioral problems in children. These results indicate that *SorCS2* methylation might mediate a reduced GMV in the precentral and posterior orbital gyri and therefore influence the pathology of children with ADHD.

Keywords: attention-deficit hyperactivity disorder (ADHD), DNA methylation, monozygotic twins, voxel-based morphometry (VBM), SorCS2

INTRODUCTION

Attention-deficit hyperactivity disorder (ADHD) is one of the most common mental disorders in childhood, characterized by inattention, hyperactivity, and impulsivity, according to the 5th edition of the Diagnostic and Statistical Manual of Mental Disorders (DSM-5) (American Psychiatric Association, 2013) and often reaching into adulthood. The prevalence of ADHD in children worldwide was estimated to be 7.2% in a meta-analysis of 175 studies (Thomas et al., 2015). Patients with ADHD have difficulties in various cognitive domains, such as cognitive control, attention, timing, and working memory (Biederman et al., 1991; Rubia, 2018), as well as in other domains involved in emotional processing, such as motivation and timing processing, such as timing dissociation and delay-related impairments (Biederman et al., 1993; Sonuga-Barke et al., 2010; Rubia, 2018). According to a prospective follow-up study, approximately 50% of children with ADHD continue to have symptoms until adulthood, and if left untreated, they can be at higher risk of psychiatric problems such as depression, substance abuse, and social problems such as unemployment and criminal offenses (Biederman et al., 2006; Molina et al., 2009).

While the heritability of ADHD has been reported to be as high as 72–88% (Larsson et al., 2014), there has been obvious discordance in ADHD diagnosis between monozygotic (MZ) twin pairs, and often differences in severity within MZ concordant cases (Larsson et al., 2014), suggesting that epigenetic factors may be involved in the etiology. Epigenetic modifications regulate gene expression independently of changes in DNA sequence, primarily through DNA methylation and histone modifications (Henikoff and Matzke, 1997), and have been suggested to serve as a critical link between external environmental factors and long-lasting phenotypic changes (Malki et al., 2016). Epigenetic changes in the brain have been found to be involved in cognitive neurological processes, including psychiatric disorders, neurogenesis, and brain development. Candidate gene studies on ADHD's DNA methylation profile based on peripheral samples such as blood or saliva have shown different methylation patterns of genes involved not only in dopaminergic, serotonergic, and neurotrophic systems including *SLC6A4*, *DRD4*, *COMT*, *BDNF*, and *NGFR*, but also neurotransmitter release or neurite outgrowth including *ERC2* and *CREB5* and associated with the symptoms and severity of ADHD (van Mil et al., 2014; Park et al., 2015; Xu et al., 2015; Dadds et al., 2016; Heinrich et al., 2017; Sengupta et al., 2017; Neumann et al., 2020).

Using disease discordant MZ twins for comparison in epidemiological epigenetic studies would be an ideal strategy, because the sex, age, perinatal environment, and other shared environmental factors that significantly influence the epigenome should be matched within MZ twins (Bell and Spector, 2011). Recent findings have revealed considerable epigenetic differences between MZ twins (Kaminsky et al., 2009), and such differences have been associated with phenotypic discordance between MZ twins, including psychiatric disorders (Kuratomi et al., 2008; Sugawara et al., 2011; Wong et al., 2014; Malki et al., 2016). Regarding ADHD, Chen et al. (2018) recently examined the relationship between brain structure and whole blood DNA methylation in 14 pairs of MZ-discordant cases, finding structural alterations in the striatum and cerebellum, as well as significant epigenetic differences in genes, such as γ-aminobutyric acid (GABA), dopamine and serotonin neurotransmitter systems, in these "discordant" brain structures (Chen et al., 2018). These findings support the role of DNA methylation in ADHD. However, given the high heterogeneity of ADHD, not only the study of DNA methylation associated significantly different brain regions in MZ discordant twins, but also examining the association between methylation array data analysis and structural alterations in the whole brain, including the cerebral cortex, can comprehensively elucidate the complex pathology of ADHD.

Here, we examined the relationship between DNA methylation differences on array data and variations in brain structures involved in the development of ADHD. Thus, our main hypothesis was that the DNA methylation sites nominated using identical MZ twins discordant for ADHD are ADHD-specific, and significantly associated with brain structures and symptoms observed in children with ADHD compared to typically developing children.

MATERIALS AND METHODS

Participants

Two pairs of MZ twins discordant for ADHD were recruited from the Department of Child and Adolescent Psychological Medicine at the University of Fukui Hospital. The twins were 9-year-old males (pair 1) and 16-year-old females (pair 2). Eighteen children with ADHD (16 males and 2 females, mean age = 9.7 ± 1.6 years) were also recruited at the department for the case-control study. The diagnosis of ADHD was assessed by licensed child and adolescent psychiatrists according to DSM-5 criteria (American Psychiatric Association, 2013). Participants were also administered an assessment module of DSM-IV ADHD from the Schedule of Affective Disorders and Schizophrenia for School-Age Children, Epidemiologic version (K-SADS-E; Orvaschel and Puig-Antich, 1994). To further assess the core symptoms of ADHD (e.g., inattentive and hyperactive/impulsive symptoms), for the pairs of MZ twins discordant for ADHD parents were asked to complete the ADHD Rating Scale (ADHD-RS) (DuPaul et al., 1998) for all children with ADHD in the case-control study, the Swanson, Nolan, and Pelham Rating Scale (SNAP-IV) (Swanson, 1992). To exclude other psychiatric conditions (e.g., anxiety disorder), subjects were administered the Mini-International Neuropsychiatric Interview for Children and Adolescents (MINI-KID; Sheehan et al., 2010) by two licensed pediatric-psychological clinicians. Two existing Cohorts of 62 children (Cohort 1: n = 28, 21 males and 7 females, mean age = 14.9 ± 1.8 years; Cohort 2: n = 34, 19 males and 15 females, mean age = 13.1 ± 2.9 years) recruited from the local community in our previous study were used as controls for the case-control study (Takiguchi et al., 2015; Shimada et al., submitted[1]). All children had normal or corrected vision and

[1]Shimada, K., Hamamura, S., Takiguchi, S., Makita, K., Yao, A., Fujisawa, T. X., et al. (submitted). Developmental differences in resting-state functional connectivity among youth in small-group family-like residential care.

normal hearing. All children, with the exception of the non-ADHD twins, were assessed using the Wechsler Intelligence Scale for Children-Fourth Edition (WISC-IV; Wechsler, 2003) or the Wechsler Adult Intelligence Scale-Third Edition (WAIS-III; Wechsler, 1997) and excluded if they had a full-scale intelligence quotient (FSIQ) <70. They were also excluded if they had any history of substance abuse, recent substance use, head trauma with loss of consciousness, significant fetal exposure to alcohol or drugs, perinatal or neonatal complications, neurological disorders, or medical conditions that might adversely affect growth and development. In the case-control study, behavioral and emotional problems were assessed using the Child Behavior Checklist (CBCL) in all children with ADHD and controls in Cohort 1 (Achenbach and Rescorla, 2001), and with the Strength and Difficulties Questionnaire (SDQ) in controls in Cohort 2 (Goodman, 1997).

Saliva Collection and DNA Extraction

Saliva samples were collected using the Oragene Discover OGR-500 kit (DNA Genotek Inc., Ottawa, ON, Canada). DNA was extracted using prepIT®•L2P reagent (DNA Genotek Inc.) and quantified using the Qubit™ dsDNA HS Assay Kit (Thermo Fisher Scientific Inc., Pittsburgh, PA, United States).

DNA Methylation Array

Genomic DNA (500 ng) was bisulfite-treated for cytosine-to-thymine conversion using the EZ DNA Methylation-Gold kit (Zymo Research, Irvine, CA, United States). The DNA was then whole-genome amplified, fragmented, and hybridized to the Human MethylationEPIC BeadChip (Illumina Inc., San Diego, CA, United States). BeadChips were scanned using iSCAN (Illumina Inc.), and the methylation level (β value) was calculated for each queried CpG locus using the GenomeStudio Methylation Module software, followed by the Psychiatric Genomics Consortium-Epigenome-Wide Association Studies quality control pipeline (Ratanatharathorn et al., 2017). Using CpGassoc (Barfield et al., 2012), samples with probe detection call rates <90% and those with an average intensity value of either <50% of the experiment-wide sample mean or <2,000 arbitrary units were excluded. Probes with detection $P > 0.001$ or those based on <3 beads were set to missing as were probes cross-hybridizing between autosomes and sex chromosomes (Teschendorff et al., 2013). CpG sites with missing data for >10% of samples within the dataset were excluded from the analysis. Probes containing single nucleotide polymorphisms (based on 1000 Genomes) within 10 base pairs of the target CpG were maintained in each dataset but flagged and tracked throughout the analysis pipeline. This decision was based on the growing recognition that sequence variants can influence DNA methylation patterns throughout the genome (Smith et al., 2014). Normalization of probe distribution and background differences between Type I and Type II probes was conducted using beta mixture quantile normalization (Teschendorff et al., 2013) after background correction. We did not remove the batch effect at this stage either for (1) MZ twins discordant for ADHD (Proband: $N = 2$, Non-proband: $N = 2$) and (2) ADHD cases ($N = 18$)–controls ($N = 62$) study since (1) those samples were scanned within the same chip and the row positional balance was identical [Pair 1: row 5 (Proband) vs. row 6 (Non-proband), pair 2: row 7 (Non-proband) vs. row 8 (Proband)], and (2) batches were completely confounded with case-control group status [Case chip ID (6 batches): 205111140162, 205111140170, 205111140171, 205134980172, 205134980191, and 205134980192; Control chip ID (8 batches): 203748260078, 203748260085, 203755070101, 203755080004, 203757350003, 203757350018, 203757350022, and 203757350023]. In such a case, it is not possible to remove technical signals when batches are confounded with variables of interest, even by employing tools such as ComBat (Johnson et al., 2007). As suggested by Nygaard et al. (2016) and Price and Robinson (2018), we decided to use chips and rows as additional covariates in our linear model instead of adjusting for batch effects in the initial processing to avoid *P*-value inflation. After quality control, 807,253 probes and 794,661 probes remained for (1) MZ twins discordant for ADHD and (2) the ADHD case-control study, respectively. We confirmed whether pair 1 and pair 2 were MZ twins using 59 "rs" probes on the EPIC chip using the R package *ewastool* (Heiss and Just, 2018), and found an identical genetic background (agreement: 0.9999891 and 0.9999893, respectively). As saliva contains a heterogeneous mixture of cell types of differing proportions in each sample, we used the EpiDISH method (Teschendorff et al., 2017) to estimate the proportion of epithelial cells derived from salivary DNA and entered it as a covariate in our statistical models.

Brain-Image Acquisition and Pre-processing

Image acquisition in the 52 participants in the case-control study (18 with ADHD, 34 controls in Cohort 2) was performed using a GE Signa PET/MR 3-Tesla scanner with an 8-channel head coil (GE Healthcare, Milwaukee, WI, United States). A T1-weighted anatomical dataset was obtained using a fast spoiled-gradient recalled imaging sequence (voxel size 1 × 1 × 1 mm, TE = 3.24 ms, TR = 8.46 ms, flip angle = 11°). Image acquisition for the other 28 controls in Cohort 1 in the case-control study was performed using a GE Discovery MR 750 3-Tesla scanner with a 32-channel head coil (GE Healthcare, Milwaukee, WI, United States). A T1-weighted anatomical dataset was obtained from each subject by a fast-spoiled gradient recalled imaging sequence (voxel size 1 × 1 × 1 mm, TE = 1.99 ms, TR = 6.38 ms, flip angle = 11°). VBM was performed as a global analytic approach using the Statistical Parametric Mapping version 12 software[2] (Wellcome Department of Imaging Neuroscience, University College London, London, United Kingdom) implemented in MATLAB 2020b (Math Works Inc., Natick, MA, United States). T1-weighted images were segmented coarsely into gray matter (GM), white matter, cerebrospinal fluid, and skull/scalp compartments using tissue probability maps. The Diffeomorphic Anatomical Registration through Exponentiated Lie Algebra algorithm was applied to the segmented brain tissues to generate a study-specific template and to achieve an accurate inter-subject registration with improved

[2]http://www.fil.ion.ucl.ac.uk/spm/software/spm12/

realignment of smaller inner structures (Ashburner, 2007). The segmented GM images were spatially normalized, and written out with an isotropic voxel resolution of 1.5 mm. Any volume change induced by normalization was adjusted via a modulation algorithm. Spatially normalized GM images were smoothed by a Gaussian kernel of 6.2 mm full width at half maximum.

Statistical Analyses

First, to clarify epigenetic associations between proband and non-proband ADHD discordant MZ twins from methylation array data, multiple regression analysis was performed using CpGassoc (Barfield et al., 2012). In this analysis, DNA methylation at each CpG probe was entered as a dependent variable, and each group (proband or non-proband) entered as an independent variable. The proportion of epithelial cells was entered as a covariate, but we did not use age and sex as covariates because they were identical between groups.

Second, to confirm the reproducibility of the probes from the MZ twin discordant pair analysis in the case-control analysis, we examined the subset probes threshold set at $P < 5.0E-05$. DNA methylation at each CpG probe was entered as a dependent variable, and each group (case or control) as an independent variable. Age, sex, FSIQ, the proportion of epithelial cells, chip, and row for batch effect adjustments as explained previously, were entered as covariates, and results were threshold at false discovery rate (FDR) <0.05 by Benjamini-Hochberg.

Third, regional differences in gray matter volume (GMV) between groups were analyzed in SPM 12 using two-sample *t*-test models. Potential confounding effects of age, sex, FSIQ, scanner, and total GMV were modeled, and their attributed variances excluded from further analysis. Total GMV was calculated from the GM images obtained from pre-processing segmentation using the "Tissue Volumes" utility from the batching system in SPM12. A GM majority optimal threshold mask, created based on a study-specific sample, was applied to the analyses to eliminate voxels of non-GM for GMV-analyses (Ridgway et al., 2009). The resulting set of voxel values used for comparison generated a statistical parametric map of the t-statistic SPM{t} that was transformed to a unit normal distribution (SPM{Z}). The statistical threshold was set at $P < 0.001$ at the voxel level and $P < 0.05$, with a family wise error (FWE) correction for multiple comparisons. The anatomical localization of significant clusters was investigated using automated anatomical labeling and Brodmann area atlases implemented in the MRIcron software package (Rorden et al., 2007).

Finally, to further examine whether the ADHD-related GMV alterations were associated with DNA methylation, a correlation analysis for the residuals of each β value (methylation, GMV) controlled by control variables was performed. To this end, the adjusted eigenvariates, representing linearly transformed estimates of GMV, were extracted from the identified cluster. The significance level was set at $P < 0.05$. All statistical analyses were performed with R 3.6.3 (R Core Team, 2020), SPM 12, IBM SPSS Statistics for Windows version 26.0. (Armonk, NY: IBM Corp.).

Meta-Analytic Decoding of Regional Function Using NeuroSynth

The functional properties of structural regions with alterations between groups were decoded using a large-scale database-informed meta-analytic approach as implemented in NeuroSynth (Yarkoni et al., 2011). A meta-analytic map associated with the identified region coordinates was derived. Further, the terms (excluding terms for brain regions) ranked by the z-score were visualized using an online word cloud generator[3].

RESULTS

Clinical Status in Monozygotic Twin Discordant Pairs

The clinical status of the MZ twin discordant pairs is shown in **Table 1**. First, regarding IQ, both pairs of children with ADHD were in the 25–75 percentile range, and no significant defects in cognitive ability were observed. Next, regarding ADHD symptoms, the inattentiveness score was >90th percentile in both ADHD children, and <75th percentile in both control children, suggesting that the inattention symptoms were significantly stronger in children with ADHD. The hyperactive/impulsive score was <50th percentile in both ADHD and control children, suggesting that there were no significant hyperactivity symptoms.

Methylation Array Data Analysis of Monozygotic Twin Discordant Pairs

No CpG probes were detected above the genome-wide significance level under the number of EPIC array probes ($P < 9.0E-08$) (Tsai and Bell, 2015; Saffari et al., 2018) as a natural consequence of the extremely small sample size. We then threshold at $P < 5.0E-05$ ($-\log(P) = 4.3$) by visual inspection of the Q-Q plot because the top probes over the threshold had residuals that steeply deviated from the expected line (**Supplementary Figure 1**). Sixty-one probes were above the threshold (**Table 2** and **Supplementary Figure 2**), which were

[3]https://www.wordclouds.com

TABLE 1 | Clinical status between monozygotic twin discordant pairs.

	Pair 1		Pair 2	
	ADHD	**Control**	**ADHD**	**Control**
Full Scale IQ (percentile)	109 (73)	–	97 (42)	–
ADHD Rating Scale-IV				
Inattentive score (percentile)	16 (94–95)	6 (50–75)	12 (92–93)	3 (50)
Hyperactive/impulsive score (percentile)	3 (25)	0 (1)	1 (25–50)	0 (1)

IQ, intelligence quotient; ADHD, attention-deficit hyperactivity disorder.

TABLE 2 | Top 61 differentially methylated CpG sites identified in ADHD-discordant monozygotic twin pairs, ranked by statistical significance and mean Δβ (calculated as DNA methylation level of control twin minus ADHD twin).

Rank	Probe ID	Gene	Chromosome	Position	Mean Δβ	*P*-value
1	cg19181132	*LRIG3*	12	59314527	0.0059	2.95E-07
2	cg00416255		15	58013677	−0.0021	7.39E-07
3	cg25395120	*KANSL1*	17	44111045	−0.0112	8.95E-07
4	cg04850211	*OBSCN*	1	228464232	0.0002	9.05E-07
5	cg02322229	*SYNE2;MIR548AZ*	14	64669716	−0.0097	1.74E-06
6	cg05803913	*MID1IP1*	X	38664442	0.0438	2.64E-06
7	cg24088250		17	75252179	0.0316	2.76E-06
8	cg03220187	*RFWD3*	16	74700945	0.0018	3.13E-06
9	cg26160626		7	155264300	−0.0055	4.68E-06
10	cg24972947	*ZNRF1*	16	75096111	−0.0248	5.83E-06
11	cg04430024	*MICAL1*	6	109778491	0.0769	6.04E-06
12	cg19670431	*SORCS2*	4	7436874	0.0454	6.77E-06
13	cg08676438	*ONECUT3*	19	1763695	0.0198	6.87E-06
14	cg23148094	*PNLIPRP1*	10	118350608	−0.0118	7.31E-06
15	cg26360087	*DCAKD*	17	43128925	0.0020	8.71E-06
16	cg06052716		7	1280607	0.0592	1.05E-05
17	cg10449882	*TMTC1*	12	29936815	−0.0043	1.08E-05
18	cg03700121	*CCDC86*	11	60610004	0.0192	1.13E-05
19	cg22641072	*CARD14*	17	78143724	0.0933	1.18E-05
20	cg09154309		2	170963987	−0.0068	1.21E-05
21	cg06111526	*ATF6B*	6	32086782	0.0062	1.33E-05
22	cg06385383	*CAND1.11*	11	10404199	0.0357	1.39E-05
23	cg05833251	*NGDN*	14	23938784	0.0048	1.54E-05
24	cg02860602		12	103356060	0.0017	1.63E-05
25	cg16524139	*TCF3*	19	1651573	0.0062	2.22E-05
26	cg03195600	*SOCS1*	16	11350371	0.0594	2.24E-05
27	cg13304638	*TBCD*	17	80834089	0.0013	2.26E-05
28	cg18007455	*LARGE*	22	34257627	0.0112	2.36E-05
29	cg03832293	*USP10*	16	84780698	−0.0124	2.48E-05
30	cg26436583	*PSTPIP2*	18	43649176	0.0148	2.70E-05
31	cg12326749	*SLC25A27*	6	46645430	−0.0066	2.94E-05
32	cg12109797		8	86414553	0.0099	3.07E-05
33	cg15451698		1	111257101	0.0179	3.25E-05
34	cg23098235	*HOXB3*	17	46634466	0.0265	3.27E-05
35	cg18430990	*TMEM240*	1	1475941	0.0068	3.28E-05
36	cg08833670	*ROBO3*	11	124746754	0.0197	3.40E-05
37	cg26486111		16	79646944	0.0009	3.40E-05
38	cg16475887	*MAPKBP1*	15	42102305	−0.0106	3.41E-05
39	cg08254353	*TMEM98*	17	31254670	0.0036	3.75E-05
40	cg17547033	*FMNL2*	2	153362087	−0.0272	3.76E-05
41	cg12507363	*DTNA*	18	32307046	−0.0346	3.78E-05
42	cg00411843		X	139584448	−0.0004	3.79E-05
43	cg25019889	*C1orf146*	1	92696685	−0.0113	3.82E-05
44	cg01980222	*TREM2*	6	41130917	0.0066	3.85E-05
45	cg02753619	*FBXW9*	19	12807497	0.0012	3.87E-05
46	cg07425090	*SYNCRIP*	6	86353447	0.0055	4.07E-05
47	cg09973105	*RNF175*	4	154681532	0.0252	4.27E-05
48	cg00966255		16	10479562	−0.0096	4.29E-05
49	cg13390059		1	88261783	−0.0277	4.40E-05
50	cg12437809	*FMO2*	1	171153544	−0.0038	4.56E-05
51	cg00025405		5	2135863	−0.0305	4.58E-05

(Continued)

TABLE 2 | (Continued)

Rank	Probe ID	Gene	Chromosome	Position	Mean Δβ	*P*-value
52	cg18265326		16	65635738	0.0499	4.59E-05
53	cg20305576	*FLT1*	13	28968481	−0.0123	4.62E-05
54	cg08973053		8	120400084	−0.0073	4.65E-05
55	cg14028653	*CDH4*	20	60448776	−0.0081	4.67E-05
56	cg05600626	*CCDC116*	22	21991401	−0.0142	4.78E-05
57	cg25259707	*SNAPIN*	1	153630934	0.1102	4.82E-05
58	cg11476326		7	139245575	−0.0041	4.88E-05
59	cg19269246		2	42325942	0.0327	4.92E-05
60	cg19851976	*CRTC1*	19	18812192	0.0262	4.92E-05
61	cg12810354	*GABRA4*	4	46996987	−0.0028	4.93E-05

ADHD, attention-deficit hyperactivity disorder.

TABLE 3 | Demographic and clinical characteristics of ADHD and control groups.

	ADHD (*n* = 18)	Controls (*n* = 62)	Statistics	*P*-value
Age (years), *Mean* (*SD*)	10.00 (1.61)	13.93 (2.69)	$t(78) = 5.88$	<0.001
Gender, *n* (male/female)	15/3	40/22	$\chi^2(1) = 2.30$	0.129
Handedness, *n* (right/left)	16/2	58/4	$\chi^2(1) = 0.44$	0.509
Full Scale IQ, *Mean* (*SD*)	98.11 (11.66)	106.98 (10.64)	$t(78) = 3.05$	0.003
CBCL Total[a], *Mean* (*SD*)	69.06 (7.02)	47.93 (8.34)	$t(44) = -8.90$	<0.001
SDQ Total[b], *Mean* (*SD*)	–	6.62 (4.28)		
SNAP-IV				
Inattention, *Mean* (*SD*)	16.16 (4.87)	–		
Hyperactivity/impulsivity, *Mean* (*SD*)	9.76 (5.21)	–		
Opposition/Defiance, *Mean* (*SD*)	7.76 (5.15)	–		
Epithelial Cells (%), *Mean* (*SD*)	28.47 (10.57)	28.63 (13.26)	$t(78) = 0.40$	0.961
Total GMV (ml), *Mean* (*SD*)	847.37 (48.94)	829.90 (74.70)	$t(78) = 1.08$	0.353
Total WMV (ml), *Mean* (*SD*)	378.93 (40.26)	392.04 (46.67)	$t(78) = -0.15$	0.283
Total Brain volume (ml), *Mean* (*SD*)	1226.30 (80.14)	1221.94 (133.16)	$t(78) = 0.05$	0.879

ADHD, attention-deficit hyperactivity disorder; IQ, intelligence quotient; CBCL, Child Behavior Checklist; SDQ, Strength and Difficulties Questionnaire; SNAP-IV, Swanson, Nolan, and Pelham questionnaire GMV, gray matter volume; WMV, white matter volume.
[a]*Data for the control group was obtained only for Cohort 1 (n = 28).*
[b]*Data obtained only from the control group of Cohort 2 (n = 34).*

confirmed to be associated with ADHD in an independent case-control dataset.

Demographic and Questionnaire Data in the Case-Control Study

The ADHD and control groups were matched for sex and handedness, but there was a significant difference in age between groups ($T(78) = 5.88$, $P < 0.001$). A two-sample *t*-test was used to compare the total FSIQ and CBCL total scores between groups. Compared to the control group, the ADHD group showed lower FSIQ ($T(78) = 3.05$, $P = 0.003$) and higher levels of ADHD-related emotional and behavioral problems (CBCL total, $T(44) = -8.90$, $P < 0.001$), although data for CBCL was only available from Cohort 1. In addition, in the control group of Cohort 2, SDQ total scores were not significantly different from the mean of standard Japanese children using one-sample *t*-test (SDQ total, $T(33) = 0.47$, $P = 0.641$), suggesting no notable emotional and behavioral problems. Multiple regression analysis was also performed to examine the effect of age on the differences in FSIQ and CBCL total score between groups, with each variable as the dependent variable; the results showed that the effect of group was significant (FSIQ: $\beta = -0.38$, $T = -2.96$, $P = 0.004$; CBCL total: $\beta = 0.93$, $T = 5.95$, $P < 0.001$) while that of age was not (FSIQ: $\beta = -0.10$, $T = -0.77$, $P = 0.445$; CBCL total: $\beta = 0.16$, $T = 0.99$, $P = 0.326$). Regarding ADHD symptoms, the inattention score of SNAP-IV in the ADHD group showed clinically mild symptoms on average, and the hyperactivity/impulsivity and opposition/defiance scores did not reach clinically significant levels. Since the ratio of epithelial cells in saliva samples affects the estimated methylation level (β value), we analyzed for the difference between groups finding no significant difference between the ADHD and control groups. We also estimated GMV, WMV, and total brain volume in the ADHD and control groups, respectively, but found no differences between groups in any of these parameters (**Table 3**).

Case-Control Subset Methylation Analysis

We extracted the top 61 probes from the initial analysis, among which 60 probes meeting the quality control criteria were

included in the case-control dataset. Among these 60 probes, three probes (cg03700121, cg18430990, and cg19670431) in the coiled-coil domain containing 86 (*CCDC86*), transmembrane protein 240 (*TMEM240*), and sortilin-related Vps10p domain containing receptor 2 (*SorCS2*) genes were significantly associated with ADHD (FDRs < 0.05, **Table 4**). However, two of these probes (cg03700121 and cg18430990) were inconsistent regarding the direction of the effect, with increased methylation in twin studies and decreased methylation in case-control studies, while only the probe involved in *SorCS2* showed consistent results in both studies. Hence, we used cg19670431 for subsequent epigenetic imaging analyses.

Structural Brain-Image Data in the Case-Control Study

A whole-brain analysis with FWE correction at the cluster level was conducted to examine regional differences in GMV between the two groups (ADHD: $n = 18$, Controls: $n = 62$). Compared with the control group, the ADHD group showed reduced GMV in the left precentral gyrus (BA6; MNI coordinates, $x = -44$, $y = 5$, $z = 57$; cluster size = 437 voxels, $P = 0.043$, FWE corrected cluster level; **Figure 1A**) and the right posterior orbital gyrus (BA47; MNI coordinates, $x = 24$, $y = 21$, $z = -21$; cluster size = 555 voxels, $P = 0.016$, FWE corrected cluster level; **Figure 1B**).

Reverse inference on the functional properties related to the local regions where structural differences between groups were observed showed that most of the terms related to the left precentral gyrus are related to language functions such as semantic memory, working memory, theory of mind, and motion imagination (**Figure 1C**); most of the terms related to the right posterior orbital gyrus are related to–mainly negative–emotional information and their regulation (**Figure 1D**).

Relationship Between Sortilin-Related Vps10p Domain Containing Receptor 2 Methylation and Brain Structural Alterations

Sortilin-related Vps10p domain containing receptor 2 methylation was both positively correlated with GMV within a cluster in the precentral gyrus and the posterior orbital gyrus (**Figures 2A,B**). This result suggests that the more methylated *SorCS2* is, the larger the GMV of the precentral and posterior orbital gyri. In addition, to verify the tissue specificity of the methylation pattern, we examined the brain-saliva correlation for the CpG probe (cg19670431) identified using a web tool based on human samples (Braun et al., 2019) and also confirmed a trend toward a positive correlation ($\rho = 0.37$, $P = 0.09$).

TABLE 4 | Three CpG sites replicated in a sample of ADHD cases vs. controls.

Probe ID	Gene	Chromosome	Position	Mean Δβ	*P*-value (FDR)
cg03700121	*CCDC86*	11	60610004	−0.1208	0.0000015
cg18430990	*TMEM240*	1	1475941	−0.0301	0.0003126
cg19670431	*SORCS2*	4	7436874	0.0230	0.0171530

FDR-adjusted P-values are corrected for multiple comparisons with 60 probes. FDR, false discovery rate.

Relationship Between Clinical Symptom Scores, Sortilin-Related Vps10p Domain Containing Receptor 2 Methylation and Brain Structural Alterations

We performed a correlation analysis investigate the association between the neurobiological basis of both *SorCS2* methylation and local GMV alterations, and clinical symptoms (core symptoms based on SNAP-IV and emotional behavior problems based on CBCL tests) associated with ADHD. As a result, a significant negative correlation was confirmed between *SorCS2* methylation and CBCL total score ($r = -0.444$, $P = 0.002$), while no significant correlation was found with SNAP total score ($r = -0.227$, $P = 0.366$); these scores also showed no correlation with both local GMV alterations. These results suggest that *SorCS2* methylation may be involved in regulating emotional behavioral problems in children rather than ADHD-specific core symptoms.

DISCUSSION

This study investigated the relationship between DNA methylation differences based on array data and brain structure involved variations in the development of ADHD. First, we investigated two pairs of MZ twins discordant for ADHD and identified 61 candidates for DNA methylation sites involved in the development of ADHD. Next, using these candidates in a case-control study we found that children with ADHD had elevated methylation in the *SorCS2* gene body region. Finally, we observed that the ADHD group had significantly reduced GMV in the precentral gyrus and posterior orbital gyrus compared to the control group and that this volume reduction was positively associated with *SorCS2* methylation. In addition, the reduced GMV regions in children with ADHD are involved in language processing and emotional control, and *SorCS2* methylation is also negatively associated with emotional behavioral problems in children. These results indicate that *SorCS2* methylation might mediate a reduced GMV in the precentral and posterior orbital gyri and therefore influence the pathology of children with ADHD.

We suggested that SorCS2 methylation is involved in ADHD through methylation array analysis of MZ twin discordant cases and case-control groups, while previous epigenome-wide studies found no evidence that *SorCS2* methylation is involved in either children or adults with ADHD (van Dongen et al., 2019; Neumann et al., 2020; Rovira et al., 2020). Although SorCS2 is known to play a crucial role in neuronal viability and function (Glerup et al., 2016), human epidemiological studies have reported that single nucleotide polymorphisms in *SorCS2* are associated with the risk of developing psychiatric disorders such as ADHD (Alemany et al., 2015), bipolar disorder (Baum et al., 2008; Ollila et al., 2009), and schizophrenia

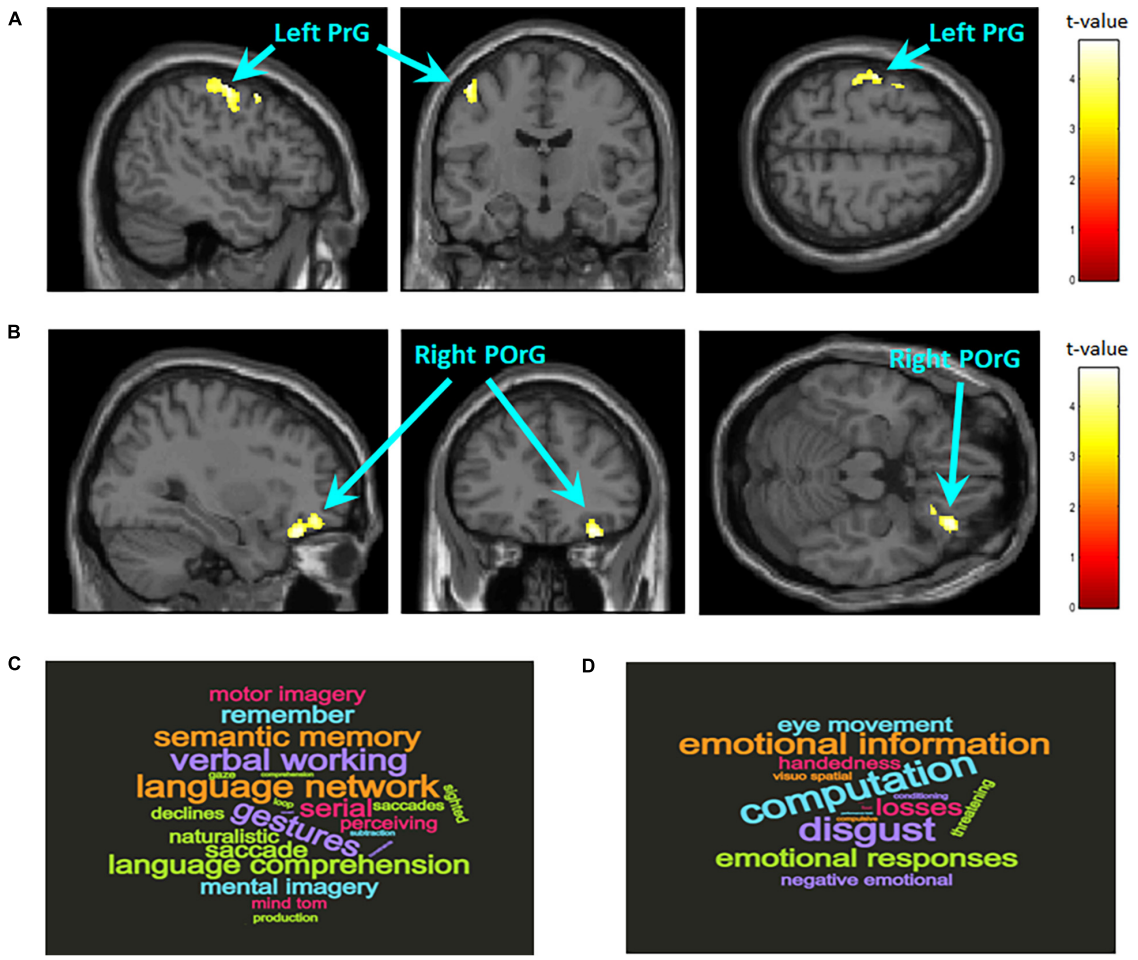

FIGURE 1 | Brain regions with significantly larger gray matter volume in the control group compared to the ADHD group. The statistical threshold for the contrasts was set at voxel-level $P < 0.001$ uncorrected for height and cluster-level $P < 0.05$ family wise error rate corrected for multiple comparisons. The color bar denotes the *t*-statistic range. **(A)** Left precentral gyrus (PrG; BA6; MNI coordinates, $x = -44$, $y = 5$, $z = 57$; cluster size = 437 voxels). **(B)** Right posterior orbital gyrus (POrG; BA47; MNI coordinates, $x = 24$, $y = 21$, $z = -21$; cluster size = 555 voxels). Reverse inference of functional properties in the left PrG **(C)** and right POrG **(D)** as decoded by NeuroSynth. The font size represents the rank according to the strength of the relationship between regions and terms.

(Christoforou et al., 2011). Although recent human genome-wide association studies have suggested that a gene set related to dopamine signaling is involved not only in ADHD alone but also in the comorbidity of ADHD with obesity and narcolepsy (Mota et al., 2020; Takahashi et al., 2020); in animal studies, lack of *SorCS2* reportedly induces ADHD-like behavior by altering the novelty response to psychostimulants and altering the dopaminergic firing pattern of the ventral tegmental area (Olsen et al., 2021). Other recent studies have revealed the significant roles of SorCS2 in brain derived neurotrophic factor (BDNF)-dependent plasticity and for social memory formation by *N*-methyl-D-aspartic (NMDA) receptor trafficking in hippocampal neurons (Glerup et al., 2016; Yang et al., 2021); in parallel, working memory deficits (Martinussen et al., 2005; Sowerby et al., 2011) and the involvement of BDNF or NMDA receptor signaling in ADHD have also been suggested (Bergman et al., 2011; Chang et al., 2014). Taken together, our results suggest that the *SorCS2* gene methylation found in this study may affect the development and certain symptoms of ADHD by affecting dopaminergic, BDNF, and/or NMDA receptor signaling pathways.

Sortilin-related Vps10p domain containing receptor 2 methylation was positively associated with GMV in the precentral and posterior orbital gyri in the ADHD group, suggesting that unmethylated *SorCS2* may lead to lower GMV. These results replicate prior results of surface area reduction in the left precentral and right orbital gyri found in another cohort of children with ADHD (Jung et al., 2019), as well as previous findings of cortical thickness reduction in the precentral gyrus and orbital gyri in a large-scale clinical sample of children (Hoogman et al., 2019). Big data analysis of structural magnetic resonance imaging of about 6,800 children found that the precentral gyrus surface area was one of the prominent local areas negatively associated with ADHD symptoms (Owens et al., 2021). Reverse inference showed that the precentral gyrus was associated with language function,

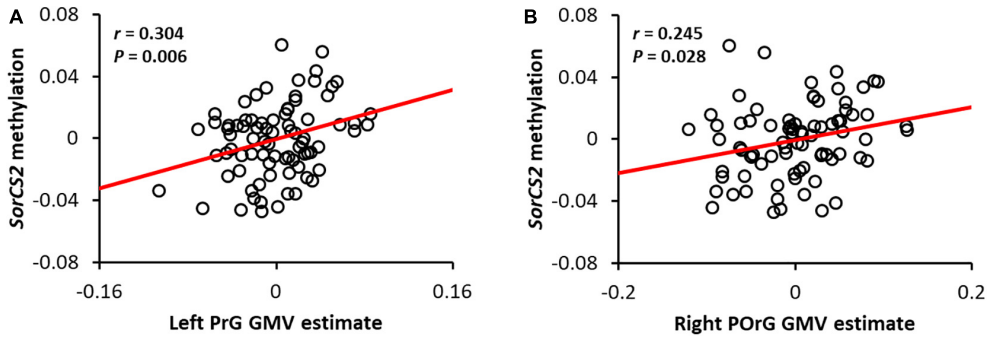

FIGURE 2 | Correlation between *SorCS2* methylation and gray matter volume in the left precentral gyrus **(A)** and the right posterior orbital gyrus **(B)**. The red line shows the regression line. Adjusted residuals with respective covariates were used as values for methylation and local GMV of SorCS2. Note that the adjusted residuals for each covariate were used as estimates of *SorCS2* methylation and local GMV.

and that children with ADHD have a higher risk of language problems (Sowerby et al., 2011; Hawkins et al., 2016; Korrel et al., 2017) which contributes to poor academic functioning (Sciberras et al., 2014). Hence, these findings suggest that *SorCS2* gene methylation may induce language-related difficulties in children with ADHD via reduced GMV in the precentral gyrus. Next, reductions in GMV and cortical thickness in the right orbital gyrus of individuals with ADHD have often been reported (Vaidya, 2012; Hoogman et al., 2019; Jung et al., 2019). Although the function of the orbital gyri appears related to emotional information and calculations, emotional information may play an important role in decision-making and executive function (Bechara et al., 2000; Rolls and Grabenhorst, 2008). Numerous imaging studies using emotional and executive function tasks have reported reduced functional activation in the right orbital gyrus (Epstein et al., 2007; Rubia et al., 2009; Cubillo et al., 2012; Godinez et al., 2015). Taken together, these findings suggest that *SorCS2* gene methylation may induce both reduced GMV in the orbital gyrus and emotional behavioral problems, although the direct association between the two could not be confirmed in this study.

Several limitations of the present study should be noted and taken into consideration for future studies. First, the sample size in this study was relatively small, including only two pairs of discordant MZ twins and 18 subjects in the ADHD group in the case-control study. In particular, the CpG sites identified in the array analysis of MZ twin discordant cases did not reach genome-wide significance level due to the small sample size; we only selected the top candidates based on their statistics. Although it is necessary to replicate the results with a larger sample size, it was particularly difficult to recruit MZ twins discordant by a single institution. Next, because we analyzed salivary DNA methylation, our data may not necessarily reflect the state of the brain due to the tissue specificity of methylation patterns (Smith et al., 2015). Regarding the tissue specificity of DNA methylation, although we tried to validate our results using a web tool that can investigate the correlation between methylation of brain, blood, saliva, and buccal cells collected from the same living human (Braun et al., 2019), another way to overcome the issue of tissue specificity is to directly examine the association between the methylation profile of *SorCS2* and the precentral or posterior orbital gyri in the postmortem brains of children with ADHD. Finally, in the case-control study, the children's age and cognitive abilities did not match and the batches for array analysis and the MR scanners for brain imaging were confounding between groups because we used two existing cohorts as control group. Although these factors were used as control variables in the statistical analysis, it made it difficult to distinguish whether the association between *SorCS2* methylation and local GMV reduction was involved in the pathophysiology of ADHD or derived from demographic factors such as age and general cognitive abilities or research artifacts by batch and scanner effects. Although no significant difference was observed between the two groups in age-sensitive brain volume, there was a significant difference in emotional behavioral problems even after controlling for age, thus, future studies need to match age and cognitive abilities and exclude batch and scanner effects. Despite these limitations, this study sheds light on the some of the pathological mechanisms of ADHD in that it suggests DNA methylation candidates associated with brain structure specific to children with ADHD.

In conclusion, this study suggests that DNA methylation of the *SorCS2* gene may induce language-related and emotional behavioral problems via brain structure alterations specific to children with ADHD. Some pharmacological or psychosocial interventions that enhance *SorCS2* gene methylation may improve ADHD symptoms by interfering with the GMV reduction in the precentral and posterior orbital gyri. In the future, the elucidation of the molecular mechanism of local brain volume changes induced by *SorCS2* methylation will be useful for understanding the pathophysiology of ADHD.

DATA AVAILABILITY STATEMENT

The DNA methylation microarray data of monozygotic twins discordant samples have been deposited in the Gene Expression Omnibus database (GEO) with the primary accession code GSE186339 (https://www.ncbi.nlm.nih.gov/geo/query/acc.cgi?acc=GSE186339). Other data that support the results of this

study are included in the article/**Supplementary Material**, further inquiries can be directed to the corresponding author.

ETHICS STATEMENT

The study protocol was approved by the Research Ethics Committee of the University of Fukui, Japan, and all procedures were conducted in accordance with the Declaration of Helsinki and the Ethical Guidelines for Clinical Studies of the Ministry of Health, Labour, and Welfare of Japan. All parents provided written informed consent for participation in the study.

AUTHOR CONTRIBUTIONS

TF, SN, and AT contributed to the conception and design of the study, performed the experiments and statistical data analysis, and wrote the first draft of the manuscript. KM, AY, ST, SH, KS, HO, and HM contributed substantially to performing the experiments and collecting the data, revised the manuscript critically for intellectual content, and approved the submitted version. All authors contributed to the article and approved the submitted version.

FUNDING

This work was supported by JSPS KAKENHI grant numbers JP19K21755, JP19H00617 (to AT), JP18K02480, JP20H04995 (to TF), and AMED under grant number JP20gk0110052 (to AT). The funders had no role in the study design, data collection and analysis, decision to publish, or preparation of the manuscript.

SUPPLEMENTARY MATERIAL

The Supplementary Material for this article can be found online at: https://www.frontiersin.org/articles/10.3389/fnins.2021.799761/full#supplementary-material

REFERENCES

Achenbach, T. M., and Rescorla, L. A. (2001). *Manual for the ASEBA School-Age Forms & Profiles*. Burlington, VT: University of Vermont, Research Center for Children, Youth, & Families.

Alemany, S., Ribasés, M., Vilor-Tejedor, N., Bustamante, M., Sánchez-Mora, C., Bosch, R., et al. (2015). New suggestive genetic loci and biological pathways for attention function in adult attention-deficit/hyperactivity disorder. *Am. J. Med. Genet. B Neuropsychiatr. Genet.* 168, 459–470. doi: 10.1002/ajmg.b.32341

American Psychiatric Association (2013). *Diagnostic and Statistical Manual of Mental Disorders, Fifth Edition (DSM-5)*. Washington, DC: American Psychiatric Association.

Ashburner, J. (2007). A fast diffeomorphic image registration algorithm. *Neuroimage* 38, 95–113. doi: 10.1016/j.neuroimage.2007.07.007

Barfield, R. T., Kilaru, V., Smith, A. K., and Conneely, K. N. (2012). CpGassoc: an R function for analysis of DNA methylation microarray data. *Bioinformatics* 28, 1280–1281. doi: 10.1093/bioinformatics/bts124

Baum, A. E., Akula, N., Cabanero, M., Cardona, I., Corona, W., Klemens, B., et al. (2008). A genome-wide association study implicates diacylglycerol kinase eta (DGKH) and several other genes in the etiology of bipolar disorder. *Mol. Psychiatry* 13, 197–207. doi: 10.1038/sj.mp.4002012

Bechara, A., Damasio, H., and Damasio, A. R. (2000). Emotion, decision making and the orbitofrontal cortex. *Cereb Cortex* 10, 295–307. doi: 10.1093/cercor/10.3.295

Bell, J. T., and Spector, T. D. (2011). A twin approach to unraveling epigenetics. *Trends Genet.* 27, 116–125.

Bergman, O., Westberg, L., Lichtenstein, P., Eriksson, E., and Larsson, H. (2011). Study on the possible association of brain-derived neurotrophic factor polymorphism with the developmental course of symptoms of attention deficit and hyperactivity. *Int. J. Neuropsychopharmacol.* 14, 1367–1376. doi: 10.1017/S1461145711000502

Biederman, J., Faraone, S. V., Spencer, T., Wilens, T., Norman, D., Lapey, K. A., et al. (1993). Patterns of psychiatric comorbidity, cognition, and psychosocial functioning in adults with attention deficit hyperactivity disorder. *Am. J. Psychiatry* 150, 1792–1798. doi: 10.1176/ajp.150.12.1792

Biederman, J., Mick, E., Surman, C., Doyle, R., Hammerness, P., Harpold, T., et al. (2006). A randomized, placebo-controlled trial of OROS methylphenidate in adults with attention-deficit/hyperactivity disorder. *Biol. Psychiatry* 59, 829–835. doi: 10.1016/j.biopsych.2005.09.011

Biederman, J., Newcorn, J., and Sprich, S. (1991). Comorbidity of attention deficit hyperactivity disorder with conduct, depressive, anxiety, and other disorders. *Am. J. Psychiatry* 148, 564–577. doi: 10.1176/ajp.148.5.564

Braun, P. R., Han, S., Hing, B., Nagahama, Y., Gaul, L. N., Heinzman, J. T., et al. (2019). Genome-wide DNA methylation comparison between live human brain and peripheral tissues within individuals. *Transl. Psychiatry* 9:47. doi: 10.1038/s41398-019-0376-y

Chang, J. P., Lane, H. Y., and Tsai, G. E. (2014). Attention deficit hyperactivity disorder and N-methyl-D-aspartate (NMDA) dysregulation. *Curr. Pharm. Des.* 20, 5180–5185. doi: 10.2174/1381612819666140110115227

Chen, Y. C., Sudre, G., Sharp, W., Donovan, F., Chandrasekharappa, S. C., Hansen, N., et al. (2018). Neuroanatomic, epigenetic and genetic differences in monozygotic twins discordant for attention deficit hyperactivity disorder. *Mol. Psychiatry*. 23, 683–690. doi: 10.1038/mp.2017.45

Christoforou, A., McGhee, K. A., Morris, S. W., Thomson, P. A., Anderson, S., McLean, A., et al. (2011). Convergence of linkage, association and GWAS findings for a candidate region for bipolar disorder and schizophrenia on chromosome 4p. *Mol. Psychiatry* 16, 240–242. doi: 10.1038/mp.2010.25

Cubillo, A., Halari, R., Smith, A., Taylor, E., and Rubia, K. (2012). A review of fronto-striatal and fronto-cortical brain abnormalities in children and adults with Attention Deficit Hyperactivity Disorder (ADHD) and new evidence for dysfunction in adults with ADHD during motivation and attention. *Cortex* 48, 194–215. doi: 10.1016/j.cortex.2011.04.007

Dadds, M. R., Schollar-Root, O., Lenroot, R., Moul, C., and Hawes, D. J. (2016). Epigenetic regulation of the DRD4 gene and dimensions of attention-deficit/hyperactivity disorder in children. *Eur. Child Adolesc. Psychiatry* 25, 1081–1089.

DuPaul, G. J., Power, T. J., Anastopoulos, A. D., and Reid, R. (1998). *ADHD Rating Scale-IV: Checklists, Norms, and Clinical Interpretation*. New York, NY: Guilford Press.

Epstein, J. N., Casey, B. J., Tonev, S. T., Davidson, M. C., Reiss, A. L., Garrett, A., et al. (2007). ADHD- and medication-related brain activation effects in concordantly affected parent-child dyads with ADHD. *J. Child Psychol. Psychiatry* 48, 899–913. doi: 10.1111/j.1469-7610.2007.01761.x

Glerup, S., Bolcho, U., Mølgaard, S., Bøggild, S., Vaegter, C. B., Smith, A. H., et al. (2016). SorCS2 is required for BDNF-dependent plasticity in the hippocampus. *Mol. Psychiatry* 21, 1740–1751. doi: 10.1038/mp.2016.108

Godinez, D. A., Willcutt, E. G., Burgess, G. C., Depue, B. E., Andrews-Hanna, J. R., and Banich, M. T. (2015). Familial risk and ADHD-specific neural activity revealed by case-control, discordant twin pair design. *Psychiatry Res.* 233, 458–465. doi: 10.1016/j.pscychresns.2015.07.019

Goodman, R. (1997). The strengths and difficulties questionnaire: a research note. *J. Child Psychol. Psychiatry* 38, 581–586. doi: 10.1111/j.1469-7610.1997.tb01545.x

Hawkins, E., Gathercole, S., Astle, D., The Calm Team, and Holmes, J. (2016). Language problems and ADHD symptoms: how specific are the links? *Brain Sci*. 6:50. doi: 10.3390/brainsci6040050

Heinrich, H., Grunitz, J., Stonawski, V., Frey, S., Wahl, S., Albrecht, B., et al. (2017). Attention, cognitive control and motivation in ADHD: Linking event-related brain potentials and DNA methylation patterns in boys at early school age. *Sci. Rep*. 7:3823. doi: 10.1038/s41598-017-03326-3

Heiss, J. A., and Just, A. C. (2018). Identifying mislabeled and contaminated DNA methylation microarray data: an extended quality control toolset with examples from GEO. *Clin. Epigen.* 10:73. doi: 10.1186/s13148-018-0504-1

Henikoff, S., and Matzke, M. A. (1997). Exploring and explaining epigenetic effects. *Trends Genet.* 13, 293–295.

Hoogman, M., Muetzel, R., Guimaraes, J. P., Shumskaya, E., Mennes, M., Zwiers, M. P., et al. (2019). Brain imaging of the cortex in ADHD: a coordinated analysis of large-scale clinical and population-based samples. *Am. J. Psychiatry* 176, 531–542. doi: 10.1176/appi.ajp.2019.18091033

Johnson, W. E., Li, C., and Rabinovic, A. (2007). Adjusting batch effects in microarray expression data using empirical Bayes methods. *Biostatistics* 8, 118–127. doi: 10.1093/biostatistics/kxj037

Jung, M., Mizuno, Y., Fujisawa, T. X., Takiguchi, S., Kong, J., Kosaka, H., et al. (2019). The effects of COMT polymorphism on cortical thickness and surface area abnormalities in children with ADHD. *Cereb Cortex*. 29, 3902–3911. doi: 10.1093/cercor/bhy269

Kaminsky, Z. A., Tang, T., Wang, S. C., Ptak, C., Oh, G. H., Wong, A. H., et al. (2009). DNA methylation profiles in monozygotic and dizygotic twins. *Nat. Genet*. 41, 240–245. doi: 10.1038/ng.286

Korrel, H., Mueller, K. L., Silk, T., Anderson, V., and Sciberras, E. (2017). Research Review: language problems in children with attention-deficit hyperactivity disorder – a systematic meta-analytic review. *J. Child Psychol. Psychiatry* 58, 640–654. doi: 10.1111/jcpp.12688

Kuratomi, G., Iwamoto, K., Bundo, M., Kusumi, I., Kato, N., Iwata, N., et al. (2008). Aberrant DNA methylation associated with bipolar disorder identified from discordant monozygotic twins. *Mol. Psychiatry* 13, 429–441. doi: 10.1038/sj.mp.4002001

Larsson, H., Chang, Z., D'Onofrio, B. M., and Lichtenstein, P. (2014). The heritability of clinically diagnosed attention deficit hyperactivity disorder across the lifespan. *Psychol. Med*. 44, 2223–2229. doi: 10.1017/S0033291713002493

Malki, K., Koritskaya, E., Harris, F., Bryson, K., Herbster, M., and Tosto, M. G. (2016). Epigenetic differences in monozygotic twins discordant for major depressive disorder. *Transl. Psychiatry*. 6:e839. doi: 10.1038/tp.2016.101

Martinussen, R., Hayden, J., Hogg-Johnson, S., and Tannock, R. (2005). A meta-analysis of working memory impairments in children with attention-deficit/hyperactivity disorder. *J. Am. Acad. Child Adolesc. Psychiatry*. 44, 377–384. doi: 10.1097/01.chi.0000153228.72591.73

Molina, B., Hinshaw, S. P., Swanson, J. M., Arnold, L. E., Vitiello, B., Jensen, P. S., et al. (2009). The MTA at 8 years: prospective follow-up of children treated for combined-type ADHD in a multisite study. *J. Am. Acad. Child Adolesc. Psychiatry*. 48, 484–500. doi: 10.1097/CHI.0b013e31819c23d0

Mota, N. R., Poelmans, G., Klein, M., Torrico, B., Fernàndez-Castillo, N., Cormand, B., et al. (2020). Cross-disorder genetic analyses implicate dopaminergic signaling as a biological link between Attention-Deficit/Hyperactivity Disorder and obesity measures. *Neuropsychopharmacology* 45, 1188–1195. doi: 10.1038/s41386-019-0592-4

Neumann, A., Walton, E., Alemany, S., Cecil, C., González, J. R., Jima, D. D., et al. (2020). Association between DNA methylation and ADHD symptoms from birth to school age: a prospective meta-analysis. *Transl. Psychiatry* 10:398. doi: 10.1038/s41398-020-01058-z

Nygaard, V., Rødland, E. A., and Hovig, E. (2016). Methods that remove batch effects while retaining group differences may lead to exaggerated confidence in downstream analyses. *Biostatistics* 17, 29–39. doi: 10.1093/biostatistics/kxv027

Ollila, H. M., Soronen, P., Silander, K., Palo, O. M., Kieseppä, T., Kaunisto, M. A., et al. (2009). Findings from bipolar disorder genome-wide association studies replicate in a Finnish bipolar family-cohort. *Mol. Psychiatry* 14, 351–353. doi: 10.1038/mp.2008.122

Olsen, D., Wellner, N., Kaas, M., de Jong, I., Sotty, F., Didriksen, M., et al. (2021). Altered dopaminergic firing pattern and novelty response underlie ADHD-like behavior of SorCS2-deficient mice. *Transl. Psychiatry* 11:74. doi: 10.1038/s41398-021-01199-9

Orvaschel, H., and Puig-Antich, J. (1994). *Schedule for Affective Disorders and Schizophrenia for School-Age Children—Epidemiologic version (K-SADS-E), Fifth Edition*. Fort Lauderdale, FL: Nova Southeastern University.

Owens, M. M., Allgaier, N., Hahn, S., Yuan, D., Albaugh, M., Adise, S., et al. (2021). Multimethod investigation of the neurobiological basis of ADHD symptomatology in children aged 9-10: baseline data from the ABCD study. *Transl. Psychiatry* 11:64. doi: 10.1038/s41398-020-01192-8

Park, S., Lee, J. M., Kim, J. W., Cho, D. Y., Yun, H. J., Han, D. H., et al. (2015). Associations between serotonin transporter gene (SLC6A4) methylation and clinical characteristics and cortical thickness in children with ADHD. *Psychol. Med*. 45, 3009–3017. doi: 10.1017/S003329171500094X

Price, E. M., and Robinson, W. P. (2018). Adjusting for batch effects in DNA methylation microarray data, a lesson learned. *Front. Genet*. 9:83. doi: 10.3389/fgene.2018.00083

Ratanatharathorn, A., Boks, M. P., Maihofer, A. X., Aiello, A. E., Amstadter, A. B., Ashley-Koch, A. E., et al. (2017). Epigenome-wide association of PTSD from heterogeneous cohorts with a common multi-site analysis pipeline. *Am. J. Med. Genet. B Neuropsychiatr. Genet*. 174, 619–630. doi: 10.1002/ajmg.b.32568

R Core Team. (2017). *R: A Language and Environment for Statistical Computing*. Vienna: R Foundation for Statistical Computing. Available online at: https://www.R-project.org/

Ridgway, G. R., Omar, R., Ourselin, S., Hill, D. L. G., Warren, J. D., and Fox, N. C. (2009). Issues with threshold masking in voxel-based morphometry of atrophied brains. *Neuroimage* 44, 99–111. doi: 10.1016/j.neuroimage.2008.08.045

Rolls, E. T., and Grabenhorst, F. (2008). The orbitofrontal cortex and beyond: from affect to decision-making. *Prog. Neurobiol*. 86, 216–244. doi: 10.1016/j.pneurobio.2008.09.001

Rorden, C., Karnath, H.-O., and Bonilha, L. (2007). Improving lesion-symptom mapping. *J. Cogn. Neurosci.* 19, 1081–1088. doi: 10.1162/jocn.2007.19.7.1081

Rovira, P., Sánchez-Mora, C., Pagerols, M., Richarte, V., Corrales, M., Fadeuilhe, C., et al. (2020). Epigenome-wide association study of attention-deficit/hyperactivity disorder in adults. *Transl. Psychiatry* 10:199. doi: 10.1038/s41398-020-0860-4

Rubia, K. (2018). Cognitive neuroscience of attention deficit hyperactivity disorder (ADHD) and its clinical translation. *Front. Hum. Neurosci*. 12:100. doi: 10.3389/fnhum.2018.00100

Rubia, K., Halari, R., Christakou, A., and Taylor, E. (2009). Impulsiveness as a timing disturbance: neurocognitive abnormalities in attention-deficit hyperactivity disorder during temporal processes and normalization with methylphenidate. *Philos. Trans. R. Soc. Lond. B Biol. Sci*. 364, 1919–1931. doi: 10.1098/rstb.2009.0014

Saffari, A., Silver, M. J., Zavattari, P., Moi, L., Columbano, A., Meaburn, E. L., et al. (2018). Estimation of a significance threshold for epigenome-wide association studies. *Genet. Epidemiol*. 42, 20–33. doi: 10.1002/gepi.22086

Sciberras, E., Mueller, K. L., Efron, D., Bisset, M., Anderson, V., Schilpzand, E. J., et al. (2014). Language problems in children with ADHD: a community-based study. *Pediatrics* 133, 793–800. doi: 10.1542/peds.2013-3355

Sengupta, S. M., Smith, A. K., Grizenko, N., and Joober, R. (2017). Locus-specific DNA methylation changes and phenotypic variability in children with attention-deficit hyperactivity disorder. *Psychiatry Res*. 256, 298–304. doi: 10.1016/j.psychres.2017.06.048

Sheehan, D. V., Sheehan, K. H., Shytle, R. D., Janavs, J., Bannon, Y., Rogers, J. E., et al. (2010). Reliability and validity of the mini international neuropsychiatric interview for children and adolescents (MINI-KID). *J. Clin. Psychiatry* 71, 313–326. doi: 10.4088/JCP.09m05305whi

Smith, A. K., Kilaru, V., Klengel, T., Mercer, K. B., Bradley, B., Conneely, K. N., et al. (2015). DNA extracted from saliva for methylation studies of psychiatric traits: evidence tissue specificity and relatedness to brain. *Am. J. Med. Genet. B Neuropsychiatr. Genet*. 168B, 36–44. doi: 10.1002/ajmg.b.32278

Smith, A. K., Kilaru, V., Kocak, M., Almli, L. M., Mercer, K. B., Ressler, K. J., et al. (2014). Methylation quantitative trait loci (meQTLs) are consistently detected across ancestry, developmental stage, and tissue type. *BMC Genom*. 15:145. doi: 10.1186/1471-2164-15-145

Sonuga-Barke, E., Bitsakou, P., and Thompson, M. (2010). Beyond the dual pathway model: evidence for the dissociation of timing, inhibitory, and

delay-related impairments in attention-deficit/hyperactivity disorder. *J. Am. Acad. Child Adolesc. Psychiatry* 49, 345–355. doi: 10.1016/j.jaac.2009.12.018

Sowerby, P., Seal, S., and Tripp, G. (2011). Working memory deficits in ADHD: the contribution of age, learning/language difficulties, and task parameters. *J. Atten. Disord.* 15, 461–472. doi: 10.1177/1087054710370674

Sugawara, H., Iwamoto, K., Bundo, M., Ueda, J., Miyauchi, T., Komori, A., et al. (2011). Hypermethylation of serotonin transporter gene in bipolar disorder detected by epigenome analysis of discordant monozygotic twins. *Transl. Psychiatry*. 1:e24. doi: 10.1038/tp.2011.26

Swanson, J. M. (1992). *School-Based Assessments and Interventions for ADD Students*. Irvine, CA: KC Publishing.

Takahashi, N., Nishimura, T., Harada, T., Okumura, A., Choi, D., Iwabuchi, T., et al. (2020). Polygenic risk score analysis revealed shared genetic background in attention deficit hyperactivity disorder and narcolepsy. *Transl. Psychiatry*. 10:284. doi: 10.1038/s41398-020-00971-7

Takiguchi, S., Fujisawa, T. X., Mizushima, S., Saito, D. N., Okamoto, Y., Shimada, K., et al. (2015). Ventral striatum dysfunction in children and adolescents with reactive attachment disorder: functional (MRI) study. *BJPsych. Open* 1, 121–128. doi: 10.1192/bjpo.bp.115.001586

Teschendorff, A. E., Breeze, C. E., Zheng, S. C., and Beck, S. (2017). A comparison of reference-based algorithms for correcting cell-type heterogeneity in Epigenome-Wide Association Studies. *BMC Bioinformatics* 18:105. doi: 10.1186/s12859-017-1511-5

Teschendorff, A. E., Marabita, F., Lechner, M., Bartlett, T., Tegner, J., Gomez-Cabrero, D., et al. (2013). A beta-mixture quantile normalization method for correcting probe design bias in Illumina Infinium 450 k DNA methylation data. *Bioinformatics* 29, 189–196. doi: 10.1093/bioinformatics/bts680

Thomas, R., Sanders, S., Doust, J., Beller, E., and Glasziou, P. (2015). Prevalence of attention-deficit/hyperactivity disorder: a systematic review and meta-analysis. *Pediatrics* 135, e994–e1001. doi: 10.1542/peds.2014-3482

Tsai, P. C., and Bell, J. T. (2015). Power and sample size estimation for epigenome-wide association scans to detect differential DNA methylation. *Int. J. Epidemiol.* 44, 1429–1441. doi: 10.1093/ije/dyv041

Vaidya, C. J. (2012). Neurodevelopmental abnormalities in ADHD. *Curr. Top. Behav. Neurosci.* 9, 49–66. doi: 10.1007/7854_2011_138

van Dongen, J., Zilhão, N. R., Sugden, K., Bios Consortium, Hannon, E. J., Mill, J., et al. (2019). Epigenome-wide association study of attention-deficit/hyperactivity disorder symptoms in adults. *Biol. Psychiatry* 86, 599–607. doi: 10.1016/j.biopsych.2019.02.016

van Mil, N. H., Steegers-Theunissen, R. P., Bouwland-Both, M. I., Verbiest, M. M., Rijlaarsdam, J., Hofman, A., et al. (2014). DNA methylation profiles at birth and child ADHD symptoms. *J. Psychiatr Res.* 49, 51–59. doi: 10.1016/j.jpsychires.2013.10.017

Wechsler, D. (1997). *Wechsler Adult Intelligence Scale*, 3rd Edn. San Antonio, TX: Psychological Corporation.

Wechsler, D. (2003). *Wechsler Intelligence Scale for Children*, 4th Edn. San Antonio, TX: Psychological Corporation.

Wong, C. C., Meaburn, E. L., Ronald, A., Price, T. S., Jeffries, A. R., Schalkwyk, L. C., et al. (2014). Methylomic analysis of monozygotic twins discordant for autism spectrum disorder and related behavioural traits. *Mol. Psychiatry* 19, 495–503. doi: 10.1038/mp.2013.41

Xu, Y., Chen, X. T., Luo, M., Tang, Y., Zhang, G., Wu, D., et al. (2015). Multiple epigenetic factors predict the attention deficit/hyperactivity disorder among the Chinese Han children. *J. Psychiatr. Res.* 64, 40–50. doi: 10.1016/j.jpsychires.2015.03.006

Yang, J., Ma, Q., Dincheva, I., Giza, J., Jing, D., Marinic, T., et al. (2021). SorCS2 is required for social memory and trafficking of the NMDA receptor. *Mol. Psychiatry* 26, 927–940. doi: 10.1038/s41380-020-0650-7

Yarkoni, T., Poldrack, R. A., Nichols, T. E., Van Essen, D. C., and Wager, T. D. (2011). Large-scale automated synthesis of human functional neuroimaging data. *Nat. Methods* 8, 665–670. doi: 10.1038/nmeth.1635

Conflict of Interest: The authors declare that the research was conducted in the absence of any commercial or financial relationships that could be construed as a potential conflict of interest.

Publisher's Note: All claims expressed in this article are solely those of the authors and do not necessarily represent those of their affiliated organizations, or those of the publisher, the editors and the reviewers. Any product that may be evaluated in this article, or claim that may be made by its manufacturer, is not guaranteed or endorsed by the publisher.

frontiers in Genetics

ORIGINAL RESEARCH
published: 01 March 2022
doi: 10.3389/fgene.2022.803584

Epigenetic Clock Deceleration and Maternal Reproductive Efforts: Associations With Increasing Gray Matter Volume of the Precuneus

Shota Nishitani[1,2,3]*, *Ryoko Kasaba*[1,2], *Daiki Hiraoka*[1,4], *Koji Shimada*[1,2,3,5], *Takashi X. Fujisawa*[1,2,3], *Hidehiko Okazawa*[3,5] *and Akemi Tomoda*[1,2,3,6]*

[1]Research Center for Child Mental Development, University of Fukui, Fukui, Japan, [2]Division of Developmental Higher Brain Functions, United Graduate School of Child Development, Hamamatsu University School of Medicine, Osaka University, Kanazawa University, Chiba University, University of Fukui, Osaka, Japan, [3]Life Science Innovation Center, University of Fukui, Fukui, Japan, [4]Japan Society for the Promotion of Science, Tokyo, Japan, [5]Biomedical Imaging Research Center, University of Fukui, Fukui, Japan, [6]Department of Child and Adolescent Psychological Medicine, University of Fukui Hospital, Fukui, Japan

OPEN ACCESS

Edited by:
Noriyoshi Usui, Osaka University, Japan

Reviewed by:
Guang-Zhong Wang, Shanghai Institute of Nutrition and Health (CAS), China
Minyoung Jung, Korea Brain Research Institute, South Korea

***Correspondence:**
Shota Nishitani
nshota@u-fukui.ac.jp
Akemi Tomoda
atomoda@u-fukui.ac.jp

Specialty section:
This article was submitted to Neurogenomics, a section of the journal Frontiers in Genetics

Received: *28 October 2021*
Accepted: *02 February 2022*
Published: *01 March 2022*

Citation:
Nishitani S, Kasaba R, Hiraoka D, Shimada K, Fujisawa TX, Okazawa H and Tomoda A (2022) Epigenetic Clock Deceleration and Maternal Reproductive Efforts: Associations With Increasing Gray Matter Volume of the Precuneus. Front. Genet. 13:803584. doi: 10.3389/fgene.2022.803584

Reproductive efforts, such as pregnancy, delivery, and interaction with children, make maternal brains optimized for child-rearing. However, extensive studies in non-human species revealed a tradeoff between reproductive effort and life expectancy. In humans, large demographic studies have shown that this is the case for the most part; however, molecular marker studies regarding aging remain controversial. There are no studies simultaneously evaluating the relationship between reproductive effort, aging, and brain structures. We therefore examined the associations between reproductive efforts (parity status, number of deliveries, motherhood period, and cumulative motherhood period), DNA methylation age (mAge) acceleration (based on Horvath's multi-tissue clock and the skin & blood clock), and the regional gray matter volumes (obtained through brain magnetic resonance imaging (MRI) using voxel-based morphometry) in 51 mothers aged 27–46 years of children in early childhood. We found that increasing reproductive efforts were significantly associated with decelerated aging in mothers with one to four children, even after adjusting for the confounding effects in the multiple linear regression models. We also found that the left precuneus gray matter volume was larger as deceleration of aging occurred; increasing left precuneus gray matter volume, on the other hand, mediates the relationship between parity status and mAge deceleration. Our findings suggest that mothers of children in early childhood, who have had less than four children, may benefit from deceleration of aging mediated via structural changes in the precuneus.

Keywords: DNA methyaltion, imaging epigenetics, longevity, maternal brain, voxel-based morphometry (VBM)

INTRODUCTION

In non-human species, the established theory (LHT: Life History Theory) is that the greater the reproductive effort, the more finite energy is expended; thus, females tradeoff life expectancy with reproductive effort (Hill and Kaplan, 1999). In humans, several large, population-based demographic studies of more than 140,000 women born between 1820 and 1920 in a preindustrial population in

Utah, North America, have also shown that women who undertook more reproductive effort lived a shorter lifespan (Penn and Smith, 2007; Bolund et al., 2016). These results are largely in line with the LHT. However, according to Bolund et al. (2016), maternal life expectancy is shortened with four or more births, per the LHT; conversely, deliveries of less than four extended life expectancy (Bolund et al., 2016). Our current monogamous society no longer has an average of nine births (as was common in this previous era); for example, the number of childbirths in first-time married couples who had been married for 15–19 years in Japan was 1.94 in 2015 (The Fifteenth Japanese National Fertility Survey in 2015, 2017). A more recent large, North America-wide demographic study of more than 20,000 women was conducted (Shadyab et al., 2017), which better reflects the current average number of births. Shadyab et al. (2017) reported that the odds ratio (OR) of longevity in Caucasians was higher for mothers who gave birth more than once (two to four children; mean OR: 1.13) compared to that of those who gave birth once (OR: 0.91) or were nulliparous (OR: 1 as reference), even after adjusting for demographic characteristics, socioeconomic status, lifestyle behaviors, reproductive factors, and health-related factors (Shadyab et al., 2017). However, it was consistent with both the LHT and previous population demographics in most aspects, especially regarding having more children; the association between the number of deliveries and longevity was attenuated, and was certainly not higher in those with five or more children. Dior et al. (2013) reported a U-shaped and nonlinear, association between the number of deliveries and all-cause maternal mortality; the lowest risk was at two to three children (Dior et al., 2013). Therefore, while it may be true that having more than four children reduces life expectancy in women, the LHT may not be consistent with births of less than four children.

Hence, recent studies using molecular metrics have attempted to provide biological evidence for the effects of reproductive effort on women's longevity. Telomere length was used as a molecular metric to reflect longevity in the initial study stages. The first study reported that mothers who had more children had shorter telomere lengths (Gray et al., 2014); by contrast, a study of the Mayan tribe in Guatemala reported that mothers who had more children had longer telomeres (Barha et al., 2016). In addition to telomere length, epigenetic age acceleration—which is obtained by calculating the deviation of DNA methylation age (mAge) from chronological age (Horvath, 2013)—has recently attracted attention, serving as a novel biomarker of aging. Using this metric, Ryan et al. showed that in 397 young, 20–22 year-old Filipino women, a higher number of pregnancies was associated with a greater mAge acceleration and shorter telomere length (Ryan et al., 2018). Kresovich *et al.* also retrospectively used this metric in more than 2,000 women aged 35–74 and living in the US, reporting that increased acceleration of aging was seen with more births (Kresovich et al., 2019). Nevertheless, the results of these studies cannot sufficiently explain why the influence of births of four or fewer children might be exceptionally non-linear. Moreover, the cause of this putative possibility might be difficult to elucidate in retrospective studies on generations that have already completed child-rearing. While the participants in the study by Ryan et al. were supposed to be rearing children, the mean age of childbearing in most developed countries is considerably higher, and was as high as 30.7 years old in Japan in 2016; therefore, while their results are applicable to younger mothers, it remains uncertain whether they can be applied to the general maternal population at present.

In addition to the phenomenon where reproductive effort affects aging and longevity, it has been affirmed that reproductive effort, including the experiences of pregnancy, delivery, and parenting, makes female brain structures more maternal and optimized for parenting (Nishitani et al., 2011; Nishitani et al., 2014; Kim, 2016). Hoekzema et al. (2017) conducted a longitudinal study that followed 25 first-time mothers from time of conception to 2 years after delivery; they found that at 10 months postpartum, the gray matter (GM) volume of the inferior and medial frontal gyrus, superior temporal sulcus, fusiform gyrus, precuneus, and hippocampus—involved in the theory-of-mind network—was reduced compared with during pregnancy (Hoekzema et al., 2017). Zhang et al. (2019) examined a similar longitudinal study and found that mothers showed changes in GM and white matter volumes, as well as the cortical thickness of several regions—including the superior and medial frontal gyrus, insula, limbic lobe, superior and middle temporal gyrus, and precentral gyrus—after 2 years of follow-up (Zhang et al., 2019). Luders et al. (2020) conducted a similar longitudinal study. They reported no decline in areas at 4–6 weeks postpartum compared with the immediate postpartum period (one to two days postpartum); however, there were increased GM volumes in certain regions, including the pre- and postcentral gyrus, thalamus, and precuneus, contrary to Hoekzema et al.'s results (Luders et al., 2020). These studies suggest that reproductive effort affects not only aging, but also elicits changes in brain structure. Contrasting with other species, humans do not reach the end of their life shortly after menopause; in fact, they live nearly twice as long as their age at menopause in this modern era. The grandmother hypothesis, explaining the existence of menopause in human life history by identifying the adaptive value of extended kin networking, has been proposed (Hawkes, 2004), as postmenopausal women have been found to have a great deal of biological and social activity (Kida et al., 2014; Hawkes and Finlay, 2018). This is unique to humans and is considered to be related to humans' high sociability, owing to their highly evolved brains (Hawkes, 2020).

Therefore, we hypothesized that reproductive effort would refine the brain structures involved in the sociability required for parenting, thereby influencing both mAge acceleration and longevity. In the present study, we examined the association between reproductive effort, mAge acceleration measured using salivary DNA, and brain structures evaluated by voxel-based morphometry (VBM), in mothers.

MATERIALS AND METHODS

Participants

A total of 57 Japanese biological mothers rearing at least one child of preschool age participated in this study; this dataset is used for

TABLE 1 | Demographic characteristics of the participants.

	(*n* = 51)
Age (years), *Mean* (*SD*)	35.4 (4.4)
Age (years) at first childbirth	29.1 (4.0)
Age (years) at last childbirth	32.3 (3.9)
Parity status, *n* (%)	11 (21.6)/40 (78.4)
Primiparity/Multiparity	
Number of deliveries, *n* (%)	11 (21.6)
One	30 (58.8)
Two	9 (17.6)
Three	1 (2.0)
Four	
Motherhood period (age of oldest child) (years)	6.2 (3.2)
Cumulative motherhood period (years)	9.9 (6.0)
Exclusive breastfeeding diet, *n* (%)	30 (58.8)
Household Income (currency = JPY), *n* (%)	
Less than 3 million	3 (5.9)
3–5 million	25 (49.0)
5–10 million	21 (41.2)
More than 10 million	2 (3.9)
MRI scanner, *n* (%)	
Discovery MR 750 3T/Signa PET/MR 3T	30 (58.8)/21 (41.2)
Proportion of Epithelial cells (%)	15.9 (5.8)
FLANDERS handedness inventory (right/mixed/left)	48 (92.3)/1 (1.9)/2 (3.8)
PSI (Total/Child/Adult)	191.5 (39.8)/86.5 (18.6)/105.1 (24.6)
BDI-II	12.0 (9.2)

PSI, Parenting Stress Index (Abidin, 1995; Namara et al., 1999); BDI-II, The Beck Depression Inventory-II (Beck, Steer, & Brown, 1996; Kojima et al., 2002).

our previous studies (Hiraoka et al., 2020; Sakakibara et al., 2021; Kasaba et al., 2021; Shimada et al., 2019). We excluded four mothers who delivered by caesarean section for multiple births, and two mothers of children with disabilities. A total of 51 mothers were included (age range = 27–46 years; mean age = 34.8 years; standard deviation (SD) = 4.5 years). Detailed demographics are shown in **Table 1**. Among the participants, 11 had one child, 30 had two children, nine had three children, and one had four children. We defined "parity status" as primiparity or multiparity, and "number of deliveries" as the number of times a mother gave live birth; these represented the reproductive effort indices. The average age of the oldest children of the participants was 6.2 years (SD = 3.2); this age was defined as the total "motherhood period" until the day of the experiment. We added up the age of all children to calculate an index, referred to as the "cumulative motherhood period"; this reflected the efforts invested in parenting more appropriately for mothers rearing multiple children (**Supplementary Figure S1** and **Supplementary Table S1**). All participants had received at least 12 years of education. Almost all (92.3 %) were right-handed, according to the FLANDERS handedness inventory (Nicholls et al., 2013; Okubo et al., 2014).

This study's protocol was approved by the Ethics Committee of the University of Fukui (FU20150109 and FU20190107), and was conducted following the Declaration of Helsinki. All participants provided written informed consent for participation in this study.

Questionnaires

The Japanese version of the Parenting Stress Index (PSI) (Namara et al., 1999)—an adaptation of the PSI (Abidin, 1995)—was used to evaluate the participants' parenting stress (PSI total). The Beck Depression Inventory-II (BDI-II) (Beck et al., 1996; Kojima et al., 2002) was used to measure the participants' depressive symptoms.

DNA Methylation

Saliva samples were collected using Oragene Discover OGR-500 kits (DNA Genotek Inc., Ottawa, ON, Canada). Saliva DNA was extracted using prepIT®•L2P reagent (DNA Genotek Inc.) and was quantified with Qubit™ dsDNA HS Assay Kit (Thermo Fisher Scientific Inc., Pittsburgh, PA, United States) (Utevsky et al., 2014). Five hundred ng of DNA was bisulfite-treated for cytosine to thymine conversion using the EZ DNA Methylation-Gold kit (Zymo Research, Irvine, CA, United States). DNA was then whole-genome amplified, fragmented, and hybridized to the HumanMethylationEPIC BeadChip (Illumina Inc., San Diego, CA, United States). The BeadChips were scanned using iSCAN (Illumina Inc.), and the methylation level (β value) was calculated for each queried CpG locus using the GenomeStudio Methylation Module software. As shown in Supplementary Figure S2, a quality check was conducted based on the Psychiatric Genomics Consortium-EWAS quality control pipeline (Ratanatharathorn et al., 2017) using CpGassoc (Barfield et al., 2012), an R package. Samples with probe detection call rates <90%, and those with an average intensity value of either <50% of the experiment-wide sample mean or <2,000 arbitrary units were excluded. Probes with detection $p > 0.001$, or those based on less than three beads, were set to missing, as were probes that cross-hybridized between autosomes and sex chromosomes. CpG sites with missing data for >10% of samples within cohorts were excluded from the analysis. After quality control, 852,775 probes were left for further analysis.

Horvath's multi-tissue clock mAge (Horvath, 2013) and the skin & blood clock mAge (Horvath et al., 2018) were calculated based on the online calculator (https://horvath.genetics.ucla.edu/html/dnamage/). The skin & blood clock is also known as a novel and highly robust DNAm age estimator for human fibroblasts, keratinocytes, buccal cells, endothelial cells, lymphoblastoid cells, skin, blood, and saliva samples, and has superior accuracy in blood and saliva samples than multi-tissue clock (Horvath et al., 2018). We regressed mAge on chronological age; the unstandardized residuals indicated epigenetic age acceleration. As saliva contains a heterogeneous mixture of cell types that differ in proportion in each sample, using the EpiDISH method (Teschendorff et al., 2017), we estimated the proportion of epithelial cells derived from salivary DNA (Epi) after the preprocessing processes similar to our previous study (Nishitani et al., 2021) and examined whether the proportion of epithelial cells affects mAge acceleration.

MRI Acquisition and Voxel-Based Morphometry

Image acquisition of 30 participants was performed using a GE Discovery MR 750 3-T scanner (GE Healthcare, Milwaukee, WI). A T1-weighted anatomical dataset was obtained from each subject by a fast-spoiled gradient recalled imaging sequence (voxel size 1 × 1 × 1 mm, TE = 1.99 ms, TR = 6.38 ms, flip angle = 11°). Image acquisition of the 21 participants was carried out using a GE Signa PET/MR 3-T scanner (GE Healthcare, Milwaukee, WI). High-resolution structural whole-brain images were acquired using a 3D T1-weighted fast spoiled-gradient recalled imaging sequence (voxel size 1 × 1 × 1 mm, TE = 3.24 ms, TR = 8.46 ms, flip angle = 11°). Given that we used two scanners, a dummy-coded covariate (0 vs. 1) was added in the analyses. VBM data were analyzed using the Statistical Parametric Mapping software (SPM12; https://www.fil.ion.ucl.ac.uk/spm) implemented in MATLAB 2014a. The T1-weighted images were preprocessed using the VBM approach with modulation, where the images were first segmented into GM, white matter, cerebrospinal fluid, and skull/scalp compartments. Using the iterative high-dimensional normalization approach provided by Diffeomorphic Anatomical Registration through an Exponentiated Lie algebra algorithm (Ashburner, 2007), the segmented GM images were spatially normalized into the stereotaxic space of the Montreal Neurological Institute (MNI). The GM images had an isotropic voxel resolution of 1.5 mm^3. Any volume change induced by normalization was adjusted via a modulation algorithm. The normalized modulated GM images were spatially smoothed by a Gaussian kernel of 8-mm full-width-at-half-maximum.

Statistical Analysis

We conducted simple linear regression using heteroscedasticity-robust standard errors, with four types of reproductive effort indices as independent variables to predict mAge acceleration: parity status, number of deliveries, motherhood period, and cumulative motherhood period. We have employed this statistical technique for our analyses since it is no needed the assumption of homoscedasticity. To investigate the extent to which reproductive effort accounts for variance in mAge acceleration in the presence of various potential confounders (chronological age, PSI total, and Epi), multiple regression using robust standard errors was conducted. In the VBM analysis, chronological age, scanner (dummy coded as 0 and 1), and total brain volume were included as covariates of no interest in the design matrix to regress out their effects. The resulting set of voxel values used for each contrast generated a statistical parametric map of the *t*-statistic, SPM (*t*), which was transformed to a unit normal distribution [SPM (*Z*)]. The statistical threshold was set to $p < 0.05$, with family-wise error correction for multiple comparisons at the cluster level (height threshold of $Z > 3.09$). Significant clusters were localized in the Automated Anatomical Labelling atlases implemented in the MRIcron software package (https://www.nitrc.org/projects/mricron).

We conducted robust mediation analysis (Alfons et al., 2021) to assess whether the GM volume mediated the link between reproductive efforts and mAge acceleration. We included chronological age as the covariate in the model. The indirect effects of each model were tested by bootstrapping confidence intervals using the robmed package (Alfons et al., 2021). The model parameters were set to give bias-corrected 95% confidence intervals and to run 5,000 bootstrap resamples. All statistical analyses were performed with R 4.0.5 and SPM 12.

RESULTS

Reproductive Effort and Epigenetic Age Acceleration

Among 353 and 391 CpG sites required to calculate Horvath's multi-tissue clock mAge (Horvath, 2013) and skin & blood mAge (Horvath et al., 2018), we used 333 and 391 CpG probes, respectively. Seventeen probes were not included in the EPIC array to begin with and three probes (cg19167673, cg27413543, and cg14329157) were removed during data processing. As expected, mAge strongly correlated with chronological age (multi-tissue clock mAge: $R^2 = 0.57$, $t = 8.13$, $P = 1.23e\text{-}10$; skin & blood clock mAge: $R^2 = 0.75$, $t = 12.17$, $P = 1.98e\text{-}16$) (**Supplementary Figure S3**). The median absolute deviation from chronological age was 3.51 years for multi-tissue clock mAge, and 2.47 years for skin & blood clock mAge. These results were comparable with 2.7 years and 2.5 or 3.0 years, respectively, as reported by Horvath (Horvath, 2013); (Horvath et al., 2018). In simple linear regression analyses, mAge acceleration calculated by the multi-tissue clock was significantly negatively associated with parity status ($\beta = -0.26$, $t = -2.30$, $P = 0.03$), number of deliveries ($\beta = -0.29$, $t = -2.45$, $P = 0.02$), motherhood period ($\beta = -0.28$, $t = -2.45$, $P = 0.02$), and cumulative motherhood period ($\beta = -0.29$, $t = -2.29$, $P = 0.03$) (**Table 2** and **Figure 1**). Conversely, mAge acceleration calculated by the skin and blood clock was significantly negatively associated with parity status ($\beta = -0.21$, $t = -2.21$, $P = 0.03$), and number of deliveries ($\beta = -0.28$, $t = -2.44$, $P = 0.02$), while no associations were found with other parameters (**Table 2** and **Figure 1**). In other words, more

TABLE 2 | Simple linear regression with robust standard errors for mAge accelerations.

	Multi-tissue clock			Skin & blood clock		
	β	*t*	*P*	*β*	*t*	*P*
Reproductive effort						
Parity status	−0.26	−2.30	0.03*	−0.21	−2.21	0.03*
Number of deliveries	−0.29	−2.45	0.02*	−0.28	−2.44	0.02*
Motherhood period	−0.28	−2.45	0.02*	−0.13	−0.92	0.36
Cumulative motherhood period	−0.29	−2.29	0.03*	−0.25	−1.84	0.07
Other variables						
Age	−0.09	−0.54	0.59	−0.04	−0.26	0.79
PSI total	−0.42	−3.15	0.003***	−0.14	−1.03	0.31
BDI-II	−0.29	−2.14	0.04*	−0.12	−0.98	0.33
Epi	−0.05	−0.35	0.73	−0.003	−0.02	0.98
Age at first childbirth	1.25	0.66	0.51	0.06	0.46	0.65
Age at last childbirth	−0.64	−0.36	0.72	0.02	0.18	0.86
Exclusive breastfeeding diet	0.09	0.59	0.56	0.24	1.93	0.06
Household income	0.04	0.27	0.79	0.18	1.44	0.16

****P < 0.05, **P < 0.01, P < 0.005.*

BDI-II, The Beck Depression Inventory-II; mAge, DNA, methylation age; PSI, parenting stress index.

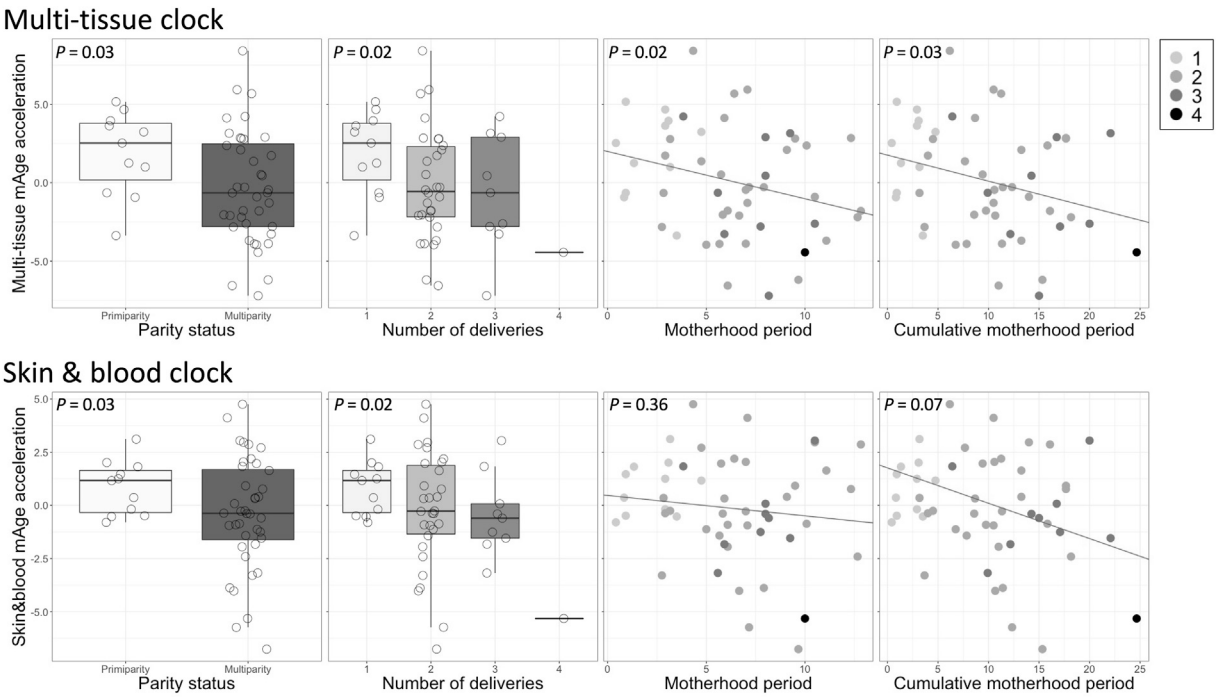

FIGURE 1 | Associations between each reproductive effort and mAge acceleration. Top: multi-tissue clock; bottom: skin & blood clock. The gray shading in the legend on the upper right reflects the number of deliveries.

reproductive efforts showed diminished mAge acceleration (**Figure 1**). PSI total (β = −0.42, t = −3.15, P = 0.003) and BDI-II (β = −0.29, t = −2.14, P = 0.04) were significantly associated with mAge acceleration calculated by the multi-tissue clock. No other demographic characteristics were associated with mAge acceleration for both calculations (**Table 2**). The correlation coefficients matrix between all the covariate combinations used in the analysis are shown in **Supplementary Figure S4**.

In addition to the simple linear regression, we also conducted multiple linear regression analyses to assess whether the other variables (chronological age, PSI total, and Epi) confounded the results (**Table 3**). Although chronological age and Epi were not significantly associated with mAge accelerations in the simple linear regression analysis, they were added in the multiple linear regression models as covariates. We chose PSI total instead of BDI-II as a covariate to avoid multi-collinearity issue in the regression model, as the two demonstrated a high correlation

TABLE 3 | Multiple linear regression with robust standard errors for mAge accelerations.

		Multi-tissue clock				Skin & blood clock			
		Parity status	Number of deliveries	Motherhood period	Cumulative motherhood period	Parity status	Number of deliveries	Motherhood period	Cumulative motherhood period
Reproductive effort	β	−0.25	−0.26	−0.29	−0.28	−0.21	−0.27	−0.14	−0.27
	t	−2.26	−2.52	−2.15	−2.14	−2.23	−2.36	−0.91	−2.09
	P	0.03*	0.02*	0.04*	0.04*	0.03*	0.02*	0.37	0.04*
Age	β	0.07	0.02	0.14	0.10	0.05	0.01	0.06	0.09
	t	0.43	0.15	0.74	0.61	0.34	0.08	0.38	0.635
	P	0.67	0.88	0.46	0.54	0.73	0.94	0.70	0.53
PSI total	β	−0.42	−0.41	−0.41	−0.42	−0.14	−0.13	−0.14	−0.14
	t	−3.06	−3.23	−3.05	−0.32	−0.96	−0.90	−0.97	−0.96
	P	0.004***	0.002***	0.004***	0.003***	0.34	0.37	0.34	0.34
Epi	β	0.03	0.03	0.06	0.06	0.04	0.03	0.04	0.06
	t	0.24	0.20	0.42	0.41	0.24	0.22	0.27	0.39
	P	0.81	0.85	0.68	0.69	0.81	.83	0.79	0.70
Model	R^2	0.16	0.18	0.17	0.17	−0.02	0.015	−0.05	0.004
	F	4.99	4.84	3.66	3.98	1.98	1.86	0.46	1.48
	P	0.002***	0.002***	0.01*	0.007**	0.11	0.13	0.77	0.22

****P < 0.05, **P < 0.01, P < 0.005.*

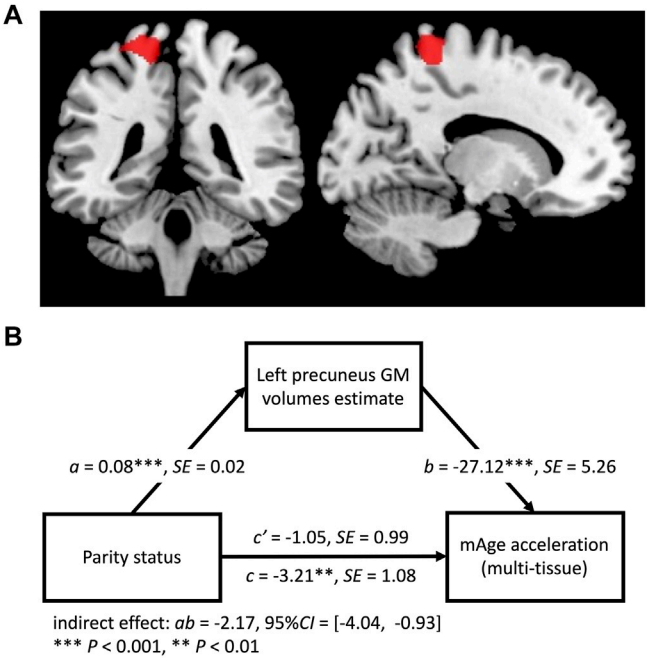

FIGURE 2 | (A) Regions of gray matter (GM) volume negatively associated with mAge acceleration (red; threshold $p < 0.05$, family-wise error corrected cluster level). **(B)** Path model for the mediation effect. GM volume of the left precuneus was a mediator in the relationship between parity status and mAge acceleration.

($r = 0.72$, $P = 2.85e\text{-}09$); additionally, the association between PSI total and mAge acceleration was greater than that of BDI-II (**Table 2**). Results showed that all four reproductive effort indices were significantly negatively associated with mAge acceleration calculated by the multi-tissue clock, even after adjusting for the confounding effects (*Ps* < 0.05, **Table 3**). Although the results of mAge acceleration calculated by the skin & blood clock showed significant associations with parity status ($P = 0.03$), number of deliveries ($P = 0.02$), and cumulative motherhood period ($P = 0.04$) in the multiple linear regression model, these models were not significant (**Table 3**). Hence, we used mAge acceleration based on the multi-tissue clock for subsequent analyses.

VBM and Path Analysis

The VBM results showed that mAge acceleration was negatively correlated with GM volume within a cluster in the left precuneus (Montreal Neurological Institute [MNI] coordinates: $x = -17$, $y = -39$, $z = 68$; cluster size = 727 voxels; $P = 0.04$, family-wise error [FWE] corrected cluster level; **Figure 2A**). There was a significant indirect effect of the precuneus GM volume on parity status and mAge acceleration (indirect effect = −2.17, 95% Confidence Interval = [−4.04, −0.93]; **Figure 2B**). No other reproductive efforts had a significant indirect effect.

DISCUSSION

This study examined the relationship between reproductive effort, mAge acceleration, and brain structure in mothers of children in early childhood. Our results showed that their reproductive effort—regarding parity status, number of deliveries, motherhood period, and cumulative motherhood period—was associated with mAge deceleration, even after adjusting for potential confounders. Although previous studies have examined the relationship between mAge acceleration or telomere length and the number of deliveries as a representative variable, this is the first time that mAge acceleration has been simultaneously examined in relation to the other reproductive effort indices, also considering daily parenting stress. We also found that the precuneus GM volume increased as mAge deceleration occurred. We also observed a mediation effect of

greater left precuneus GM volume on the relationship between parity status and mAge deceleration. This suggests that the precuneus—a central node in the human brain that supports complex cognition and behavior—may be associated with age deceleration in child-rearing mothers. This also suggests that multiparity between two to four births lead to maternal brain changes in the left precuneus, which contributes more to mAge deceleration than just one birth.

Our results were limited as we only included mothers who gave birth to one to four children; thus, we do not know how this would have affected women with more than four births. Still, among mothers who gave birth to one to four children, our results seemed to contradict the LHT (Hill and Kaplan, 1999). Our results suggest that mothers who gave birth to less than four children and have currently been rearing them have aged more slowly, depending on their reproductive efforts. Our findings are consistent with previous large demographic studies reporting that deliveries of less than four children extended, rather than diminished, life expectancy (Dior et al., 2013; Bolund et al., 2016; Shadyab et al., 2017). We speculate that this avoids a downward trend in the birth rate, since having only one offspring born to each couple would lead to a decline in population in a monogamous society. While childbearing certainly comes at the cost of energy based on the LHT, giving birth to two or more children while having fewer than four may benefit the mother's lifespan, even accounting for the tradeoffs of childbirth.

One possible biological cause underlying this phenomenon could be due to maternal brain alteration. Human mothers' brains undergo dynamic structural and functional changes during pregnancy and the early postpartum period to facilitate their psychological and behavioral adaptation to parenting (Kim, 2016; Hoekzema et al., 2017; Zhang et al., 2019; Luders et al., 2020). This transition to the maternal brain seems to particularly enhance the functioning of the reward, social information, and emotion regulation circuits (Ho et al., 2014). We identified that mAge deceleration associated with parity status was linked to an increase in precuneus GM volume in mothers, which is similar to the findings of the study by Luders et al. where an increase in precuneus GM volume was observed at 4–6 weeks postpartum, compared with 1–2 days postpartum (Luders et al., 2020). The precuneus is included in the social information circuit and is a hub for the default mode network (DMN), which involves empathy, as well as self-monitoring and reflection (Utevsky et al., 2014). In other words, becoming a mother of two or more children may have led to more complex social interactions, which may have contributed to a greater precuneus GM volume than in the past. It has also been found that patients with Alzheimer's disease (AD) and in the prodromal stage of AD have decreased DMN functions and precuneus GM volume compared to controls (Goto et al., 2015). Using postmortem brains, a telomere length analysis of each brain region comprising the DMN showed that the precuneus telomere length was shorter in AD and the prodromal stage of AD than in controls, whereas there were no differences in the frontal, inferior temporal, posterior cingulate gyrus or visual cortex (Mahady et al., 2020). Furthermore, this telomere length reduction in the precuneus also correlated with cognitive task performance. One of the main symptoms of PTSD is an elevated rumination characterized by repetitive, negative self-focused cognition; it has been reported that reduced functional connectivity between the isthmus cingulate and the left precuneus within the DMN is linked to this high level of rumination (Philippi et al., 2020). Lifetime trauma burden and suffering from both current and lifetime PTSD have been reported to cause GrimAge acceleration (Katrinli et al., 2020). These studies support the notion that aging and mental stress that accelerates aging may affect the functional connectivity between the precuneus and the other brain network region. The sophistication of the social information and DMN functions involved in becoming a mother may have contributed to the mAge deceleration via enhancing precuneus function and volume; however, this finding is not related to the number of deliveries—which accounts for the major reproductive effort—but rather to parity status (whether a baby is born to a mother once or twice or more), and is not a model that is valid as the number of deliveries increases.

Our results were partially inconsistent with previous studies. Ryan et al. reported mAge acceleration in mothers who had given birth to one to five children, as well as in nulliparous women (Ryan et al., 2018). However, their study participants were 20–22 years-old, which is relatively young compared with the average age of a primipara in modern, developed countries. Some reports suggest that a higher age at first birth is associated with longer telomere length (Fagan et al., 2017) and longer life expectancy (Shadyab et al., 2017). Thus, the association may be linear, rather than U-shaped, when the age at first birth is relatively young, as in this previous study. In addition, various environmental factors have been reported to influence mAge acceleration, most notably stress (Hoare et al., 2020; Katrinli et al., 2020). While Ryan et al. adjusted for socioeconomic status, they did not consider the effects of psychological aspects, such as parental stress; therefore, an analysis adjusting for these effects may also be necessary. In our results, higher parental stress, not only reproductive effort, was associated with the deceleration of aging. Conversely, Kresovich et al. reported accelerated aging in mothers who gave birth to one to four or more children, as well as in nulliparous women (Kresovich et al., 2019). However, their study was retrospective and included those who were currently out of the child-rearing phase (an average age of 55 years when the blood samples were collected), which is different from the present study, involving mothers of children in early childhood. Their results may thus be confounded by menopause (Gray et al., 2014) and the higher genetic risks for developing breast cancer, which is a unique characteristic of this cohort population (Sandler et al., 2017). By contrast, Barha et al. found longer telomeres in mothers who gave birth to one to six babies (Barha et al., 2016). Although this study did not measure mAge acceleration, telomere length results indicate that age deceleration may have occurred, perhaps akin to our findings. Additionally, our studies were similar in that the DNA was saliva-derived. Our method of estimating mAge by using Horvath's multi-tissue clock should not be noticeably affected, even if the tissue from which the DNA was derived was different (Horvath, 2013). Still, the similarities regarding the type of sample may not be particularly relevant. Additionally, the participants in their study were, on average,

39.4 years old, premenopausal, and probably still rearing their children. This consistency in age and rearing young children may be related to the directional consistency of the two results. Although their results were linearly regressed, on closer inspection, an inverted U-shaped approximation with a peak at two to three births appears to be more appropriate.

There are at least six potential limitations concerning our study's results. First, the small number of participants; we only had one participant with more than four children, limiting the ability to observe the U-shaped association that we hypothesized. Small group sizes may preclude drawing significant conclusions and limit generalizability of the results; thus, we will confirm these pilot results by increasing the sample size in future studies. Second, there were no nulliparous participants. Shadyab et al. (2017) reported that mothers had a longer life expectancy than nulliparous women (Shadyab et al., 2017). It is also known that changes in brain morphology and cognitive function occur when women become mothers (Hoekzema et al., 2017; Zhang et al., 2019; Luders et al., 2020); therefore, it is necessary to include nulliparous women to show the association between mAge acceleration and precuneus GM volume with brain materialization. Third, we used saliva DNA samples for mAge and mAge acceleration calculation. This limits the use of other newly developed blood DNA composite biomarkers, including: PhenoAge, which more effectively captures the epigenetic biomarkers of physiological age and discriminates between morbidity and mortality more definitively in individuals of the same chronological age (Levine et al., 2018); and GrimAge—named after the Grim Reaper—which predicts lifespan and healthspan in units of years (Lu et al., 2019). However, Horvath's multi-tissue clock can be used for any type of tissues, enabling a direct comparison with most previous studies based on blood DNA (Ryan et al., 2018; Kresovich et al., 2019). Forth, there was a significant association that higher the PSI, the more age deceleration based on the multi-tissue clock ($p = 0.003$), but not for skin & blood clock ($p = 0.31$). Zannas et al. (2015) have reported that lifetime stress accelerates epigenetic aging since the multi-tissue clock has 85 probes located within glucocorticoid response elements (Zannas et al., 2015). Thus, these specific probes included in the multi-tissue clock might have affected the association with PSI. However, the effect directionality of our results was different. This may suggest that the age deceleration was not effortlessly obtained as it was also associated with the length of the motherhood period. Fifth, we do not have information whether these participants cohabit with their parent or parent-in-law. According to the public demographics, nuclear families in Japan were 82.7% (2016) (Graphical Review of Japanese Household, 2016) and this might have influenced the results. Finally, we have focused only on mAge acceleration, but it is necessary to explore the relationship with the genome-wide profile, which is a future research goal.

CONCLUSION

Despite these limitations, our results suggest that reproductive effort in mothers may refine the brain structures involved in the sociability required for parenting, conversely influencing mAge acceleration and longevity. Our results also suggest that the mAge deceleration associated with changes in the precuneus may be one of the phenomena linked to the maternalization of the brain.

DATA AVAILABILITY STATEMENT

The original contributions presented in the study are included in the article/**Supplementary Material**, further inquiries can be directed to the corresponding authors.

ETHICS STATEMENT

The studies involving human participants were reviewed and approved by The Ethics Committee of the University of Fukui. The patients/participants provided their written informed consent to participate in this study.

AUTHOR CONTRIBUTIONS

SN and AT conceived and designed the project. SN, RK, DH, KS, TXF, and HO performed the experiments, collected, and analyzed the data. SN drafted the manuscript.

FUNDING

All phases of this study were supported by AMED under Grant Number JP20gk0110052 (AT and SN), JSPS KAKENHI Scientific Research (A) (JP19H00617 to AT), Scientific Research (C) (JP20K02700 to SN), Grant-in-Aid for "Creating a Safe and Secure Living Environment in the Changing Public and Private Spheres" from the Japan Science and Technology Agency (JST)/Research Institute of Science and Technology for Society (RISTEX), Research grant from Japan-United States Brain Research Cooperative Program (AT), Research Grants from the University of Fukui (FY 2019 and 2020 to SN), Grant-in-Aid for Translational Research from the Life Science Innovation Center, University of Fukui (LSI20305 to SN), and Grant for Life Cycle Medicine from Faculty of Medical Sciences, University of Fukui (SN).

ACKNOWLEDGMENTS

We would like to thank all the participants and the staff at the Research Center for Child Mental Development.

SUPPLEMENTARY MATERIAL

The Supplementary Material for this article can be found online at: https://www.frontiersin.org/articles/10.3389/fgene.2022.803584/full#supplementary-material

REFERENCES

Abidin, R. R. (1995). *Parenting Stress Index (PSI), Manual*. 3rd ed. Charlottesville, VA: Pediatric Psychology Press.

Alfons, A., Ates, N. Y., and Groenen, P. J. F. (2021). A Robust Bootstrap Test for Mediation Analysis, 2021 for Mediation Analysis. *Organizational Res. Methods press*. doi:10.1177/1094428121999096

Ashburner, J. (2007). A Fast Diffeomorphic Image Registration Algorithm. *Neuroimage* 38, 95–113. doi:10.1016/j.neuroimage.2007.07.007

Barfield, R. T., Kilaru, V., Smith, A. K., and Conneely, K. N. (2012). CpGassoc: an R Function for Analysis of DNA Methylation Microarray Data. *Bioinformatics* 28, 1280–1281. doi:10.1093/bioinformatics/bts124

Barha, C. K., Hanna, C. W., Salvante, K. G., Wilson, S. L., Robinson, W. P., Altman, R. M., et al. (2016). Number of Children and Telomere Length in Women: A Prospective, Longitudinal Evaluation. *PLoS One* 11, e0146424. doi:10.1371/journal.pone.0146424

Beck, A. T., Steer, R. A., and Brown, G. K. (1996). *Manual for the Beck Depression Inventory-II*. San Antonio, TX: Psychological Corporation.

Bolund, E., Lummaa, V., Smith, K. R., Hanson, H. A., and Maklakov, A. A. (2016). Reduced Costs of Reproduction in Females Mediate a Shift from a Male-Biased to a Female-Biased Lifespan in Humans. *Sci. Rep.* 6, 24672. doi:10.1038/srep24672

Dior, U. P., Hochner, H., Friedlander, Y., Calderon-Margalit, R., Jaffe, D., Burger, A., et al. (2013). Association between Number of Children and Mortality of Mothers: Results of a 37-year Follow-Up Study. *Ann. Epidemiol.* 23, 13–18. doi:10.1016/j.annepidem.2012.10.005

Fagan, E., Sun, F., Bae, H., Elo, I., Andersen, S. L., Lee, J., et al. (2017). Telomere Length Is Longer in Women with Late Maternal Age. *Menopause* 24, 497–501. doi:10.1097/gme.0000000000000795

Goto, M., Abe, O., Aoki, S., Hayashi, N., Ohtsu, H., Takao, H., et al. (2015). Longitudinal gray-matter Volume Change in the Default-Mode Network: Utility of Volume Standardized with Global gray-matter Volume for Alzheimer's Disease: a Preliminary Study. *Radiol. Phys. Technol.* 8, 64–72. doi:10.1007/s12194-014-0295-9

Graphical Review of Japanese Household, *from Comprehensive Survey of Living Conditions*, Ministry of Health Labour and Welfare, Tokyo, 2016.

Gray, K. E., Schiff, M. A., Fitzpatrick, A. L., Kimura, M., Aviv, A., and Starr, J. R. (2014). Leukocyte Telomere Length and Age at Menopause. *Epidemiology* 25, 139–146. doi:10.1097/ede.0000000000000017

Hawkes, K. (2020). Cognitive Consequences of Our Grandmothering Life History: Cultural Learning Begins in Infancy. *Phil. Trans. R. Soc. B* 375, 20190501. doi:10.1098/rstb.2019.0501

Hawkes, K., and Finlay, B. L. (2018). Mammalian Brain Development and Our Grandmothering Life History. *Physiol. Behav.* 193, 55–68. doi:10.1016/j.physbeh.2018.01.013

Hawkes, K. (2004). The Grandmother Effect. *Nature* 428, 128–129. doi:10.1038/428128a

Hill, K., and Kaplan, H. (1999). Life History Traits in Humans: Theory and Empirical Studies. *Annu. Rev. Anthropol.* 28, 397–430. doi:10.1146/annurev.anthro.28.1.397

Hiraoka, D., Nishitani, S., Shimada, K., Kasaba, R., Fujisawa, T. X., and Tomoda, A. (2020). Epigenetic Modification of the Oxytocin Gene Is Associated with gray Matter Volume and Trait Empathy in Mothers. *Psychoneuroendocrinology* 123, 105026. doi:10.1016/j.psyneuen.2020.105026

Ho, S. S., Konrath, S., Brown, S., and Swain, J. E. (2014). Empathy and Stress Related Neural Responses in Maternal Decision Making. *Front. Neurosci.* 8, 152. doi:10.3389/fnins.2014.00152

Hoare, J., Stein, D. J., Heany, S. J., Fouche, J.-P., Phillips, N., Er, S., et al. (2020). Accelerated Epigenetic Aging in Adolescents from Low-Income Households Is Associated with Altered Development of Brain Structures. *Metab. Brain Dis.* 35, 1287–1298. doi:10.1007/s11011-020-00589-0

Hoekzema, E., Barba-Müller, E., Pozzobon, C., Picado, M., Lucco, F., García-García, D., et al. (2017). Pregnancy Leads to Long-Lasting Changes in Human Brain Structure. *Nat. Neurosci.* 20, 287–296. doi:10.1038/nn.4458

Horvath, S. (2013). DNA Methylation Age of Human Tissues and Cell Types. *Genome Biol.* 14, R115. doi:10.1186/gb-2013-14-10-r115

Horvath, S., Oshima, J., Martin, G. M., Lu, A. T., Quach, A., Cohen, H., et al. (2018). Epigenetic Clock for Skin and Blood Cells Applied to Hutchinson Gilford Progeria Syndrome and *Ex Vivo* Studies. *Aging* 10, 1758–1775. doi:10.18632/aging.101508

Kasaba, R., Shimada, K., and Tomoda, A. (2021). Neural Mechanisms of Parental Communicative Adjustments in Spoken Language. *Neuroscience* 457, 206–217. doi:10.1016/j.neuroscience.2020.12.002

Katrinli, S., Stevens, J., Wani, A. H., Lori, A., Kilaru, V., van Rooij, S. J. H., et al. (2020). Evaluating the Impact of Trauma and PTSD on Epigenetic Prediction of Lifespan and Neural Integrity. *Neuropsychopharmacol.* 45, 1609–1616. doi:10.1038/s41386-020-0700-5

Kida, T., Nishitani, S., Tanaka, M., Takamura, T., Sugawara, M., and Shinohara, K. (2014). I Love My Grandkid! an NIRS Study of Grandmaternal Love in Japan. *Brain Res.* 1542, 131–137. doi:10.1016/j.brainres.2013.10.028

Kim, P. (2016). Human Maternal Brain Plasticity: Adaptation to Parenting. *New Dir. Child Adolesc. Develop.* 2016, 47–58. doi:10.1002/cad.20168

Kojima, M., Furukawa, T. A., Takahashi, H., Kawai, M., Nagaya, T., and Tokudome, S. (2002). Cross-cultural Validation of the Beck Depression Inventory-II in Japan. *Psychiatry Res.* 110, 291–299. doi:10.1016/s0165-1781(02)00106-3

Kresovich, J. K., Harmon, Q. E., Xu, Z., Nichols, H. B., Sandler, D. P., and Taylor, J. A. (2019). Reproduction, DNA Methylation and Biological Age. *Hum. Reprod.* 34, 1965–1973. doi:10.1093/humrep/dez149

Levine, M. E., Lu, A. T., Quach, A., Chen, B. H., Assimes, T. L., Bandinelli, S., et al. (2018). An Epigenetic Biomarker of Aging for Lifespan and Healthspan. *Aging* 10, 573–591. doi:10.18632/aging.101414

Lu, A. T., Quach, A., Wilson, J. G., Reiner, A. P., Aviv, A., Raj, K., et al. (2019). DNA Methylation GrimAge Strongly Predicts Lifespan and Healthspan. *Aging* 11, 303–327. doi:10.18632/aging.101684

Luders, E., Kurth, F., Gingnell, M., Engman, J., Yong, E.-L., Poromaa, I. S., et al. (2020). From Baby Brain to Mommy Brain: Widespread gray Matter Gain after Giving Birth. *Cortex* 126, 334–342. doi:10.1016/j.cortex.2019.12.029

Mahady, L., He, B., Malek-Ahmadi, M., and Mufson, E. J. (2020). Telomeric Alterations in the Default Mode Network during the Progression of Alzheimer's Disease: Selective Vulnerability of the Precuneus. *Neuropathol. Appl. Neurobiol.* 47 (3), 428–440. doi:10.1111/nan.12672

The Fifteenth Japanese National Fertility Survey in 2015 (2017). Marriage Process and Fertility of Married Couples Attitudes toward Marriage and Family Among Japanese Singles. *Natl. Inst. Popul. Soc. Security Res. (Japan)*, 1–26. https://www.ipss.go.jp/ps-doukou/e/doukou15/Nfs15_points_eng.pdf.

Namara, M., Kanematsu, Y., Araki, A., Maru, M., Nakamura, N., Takeda, J., et al. (1999). Validity and Reliability of the Japanese Version of the Parenting Stress Index. *J. Child Health* 58 (5), 610–616.

Nicholls, M. E. R., Thomas, N. A., Loetscher, T., and Grimshaw, G. M. (2013). The Flinders Handedness Survey (FLANDERS): a Brief Measure of Skilled Hand Preference. *Cortex* 49, 2914–2926. doi:10.1016/j.cortex.2013.02.002

Nishitani, S., Doi, H., Koyama, A., and Shinohara, K. (2011). Differential Prefrontal Response to Infant Facial Emotions in Mothers Compared with Non-mothers. *Neurosci. Res.* 70, 183–188. doi:10.1016/j.neures.2011.02.007

Nishitani, S., Kuwamoto, S., Takahira, A., Miyamura, T., and Shinohara, K. (2014). Maternal Prefrontal Cortex Activation by Newborn Infant Odors. *Chem. Senses* 39, 195–202. doi:10.1093/chemse/bjt068

Nishitani, S., Suzuki, S., Ochiai, K., Yao, A., Fujioka, T., Fujisawa, T. X., et al. (2021). Altered Epigenetic Clock in Children Exposed to Maltreatment. *Psychiatry Clin. Neurosci.* 75, 110–112. doi:10.1111/pcn.13183

Okubo, M., Suzuki, H., and Nicholls, M. E. R. (2014). A Japanese Version of the FLANDERS Handedness Questionnaire. *Jpn. J. Psychol.* 85, 474–481. doi:10.4992/jjpsy.85.13235

Penn, D. J., and Smith, K. R. (2007). Differential Fitness Costs of Reproduction between the Sexes. *Proc. Natl. Acad. Sci.* 104, 553–558. doi:10.1073/pnas.0609301103

Philippi, C. L., Pessin, S., Reyna, L., Floyd, T., and Bruce, S. E. (2020). Cortical Midline Structures Associated with Rumination in Women with PTSD. *J. Psychiatr. Res.* 131, 69–76. doi:10.1016/j.jpsychires.2020.09.001

Ratanatharathorn, A., Boks, M. P., Maihofer, A. X., Aiello, A. E., Amstadter, A. B., Ashley-Koch, A. E., et al. (2017). Epigenome-wide Association of PTSD from Heterogeneous Cohorts with a Common Multi-Site Analysis Pipeline. *Am. J. Med. Genet.* 174, 619–630. doi:10.1002/ajmg.b.32568

Ryan, C. P., Hayes, M. G., Lee, N. R., McDade, T. W., Jones, M. J., Kobor, M. S., et al. (2018). Reproduction Predicts Shorter Telomeres and Epigenetic Age Acceleration Among Young Adult Women. *Sci. Rep.* 8, 11100. doi:10.1038/s41598-018-29486-4

Sakakibara, N., Makita, K., Hiraoka, D., Kasaba, R., Kuboshita, R., Shimada, K., et al. (2021). Increased Resting-state Activity in the Cerebellum with Mothers Having Less Adaptive Sensory Processing and Trait Anxiety. *Hum. Brain Mapp.* 42, 4985–4995. doi:10.1002/hbm.25594

Sandler, D. P., Hodgson, M. E., Deming-Halverson, S. L., Juras, P. S., D'Aloisio, A. A., Suarez, L. M., et al. (2017). The Sister Study Cohort: Baseline Methods and Participant Characteristics. *Environ. Health Perspect.* 125, 127003. doi:10.1289/ehp1923

Shadyab, A. H., Gass, M. L. S., Stefanick, M. L., Waring, M. E., Macera, C. A., Gallo, L. C., et al. (2017). Maternal Age at Childbirth and Parity as Predictors of Longevity Among Women in the United States: The Women's Health Initiative. *Am. J. Public Health* 107, 113–119. doi:10.2105/ajph.2016.303503

Shimada, K., Kasaba, R., Yao, A., and Tomoda, A. (2019). Less Efficient Detection of Positive Facial Expressions in Parents at Risk of Engaging in Child Physical Abuse. *BMC Psychol.* 7, 56. doi:10.1186/s40359-019-0333-9

Teschendorff, A. E., Breeze, C. E., Zheng, S. C., and Beck, S. (2017). A Comparison of Reference-Based Algorithms for Correcting Cell-type Heterogeneity in Epigenome-wide Association Studies. *BMC Bioinformatics* 18, 105. doi:10.1186/s12859-017-1511-5

Utevsky, A. V., Smith, D. V., and Huettel, S. A. (2014). Precuneus Is a Functional Core of the Default-Mode Network. *J. Neurosci.* 34, 932–940. doi:10.1523/jneurosci.4227-13.2014

Zannas, A. S., Arloth, J., Carrillo-Roa, T., Iurato, S., Röh, S., Ressler, K. J., et al. (2015). Lifetime Stress Accelerates Epigenetic Aging in an Urban, African American Cohort: Relevance of Glucocorticoid Signaling. *Genome Biol.* 16, 266. doi:10.1186/s13059-015-0828-5

Zhang, K., Wang, M., Zhang, J., Du, X., and Chen, Z. (2019). Brain Structural Plasticity Associated with Maternal Caregiving in Mothers: A Voxel- and Surface-Based Morphometry Study. *Neurodegener Dis.* 19, 192–203. doi:10.1159/000506258

Conflict of Interest: The authors declare that the research was conducted in the absence of any commercial or financial relationships that could be construed as a potential conflict of interest.

Publisher's Note: All claims expressed in this article are solely those of the authors and do not necessarily represent those of their affiliated organizations, or those of the publisher, the editors and the reviewers. Any product that may be evaluated in this article, or claim that may be made by its manufacturer, is not guaranteed or endorsed by the publisher.

frontiers in Genetics

ORIGINAL RESEARCH
published: 03 March 2022
doi: 10.3389/fgene.2022.815089

Short Tandem Repeat Variation in the *CNR1* Gene Associated With Analgesic Requirements of Opioids in Postoperative Pain Management

Shinya Kasai[1], *Daisuke Nishizawa*[1], *Junko Hasegawa*[1], *Ken-ichi Fukuda*[2], *Tatsuya Ichinohe*[3], *Makoto Nagashima*[4], *Masakazu Hayashida*[5] *and Kazutaka Ikeda*[1]*

[1]*Addictive Substance Project, Department of Psychiatry and Behavioral Sciences, Tokyo Metropolitan Institute of Medical Science, Tokyo, Japan,* [2]*Department of Oral Health Science, Tokyo Dental College, Tokyo, Japan,* [3]*Department of Dental Anesthesiology, Tokyo Dental College, Tokyo, Japan,* [4]*Department of Surgery, Toho University Sakura Medical Center, Sakura, Japan,* [5]*Department of Anesthesiology and Pain Medicine, Juntendo University School of Medicine, Tokyo, Japan*

OPEN ACCESS

Edited by:
Noriyoshi Usui, Osaka University, Japan

Reviewed by:
Kazutaka Ohi, Gifu University, Japan
Yuta Yoshino, Ehime University, Japan

***Correspondence:**
Kazutaka Ikeda
ikeda-kz@igakuken.or.jp

Specialty section:
This article was submitted to Neurogenomics, a section of the journal Frontiers in Genetics

Received: *15 November 2021*
Accepted: *02 February 2022*
Published: *03 March 2022*

Citation:
Kasai S, Nishizawa D, Hasegawa J, Fukuda K-i Ichinohe T, Nagashima M, Hayashida M and Ikeda K (2022) Short Tandem Repeat Variation in the CNR1 Gene Associated With Analgesic Requirements of Opioids in Postoperative Pain Management. Front. Genet. 13:815089. doi: 10.3389/fgene.2022.815089

Short tandem repeats (STRs) and variable number of tandem repeats (VNTRs) that have been identified at approximately 0.7 and 0.5 million loci in the human genome, respectively, are highly multi-allelic variations rather than single-nucleotide polymorphisms. The number of repeats of more than a few thousand STRs was associated with the expression of nearby genes, indicating that STRs are influential genetic variations in human traits. Analgesics act on the central nervous system via their intrinsic receptors to produce analgesic effects. In the present study, we focused on STRs and VNTRs in the *CNR1*, *GRIN2A*, *PENK*, and *PDYN* genes and analyzed two peripheral pain sensation-related traits and seven analgesia-related traits in postoperative pain management. A total of 192 volunteers who underwent the peripheral pain sensation tests and 139 and 252 patients who underwent open abdominal and orthognathic cosmetic surgeries, respectively, were included in the study. None of the four STRs or VNTRs were associated with peripheral pain sensation. Short tandem repeats in the *CNR1*, *GRIN2A*, and *PENK* genes were associated with the frequency of fentanyl use, fentanyl dose, and visual analog scale pain scores 3 h after orthognathic cosmetic surgery (Spearman's rank correlation coefficient ρ = 0.199, p = 0.002, ρ = 0.174, p = 0.006, and ρ = 0.135, p = 0.033, respectively), analgesic dose, including epidural analgesics after open abdominal surgery (ρ = –0.200, p = 0.018), and visual analog scale pain scores 24 h after orthognathic cosmetic surgery (ρ = 0.143, p = 0.023), respectively. The associations between STRs in the *CNR1* gene and the frequency of fentanyl use and fentanyl dose after orthognathic cosmetic surgery were confirmed by Holm's multiple-testing correction. These findings indicate that STRs in the *CNR1* gene influence analgesia in the orofacial region.

Keywords: analgesic requirement, cannabinoid receptor 1, ionotropic glutamate receptor NMDA type subunit 2A, preproenkephalin, prodynorphin, short tandem repeat

INTRODUCTION

Pain sensation is an inherent mechanism to avoid tissue damage from injuries and burns. It is an essential system for the living body, but excessive pain is a harmful sensation that evokes unpleasant and aversive reactions. Therefore, there is a clinical need to adequately control severe pain. Opioids, including morphine and fentanyl, have been used as analgesics to alleviate severe pain in many medical situations, such as cancer pain treatment and postoperative pain management. Opioid analgesic consumption varies widely among countries. Palliative care has been reported to be practiced adequately or moderately in the United States, Canada, Europe, and Australia (Duthey and Scholten, 2014). However, in recent years, opioid use disorder, including opioid misuse and addiction, has caused a serious public health crisis in these countries (Volkow and Collins, 2017). The morbidity and mortality of opioid use disorder increased during the coronavirus disease 2019 pandemic in the United States and Canada. Thus, proper opioid use is required now more than ever (Patel et al., 2021; Wang et al., 2021).

A great deal of variation in opioid requirements has been observed for adequate pain relief among individuals (Aubrun et al., 2003; Fukuda et al., 2010). Individual differences in opioid analgesia are attributable to multiple and interacting genetic, psychological, and environmental factors. Twin studies that compared morbidity between monozygotic and dizygotic twins reported that 12–60, 30, 59, and 36% were heritable for opioid-induced analgesic effects, respiratory depression, nausea, and drug dislike, respectively (Angst et al., 2012a; Angst et al., 2012b). Recently, genetic studies of personalized pain treatment have been performed, and some genetic variations have been shown to be associated with individual differences in analgesic effects of opioids (reviewed in Kumar et al., 2019). The A118G single nucleotide polymorphism (SNP; rs1799971) in the μ-opioid receptor (*OPRM1*) gene is the most studied genetic variation that is associated with individual differences in opioid analgesia (Kasai and Ikeda, 2011). Single-nucleotide polymorphisms in the ATP-binding cassette subfamily B member 1 (*ABCB1*), adrenoceptor β1 (*ADRB1*), catechol-*O*-methyltransferase (*COMT*), cytochrome P450 family 2 subfamily D member 6 (*CYP2D6*), cytochrome P450 family 3 subfamily A member 4 (*CYP3A4*), solute carrier family 22 member 1 (*SLC22A1*), and UDP glucuronosyltransferase family 2 member B7 (*UGT2B7*) genes were also shown to be associated with analgesic effects of opioids (Reyes-Gibby et al., 2007; Stamer et al., 2007; Rakvåg et al., 2008; Tzvetkov et al., 2011; Sistonen et al., 2012; Candiotti et al., 2013; Bastami et al., 2014; Dong et al., 2015; Wei et al., 2015; Dzambazovska-Trajkovska et al., 2016; Lv et al., 2018).

Besides SNPs, various types of genetic variations, including insertions and deletions (i.e., indels), short tandem repeats (STRs), variable number of tandem repeats (VNTRs), copy number variations (CNVs), and retrotransposons, exist in the human genome. Short tandem repeats and VNTRs are typically classified as repetitive sequence motifs of less than six base pair (bp) nucleotides and more than six bp, respectively. Short tandem repeats and VNTRs were identified in the human genome at approximately 0.7 and 0.5 million loci, respectively, which are less than the 85 million loci for SNPs (Willems et al., 2014; Genomes Project Consortium et al., 2015; Bakhtiari et al., 2021). However, repeat variations of STRs vary widely because of the high mutation rate by DNA slippage (Fan and Chu, 2007). The rate of mutation of STRs in the human germline was estimated to be approximately $3–7 \times 10^{-3}$ per locus per gamete per generation (Brinkmann et al., 1998; Ellegren, 2000; Kayser et al., 2000). The genome-wide mutation rate in the human germline is relatively low compared with STRs (approximately 10^{-8} to 10^{-9} per locus per generation; Scally, 2016; Xue et al., 2009). VNTRs are repeat sequences of approximately 10–100 nucleotides with 5–50 repeats and the large nucleotide differences would affect chromosomal structures (Brookes, 2013). Therefore, STRs and VNTRs highly contribute to the heritability of individual differences in human traits.

Short tandem repeats and VNTRs in the cannabinoid receptor 1 (*CNR1*), glutamate ionotropic receptor NMDA type subunit 2A (*GRIN2A*), prodynorphin (*PDYN*), and proenkephalin (*PENK*) genes were reported to be associated with the vulnerability to schizophrenia and substance dependence (Comings et al., 1997; Comings et al., 1999; Chen et al., 2002; Itokawa et al., 2003). Opioid analgesics act through opioid receptors, which mediate almost all opioid effects and comprise the endogenous opioid system with their endogenous peptide ligands, including enkephalins and dynorphins. The *PDYN* and *PENK* genes encode prodynorphin and preproenkephalin, which are precursors of dynorphin and enkephalin peptides, respectively. The *CNR1* gene encodes cannabinoid receptor 1, which is mainly expressed in the central and peripheral nervous systems, including the hippocampus, frontal cortex, amygdala, hypothalamus, cerebellum, and midbrain (Glass et al., 1997). The endocannabinoid system via CNR1 was reported to interact closely with the endogenous opioid system. The allosteric modulation of CNR1 signaling altered opioid function, including antinociception, in rodents (Datta et al., 2020; Slivicki et al., 2020). The *GRIN2A* gene encodes the ionotropic glutamate receptor NMDA2A (ε1), which is a subunit of NMDA receptor channels. *GRIN2A* gene expression is abundant in the central nervous system and increases during development in humans and mice (Bagasrawala et al., 2017; Rodenas-Ruano et al., 2012; Sanz-Clemente et al., 2010, Sanz-Clemente et al., 2013). Opioid effects, including tolerance and reward, were reduced in *Grin2a* knockout mice (Miyamoto et al., 2004).

In the present study, STRs and VNTR in the *CNR1*, *GRIN2A*, *PDYN*, and *PENK* genes were examined to assess genetic vulnerability to peripheral pain sensation and analgesic requirements for opioids, based on the latency to cold or mechanical pain perception, frequency of fentanyl and analgesic use, dose of fentanyl and analgesic use, and visual analog scale (VAS) score after surgery in postoperative pain management.

MATERIALS AND METHODS

Participants

The present study was conducted with clinical data from 192 participants to assess peripheral pain sensation, 139 patients who

underwent major abdominal surgery, and 252 patients who underwent orthognathic cosmetic surgery. Volunteers who lived in the Kanto area of Japan were enrolled in the study to assess peripheral pain sensation. The patients who underwent major open abdominal surgery with combined general and epidural anesthesia were enrolled at the Research Hospital, Institute of Medical Science, The University of Tokyo, or Toho University Sakura Hospital. Patients who were scheduled to undergo orthognathic cosmetic surgery (bilateral mandibular sagittal split ramus osteotomy) for mandibular prognathism were enrolled at Tokyo Dental College Suidoubashi Hospital. All of the subjects provided written informed consent before participating in the study.

The study protocol was approved by each Institutional Review Board at the Institute of Medical Science, The University of Tokyo (Tokyo, Japan), Toho University Sakura Hospital (Chiba, Japan), Tokyo Dental College (Chiba, Japan), and the Tokyo Metropolitan Institute of Medical Science (Tokyo, Japan).

Clinical Data on Peripheral Pain Sensation and Analgesic Requirements of Opioids

In the study of peripheral pain sensation, latencies to cold and mechanical pain perception were measured in the cold pressor- and mechanical stimulation-induced pain tests, respectively. The cold pressor-induced pain test was slightly modified from original methods (Bisgaard et al., 2001; Martikainen et al., 2004). Briefly, each index and middle finger was placed in ice-cold water up to the second joint, and the time to feel a pain sensation was measured with a 15 s cut-off time to prevent tissue damage. The average of the two fingers was considered the latency to cold pain perception. A DPS-20 digital force gauge (Imada, Northbrook, IL, United States) was used in the mechanical stimulation-induced pain test. The nail of each index finger to pinky finger was pressed with the digital force gauge, and the force to feel pain sensation was recorded. The average of the four fingers was considered the latency to mechanical pain perception (Nishizawa et al., 2014).

Postoperative pain management after open abdominal surgery was previously described (Hayashida et al., 2008). Briefly, postoperative pain management was primarily performed with continuous epidural anesthesia with fentanyl or morphine. For patients who complained of significant postoperative pain despite the administration of continuous epidural analgesics, appropriate doses of opioids, including morphine, buprenorphine, pentazocine, and pethidine, and/or nonsteroidal antiinflammatory drugs (NSAIDs), including diclofenac and flurbiprofen, were systemically administered as rescue analgesics and antipyretics. The doses of opioids and NSAIDs that were administered as rescue analgesics during the postoperative period were converted to equivalent doses of systemic pentazocine. The frequency of rescue analgesic use during the 24 h postoperative period, total dose of rescue analgesics during the 24 h postoperative period (converted to equivalent doses of systemic pentazocine), and total dose of rescue analgesics, excluding antipyretics, during the 24 h postoperative period (converted to equivalent doses of systemic pentazocine) were calculated and analyzed.

The clinical data on postoperative pain management after orthognathic cosmetic surgery were previously reported (Fukuda et al., 2009). Briefly, intravenous patient-controlled analgesia (PCA) with 20 μg/ml fentanyl began immediately after tracheal extubation using a CADD-Legacy PCA pump (Smiths Medical Japan, Tokyo, Japan). A bolus dose of fentanyl (20 μg) was administered upon patient request. Patient-controlled analgesia was continued during the 24 h postoperative period. The frequency and dose of fentanyl (μg/kg) during the postoperative period were calculated from PCA pump records and normalized to body weight. The intensity of pain sensation was assessed at 3 and 24 h postoperatively using a 100 mm VAS, with 0 mm indicating no pain and 100 mm indicating the worst pain imaginable.

Genotyping

Either whole blood or oral mucosa samples were collected from all subjects for the genetic analysis. DNA was extracted from whole blood or oral mucosa samples using the conventional phenol-chloroform method or QIAamp DNA Mini Kit (Qiagen K.K., Tokyo, Japan) according to the manufacturer's instructions.

Genotyping STRs in the *CNR1*, *GRIN2A*, and *PENK* genes was performed by Aoba Genetics, Inc., (Yokohama, Japan). Approximately 15 ng of genomic DNA from each participant was used as the template for genotyping using polymerase chain reaction (PCR) with fluorescent dye-labeled primers and an ABI PRISM 3130xl Genetic Analyzer (Applied Biosystems Japan, Tokyo, Japan). Briefly, PCRs were performed with a 5′-VIC-labeled specific forward primer for each STR and Invitrogen AccuPrime *Taq* DNA polymerase, High Fidelity (Thermo Fisher Scientific K.K., Tokyo, Japan), under the following conditions: 94°C for 2 min, 35 cycles of 94°C for 30 s, 57°C for 30 s, and 68°C for 30 s, followed by 68°C for 7 min. The specific primers for STRs in the *CNR1*, *GRIN2A*, and *PENK* genes were the following: *CNR1* STR (forward, 5′-GCTGCTTCTGTTAACCCTGC-3′; reverse, 5′-TACATCTCCGTGTGATGTTCC-3′), *GRIN2A* STR (forward, 5′-GAAGGAAGCATGTGGGAAATGCAG-3′; reverse, 5′-GTTTCTTGCTGGGTACAGTTATCCCCCT-3′), *PENK* STR forward, 5′-TAATAAAGGAGCCAGCTATG-3′; reverse, 5′-ACATCAGATGTAAATGCAAGT-3′; Chan et al., 1994; Comings et al., 1997; Itokawa et al., 2003). The nucleotide lengths of the PCR products were determined using an ABI PRISM 3130xl Genetic Analyzer and GeneMapper 4.0 software (Applied Biosystems Japan). To evaluate the actual repeat numbers of the STRs, direct sequencing was performed with PCR products that were amplified from samples whose repeat numbers were determined to be homozygous by GeneMapper (**Supplementary Material**). The cycle sequencing reaction with the BigDye Terminator 3.1 Cycle Sequencing Kit (Applied Biosystems Japan) was performed according to the manufacturer's instructions, and the reaction products were purified. Nucleotide sequences of the products, including the STRs, were determined using an ABI PRISM 3100 Genetic Analyzer (Applied Biosystems Japan).

TABLE 1 | Patients' demographic and clinical data.

Demographic data	Clinical data
Volunteers:	
Number of patients (male/female)	192 (121/71)
Age (years)	36.14 ± 12.69 (20–65)
Peripheral pain sensation-related traits:	
Latency to cold pain perception (s)	23.75 (17.13–36.88); 6.00–180.00
Latency of mechanical pain perception (kg)	2.30 (1.79–3.02); 0.77–5.31
Patients who underwent open abdominal surgery:	
Number of patients (male/female)	139 (81/58)
Age (years)	63.63 ± 9.96 (28–80)
Body weight (kg)	56.52 ± 10.44 (35–80)
BMI (kg/m^2)	22.47 ± 3.50 (14.50–35.03)
Analgesic requirements of opioid-related traits:	
Frequency of analgesic use during the 24 h postoperative period	0 (0–1); 0–6
24 h postoperative analgesic dose converted to systemic pentazocine (mg)	0.00 (0.00–15.00); 0.00–135.00
24 h postoperative analgesic dose (including epidural analgesics) converted to systemic pentazocine (mg)	127.50 (96.00–177.00); 36.00–315.00
Patients who underwent orthognathic cosmetic surgery:	
Number of patients (male/female)	252 (89/163)
Age (years)	25.58 ± 7.44 (15–50)
Body weight (kg)	58.22 ± 11.23 (38–128)
BMI (kg/m^2)	21.36 ± 3.02 (14.88–37.10)
Analgesic requirements of opioid-related traits:	
Frequency of fentanyl use during the 24 h postoperative period	6 (3–12); 0–111
24 h postoperative fentanyl dose (μg/kg)	2.32 (1.14–4.08); 0.00–13.82
VAS pain score at 3 h (mm)	25 (13–48); 0–90
VAS pain score at 24 h (mm)	24 (10–40); 0–83

The data are expressed as numbers, mean ± standard deviation (range), or median (interquartile range); range.

Genotyping for the 68 bp VNTR in the *PDYN* gene was previously described (Zimprich et al., 2000). Briefly, PCRs were performed with the primers 5′-AGCAATCAGAGGTTG AAGTTGGCAGC-3′ and 5′-GCACCAGGCGGTTAGGTA GAGTTGTC-3′ under the following thermal cycle conditions: 95°C for 2 min, 35 cycles of 95°C for 30 s, 70°C for 30 s, and 72°C for 1 min, followed by 72°C for 8 min. The 68 bp repeat number of each sample was determined by electrophoretic mobility of the PCR product in agarose gel electrophoresis.

Statistical Analysis

All of the statistical analyses were performed using SPSS Statistics 24 software (IBM Japan Ltd., Tokyo, Japan). All of the clinical data, including the participants' demographic data and analgesic requirements of opioids after open abdominal surgery and orthognathic cosmetic surgery, were first analyzed for normal probability distributions and homoscedastic variance using the Kolmogorov-Smirnov test and *F*-test, respectively. These clinical parameters did not have a normal probability distribution; thus, subsequent statistical analyses were performed using nonparametric methods. Associations between the participants' demographic characteristics and clinical data, including peripheral pain sensation and analgesic requirements of opioids, were examined using the Mann-Whitney *U* test. Associations between variances of STRs or VNTRs and clinical data were statistically analyzed using the Spearman's rank correlation test. Multiple-testing corrections were performed using Holm's method to adjust p values that were derived from multiple comparisons in the association analyses. Values of $p < 0.05$ were considered statistically significant.

RESULTS

The present study included three association analyses with clinical data on peripheral pain sensation and analgesic requirements of opioids after open abdominal surgery and orthognathic cosmetic surgery (**Table 1**). The distributions of the participants' demographic data, including age, body weight, and body mass index (BMI), were different between the association analyses. The distribution of the age of patients who underwent open abdominal surgery was significantly different from participants whose peripheral pain sensation was assessed and patients who underwent orthognathic cosmetic surgery (U = 1,363.50 and U = 219.50, respectively, $p < 0.001$, Mann-Whitney *U* test). The distribution of the participants' ages in the study of peripheral pain sensation was significantly associated with latencies to cold and mechanical pain perception (Spearman's rank correlation coefficient $\rho = 0.324$, $p < 0.001$, and $\rho = 0.185$, $p < 0.05$, respectively). The latency to mechanical pain perception were significantly different between sexes (U = 2306.50, $p < 0.001$, Mann-Whitney *U* test). The latency to cold pain perception was associated with mechanical pain perception ($\rho = 0.366$, $p < 0.001$). The distribution of ages of patients who underwent open abdominal surgery was significantly associated with the frequency of analgesic use during the 24 h postoperative period ($\rho = -0.168$, $p < 0.05$). The body weight and BMI distributions for patients who underwent orthognathic cosmetic surgery were significantly associated with 24 h postoperative fentanyl dose ($\rho = -0.164$, $p < 0.01$, and $\rho = -0.144$, $p < 0.05$, respectively).

We focused on STRs in the *CNR1*, *GRIN2A*, and *PENK* genes and VNTRs in the *PDYN* gene and examined whether STRs and

TABLE 2 | Short tandem repeats analyzed in the present study.

Gene	Coding protein	dbSNP rs#	Position	Location in gene	STR/ VNTR
CNR1	cannabinoid receptor 1	rs72426053, rs1562491880, rs1244069759, rs1164873271	6q15	3′ flanking region	(AAT)n
GRIN2A	Ionotropic glutamate receptor NMDA type subunit 2A	rs3219790	16p13.2	5′ flanking region	(GT)n
PENK	proenkephalin	rs3138832	8q12.1	3′ flanking region	(CA)n
PDYN	prodynorphin	rs1568548100, rs869080647, rs1568548112, rs1568548137, rs1568548201	20p13	5′ flanking region	(68 bp)n

TABLE 3 | Associations between S and L alleles of STRs and peripheral pain sensation.

		CNR1		***GRIN2A***		***PENK***		***PDYN***	
		S allele	**L allele**	**S allele**	**L allele**	**S allele**	**L allele**	**S allele**	**L allele**
Number of repeats:Number of alleles (allelic frequency in S and L alleles)		9: 43 (0.224)	9: 1 (0.005)	20: 25 (0.130)	20: 1 (0.005)	12: 31 (0.161)	12: 1 (0.005)	1: 13 (0.068)	
		12: 22 (0.115)	12: 1 (0.005)	21: 9 (0.047)	21: 2 (0.010)	13: 91 (0.474)	13: 32 (0.167)	2: 171 (0.891)	2: 141 (0.734)
		13: 9 (0.047)		22: 20 (0.104)	22: 5 (0.026)	14: 68 (0.354)	14: 155 (0.807)	3: 8 (0.042)	3: 48 (0.250)
		14: 48 (0.250)	14: 15 (0.078)	23: 27 (0.141)	23: 3 (0.016)		15: 2 (0.01)		4: 3 (0.016)
		15: 54 (0.281)	15: 80 (0.417)	24: 28 (0.146)	24: 12 (0.063)				
		16: 13 (0.068)	16: 75 (0.391)	25: 65 (0.339)	25: 66 (0.344)				
		17: 1 (0.005)	17: 18 (0.094)	26: 9 (0.047)	26: 29 (0.151)				
				27: 6 (0.031)	27: 42 (0.219)				
				28: 1 (0.005)	28: 17 (0.089)				
				29: 2 (0.010)	29: 7 (0.036)				
					31: 5 (0.026)				
					32: 1 (0.005)				
					34: 1 (0.005)				
				35: 1 (0.005)					
Latency to cold pain perception	ρ	−0.047	0.027	0.003	−0.035	0.019	−0.041	0.079	−0.019
	p	0.520	0.713	0.963	0.632	0.796	0.571	0.277	0.790
Latency to mechanical pain perception	ρ	−0.077	0.125	−0.036	0.015	−0.021	−0.048	0.011	-0.115
	p	0.293	0.086	0.622	0.837	0.774	0.511	0.878	0.112

Spearman's rank correlation tests were conducted to examine associations between shorter (S) and longer (L) alleles in each STR or VNTR and the latency to pain perception. ρ: Spearman's rank correlation coefficient.

VNTRs in these genes were associated with peripheral pain sensation and analgesic requirements of opioids. Short tandem repeats in the *CNR1*, *GRIN2A*, and *PENK* genes were AAT trinucleotide, GT dinucleotide, and CA dinucleotide repeat polymorphisms, respectively. The VNTR in the *PDYN* gene was 68 bp repeats (**Table 2**). These repeat polymorphisms widely varied with many alleles (repeat number) and genotypes (repeat number/repeat number). Two alleles of STRs and VNTRs in each subject were defined as shorter (S) and longer (L) alleles according to their repeat numbers in each patient. Associations between STRs or VNTRs and the clinical data were analyzed according to the S and L alleles of each STR.

The distribution of the STR in the *CNR1* gene showed a large repeat number and wide variation as 9–18 repeats (6-7 variations) in the both S and L alleles (**Table 3**). In contrast, although the repeat number of the STR in the *GRIN2A* gene was also as large as 20–35 (14 variations), the distributions of repeat numbers were different between the S and L alleles (S allele: 20–29 repeats; L allele: 20–35 repeats). Variations of the STR in the *PENK* gene and VNTR in the *PDYN* gene were as low as five variations (11–15 repeats) and four variations (1–4 repeats), respectively. Associations between STRs or VNTRs and clinical data on peripheral pain sensation, including latencies to cold and mechanical pain perception, were examined using the

TABLE 4 | Associations between S and L alleles of STRs and postoperative analgesia in patients who underwent open abdominal surgery.

		CNR1		*GRIN2A*		*PENK*		*PDYN*	
		S allele	**L allele**	**S allele**	**L allele**	**S allele**	**L allele**	**S allele**	**L allele**
Number of repeats:Number of alleles (allelic frequency in S and L alleles)		9: 19 (0.137)	9: 3 (0.022)	20: 15 (0.108)	20: 3 (0.022)	11: 1 (0.007)		1: 17 (0.122)	
		10: 1 (0.007)		21: 11 (0.079)	21: 3 (0.022)	12: 22 (0.158)	12: 2 (0.014)	2: 119 (0.856)	2: 98 (0.705)
		11: 1 (0.007)		22: 15 (0.108)	22: 2 (0.014)	13: 59 (0.424)	13: 21 (0.151)	3: 3 (0.022)	3: 36 (0.259)
		12: 14 (0.101)	12: 1 (0.007)	23: 15 (0.108)	23: 4 (0.029)	14: 57 (0.410)	14: 110 (0.791)		4: 5 (0.036)
		13: 8 (0.058)	13: 1 (0.007)	24: 27 (0.194)	24: 12 (0.086)		15: 6 (0.043)		
		14: 28 (0.201)	14: 10 (0.072)	25: 39 (0.281)	25: 34 (0.245)				
		15: 49 (0.353)	15: 45 (0.324)	26: 11 (0.079)	26: 24 (0.173)				
		16: 13 (0.094)	16: 60 (0.432)	27: 6 (0.043)	27: 24 (0.173)				
			17: 12 (0.086)		28: 16 (0.115)				
			18: 1 (0.007)		29: 6 (0.043)				
					30: 3 (0.022)				
					31: 4 (0.029)				
					32: 2 (0.014)				
					33: 1 (0.007)				
					34: 1 (0.007)				
Frequency of analgesic use	ρ	–0.153	–0.140	-0.093	0.015	0.107	–0.010	–0.066	0.029
	p	0.078	0.109	0.275	0.859	0.211	0.903	0.437	0.735
Analgesic dose	ρ	–0.134	–0.121	–0.104	–0.005	0.099	–0.005	–0.009	0.046
	p	0.123	0.165	0.221	0.953	0.246	0.954	0.915	0.592
Analgesic dose including epidural analgesics	ρ	0.068	–0.050	–0.200	0.009	0.050	0.028	–0.048	0.011
	p	0.440	0.566	0.018	0.914	0.557	0.745	0.575	0.900

Spearman's rank correlation tests were conducted to examine associations between shorter (S) and longer (L) alleles in each STR or VNTR and the frequency of analgesic use during the 24 h postoperative period (frequency of analgesic use), 24 h postoperative analgesic dose converted to systemic pentazocine (analgesic dose), and 24 h postoperative analgesic dose, including epidural analgesics (analgesic dose, including epidural analgesics). ρ: Spearman's rank correlation coefficient.

Spearman's rank correlation test after the correction for age and sex. The repeat number of the L allele of the *CNR1* STR was slightly associated with the latency to mechanical pain perception in male volunteers (Spearman's rank correlation coefficient $\rho = 0.186$, $p = 0.043$), but this association was not confirmed after multiple-testing correction using the Holm method for each STR.

Repeat numbers of STRs and VNTRs in patients who underwent open abdominal surgery showed a similar distribution as participants whose peripheral pain sensation was assessed (**Table 4**). The surgical procedures for open abdominal surgery mostly included gastrectomy for gastric cancer and colectomy for colorectal cancer. The frequency of analgesic use during the 24 h postoperative period (frequency of analgesic use), 24 h postoperative analgesic dose (converted to systemic pentazocine; analgesic dose), and 24 h postoperative analgesic dose, including epidural analgesics (analgesic dose including epidural analgesics) were analyzed as an index for analgesic requirements of opioids in this association analysis. The repeat variation of the S allele of the *GRIN2A* STR was significantly associated with analgesic dose, including epidural analgesics (Spearman rank correlation coefficient $\rho = -0.200$, $p = 0.018$), but this association was not confirmed after multiple-testing correction using the Holm method for each STR.

Repeat numbers of the STRs and VNTRs in patients who underwent orthognathic cosmetic surgery showed a similar distribution as participants whose peripheral pain sensation was assessed (**Table 5**). The index for analgesic requirements of opioids, including the frequency of fentanyl use during the 24 h postoperative period (frequency of fentanyl use), 24 h postoperative fentanyl dose (fentanyl dose), VAS pain score at 3 h, and VAS pain score at 24 h, were analyzed. The repeat number of the L allele of the *PENK* STR was significantly associated with VAS pain score at 24 h (Spearman's rank correlation test; $\rho = 0.143$, $p = 0.023$), but no significant association was found after Holm's multiple-testing correction. The repeat number of the S allele of the *CNR1* STR was significantly associated with the frequency of fentanyl use, fentanyl dose, and VAS pain score at 3 h ($\rho = 0.199$, $p = 0.002$, $\rho = 0.174$, $p = 0.006$, and $\rho = 0.135$, $p = 0.033$, respectively). Associations with the frequency of fentanyl use and fentanyl dose were also statistically significant after Holm's multiple-testing correction.

TABLE 5 | Associations between S and L alleles of STRs and postoperative analgesia in patients who underwent orthognathic cosmetic surgery.

		CNR1		*GRIN2A*		*PENK*		*PDYN*	
		S allele	**L allele**	**S allele**	**L allele**	**S allele**	**L allele**	**S allele**	**L allele**
Number of repeats:Number of alleles (allelic frequency in S and L alleles)		9: 41 (0.163) 12: 30 (0.119) 13: 8 (0.032) 14: 55 (0.218) 15: 96 (0.381) 16: 20 (0.079) 17: 1 (0.004)	9: 2 (0.008) 12: 3 (0.012) 14: 27 (0.107) 15: 76 (0.302) 16: 125 (0.496) 17: 17 (0.067) 18: 1 (0.004)	18: 1 (0.004) 19: 1 (0.004) 20: 28 (0.111) 21: 17 (0.067) 22: 28 (0.111) 23: 42 (0.167) 24: 43 (0.171) 25: 61 (0.242) 26: 18 (0.071) 27: 11 (0.044) 28: 1 (0.004)	20: 1 (0.004) 21: 1 (0.004) 22: 5 (0.020) 23: 3 (0.012) 24: 19 (0.075) 25: 91 (0.361) 26: 46 (0.183) 27: 43 (0.171) 28: 20 (0.079) 29: 7 (0.028) 30: 3 (0.012) 31: 2 (0.008) 32: 7 (0.028) 33: 2 (0.008) 35: 1 (0.004)	12: 34 (0.135) 13: 127 (0.504) 14: 90 (0.357)	13: 39 (0.155) 14: 209 (0.829) 15: 3 (0.012)	1: 9 (0.083) 2: 94 (0.870) 3: 4 (0.037)	2: 68 (0.630) 3: 35 (0.324) 4: 5 (0.046)
Frequency of fentanyl use	ρ	0.199 *	–0.006	–0.070	–0.020	0.021	0.081	–0.152	–0.079
	p	0.002	0.922	0.268	0.750	0.746	0.200	0.117	0.415
Fentanyl dose	ρ	0.174 *	–0.016	–0.103	–0.044	0.053	0.070	–0.132	–0.118
	p	0.006	0.802	0.106	0.486	0.408	0.269	0.173	0.226
VAS pain score at 3 h	ρ	0.135	0.036	0.003	0.078	–0.067	0.085	–0.025	–0.060
	p	0.033	0.569	0.957	0.219	0.293	0.181	0.796	0.540
VAS pain score at 24 h	ρ	0.059	–0.061	0.000	–0.076	0.015	0.143	–0.031	–0.103
	p	0.354	0.340	0.994	0.230	0.815	0.023	0.752	0.289

*Spearman's rank correlation tests were conducted to examine associations between shorter (S) and longer (L) alleles in each STR or VNTR and the frequency of fentanyl use during the 24 h postoperative period (frequency of fentanyl use), 24 h postoperative fentanyl dose (fentanyl dose), VAS pain score at 3 h, and VAS pain score at 24 h. ρ: Spearman's rank correlation coefficient. *p < 0.05, significant difference between repeat number of STR and postoperative analgesia after Holm's multiple-testing correction.*

DISCUSSION

The present study was performed with clinical data on peripheral pain sensation and analgesic requirements of opioids in patients who underwent open abdominal surgery and orthognathic cosmetic surgery. The frequency of fentanyl use during the 24 h postoperative period in patients who underwent orthognathic cosmetic surgery showed a wide distribution in the range of 0–111 (**Table 1**). The lockout time of the PCA pump was set at 10 min. Thus, patients could receive fentanyl at most 144 times during the 24 h postoperative period. The VAS scores of the patient who received fentanyl 111 times were 5 and 25 at 3 and 24 h postoperatively, respectively. The duration of anesthesia and surgery for this patient was 185 min (interquartile range: 156, 185) and 120 min (interquartile range: 90, 119), respectively. This patient was included in the study because this patient met all of the inclusion criteria and none of the exclusion criteria. In the participants' demographic data, age was positively associated with latencies to cold and mechanical pain perception (Spearman's rank correlation coefficient $\rho = 0.324$, $p < 0.001$, and $\rho = 0.185$, $p < 0.05$, respectively). Thus, pain sensitivity was considered to decrease with age. The age of the patients who underwent open abdominal surgery was also negatively associated with the frequency of analgesic use (Spearman rank correlation coefficient $\rho = -0.168$, $p = 0.049$). The lower frequency of analgesic use would be caused by lower pain sensitivity in older patients. The latency to mechanical pain perception in females was lower than in males (Mann-Whitney $U = 6284.50$, $p < 0.001$), but no difference in cold pain perception was found between sexes, indicating that females are more sensitive to mechanical pain but not too cold pain compared with males (data not shown). The latency to cold pain perception was measured by the cold-pressor test immediately before surgery in patients who underwent orthognathic cosmetic surgery. In patients who underwent open abdominal surgery, the latencies to cold and mechanical pain perception were not examined. The cold-pressor test was slightly different from the peripheral pain perception test that was performed in volunteers (Fukuda et al., 2009). The distribution of the latency to cold pain perception in patients who underwent orthognathic cosmetic surgery was 2.0–150 s (median: 14.0, interquartile range: 9.0, 23.0) and was slightly associated with fentanyl dose and VAS pain score at 24 h (Spearman rank correlation coefficient $\rho = -0.128$, $p = 0.042$, and $\rho = -0.126$, $p = 0.047$, respectively), but these associations were not confirmed after multiple-testing correction using the Holm method to analyze the latency to cold pain perception with four clinical parameters, including the frequency of fentanyl use, fentanyl dose, VAS pain score at 3 h, and VAS pain score at 24 h. The distribution of the latency to cold pain perception in patients who underwent orthognathic cosmetic surgery was not associated with the patients' ages ($\rho = -0.022$, $p = 0.734$).

The low standard deviation of the patients' ages (mean ± standard deviation: 25.58 ± 7.44 years; **Table 1**) suggested that patients who underwent orthognathic cosmetic surgery and enrolled in the study were within a narrow age range and may be expected to be uniform with regard to pain perception.

Variations of repeat numbers were different between three STRs and VNTRs in the present study. The repeat numbers and variations of STRs in the *CNR1*, *GRIN2A*, and *PENK* genes were 9–18 repeats (10 variations), 18–35 repeats (18 variations), and 11–15 repeats (five variations), respectively. On the contrary, the repeat number and variation of the VNTR in the *PDYN* gene was 1-4 repeats and four variations. The repeat numbers of STRs in the *CNR1*, *GRIN2A*, and *PENK* genes were large, rather than the VNTR in the *PDYN* gene. Among these STRs, high variations of repeat numbers of STRs were found in the *CNR1* and *GRIN2A* genes rather than the *PENK* gene, indicating that not all STR variations are high. Replication slippage events outnumber point mutations by one or two orders of magnitude in STRs (Pumpernik et al., 2008). Mutations that are caused by DNA slippage in STRs occurred without a minimal threshold length, and mutation rates decreased and increased with the repeat length and total length of STRs, respectively (Leclercq et al., 2010), which can support the difference in repeat number variations between STRs in the *CNR1*, *GRIN2A*, and *PENK* genes. However, mutation rates in STRs converged at the upper limit (0.001–0.01) at over 20 nucleotides of the total length of STRs, although the repeat length and differences in STR variations (e.g., repeat number and total length of STRs) could be influenced by other factors, such as chromosomal background near the STRs. The STR in the *CNR1* gene showed multiple peaks in the distribution of repeat numbers at 9–12 and 15 repeats. This unusual allelic distribution of the STR in the *CNR1* gene was described in previous studies, which suggests our data on allelic distribution in the *CNR1* gene was not a genotyping error (Comings et al., 1997; Li et al., 2000; Siegfried et al., 2004; Ruiz-Contreras et al., 2013). The present study was conducted with different races and ethnicities, indicating that the multiple peaks of allelic frequency of the STR in the *CNR1* gene was not attributable to racial or ethnic differences in allelic frequency. Such multiple peaks of the allelic frequency of STRs were also shown at another microsatellite loci, DYS385a/b in the Y chromosome, although allelic frequencies of most STRs had a single peak (Kayser et al., 2000). Considering these studies together, the mutation rate in the *CNR1* STR would change at multiple stages with the length of the STR, which would be a structural characteristic of the STR in the *CNR1* gene.

Short tandem repeats have been reported to be associated with gene expression and human traits (Jakubosky et al., 2020). Approximately 2,000 significant expression STRs colocalized with regulatory elements and were considered to modulate certain histone modifications (Gymrek et al., 2016). These expression STRs also contributed 10–15% of the heritability that was mediated by all common variants and were enriched in various clinical conditions that were reported by genome-wide association studies. Expression-mediating VNTRs also exerted a strong influence on the expression of proximal genes, and 80% of these VNTRs have a maximum effect size of at least 0.3 (Bakhtiari et al., 2021). Short tandem repeats and VNTRs in regulatory elements of genes can influence gene expression. The influence of each allele of STRs and VNTRs on gene expression would be expected to be different according to lengths of STRs and VNTRs. If the elongation of an STR is recessive for a phenotype, then the phenotype would be attributable to the S allele of the STR. Conversely, if the elongation of an STR is dominant for a phenotype, then the phenotype would be attributable to the L allele of the STR. Investigating STRs and VNTRs according to the S and L alleles rather than according to groups that are divided by the threshold of the length of STRs and VNTRs effectively assesses the genetic vulnerability to a phenotype. In the present study, the S allele of the AAT trinucleotide STR in the *CNR1* gene was positively associated with the frequency and dose of postoperative fentanyl use in patients who underwent orthognathic cosmetic surgery, indicating that analgesic effects of opioids would be low in patients with long AAT repeats. The elongation of AAT repeats of the STR in the *CNR1* gene would be recessive for the analgesic effects of opioids in patients who underwent orthognathic cosmetic surgery. The protein expression of CNR1 in lymphocytes from patients with long AAT repeats of the STR in the *CNR1* gene (≥12 repeats in both alleles) was significantly lower than in patients with short AAT repeats (homozygous or heterozygous for alleles with ≤11 repeats; Rossi et al., 2013). This report also indicated that the long repeat of the STR in the *CNR1* gene would be recessive for phenotypes that are related to the *CNR1* gene. AAT STRs are the most representative trinucleotide repeats in the human genome, but they are less frequent in exons (Kozlowski et al., 2010). AAT STRs are mainly located in the 3′-untranslated region (UTR). The 3′UTRs of genes are related to the stability of mRNA, and extension of the 3′UTR generally causes lower stability and expression of mRNA. The lower protein expression of CNR1 in carriers of long AAT repeats of the *CNR1* STR may be caused by the lower stability of *CNR1* mRNA.

Short tandem repeats in the *CNR1* gene were reported to be associated with the vulnerability to irritable bowel syndrome (Park et al., 2011; Jiang et al., 2014), multiple sclerosis (Ramil et al., 2010; Rossi et al., 2011, 2013), schizophrenia (Ujike et al., 2002; Martínez-Gras et al., 2006), and substance use disorders (Comings et al., 1997; Zhang et al., 2004; Ballon et al., 2006). The T2-weighted lesion load was inversely correlated with gray matter volume in the left frontal and cingulate cortex and right temporal cortex in multiple sclerosis patients with long AAT repeats of the *CNR1* STR (Rossi et al., 2013). The previous study indicated the possibility that some gray matter regions that are related to the analgesic effects of opioids would be vulnerable to inflammatory stimulation in carriers of long AAT repeats of the *CNR1* STR. Additionally, CNR1 colocalized with μ-opioid receptors in the same presynaptic nerve terminals in the nucleus accumbens, caudate putamen, and dorsal horn in rats (López-Moreno et al., 2010). A positive allosteric modulator of CNR1 signaling enhanced morphine antinociception in mice (Slivicki et al., 2020). These results indicate the critical role of the endogenous cannabinoid system *via* CNR1 in modulating the analgesic effects of opioids for orofacial surgery.

Genetic contributions to analgesic effects of opioids are influenced by psychological and environmental factors, including race, ethnicity, culture, and pain sensation status. To further elucidate genetic variability of the STR in the *CNR1* gene that contributes to analgesic effects of opioids, replication studies will be required in different races/ethnicities with sufficient sample sizes for each effect size. Additionally, elucidating the molecular mechanisms that underlie the association between repeat polymorphisms, including STRs and VNTRs, and analgesic effects of opioids may lead to a precise understanding of individual differences in analgesic effects of opioids and improve treatment strategies for pain.

DATA AVAILABILITY STATEMENT

The datasets presented in this study can be found in online repositories. The names of the repository/repositories and accession number(s) can be found in the article/ **Supplementary Material**.

ETHICS STATEMENT

The studies involving human participants were reviewed and approved by Human Research Ethics Review Board (Institute of Medical Science, The University of Tokyo) Human Research Ethics Review Board (Toho University Sakura Hospital) Human Research Ethics Review Board (Tokyo Dental College) Human Research Ethics Review Board (Tokyo Metropolitan Institute of Medical Science). Written informed consent to participate in this study was provided by the participants' legal guardian/next of kin.

AUTHOR CONTRIBUTIONS

SK designed the study, involved in genotyping, and performed statistical data analysis, data interpretation, and manuscript drafting. DN involved in interpretation of clinical data. JH involved in genotyping. KF, TI, MN, and MH involved in collection of clinical data and DNA samples. KI conceived the study and performed data interpretation. All authors contributed to the manuscript and approved the submitted version.

FUNDING

This study was supported by Grants-in-Aid for Scientific Research from JSPS JP16H06276 AdAMS, 21H03028, and 19KK0225.

ACKNOWLEDGMENTS

The authors thank Mr M Arends for proofreading the manuscript. The authors are grateful to all of the participants and patients who enrolled in the study and the anesthesiologists and surgeons at the Research Hospital of the Institute of Medical Science, Toho University Sakura Hospital, and Tokyo Dental College Suidoubashi Hospital for collecting blood and oral mucosa samples and clinical data.

SUPPLEMENTARY MATERIAL

The Supplementary Material for this article can be found online at: https://www.frontiersin.org/articles/10.3389/fgene.2022.815089/full#supplementary-material

REFERENCES

Angst, M. S., Lazzeroni, L. C., Phillips, N. G., Drover, D. R., Tingle, M., Ray, A., et al. (2012b). Aversive and Reinforcing Opioid Effects. *Anesthesiology* 117, 22–37. doi:10.1097/ALN.0b013e31825a2a4e

Angst, M. S., Phillips, N. G., Drover, D. R., Tingle, M., Ray, A., Swan, G. E., et al. (2012a). Pain Sensitivity and Opioid Analgesia: a Pharmacogenomic Twin Study. *Pain* 153, 1397–1409. doi:10.1016/j.pain.2012.02.022

Aubrun, F., Langeron, O., Quesnel, C., Coriat, P., and Riou, B. (2003). Relationships between Measurement of Pain Using Visual Analog Score and Morphine Requirements during Postoperative Intravenous Morphine Titration. *Anesthesiology* 98, 1415–1421. doi:10.1097/00000542-200306000-00017

Bagasrawala, I., Memi, F., V. Radonjić, N., and Zecevic, N. (2017). *N*-methyl D-Aspartate Receptor Expression Patterns in the Human Fetal Cerebral Cortex. *Cereb. Cortex* 27, 5041–5053. doi:10.1093/cercor/bhw289

Bakhtiari, M., Park, J., Ding, Y.-C., Shleizer-Burko, S., Neuhausen, S. L., Halldórsson, B. V., et al. (2021). Variable Number Tandem Repeats Mediate the Expression of Proximal Genes. *Nat. Commun.* 12, 2075. doi:10.1038/s41467-021-22206-z

Ballon, N., Leroy, S., Roy, C., Bourdel, M. C., Charles-Nicolas, A., Krebs, M. O., et al. (2006). (AAT)n Repeat in the Cannabinoid Receptor Gene (CNR1): Association with Cocaine Addiction in an African-Caribbean Population. *Pharmacogenomics J.* 6, 126–130. doi:10.1038/sj.tpj.6500352

Bastami, S., Gupta, A., Zackrisson, A.-L., Ahlner, J., Osman, A., and Uppugunduri, S. (2014). Influence ofUGT2B7,OPRM1andABCB1 Gene Polymorphisms on Postoperative Morphine Consumption. *Basic Clin. Pharmacol. Toxicol.* 115, 423–431. doi:10.1111/bcpt.12248

Bisgaard, T., Klarskov, B., Rosenberg, J., and Kehlet, H. (2001). Characteristics and Prediction of Early Pain after Laparoscopic Cholecystectomy. *Pain* 90, 261–269. doi:10.1016/S0304-3959(00)00406-1

Brinkmann, B., Klintschar, M., Neuhuber, F., Hühne, J., and Rolf, B. (1998). Mutation Rate in Human Microsatellites: Influence of the Structure and Length of the Tandem Repeat. *Am. J. Hum. Genet.* 62, 1408–1415. doi:10.1086/301869

Brookes, K. J. (2013). The VNTR in Complex Disorders: the Forgotten Polymorphisms? A Functional Way Forward. *Genomics* 101, 273–281. doi:10.1016/j.ygeno.2013.03.003

Candiotti, K., Yang, Z., Xue, L., Zhang, Y., Rodriguez, Y., Wang, L., et al. (2013). Single-nucleotide Polymorphism C3435T in the ABCB1 Gene Is Associated with Opioid Consumption in Postoperative Pain. *Pain Med.* 14, 1977–1984. doi:10.1111/pme.12226

Chan, R. J., McBride, A. W., Thomasson, H. R., Ykenney, A., and Crabb, D. W. (1994). Allele Frequencies of the Preproenkephalin A (*PENK*) Gene CA Repeat in Asians, African-Americans, and Caucasians: Lack of Evidence for Different Allele Frequencies in Alcoholics. *Alcohol. Clin. Exp. Res.* 18, 533–535. doi:10.1111/j.1530-0277.1994.tb00905.x

Chen, A. C. H., LaForge, K. S., Ho, A., McHugh, P. F., Kellogg, S., Bell, K., et al. (2002). Potentially Functional Polymorphism in the Promoter Region of Prodynorphin Gene May Be Associated with protection against Cocaine

Dependence or Abuse. *Am. J. Med. Genet.* 114, 429–435. doi:10.1002/ajmg.10362

Comings, D. E., Blake, H., Dietz, G., Gade-Andavolu, R., Legro, R. S., Saucier, G., et al. (1999). The Proenkephalin Gene (*PENK*) and Opioid Dependence. *Neuroreport* 10, 1133–1135. doi:10.1097/00001756-199904060-00042

Comings, D. E., Muhleman, D., Gade, R., Johnson, P., Verde, R., Saucier, G., et al. (1997). Cannabinoid Receptor Gene (CNR1): Association with IV Drug Use. *Mol. Psychiatry* 2, 161–168. doi:10.1038/sj.mp.4000247

Datta, U., Kelley, L. K., Middleton, J. W., and Gilpin, N. W. (2020). Positive Allosteric Modulation of the Cannabinoid Type-1 Receptor (CB1R) in Periaqueductal gray (PAG) Antagonizes Anti-nociceptive and Cellular Effects of a Mu-Opioid Receptor Agonist in Morphine-Withdrawn Rats. *Psychopharmacology* 237, 3729–3739. doi:10.1007/s00213-020-05650-5

Dong, H., Lu, S.-j., Zhang, R., Liu, D.-d., Zhang, Y.-z., and Song, C.-y. (2015). Effect of the *CYP2D6* Gene Polymorphism on Postoperative Analgesia of Tramadol in Han Nationality Nephrectomy Patients. *Eur. J. Clin. Pharmacol.* 71, 681–686. doi:10.1007/s00228-015-1857-4

Duthey, B., and Scholten, W. (2014). Adequacy of Opioid Analgesic Consumption at Country, Global, and Regional Levels in 2010, its Relationship with Development Level, and Changes Compared with 2006. *J. Pain Symptom Manage.* 47, 283–297. doi:10.1016/j.jpainsymman.2013.03.015

Dzambazovska-Trajkovska, V., Nojkov, J., Kartalov, A., Kuzmanovska, B., Spiroska, T., Seljmani, R., et al. (2016). Association of Single-Nucleotide Polymorhism C3435T in the ABCB1 Gene with Opioid Sensitivity in Treatment of Postoperative Pain. *Pril* 37, 73–80. doi:10.1515/prilozi-2016-0019

Ellegren, H. (2000). Heterogeneous Mutation Processes in Human Microsatellite DNA Sequences. *Nat. Genet.* 24, 400–402. doi:10.1038/74249

Fan, H., and Chu, J.-Y. (2007). A Brief Review of Short Tandem Repeat Mutation. *Genomics, Proteomics & Bioinformatics* 5, 7–14. doi:10.1016/S1672-0229(07)60009-6

Fukuda, K.-i., Hayashida, M., Ikeda, K., Koukita, Y., Ichinohe, T., and Kaneko, Y. (2010). Diversity of Opioid Requirements for Postoperative Pain Control Following Oral Surgery-Is it Affected by Polymorphism of the μ-Opioid Receptor. *Anesth. Prog.* 57, 145–149. doi:10.2344/0003-3006-57.4.145

Fukuda, K., Hayashida, M., Ide, S., Saita, N., Kokita, Y., Kasai, S., et al. (2009). Association between *OPRM1* Gene Polymorphisms and Fentanyl Sensitivity in Patients Undergoing Painful Cosmetic Surgery. *Pain* 147, 194–201. doi:10.1016/j.pain.2009.09.004

Genomes Project ConsortiumAuton, A., Auton, A., Brooks, L. D., Durbin, R. M., Garrison, E. P., Kang, H. M., et al. (2015). A Global Reference for Human Genetic Variation. *Nature* 526, 68–74. doi:10.1038/nature15393

Glass, M., Faull, R. L. M., and Dragunow, M. (1997). Cannabinoid Receptors in the Human Brain: a Detailed Anatomical and Quantitative Autoradiographic Study in the Fetal, Neonatal and Adult Human Brain. *Neuroscience* 77, 299–318. doi:10.1016/s0306-4522(96)00428-9

Gymrek, M., Willems, T., Guilmatre, A., Zeng, H., Markus, B., Georgiev, S., et al. (2016). Abundant Contribution of Short Tandem Repeats to Gene Expression Variation in Humans. *Nat. Genet.* 48, 22–29. doi:10.1038/ng.3461

Hayashida, M., Nagashima, M., Satoh, Y., Katoh, R., Tagami, M., Ide, S., et al. (2008). Analgesic Requirements after Major Abdominal Surgery Are Associated with *OPRM1* Gene Polymorphism Genotype and Haplotype. *Pharmacogenomics* 9, 1605–1616. doi:10.2217/14622416.9.11.1605

Itokawa, M., Yamada, K., Yoshitsugu, K., Toyota, T., Suga, T., Ohba, H., et al. (2003). A Microsatellite Repeat in the Promoter of the N-Methyl-D-Aspartate Receptor 2A Subunit (*GRIN2A*) Gene Suppresses Transcriptional Activity and Correlates with Chronic Outcome in Schizophrenia. *Pharmacogenetics* 13, 271–278. doi:10.1097/00008571-200305000-00006

Jakubosky, D., D'Antonio, M., Bonder, M. J., Smail, C., Donovan, M. K. R., Young Greenwald, W. W., et al. (2020). Properties of Structural Variants and Short Tandem Repeats Associated with Gene Expression and Complex Traits. *Nat. Commun.* 11, 2927. doi:10.1038/s41467-020-16482-4

Jiang, Y., Nie, Y., Li, Y., and Zhang, L. (2014). Association of Cannabinoid Type 1 Receptor and Fatty Acid Amide Hydrolase Genetic Polymorphisms in Chinese Patients with Irritable Bowel Syndrome. *J. Gastroenterol. Hepatol.* 29, 1186–1191. doi:10.1111/jgh.12513

Kasai, S., and Ikeda, K. (2011). Pharmacogenomics of the Human M-Opioid Receptor. *Pharmacogenomics* 12, 1305–1320. doi:10.2217/pgs.11.68

Kayser, M., Roewer, L., Hedman, M., Henke, L., Henke, J., Brauer, S., et al. (2000). Characteristics and Frequency of Germline Mutations at Microsatellite Loci from the Human Y Chromosome, as Revealed by Direct Observation in Father/son Pairs. *Am. J. Hum. Genet.* 66, 1580–1588. doi:10.1086/302905

Kozlowski, P., de Mezer, M., and Krzyzosiak, W. J. (2010). Trinucleotide Repeats in Human Genome and Exome. *Nucleic Acids Res.* 38, 4027–4039. doi:10.1093/nar/gkq127

Kumar, S., Kundra, P., Ramsamy, K., and Surendiran, A. (2019). Pharmacogenetics of Opioids: a Narrative Review. *Anaesthesia* 74, 1456–1470. doi:10.1111/anae.14813

Leclercq, S., Rivals, E., and Jarne, P. (2010). DNA Slippage Occurs at Microsatellite Loci without Minimal Threshold Length in Humans: a Comparative Genomic Approach. *Genome Biol. Evol.* 2, 325–335. doi:10.1093/gbe/evq023

Li, T., Liu, X., Zhu, Z.-H., Zhao, J., Hu, X., Ball, D. M., et al. (2000). No Association between (AAT)n Repeats in the Cannabinoid Receptor Gene (CNR1) and Heroin Abuse in a Chinese Population. *Mol. Psychiatry* 5, 128–130. doi:10.1038/sj.mp.4000670

Lopez-Moreno, J., Lopez-Jimenez, A., Gorriti, M., and de Fonseca, F. (2010). Functional Interactions between Endogenous Cannabinoid and Opioid Systems: Focus on Alcohol, Genetics and Drug-Addicted Behaviors. *Cdt* 11, 406–428. doi:10.2174/138945010790980312

Lv, J., Liu, F., Feng, N., Sun, X., Tang, J., Xie, L., et al. (2018). CYP3A4 Gene Polymorphism Is Correlated with Individual Consumption of Sufentanil. *Acta Anaesthesiol Scand.* 62, 1367–1373. doi:10.1111/aas.13178

Martikainen, I. K., Närhi, M. V., and Pertovaara, A. (2004). Spatial Integration of Cold Pressor Pain Sensation in Humans. *Neurosci. Lett.* 361, 140–143. doi:10.1016/j.neulet.2003.12.060

Martínez-Gras, I., Hoenicka, J., Ponce, G., Rodríguez–Jiménez, R., Jiménez-Arriero, M. A., Pérez-Hernandez, E., et al.AAT (2006). (AAT)n Repeat in the Cannabinoid Receptor Gene, CNR1: Association with Schizophrenia in a Spanish Population. *Eur. Arch. Psychiatry Clin. Neurosci.* 256, 437–441. doi:10.1007/s00406-006-0665-3

Miyamoto, Y., Yamada, K., Nagai, T., Mori, H., Mishina, M., Furukawa, H., et al. (2004). Behavioural Adaptations to Addictive Drugs in Mice Lacking the NMDA Receptor Epsilon1 Subunit. *Eur. J. Neurosci.* 19, 151–158. doi:10.1111/j.1460-9568.2004.03086.x

Nishizawa, D., Fukuda, K.-i., Kasai, S., Ogai, Y., Hasegawa, J., Sato, N., et al. (2014). Association between *KCNJ6* (*GIRK2*) Gene Polymorphism Rs2835859 and post-operative Analgesia, Pain Sensitivity, and Nicotine Dependence. *J. Pharmacol. Sci.* 126, 253–263. doi:10.1254/jphs.14189fp

Park, J. M., Choi, M.-G., Cho, Y. K., Lee, I. S., Kim, S. W., Choi, K. Y., et al. (2011). Cannabinoid Receptor 1 Gene Polymorphism and Irritable Bowel Syndrome in the Korean Population. *J. Clin. Gastroenterol.* 45, 45–49. doi:10.1097/MCG.0b013e3181dd1573

Patel, I., Walter, L. A., and Li, L. (2021). Opioid Overdose Crises during the COVID-19 Pandemic: Implication of Health Disparities. *Harm Reduct J.* 18, 89. doi:10.1186/s12954-021-00534-z

Pumpernik, D., Oblak, B., and Borštnik, B. (2008). Replication Slippage versus point Mutation Rates in Short Tandem Repeats of the Human Genome. *Mol. Genet. Genomics* 279, 53–61. doi:10.1007/s00438-007-0294-1

Rakvåg, T. T., Ross, J. R., Sato, H., Skorpen, F., Kaasa, S., and Klepstad, P. (2008). Genetic Variation in theCatechol-O-Methyltransferase (COMT)Gene and Morphine Requirements in Cancer Patients with Pain. *Mol. Pain* 4, 1744–8069. doi:10.1186/1744-8069-4-64

Ramil, E., Sánchez, A., González-Pérez, P., Rodríguez-Antigüedad, A., Gómez-Lozano, N., Ortiz, P., et al. (2010). The Cannabinoid Receptor 1 Gene (CNR1) and Multiple Sclerosis: an Association Study in Two Case-Control Groups from Spain. *Mult. Scler.* 16, 139–146. doi:10.1177/1352458509355071

Reyes-Gibby, C. C., Shete, S., Rakvåg, T., Bhat, S. V., Skorpen, F., Bruera, E., et al. (2007). Exploring Joint Effects of Genes and the Clinical Efficacy of Morphine for Cancer Pain: *OPRM1* and *COMT* Gene. *Pain* 130, 25–30. doi:10.1016/j.pain.2006.10.023

Rodenas-Ruano, A., Chávez, A. E., Cossio, M. J., Castillo, P. E., and Zukin, R. S. (2012). REST-dependent Epigenetic Remodeling Promotes the Developmental Switch in Synaptic NMDA Receptors. *Nat. Neurosci.* 15, 1382–1390. doi:10.1038/nn.3214

Rossi, S., Bozzali, M., Bari, M., Mori, F., Studer, V., Motta, C., et al. (2013). Association between a Genetic Variant of Type-1 Cannabinoid Receptor and

Inflammatory Neurodegeneration in Multiple Sclerosis. *PLoS One* 8, e82848. doi:10.1371/journal.pone.0082848

Rossi, S., Buttari, F., Studer, V., Motta, C., Gravina, P., Castelli, M., et al. (2011). The (AAT)n Repeat of the Cannabinoid CB1 Receptor Gene Influences Disease Progression in Relapsing Multiple Sclerosis. *Mult. Scler.* 17, 281–288. doi:10.1177/1352458510388680

Ruiz-Contreras, A. E., Carrillo-Sánchez, K., Gómez-López, N., Vadillo-Ortega, F., Hernández-Morales, S., Carnevale-Cantoni, A., et al. (2013). Working Memory Performance in Young Adults Is Associated to the AATn Polymorphism of the *CNR1* Gene. *Behav. Brain Res.* 236, 62–66. doi:10.1016/j.bbr.2012.08.031

Sanz-Clemente, A., Matta, J. A., Isaac, J. T. R., and Roche, K. W. (2010). Casein Kinase 2 Regulates the NR2 Subunit Composition of Synaptic NMDA Receptors. *Neuron* 67, 984–996. doi:10.1016/j.neuron.2010.08.011

Sanz-Clemente, A., Nicoll, R. A., and Roche, K. W. (2013). Diversity in NMDA Receptor Composition. *Neuroscientist* 19, 62–75. doi:10.1177/1073858411435129

Scally, A. (2016). The Mutation Rate in Human Evolution and Demographic Inference. *Curr. Opin. Genet. Dev.* 41, 36–43. doi:10.1016/j.gde.2016.07.008

Siegfried, Z., Kanyas, K., Latzer, Y., Karni, O., Bloch, M., Lerer, B., et al. (2004). Association Study of Cannabinoid Receptor Gene (CNR1) Alleles and Anorexia Nervosa: Differences between Restricting and Bingeing/purging Subtypes. *Am. J. Med. Genet.* 125B, 126–130. doi:10.1002/ajmg.b.20089

Sistonen, J., Madadi, P., Ross, C. J., Yazdanpanah, M., Lee, J. W., Landsmeer, M. L. A., et al. (2012). Prediction of Codeine Toxicity in Infants and Their Mothers Using a Novel Combination of Maternal Genetic Markers. *Clin. Pharmacol. Ther.* 91, 692–699. doi:10.1038/clpt.2011.280

Slivicki, R. A., Iyer, V., Mali, S. S., Garai, S., Thakur, G. A., Crystal, J. D., et al. (2020). Positive Allosteric Modulation of CB1 Cannabinoid Receptor Signaling Enhances Morphine Antinociception and Attenuates Morphine Tolerance without Enhancing Morphine- Induced Dependence or Reward. *Front. Mol. Neurosci.* 13, 54. doi:10.3389/fnmol.2020.00054

Stamer, U. M., Musshoff, F., Kobilay, M., Madea, B., Hoeft, A., and Stuber, F. (2007). Concentrations of Tramadol and *O*-Desmethyltramadol Enantiomers in Different *CYP2D6* Genotypes. *Clin. Pharmacol. Ther.* 82, 41–47. doi:10.1038/sj.clpt.6100152

Tzvetkov, M. V., Saadatmand, A. R., Lötsch, J., Tegeder, I., Stingl, J. C., and Brockmöller, J. (2011). Genetically Polymorphic OCT1: Another Piece in the Puzzle of the Variable Pharmacokinetics and Pharmacodynamics of the Opioidergic Drug Tramadol. *Clin. Pharmacol. Ther.* 90, 143–150. doi:10.1038/clpt.2011.56

Ujike, H., Takaki, M., Nakata, K., Tanaka, Y., Takeda, T., Kodama, M., et al. (2002). CNR1, central Cannabinoid Receptor Gene, Associated with Susceptibility to Hebephrenic Schizophrenia. *Mol. Psychiatry* 7, 515–518. doi:10.1038/sj.mp.4001029

Volkow, N. D., and Collins, F. S. (2017). The Role of Science in the Opioid Crisis. *N. Engl. J. Med.* 377, 1797–1798. doi:10.1056/NEJMc1711494

Wang, Q. Q., Kaelber, D. C., Xu, R., and Volkow, N. D. (2021). COVID-19 Risk and Outcomes in Patients with Substance Use Disorders: Analyses from Electronic Health Records in the United States. *Mol. Psychiatry* 26, 30–39. doi:10.1038/s41380-020-00880-7

Wei, W., Tian, Y., Zhao, C., Sui, Z., Liu, C., Wang, C., et al. (2015). Correlation of ADRB1 Rs1801253 Polymorphism with Analgesic Effect of Fentanyl after Cancer Surgeries. *Med. Sci. Monit.* 21, 4000–4005. doi:10.12659/msm.894060

Willems, T., Gymrek, M., Highnam, G., Mittelman, D., and Erlich, Y. (2014). The Landscape of Human STR Variation. *Genome Res.* 24, 1894–1904. doi:10.1101/gr.177774.114

Xue, Y., Wang, Q., Long, Q., Ng, B. L., Swerdlow, H., Burton, J., et al. (2009). Human Y Chromosome Base-Substitution Mutation Rate Measured by Direct Sequencing in a Deep-Rooting Pedigree. *Curr. Biol.* 19, 1453–1457. doi:10.1016/j.cub.2009.07.032

Zhang, P.-W., Ishiguro, H., Ohtsuki, T., Hess, J., Carillo, F., Walther, D., et al. (2004). Human Cannabinoid Receptor 1: 5′ Exons, Candidate Regulatory Regions, Polymorphisms, Haplotypes and Association with Polysubstance Abuse. *Mol. Psychiatry* 9, 916–931. doi:10.1038/sj.mp.4001560

Zimprich, A., Kraus, J., Woltje, M., Mayer, P., Rauch, E., and Hollt, V. (2000). An Allelic Variation in the Human Prodynorphin Gene Promoter Alters Stimulus-Induced Expression. *J. Neurochem.* 74, 472–477. doi:10.1046/j.1471-4159.2000.740472.x

Conflict of Interest: The authors declare that the research was conducted in the absence of any commercial or financial relationships that could be construed as a potential conflict of interest.

Publisher's Note: All claims expressed in this article are solely those of the authors and do not necessarily represent those of their affiliated organizations, or those of the publisher, the editors, and the reviewers. Any product that may be evaluated in this article, or claim that may be made by its manufacturer, is not guaranteed or endorsed by the publisher.

Advantages of publishing in Frontiers

OPEN ACCESS
Articles are free to read for greatest visibility and readership

FAST PUBLICATION
Around 90 days from submission to decision

HIGH QUALITY PEER-REVIEW
Rigorous, collaborative, and constructive peer-review

TRANSPARENT PEER-REVIEW
Editors and reviewers acknowledged by name on published articles

Frontiers
Avenue du Tribunal-Fédéral 34
1005 Lausanne | Switzerland

Visit us: www.frontiersin.org
Contact us: frontiersin.org/about/contact

REPRODUCIBILITY OF RESEARCH
Support open data and methods to enhance research reproducibility

DIGITAL PUBLISHING
Articles designed for optimal readership across devices

FOLLOW US
@frontiersin

IMPACT METRICS
Advanced article metrics track visibility across digital media

EXTENSIVE PROMOTION
Marketing and promotion of impactful research

LOOP RESEARCH NETWORK
Our network increases your article's readership